Power Quality Enhancement in Electricity Networks Using Grid-connected Solar and Wind Based DGs

Department of Electrical Engineering
University of Cape Town

Prepared by:
Tlhoriso Matlokotsi
MTLTLH003

Prepared for:
A/Prof. Sunetra Chowdhury

****DEPARTMENT OF ELECTRICAL ENGINEERING****
University of Cape Town

February 2017

Submitted to the Department of Electrical Engineering at the University of Cape Town in partial fulfilment of the academic requirements for a Master of Science degree in Electrical Engineering;

Key Words: Power Quality, Voltage profile, Distributed Generation, Solar photovoltaic, Doubly Fed Induction generator, Grid integration

Declaration

I know the meaning of plagiarism and declare that all the work in this document, save for that which has been properly acknowledged, is my own. This dissertation has been submitted to Turnitin for plagiarism checking and I confirm that my supervisor has seen my report and any concerns revealed by such have been resolved with my supervisor.

Name: Tlhoriso Matlokotsi

Signature: Signed by candidate

Date: 20 February 2017

Acknowledgements

First and foremost, my sincere gratitude goes to God the Almighty for the gift of life and the blessings throughout the course of my studies. He has always been my provider.

I would also whole like to show my sincere appreciation to A/Prof. Sunetra Chowdhury for the support throughout this research work. Prof. Chowdhury has been exceptional and significantly enhanced my research capabilities. It is through her support that I had a significant exposure to academic activities such as presentations and solid academic writing.

Special thanks go to MasterCard Foundation for funding my research work. Their support enabled me to perform to the best of my ability.

A token of acknowledgement goes to my mother, Mrs. Mmamokete Matlokotsi and my siblings for being there for me during the course of academic career. Indeed, family is one of nature's masterpieces. Special thanks also go to my beloved partner and lover Thakane Monaheng for the support during the course of my entire postgraduate journey.

Abstract

The integration of DG into utility networks has significantly increased over the past years primarily as a result of growing energy demand, coupled with the environmental impacts posed by conventional fossil fuel-based power generation. The prominent DG technologies which are capable of meeting bulk energy demands and are clean energy sources are wind and solar energy sources. The resources for solar and wind based DG are available in abundance in most geographical locations in South Africa and the rest of Africa. Through the Renewable Energy Independent Power Producer Procurement Programme (REIPPPP) introduced by the South African government in 2011, 3 920 MW of renewable energy has been procured to date. Out of this, solar and wind energy constitute 2 200 MW and 960 MW, respectively.

Grid integration of solar and wind-based intermittent DGs may however pose negative impacts on the quality of power supplied by the utility network. Some of the detrimental impacts of DG include voltage fluctuations, flicker, etc. which are in general categorised as power quality (PQ) problems. The proper planning of DG integration is required to mitigate the negative impacts they pose on system's PQ to ensure that the performance of the utility network is enhanced in terms of the overall PQ improvement of the system.

This dissertation reviews general PQ problems in utility networks with DG integration and whether poor planning of DG integration affects PQ negatively. The work emphasizes on the impacts of grid integration of wind and solar PV sources on power quality. It investigates the manner in which wind and solar energy systems differ in their impacts and capacity to improve PQ of the network in terms of a number of factors such as point of integration and capacity of DG, type of DG, network loading, etc. The role of grid-integrated DG in PQ improvement in electricity network is also investigated by exploring different PQ improvement techniques. The networks considered for the grid integration of DG for PQ improvement in this work are the IEEE 9-bus sub-transmission network at the nominal voltage of 230kV and the IEEE 33-bus distribution network at the nominal voltage of 12 kV. The aspects essential for facilitating proper planning of DG integration for PQ improvement and total loss reduction are investigated and the comparative analysis is made between grid integration of wind and solar PV based DGs.

The simulations of different case studies in this work are done using DIgSILENT PowerFactory version 14.1 as well as coding in MATLAB. The cases studies conducted are aimed at facilitating the proper planning of grid integration of wind and solar PV-based DGs by comparing their PQ

improvement capabilities under different scenarios. First the investigation of how their location and capacity affect the network voltage profiles and active power losses is conducted. Their ability to improve the system's PQ is also studied by observing PQ improvement strategies such as voltage control, installation of energy storage and the optimal placement of DGs under different scenarios. In order to account for the weakness of most South African utility grids, PQ improvement in weak networks with DG integration is also studied by investigating how DG integration in networks with different grid strengths affect the system's PQ.

The results provide an understanding of the role of grid integration of wind and solar based DGs on PQ which is useful in the planning of grid integration of RE, particularly in South African electricity networks. The results revealed that the location and capacity of integrated DGs indeed affect the quality of power as well as active power losses in the grid. It is also established that a significant improvement in network's PQ and line loss reduction can be achieved in networks with wind and solar integration. The results however indicated that wind and solar PV based DGs differ in their impacts and capacity to improve the quality of power in the network. Furthermore, the results revealed that wind and solar plants integration into weak utility grids may pose adverse impacts on the system's PQ. It was however established that including reactive power control devices such as STATCOM and SVC at the PCC can successfully improve the system's PQ and enable grid code compliance in electricity networks with DG integration.

Table of Contents

List of Figures

List of Illustrations

List of Tables

1. Introduction

1.1 Background to the study

The ever rising demand for electrical energy as a result of increasing population across the globe has called for a need to increase electrical energy generation. Currently the greater percentage of electrical energy is generated by burning of fossil fuels which have negative environmental impacts. The sustainable solution is therefore to consider the deployment of cleaner renewable energy sources to generate additional power to meet energy demands. South Africa in particular has taken an initiative of integrating small renewable-based power plants to the utility grid through the Renewable Energy Independent Power Producer Procurement Program (REIPPPP). The most popular renewable energy sources which have the potential to alleviate the energy crisis are wind and solar PV because these resources are available in abundance in most geographical locations in the African continent, including South Africa.

One of the main issues concerning grid-integration of Renewable Energy Sources (RES) is their impacts on the system's power quality (PQ). The continuing usage of PQ-sensitive equipment in domestic and industrial applications requires high PQ in the utility grids. Customers and utilities are affected by poor PQ as it may deteriorate the network's performance and result in shutdown or mal-operation of certain equipment. The quality of power, particularly in distribution grid is a primary challenge in planning grid integration of DGs since most network loads are supplied from the distribution level of a network. The grid integration of wind and solar PV based DGs pose a number of challenges which may affect system's PQ and hence affect the normal operation of the power network. Their intermittent nature contributes to frequency and voltage variations (rises and dips) in the network. Power quality is an important issue in electricity network because most modern loads employed in critical processes and applications are sensitive to poor PQ.

The traditional design of conventional electricity networks is based on bulk power generation from the power stations situated far from the end user and closer to the primary resource. This operational structure of the network was designed on the basis of economics, reliability and quality of supply. The flow of power in conventional networks has always been unidirectional, flowing from higher voltage levels to lower voltage levels. The conventional electrical grids were therefore not designed to accommodate any integration of DG, particularly at the distribution level. Connecting DG units into utility grids therefore adversely affect the network operation and may deteriorate the quality of power in the network, if integration planning is done poorly. Hence, in light of the PQ issues brought about by grid integration of DGs, particular attention should be paid to proper planning of their grid

connection such that the overall PQ of the network remains unaffected or enhanced. This calls for exploring the role of their grid integration DGs on PQ enhancement.

With the deployment of renewable energy systems (RESs) as DGs of different capacities, the future electricity networks now have multiple small generating units connected at different parts of the network, particularly at the sub transmission and distribution parts due to their close proximity to load centres. The network will therefore be active, with generation and consumption within close proximity of each other. This will affect the conventional flow of power from higher voltage levels to lower voltage levels as high penetration levels of DG may result in over voltages at the point of common coupling (PCC). As a result, the voltage may rise above the limits permitted by the grid codes. Some of the negative impacts resulting from grid integration of DGs include voltage fluctuations, flicker, harmonic injection, frequency deviation, etc. The poor planning of grid integration of DG have negative impacts on the system's PQ and may accelerate the problems stated above.

For proper planning of grid-integration of solar and wind energy sources, it is first vital to establish how grid integration of each RES affects the system's PQ. This will help establish whether poor planning of grid integration of DG have a negative impact on the system's PQ. The investigation and understanding of the role of grid integration of DGs in network's PQ improvement will also enable an effective planning of DG grid integration. The effective utilization of DG for PQ improvement can be achieved by exploring a number options essential for mitigating PQ problems such as voltage variations. Apart from the issue of PQ, careful consideration should be made towards active power loss reduction, protection coordination and stability in planning the grid with DG penetration.

A comprehensive analysis of the impacts of grid integration of solar PV and wind based DGs is essential and has been taken up in this dissertation. One of the main challenge to proper grid integration of DGs is their optimal location in the network as well as their capacity. The optimal location and capacity of DGs in this context refers to the best PCC and capacity of DG which will ensure improved PQ in the system. This is because improper placement and sizing of DGs may pose negative impacts on the quality of power and contribute to increased power losses in the network. It is therefore imperative to be able determine the optimal locations for placement of DGs under different scenarios, such that the overall quality of power in the network can be enhanced while the efficiency of the power system is also enhanced. In addition to improving the system's PQ, the optimal allocation of DGs in electricity networks should also ensure improved system's reliability for enhanced security of electricity supply.

Some parts of the South African sub-transmission and distribution networks, particularly those supplying remote areas are characterized by long and weak lines. Wind and solar energy resources may be found in abundance at locations close to the parts where the network is electrically weak. For economical purposes, the suitable PCC will potentially be the bus or substation located within the weak grid. DG integration in weak networks may pose adverse impacts on the system's PQ due to the stress imposed on the lines. The integration of DGs in electrically weak networks may therefore require a significant level of network strengthening, with associated high costs and long implementation times. In order to facilitate the proper planning of DG integration in weak grids, their impacts on PQ must be understood so that appropriate measures can be put in place to enhance the network's PQ. This requires relevant network studies to assess the grid integration feasibility and propose relevant techniques to allow for a higher DG penetration level.

1.1.1 *Purpose of the study*

The significance of improving PQ in networks with DG integration is motivated by the prevailing PQ problems as a result of poor planning of DG integration. The strictness of the grid codes governing grid integration of DGs also calls for a need to ensure that the grid codes requirements are met upon DG integration. Wind and solar energy resources are usually available in abundance at locations far from the utility network and the closest connection point may be the parts of the network with weak grid strength. Weak networks characterize most parts of the transmission, sub-transmission and distribution networks of most South African utility grids and need to be evaluated for capability to accommodate DG penetrations without violating the grid code requirements.

1.2 Research questions

The impacts of grid integration of DGs on PQ is the challenge which brings a major concern to utilities and network planners particularly when large penetration levels of DG are to be integrated. Wind and solar plants penetration level is likely to increase due to high availability of their resources, their intermittent nature may pose detrimental impacts on the system's PQ. The grid codes however require them to operate within acceptable PQ limits in addition to providing additional power to the network. The research questions which this work attempt to answer while analysing the role of grid integration of DGs for PQ enhancement are as listed below:

- Does poor planning of solar PV and Wind based DGs integration affects the system's PQ?
- How can DGs be effectively used for enhancing power quality?

- How does wind and solar power plants differ in their impacts or capacity to improve the system's PQ?

1.3 Objectives of research

For the purpose of achieving PQ improvement in utility networks with DG integration, the following were addressed in this work in order to facilitate proper planning their integration:

- To review the general PQ problems in electricity networks with DG integration;
- To establish whether poor planning of DG integration affects PQ negatively;
- To establish how wind and solar plants integrated into utility grids differ in their impacts and capacity to improve PQ;
- To investigate the effect of DG location, penetration level and network loading on system's PQ and total power losses and compare the results obtained as a result of solar PV and DFIG type wind power plant integration;
- To explore PQ improvement techniques in utility grids with solar and wind plants integration and compare the level on improvement between the two technologies;
- To investigate the impacts of connecting DGs in utility grids with different grid strengths and apply measures necessary to improve the system's PQ such as reactive power control by Static Var Systems (SVS);
- To optimally locate and size DGs in the network given the network characteristics for the purpose of improving the system's PQ
- To formulate a multi-objective function which considers voltage profile improvement and active power reduction to facilitate the optimal allocation of DGs for PQ enhancement;
- To observe and compare PQ improvement as result of optimal placement of wind and solar plants into utility grid under different scenarios;

1.4 Scope of dissertation and scientific approach

The analysis in this dissertation focuses on voltage profiles before and after the integration of DGs during the normal network operation and when disturbances are introduced in the form of three phase faults. In cases when there is a fault in the system, the focus is made on the transient response of the system by observing the post-fault voltage profile in the presence of DGs. In the case studies conducted, the system's PQ is evaluated using the grid code requirement for connection of renewable energy sources in to South African networks as a reference.

Power losses in power systems are one of the fundamental indicators of an economic operation of the power system and hence cannot be ignored in PQ improvement analysis. The overall active power losses as a result of DG integration in the case studies conducted are also investigated. The case studies conducted focus on voltage profile improvement and do not consider the stability of the system. The frequency variations as a result of variations of the real power generated and consumed are also excluded in the analysis. The harmonic injections due to DG integration are also not included in PQ analysis of the network. The systems' frequency variation and harmonic injection issues are disregarded because the modern technology and control strategies are capable of mitigating their adverse impact, even at higher DG penetration levels. Voltage profiles fluctuations have however been identified as major PQ issues pertaining to large penetration levels of DG and hence require a special attention.

The enhancement of PQ in networks with DG integration is carried out using the standard test systems which are IEEE 9-bus system and IEEE 33-bus distribution test feeder. The IEEE 9-bus system represents the sub transmission system while the latter represents the distribution system with loads integrated at all system's buses except bus 1. The software tools employed to achieve PQ improvement are DIgSILENT Power factory and necessary coding in MATLAB environment. Most cases are however conducted in DIgSILENT power factory program which has numerous functionalities required to model and simulate the network and components in this work. The following overview details the studies conducted by each tool;

- DIgSILENT power factory is employed studies pertaining to modelling and simulations of network and DG models to observe the behaviour of the network upon DG integration. The studies seeking to observe the transient behaviour of the system upon Dg integration are also conducted in power factory.
- The GA algorithm is developed to find the optimal placement and sizing of DGs for PQ enhancement in the network in MATLAB environment. The optimization problem is achieved by defining the objective function as well as the necessary calculations such as load flow in MATLAB code.

From the above tasks conducted, the resulting voltage profiles and total power losses as a result of DG integration are compared to that obtained when the base case (network without DG integration) is simulated. Furthermore, the results obtained are also used to compare the performance of grid integrated solar and wind plants in terms of PQ enhancement capabilities of each technology.

1.5 Assumptions

The assumptions made in PQ enhancement in utility networks using solar and wind-based DGs are aimed at simplifying some of the complexities associated with modelling and obtaining accurate results. The assumptions made for the purpose of this work are as follows:

- The demand for load in the networks is less than the total installed capacity.
- The configuration of the distribution system is radial and is fed by the high-voltage/medium-voltage (HV/MV) substations. The addition of DG to the distribution network structure will therefore not disturb the radial configuration of the network.
- The protection settings of the relays and circuit breakers between the network components and DG systems are in place and have been coordinated to adequately protect network components against short circuits. The relays and circuit breakers are placed at the beginning and end of each line for protection of loads at the respective nodes.
- All buses in the test networks are considered as potential locations for DG installation with only the slack bus being an exception.
- In reality, planning of intermittent DG sources such as wind turbines and PVs is highly dependent on the availability of their resources. It is therefore assumed that a feasibility study evaluating the possibility of their exploitation has been performed beforehand such that their optimal placement in the network can be attained.

1.6 Delimitations of the work

The boundaries set for the study are mainly pertaining to the indicators of system PQ such as frequency profiles and harmonics. The impacts of DG integration on frequency and harmonics are only reviewed in the literature review but are not considered in the simulations section of the work. The analysis of network's PQ will be conducted by observing only the voltage profiles and active power losses to observe the DG impacts of system's efficiency. The study also does not consider the transient stability analysis which could also influence the PQ in the network.

1.7 Dissertation outline

The dissertation consists of 8 chapters as outlined below:

Chapter 1: This chapter provides an introductory overview of the work and includes the background to the study, objectives of the study, scope of the work and scientific approach as well as the outline of the dissertation.

Chapter 2: This chapter presents the review of relevant research and technical literature on general PQ problems as a result of DG integration and the role of grid integration of DGs on PQ enhancement. An overview of planning of utility grids with DG integration is also presented.

Chapter 3: This chapter presents theory development of PQ enhancement in utility networks with DG integration in terms of voltage quality during normal network operation and in instances of faults. The various techniques essential for mitigating DG impacts for maximum penetration are also discussed.

Chapter 4: This chapter presents an overview of different optimization techniques essential for determination of optimal DG sizes and locations in distribution networks, taking into consideration, the power quality improvement and power loss reduction.

Chapter 5: This chapter presents the research method undertaken to conduct the case studies. The necessary models of test networks and DGs are discussed in this chapter. The problem formulation of the optimization procedure is also presented in this chapter.

Chapter 6: The case studies conducted for the purpose of investigating the role of grid integration of DG units for PQ enhancement are presented in this chapter. The detailed simulation procedure is also discussed in this chapter.

Chapter 7: The results of the case studies described in Chapter 6 are presented and discussed in this chapter.

Chapter 8: This chapter presents the conclusions drawn from the results obtained from the simulations and details the necessary recommendations for future work.

2. Literature Review

The current energy sources dominating the energy industry are based on fossil fuels, which have brought concerns due to their impacts on the environment. Coal has remained the largest global energy resource with over 82% of the world's energy being generated from coal powered stations [1]. The techniques employed in coal powered stations release particulate matters and harmful greenhouse gases which destroy the ozone layer and are the major causes of climate change and environmental pollution as a whole.

Apart from environmental pollution and climate change, generating utilities are facing a challenge of supplying adequate amount of electrical power to consumers due to rising energy demand. Demand for excess energy is motivated by an increase in population, economic improvements as well as advancement in technology systems, most of which require electricity to operate. It is therefore crucial for energy utilities to meet energy demands by considering alternative means to generate energy. This calls for a need to consider generating energy from renewable energy sources to partially replace the conventional energy sources.

Renewable energy sources such as wind, solar, biomass, hydro-power, geothermal and marine energies provided an estimated 19% of global energy consumption in 2012 and continued to grow in 2013 [1]. These power generating units fall under Distributed Generation (DG). DG sources differ from large central power systems in that they are relatively smaller sources of electrical power generation or storage, typically in the range of 1kW to 50MW, located within close proximity to consumer loads or connected to an electric distribution system [2]. Integration of DG units to electricity networks is increasing and is expected to continue growing over the next coming years [3]. It is therefore expected that DG will contribute in substantially to power generation in the near future. Wind and solar photovoltaic are the fastest growing DG technologies which have drawn the global attention of the 21st century. However, challenges associated with their integration to the utility grid affect the power quality of the power system.

The literature review provides a brief overview of the definitions of DG and the PQ phenomenon. The chapter then provides a brief background to PQ phenomenon and classification of PQ problems. The chapter then covers a review on planning of grid-integration of DGs. The utilization of DGs for PQ enhancement in electricity networks is also covered with particular emphasis made on techniques that contribute to PQ enhancement. The impacts of grid-integration of wind and solar PV-based DGs on PQ are also included followed by the review of PQ enhancement by optimal DG placement and sizing. The review of PQ grid-connected wind and solar PV based DGs is structured as per Table 2-1 below:

Table 2-1: The criteria followed in structuring of the literature review

Topics reviewed	Items covered
Description of Distributed Generation	DG definition, Motivations for DG deployment.
Review of PQ phenomena	PQ definition, PQ problems, motivations for PQ.
Planning of DG grid-integration	Challenges for current networks, Grid planning, DG integration into weak networks, Grid code assessment for DG integration into SA networks.
DG deployment for PQ enhancement	DG coupling with energy storage, Using power electronics for PQ enhancement, Strategic implementation of DGs for PQ improvement.
Impacts of wind and solar PV on PQ enhancement	DG impacts on voltage profiles, system power losses, frequency and harmonics.
Optimal placement and sizing of DGs	Optimal DG allocation for voltage profile improvement, reliability improvement and economic performance enhancement.

2.1 Distributed generation

2.1.1 *Definition*

Distributed generation is one of the new trends in power systems and is generally defined as generating units sufficiently smaller than the central generating plants. The term is used differently in some countries by using notations such as “dispersed generation”, embedded generation” or “decentralized generation” [4]. Numerous definitions for DG had been proposed by different professional bodies such as the International Energy Agency (IEA) and Institute of Electrical and Electronic Engineers (IEEE). Most DG definitions are generally based on the size and location of the generating unit with respect to centralized generating plants.

IEA defines DG as generating plants supplying a customer on-site, or providing support to the network, and are integrated to the grid at distribution voltage levels [4]. The IEEE on the other hand, defines DG as electricity generation by units that are smaller than the centralized generating plants such that interconnection at nearly any point in a network is possible [5]. In this research, the adopted DG definition is that proposed by Gonzalez et al. wherein DG is defined as the source of electrical power integrated to the network at the sub-transmission and distribution levels including those connected on the customer side of the meter, and smaller than central generating plants [6].

DG technologies are classified into renewable DGs and non-renewable DGs and the latter is an unattractive solution for utilities due to its environmental and sustainability concerns. Electrical energy storage systems are also classified as part of DG technologies because they are sometimes concurrently integrated with DG sources. Renewable DGs are preferred due to cleanness of their technology and high availability in most geographic locations. Various DG technologies are shown in Figure 2-1 below:

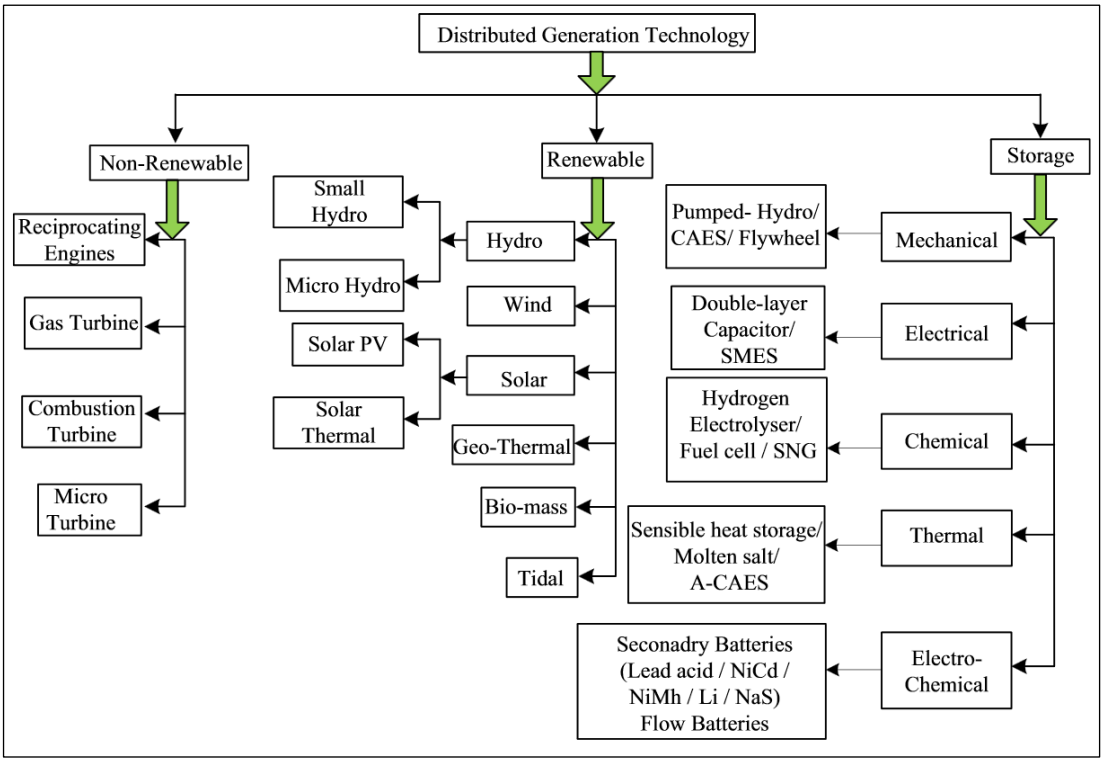

Figure 2-1: Classification of various distributed generation technologies **[7]**

DG technologies include a wide range of energy sources that can be classified as renewable and non-renewable energy sources. Renewable DGs include mainly wind turbines and solar photovoltaic (PV) while non-renewable DGs include diesel generators and fuel cells. The combination of heat and electricity generation is also among well-established DG technologies mostly used in large industries. The interest in combined heat and power (CHP) among other DG technologies is due to its flexibility of operation, size and expandability [8]. However this work is primarily concerned only with wind power and solar PV type DGs.

DG units can be operated in two main modes which are islanded mode and grid-connected mode. In the former case, DGs generate power independently of the grid. In grid-connected mode, the power generated by DG is fed directly into the grid either at sub-transmission or distribution networks, close to customer equipment [9]. The integration of DGs within existing grids results in numerous

challenges ranging from infrastructure requirement, technical performance and power quality [9]. Power quality (PQ) in networks with DG integration is a major challenge as poor PQ can pose adverse impacts on network loads.

2.1.2 *Motivations for DG deployment*

It is expected that DG technologies will contribute significantly to the total energy generation of the future due to improvements in the development of a wide number of DG technologies. According to the IEA, an interest in DG has significantly been motivated by the following major factors [4]:

- Diversity and advancements in developed DG technologies
- Customers demand for reliable electricity
- Liberalization of the electricity market
- Climate change concerns as a result of conventional electricity generation technologies
- Restrictions on contractions of new transmission lines and the associated costs
- Fuel costs uncertainties

There has been a significant increase in deployment of wind and solar PV based DGs and their optimal integration to the grid is the current trend in renewable energy industry. The increase, according to Paska et al. [10] is attributed to a declining trend in the cost associated with their large scale deployment. The traditional grid architecture based on centralized generation has also given a way to a modular architecture that will include strategically interconnected DG [10].

Apart from them being clean energy sources, one of the motivations for grid integration of wind and solar energy sources is their ability to improve the grid's PQ , reduce system's active power losses and improve reliability. PV systems have a fairly large footprint in the global energy paradigm due to their use of inexhaustible energy from the sun and environmental benefits [10]. Wind energy has also grown tremendously in the past years due to its potential to alleviate energy crises in the growing energy industry as well as the clean nature of wind resource.

Network operators as well as electricity customers are becoming increasingly concerned about poor PQ which can have adverse impacts on network's efficiency, reliability and security of supply in DG-integrated networks [11]. The sensitivity of most equipment used in commercial and industrials processes require that the quality of power supply is of good standard. Any fluctuations in the power system's PQ such as voltage and frequency or injection of harmonics may result in mal-operation or even shutdown of equipment. This has led to utilities and distribution network operators to develop the grid codes setting out system's operational constraints in terms of the parameters such as

acceptable voltage/frequency ranges and harmonic levels at different network sections. The grid code requirements for DG integration into South African networks will be reviewed in the following sections. The focus of this work is on power quality problems and its improvement strategies in electricity networks with further penetration of DG into the energy mix.

2.2 Power Quality Phenomena

2.2.1 *Definition of Power Quality*

Different literature define power quality in different ways but their definitions all converge to a common meaning, ensuring a reliable performance of an electrical system with no adverse impacts to the system. IEEE defines power quality as "the concept of powering and grounding sensitive electronic equipment in a manner suitable for the equipment and compatible with the premise wiring system as well as other connected equipment" [12]. It is also defined as any power system problem demonstrated in voltage, current and frequency deviations which results in significant loss of performance in electrical equipment or life expectancy [12]. Power quality (PQ) is also assessed by the ability of electrical equipment to operate in a satisfactory manner and without having adverse impacts on other electrical equipment connected to electrical networks. The system's PQ can be identified by observing different parameters such as voltage profiles, frequency, reliability, etc.

2.2.2 *Motivations for Power Quality Concern*

The increasing energy demands and technology advances are major motivations for power quality concern. Utilities are facing a challenge of supplying high quality electrical power due to number of factors, some of which are influenced by improvements in technology. The issue of PQ in electrical systems is important and strongly motivated by the following reasons:

- The world population is becoming increasingly dependent on the electrical power and utilities have to keep up with this demand. While a small power outage can have a huge economic impact on industrial customers, longer interruptions harm almost all operations of the modern society where millions of people are predominantly dependent on electricity [13].
- The vast majority of industrial and residential processes use electrical equipment that is more sensitive to power quality variations. The availability of electrical power with improved power quality is therefore an important factor for competitiveness in numerous sectors, particularly in continuous process industries and the information systems technology services.
- Increasing usage of power electronic equipment such as variable speed drives and computers now demands stricter compliance of PQ to grid codes [14].

- Higher penetration levels of wind and solar-based DGs in electricity networks have impacts on the PQ of the network due to their fluctuating power outputs. These technologies make use of power electronic devices for effective grid integration thus increasing the chances of voltage and current harmonic distortions [14].

2.2.3 *Power Quality Problems*

Different types of PQ problems are classified based on their impacts on electrical systems as well as their duration. The fundamental concept of electrical power quality seeks to identity parameters such as voltage and frequency of the power system and the degree at which they vary from their nominal magnitudes. These parameter variations are the main reason for PQ degradation and are hence of utmost importance in reliable power systems operation [15]. Addition of a large number of modern sophisticated equipment to the power system has also called for a need for improved PQ at the consumer's premises.

Determination of the exact power quality problems in the power system may require some sophisticated electronic test equipment. Fortunately, the presence of problems related to poor PQ in electrical systems can be recognized by observing the behaviour of connected electrical equipment. As indicated in a research done by Khalid et al. the following symptoms are major indicators of PQ problems [13]:

- Circuit breakers tripping without being overloaded
- Equipment failing during a thunder storm
- Electronics systems work in one location and fail to work in another
- Electronic systems failing or not operating rather frequently

PQ in electrical systems is defined by various parameters such as the behaviour of system's voltage and harmonics. The common parameters considered in evaluating power quality problems are discussed in the sections to follow.

2.2.4 *Voltage fluctuations*

Voltage fluctuations are defined as continuous variations of the voltage or a series of random voltage changes normally with the magnitude within the voltage ranges [16] [11]. Voltage fluctuations are the results of sudden changes in the apparent power drawn by loads. Other causes of voltage variation include connecting variable power sources such as wind generators and PV's in to electrical networks. The fluctuating nature of wind velocities result in variations in the output voltage of the wind energy conversion system (WECS) and consequently results in poor PQ. Similarly, the output power of the

solar PV systems is dependent on the irradiance from the sun which is inconsistent and consequently causes variations in the system's voltage profiles.

Voltage variations are classified into long and short duration variations depending on the duration of an interruption. Long duration voltage variations exist for more than 1 minute and may be either over voltage or under voltage [17]. An overvoltage occurs when an r.m.s. AC voltage rises above 110 % of the nominal voltage for more than one minute [11]. Conversely, under voltage occurs when the value of r.m.s AC voltage decreases to 90% of the nominal voltage for over one minute. The most prominent causes of long duration voltage variations include overloading of distribution system, variations in local loads and switching operations.

Short duration voltage variations on the other hand are variations in the r.m.s voltage from the nominal voltage for longer than 0.5 AC cycles but less than or equal to 1 minute [17]. Short term voltage variations are different from steady state changes in the waveform such as harmonics and noise which also have a short duration but repeat for each cycle of a sinusoidal waveform. The major causes of short duration voltage variations include voltage disturbance conditions resulting from energizing of large electric loads which require high starting currents or transformer switching with high inrush current [17]. The loose connections in the current carrying conductors can also result in short duration voltage variations.

2.2.5 *Voltage sags/ Voltage dips*

Voltage sag is described as a temporary decrease in the r.m.s. magnitude of the nominal voltage magnitude between 10% and 90% of the nominal voltage, normally lasting from 0.5 to 60 cycles [18]. The lost voltage and retained voltage are considered in evaluating the voltage dips. The lost voltage is the difference between the pre-fault voltage magnitude and that during the dip, while retained voltage is the percentage of the nominal r.m.s voltage remaining at the lowest point of the dip. The seriousness of the voltage sag on power systems is determined by observing the magnitude and duration of the sag. There are numerous causes of voltage sags in the power systems and the European standard EN50160 [19], states that voltage dips depth of 10% to 15% may occur as a result of switching of loads whereas large voltage sags may occur as a result of faults in the system. Mohod et al. [18] described other causes of voltage sags to be startup of wind turbines, faults on the electrical network and consumer installations, switching of heavy loads and startup of large motors. It is therefore crucial for electrical network's components to be able to operate efficiently even when the afore-mentioned activities occur at any point of the network to ensure satisfactory performance of the system.

The system's voltage and power are directly related, thus the occurrence of voltage dips in the power system will affect the PQ the electrical system. According to Mohod et al. [18], consequences of voltage sags include malfunctioning of electrical equipment such as microprocessor based control systems, adjustable speed drives and programmable logic controller. Therefore voltage sags may force important processes to a halt while causing loss of efficiency in electrical machines as well as delays in contractors or relay drippings for voltage sensitive loads.

2.2.6 *Harmonics*

Currently, the use of power electronic converters in electrical networks has increased as they play a vital role in DG deployment and integration to the electrical grid. Power electronic converters used to interface DG units to the grid, particularly wind and solar PV-based DGs may introduce a lot of harmonics in to the power system. Harmonics are the alternating quantities with frequencies other than the fundamental present in current and voltage signals. This causes the current or voltage waveforms to assume a non-sinusoidal shape corresponding to the sum of different sine-waves having frequencies that are multiples of the power-system's fundamental frequency (50Hz for South Africa), consequently affecting the system's PQ [20].

Power electronic converters used to interface DGs to utility grid are not the only sources of harmonics. Other factors contributing to this include the excessive use of semiconductor based switching devices and inverters [20]. The nonlinearity of loads may also contribute to harmonic emissions in the power system. It is therefore vital to consider the level of harmonic emission by various components in order to develop control systems capable of reducing the network harmonic content.

Harmonics are classified based on their fundamental frequency and are categorized as integer harmonics, inter harmonics and sub harmonics. The respective harmonics classes had been defined in [15] based on the relationship of their respective frequencies with the power system's frequency. Harmonics having integer multiples of the fundamental frequency are described as integer harmonics while inter and sub harmonics have frequencies greater or smaller than that of the fundamental frequency [15]. Harmonics are undesirable in power systems as they have adverse impacts on generation, transmission, distribution as well as on consumer's loads. The acceptable limits of the maximum harmonic distortion are set out by regulating bodies for different parts of the power system. According to IEEE standard 1250, the acceptable maximum total harmonic distortion is 5% at 2.3kV - 69kV, 2.5 % at 69kV – 138kV and 1.5% at voltage levels higher than 138kV [20].

2.2.7 *Frequency variations*

Variations in the system's frequency can also have negative impacts on the system's PQ. Frequency variations are fairly rare in stable utility systems but certain application such as voltage source converters in the power systems can cause frequency deviations due to the level of their harmonics emissions [14]. Frequency variation is also common in systems with poor power infrastructure and can be worse when the generator is heavily loaded [17]. Generally, when integrating DGs to the grid, the main control is focused on maintaining the voltage at the PCC within the permissible limits while the frequency at PCC is expected to adapt to that of the power system.

Several grid codes and standards provide permissible frequency ranges for desirable power systems. The IEEE standard 1547 states that electrical frequency in distribution systems must only vary between 59.3 Hz and 60.5 Hz [21]. The South African grid connection code for DG on the other hand requires the operating frequency range of 49Hz to 51Hz for all categories of DGs [22]. It should however be noted that the nominal system's frequency of the South African grid is 50Hz, thus the probable reason why it differs from that specified in IEEE standard. Frequency variation problem can be corrected by assessing all power sources causing frequency variation and repairing or replacing them, if necessary [17].

2.3 Planning of grid integration of DG for PQ enhancement

The current power grid consists of large power plants normally located close to their primary energy source which is usually far away from customers [11]. Electrical power is therefore delivered at high voltage (HV) to customers using long distance transmission lines to minimize power losses. The distribution system delivers power at medium voltage (MV) and low voltage (LV) and are operated radially with power flowing from higher voltage levels down to the end users located at lower voltage levels. Power is also said to flow from upstream (generation) to downstream (load) side of the network.

Integration of DGs at MV and LV networks is currently a trend followed in power systems to meet the rising energy demands. The emerging new technologies allow for multiple DG integration at different points of electricity networks [23]. However, integration of very large capacities of intermittent DGs such as wind and solar PV in sub-transmission and distribution systems may deteriorate the network's PQ. Optimal planning of DG integration into distribution networks is therefore a crucial aspect in ensuring improved PQ and security of supply in power systems. The challenge in DG planning is finding the optimal location and capacity of DG with respect to network

configuration and load distribution such that an economic and technically sound power system operation is maintained [24].

2.3.1 *Key Challenges for Current Sub-transmission and Distribution Networks*

A) Grid reinforcement

The current sub-transmission and distribution networks present complexities when DGs are integrated. The main reason is that they were initially designed to distribute power from generating stations via the transmission system to end users at distribution level without considering potential future connection of DG technologies at more downstream locations. In order to integrate DGs effectively to the grid, the current electricity networks will need to be reinforced such that new DG connections and the ever increasing network loads are accommodated. For long term power security, the sub-transmission and distribution networks should be adjusted such that they operate optimally under possible combinations of generation and loading conditions [24].

The power system should therefore have the capability of handling the potential future growth of decentralized generation and network loads in grid reinforcement and planning stages. This challenge can be effectively addressed by considering several approaches that will facilitate the improvement of PQ and reliable operation of the sub-transmission and distribution networks with DG integration. The potential solutions for proper planning of DG integration differ in their effectiveness and economic implications. The possible types of network optimization techniques may be as listed below [25] [11]:

- Design and extension of new transmission lines and substations depending on the capacity of DG and PCC [26]
- Design of the whole network with the assumption that there is no real existing network.
- Utilizing intelligent planning techniques both for the design of new network and expansion of the current network.

B) Operation of the Sub-transmission and Distribution Networks

The sub-transmission and distribution networks are integral parts of the grid and must effectively ensure that electrical power delivered to customers is of satisfying quality. As stated earlier, electrical power flow in these networks flows is unidirectional and depends on voltage levels between two points. The increased penetration of DG's, particularly wind and PV which are intermittent in nature may result in variations in their output power and hence affect the grid's PQ. They also pose a challenge for system's power balancing and network operation [26]. The power flow direction in distribution networks is likely to as a result of rising voltage profile at the PCC.

Utilities have experienced instances of over voltage at PCC of DG units and have thus set mandatory limits on the maximum size of integrated DG units to ensure that technical limits of the network are maintained [27]. The network bus bars which are more vulnerable to over voltages are those situated at low local load conditions such as those in remote rural areas [11]. In this case, DG generation is more likely to exceed local demand and this could cause power to flow from distribution to transmission networks, resulting in reverse power flow [26]. Grid-connected DG units do not necessarily regulate the voltage at the customer connection points, specifically at low voltage levels due to absence of active voltage control schemes at these points. The voltage rise problem increases in proportion to the degree at which local generation exceeds local demand and can pose adverse impacts to the distribution systems if not regulated.

In systems with high DG penetration, the power flow is likely to exceed the maximum capacity of the sub-transmission and distribution systems. The system becomes congested when the physical capacity limits such as the current carrying capacity of the lines are exceeded due to excessive DG feed-in [26]. The physical capacity limits of the system are exceeded when the difference of the generated power and load power is greater than the system's maximum rated power. Similarly, in cases where the system experiences excessive demand, congestion may also occur if generated power is insufficient to meet the demand [26]. Equations (2-1) and (2-2) below define clearly the conditions that cause occurrence of congestions in distribution systems:

$$P_G - P_L > P_{Max} \quad (2\text{-}1)$$

$$P_L - P_G > P_{Max} \quad (2\text{-}2)$$

where P_G and P_L represent generated and load power respectively and P_{Max} is the maximum rated power of the distribution network.

From the above equations, it can be seen that congestion conditions in distribution systems may require distribution network operators to reduce or increase DG production depending on the cause, to ensure reliable and secure operation. This may cause unnecessary interruptions which will consequently affect the reliability of supply. It is therefore important that DSO consider and cater for congestion problems in design of distribution networks by utilizing technologies essential for mitigating congestion problems.

C) Traditional Design of Sub-transmission and Distribution networks

The design of traditional sub-transmission and distribution networks is mainly based on unidirectional power flows towards connected customers. The topological design of the grid has not changed much to allow effective DG integration, especially in distribution networks [8]. The main challenge is that conventional grids are designed on a top-down basis and do not require excessive use of monitoring tools since power flows are predictable [26]. However the continuing demand as well as economic advantages offered by DG technologies has urged utilities to integrate DG units at distribution networks. This will change the traditional topology of the power systems to cater for generation at distribution grids.

2.3.2 *Grid planning including DG*

The growing connection of DG technologies in electricity networks, particularly at distribution level will require a properly planned grid. Despite the promising merits of DG integration, their installation into electrical power grid is not a simple plug-and-play problem [28]. The quality of power in distribution grid is of primary concern in grid planning with DG since most network loading is connected to the distribution network. Apart from the issue of PQ, careful consideration should be made towards reliability, protection coordination, stability and power losses in planning the grid with DG penetration [28]. The main objectives of optimal DG planning for effective power system performance as discussed in [29] are summarized below:

i) Enabling integration of large DG capacities
ii) Reduction of line losses as well as overall system's losses
iii) Maximization of voltage limit loadability
iv) Reduction of variations in voltage profile
v) Improvement of social welfare by provision of affordable clean energy, better community services and creation of employment and business opportunities

However, the major focus is to determine whether poor planning of DG integration affects PQ negatively. In order to achieve a better quality of power as well as the afore-mentioned objectives, several factors have to be taken into consideration in DG planning scenarios. The effect of DG units on PQ is strongly dependent on the type of DG unit and connection point on the network, i.e. the PCC [3]. DG units can be integrated directly to the network or indirectly through converters depending on the type of DG technology under consideration. In both scenarios, the network's PQ and power flow are affected [3]. Choice of PCC is fundamental since the impacts of DG integration on the system's PQ differ according to their placement with respect to conventional utility generators.

A. Impact of DG location on power quality

The PCC plays a vital role in determination of the system's PQ. DG units are connected at sub-transmission or distribution networks depending on their size and resource availability at a particular site. However, the most crucial aspect of proper allocation of DG units is to ensure compliance with the grid codes. Certain requirements need to be met at the point of common coupling to ensure efficient performance and operation of the power system. For instance, the IEEE 1547 – *Standard for Interconnecting Distributed Resources with Electric Power Systems*, sets out the technical specifications and requirements to be met at the PCC [21].

The location and PCC in the electricity network are also dependent on the network voltage level. Connecting DG units at the distribution level of the network may result in significant voltage fluctuation problems such as under- or over voltages at the PCC [30]. The major cause of these problems is electrical parameters of wind generators or PV systems and the technologies employed in their integration to the grid. The IEEE 1547 standard requires DG units to be in parallel with the grid without causing voltage variations greater than ±5% of the nominal PCC voltage magnitude [21]. It is therefore imperative that grid planning including DG technologies considers the acceptable voltage limits in grid integration stages for enhanced power system performance.

Placement of DG units has been found to be the fundamental aspect of DG planning since it impacts critically the operation of the sub-transmission and distribution networks. Unplanned location of DGs has been found to have negative effects on the system's PQ as well as efficiency [29]. On the other hand, optimal DG placement can significantly improve network's voltage profiles and overall power loss reduction; the attributes which ensure improved PQ and supply reliability [11] [29].

Several optimization methods and algorithms for optimal placement of DG technologies have thus been developed. These algorithms consider factors such as type and size of DG technology, network configuration and load distribution in determination of optimal locations and sizes of DG units [24]. One such algorithm is Genetic Algorithm (GA) which is used to determine the optimal DG size and location in a radial distribution system by minimizing real power losses, Total Harmonic Distortions (THDs) and voltage sag [24]. It is therefore crucial for DG integration planners to carry out some optimization algorithms in determining the optimal location of a DG for enhanced system's operation.

B. Impact of DG sizing on power quality

The size or capacity of DG units can be defined in terms of their power output or number integrated units. Penetration level is a term used to describe total capacity of DG units connected to the network. DG penetration level is obtained by the total power that DG units inject to the grid with respect to

active power provided by centralized utility generation [11]. DG penetration level also dependents on the loading of the feeder. The Equations (2-3) and (2-4) are used to express the percentage of DG penetration level in the power systems and are as given below [31]:

$$\%DG_{Penetration\_level} = \frac{P_{DG}}{P_{DG} - P_{CG}} \times 100 \quad (2\text{-}3)$$

$$\%DG_{Penetration\_level} = \frac{P_{DG}}{P_{L.max}} \times 100 \quad (2\text{-}4)$$

where P_{DG} and P_{CG} represent the amount of total active power generated by DG and centralized generation respectively and $P_{L.max}$ is the maximum load of the feeder.

Electrical networks should be strong enough to accommodate large penetration of DG units. Developed countries such as Denmark have strong interconnected grids that allow integration of large capacity of DG units [32] . South Africa on the other hand has long and weak networks that limit DG penetration levels [33]. However, South Africa plans to integrate higher DG capacities to the sub-transmission and distribution networks at voltage levels of 11kV, 22kV and 220 kV [33]. It has been observed that when penetration level of DG is low, the impacts of DG on PQ at the transmission and distribution networks are the least [31]. The increasing DG penetration will however impact not only the sub-transmission and distribution networks but the whole system.

The increasing integration of DGs requires new techniques for improved network operation for optimal operation of the power system. South Africa in particular, plans to increase electricity generated by DG technologies to 20GW by 2030 [33]. Grid connection codes for renewable power plants (RPPs) connected to the electricity transmission or distribution systems in South Africa have thus been developed to achieve this target. The detailed discussion of the South African grid connection code will be found in preceding sections.

DG penetration level in electricity networks should be able to comply with the technical constraints while serving the local loads with substantial power. Several approaches essential for allowing higher penetration level of DG in electricity networks have been developed. These include employing energy storage systems in grid connected DGs so that any excess power that cannot be consumed locally can be stored. Power electronics essential for offering voltage or frequency control at the PCC can also play a significant role in allowing increased DG penetration level. Also, several power flow optimization algorithms that are essential in finding the optimal size of DG at each load bus have been developed.

2.3.3 *DG integration into weak power grids*

The availability of renewable energy sources such as wind and solar is influenced by numerous factors such as geographic location. Resources are usually available in abundance in remote areas which are far from the power consumption centers. DG units will therefore need to be connected at sub-stations, close to their physical locations, which is likely to be the transmission or sub-transmission grid part characterized by long transmission lines. At these parts of the network, the grid is usually weak and may not be able to accommodate high penetration levels of DGs without violating grid codes. The strength of the grid is determined by its impedance and mechanical inertia [34]. The grid strength can therefore be calculated by using the grid stiffness index such as the Short-Circuit Ratio (SCR) which takes into account the generation connected at the PCC as defined by Equation (2-5) below.

$$SCR = \frac{S_C}{S_N} \tag{2-5}$$

where,

S_N represents the total capacity of the generation power plant.

S_C represents the short-circuit capacity of the grid at the PCC.

The application of the SCR to determine the strength of an electrical grid is an acceptable method to decide whether the grid is strong or weak. If the SCR is lower 10, the grid is considered weak and may pose adverse impact upon integration of DG [35]. The SCR values higher than 10 therefore indicate that the grid is strong and can accommodate high penetration level of renewable or non-renewable DGs without violating the grid code requirements. On the other hand, the reactance to resistance ratio is also an indicator of the grid strength and the grid is considered weak if this ratio is less than 0.5. The weak DG-integrated networks can be classified according to the following types [36]:

- Low SCR as a result of connecting DGs to low impedance grid through long lines
- Low SCR as a result of high grid impedance
- The internal fault in the grid caused by an increase of grid impedance and transient SCR drop

The strength of an electrical grid is one of the important factors to be considered when planning grid integration of DGs into utility grids. This is because the voltage levels are generally not constant in in weak grids and connection of DG may further deteriorate the system's PQ. DGs can however be beneficial to weak grids if proper planning of their integration is executed since they can be used to maintain the voltage at the nominal value by injecting reactive power at the PCC.

2.3.4 *Grid codes assessment for renewable energy power plants in South Africa*

The South African renewable energy grid code [22] has been developed to allow renewable energy power producers to effectively plan the connection of DG units to the Transmission System (TS) or Distribution system (DS). The primary objective of this code is to present a set of minimum technical and grid-connection requirements that should be met by DGs already connected to or seeking connection to the South African network. The code applies to a number of different RPP technologies including solar PV and wind energy systems which are the main focus of this work. Irrespective of the type of DG technology, the grid code compliance is applicable to all RPP [22]. The term DG will be used interchangeably with RPPs as they are considered to have the same meaning in the context of this work.

DG systems are classified into three main categories based on their rated power and the voltage level at which they are connected. These categories are classified as categories A, B and C, with category A further divided into 3 sub-categories A1, A2 and A3. Category A includes DGs with rated power in the range of 0 to 1 MVA connected to low voltage (LV) part of the network; Category B includes DGs with the rated power in the range equal to 1MVA but less than 20MVA connected to the medium voltage (MV) part of the network; category C includes any DG unit integrated at the MV or high voltage (HV) network part and having the power rating equal to or greater than 20MVA. Each category has its own set of requirements in terms of operating voltage ranges, low voltage ride through and operating power factor range. The operating frequency and the power ranges are however the same for all categories. The summary of the requirements for grid connection is presented in Table 2-2:

Table 2-2: The summary of grid code requirements for each DG category **[22]**

Category	**A1**	**A2**	**A3**	**B**	**C**
Output power [KVA]	0 – 13.8	13.8 - 100	100 - 1000	>1000 - 20000	>20000
Voltage level	LV			MV	MV/HV
Operating frequency	49 – 51Hz				
Operating voltage range	-15 to +10%			±5%	
Operating power range	20 – 100%				
Low voltage ride through	60% for 0.15s			0% for 0.15s	
High voltage ride through	NA			120% for 2 s	

Power factor operating range (leading and lagging)	0.95	0.975	0.95

The technical operating requirements for grid connected DGs are presented for normal and abnormal operating conditions of the network. Although the requirements may differ according to the location of the DG unit, the grid code requires that DGs withstand frequency and voltage fluctuations at the PCC under normal and abnormal operating conditions [22]. The actual operating voltage differs based on location of DGs and is decided by national energy utility ESKOM in proper consultation with concerned customers. The fundamental requirements that must be met in grid integration of DGs include voltage and frequency deviation limits which are essential in maintaining the system's PQ.

A. Normal operating conditions

The South African grid connection code requires that DGs of all categories be designed such that they continuously operate within the voltage ranges specified in Table 2-1, taking into account the available voltage level at PCC. The minimum and maximum operating voltages at PCC become stricter for DG units connected at high voltage levels. The minimum operating voltage that can be reached at the PCC should be 0.9 p.u for DGs integrated on 11kV up to 132kV networks. The connection code however restrict the maximum operating voltage at 1.08 p.u. for DGs integrated at 11kV and 1.0985 p.u. for DGs integrated at 132kV networks [22].

Grid integrated DGs should also be designed such that they are capable of operating within the frequency ranges specified in the grid connection code. The decision of connecting or disconnecting the DGs to the grid is subject to the duration of system's frequency variation from the nominal. Although frequency disturbance may force DGs to be disconnected, category A units can reconnect after 60 seconds and category B and C after 3 seconds, provided that the frequency has returned to acceptable limits. Figure 2-2 presents the frequency ranges at which DG units should operate in and the time that has to elapse to remain integrated at particular frequencies.

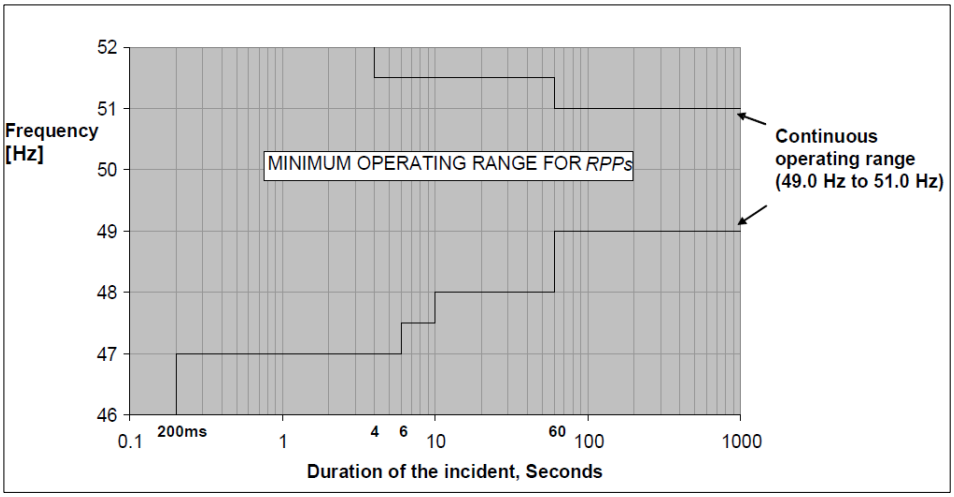

Figure 2-2: The acceptable frequency ranges of DG units during a frequency disturbance **[22]**

B. Abnormal operating conditions

The South African grid code also provides requirements for the design and operation of DGs during voltage and frequency disturbances. The DGs may need to be disconnected from the grid during a system disturbance at the PCC. DGs are however required to resume normal operation no later than 5 seconds after network conditions return to normal. The voltage ride through conditions that the three DG categories are required to withstand are presented in Figure 2-3 and Figure 2-4 below.

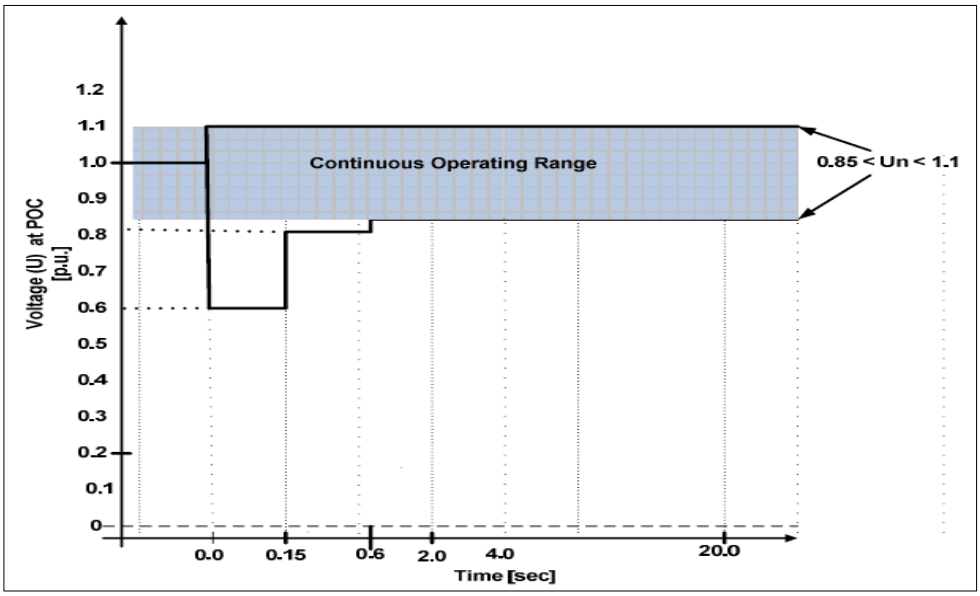

Figure 2-3: Voltage-ride-through capability of DGs in category A1 and A2 **[22]**

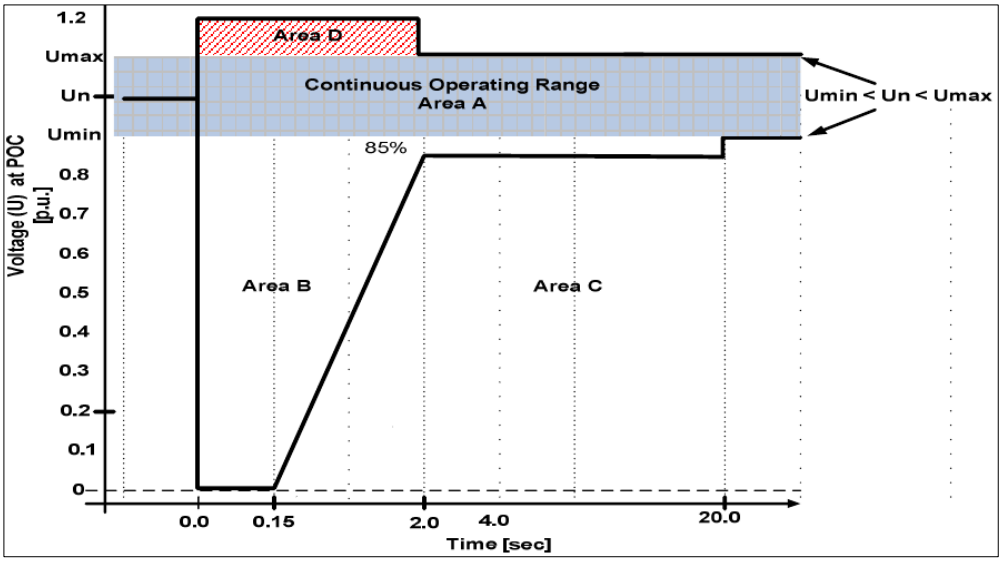

Figure 2-4: Voltage-ride-through capabilities for the DG technologies of category A3, B and C **[22]**

DG units integrated to the grid should be designed such that they are capable of withstanding voltage drops and peaks at the PCC for a certain period of time before disconnecting as depicted in Figures 2-3 and 2-4. Categories A1 and A2 have to continue normal operation under minor grid disturbances since they have minimum impact on voltage support and grid stability. Categories A3, B and C on the other hand have stricter requirements in terms of the duration of the voltage drop and the minimum time for which DG should remain connected to the network. The voltage ride through requirements for the latter three categories is sub-divided into operating areas, A-D which determine whether the DG remains connected to or is to be disconnected from the grid.

In Area A, the DG is required to remain connected and continue normal generation of power. Area B shows the drop in voltage for a short duration of time and the grid code requires the DG to offer maximum voltage support by injecting reactive current to stabilize the voltage as shown in Figure 2-4. Conversely, DGs are required to remain connected in Area D and provide voltage support by absorbing reactive current. Disconnection only happens when DGs in category A3, B and C operate in Area C as shown in Figure 2-4. However, reconnection is required once the operating conditions revert back to normal, with category A reconnecting after 60 seconds and category B and C reconnecting after 3 seconds following a voltage disturbance. From Figures 2-3 and 2-4, it can be observed that DGs are required to continue operation even when the range of normal network operating conditions are exceeded for a particular time.

The reactive power support requirements during voltage variations at the PCC are also presented in terms of the operating areas as depicted in Figure 2-5. The control of voltage is required to comply with that shown in Figure 2-5 such that reactive currents follow the control characteristics at corresponding time. During the voltage drop depicted in Area B, the supply of reactive power is given

the first priority, while that of active power has the second priority. The system's active power is however expected to be maintained during voltage drops and is only allowed when the voltage drops below 85% of the nominal voltage value. Each DG category is further required to restore active power generation to at least 90% of the initial production within 1 second of fault clearance.

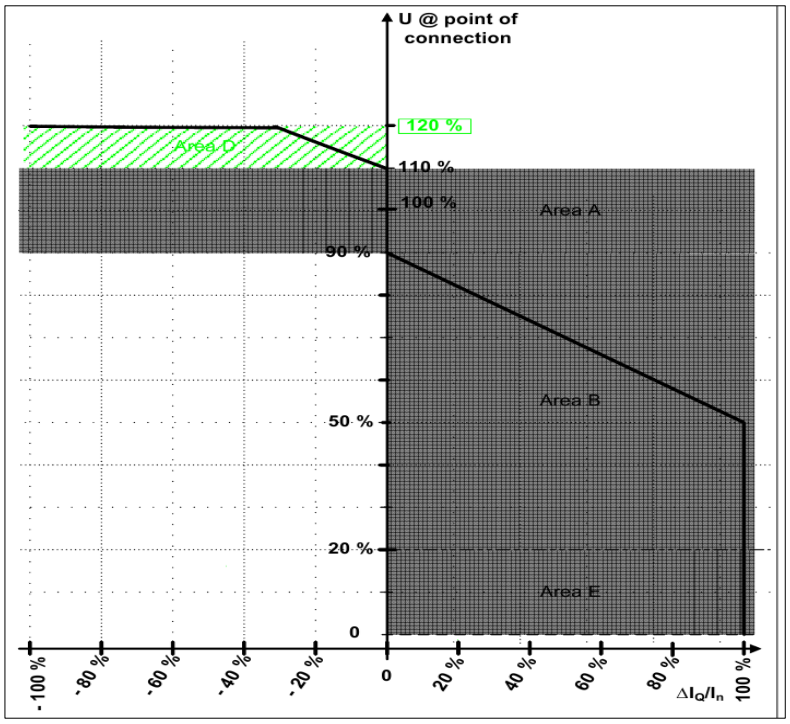

Figure 2-5: The requirements for reactive power support during voltage drops or peaks at the PCC **[22]**

The three categories of DGs are strictly expected to adhere to a particular operating power factor which is category dependent. DGs must therefore be designed such that they are able to vary reactive power support at the PCC within the ranges defined in Figure 2-6 below. The default power factor at which DG should be operated is unity power factor and would only differ if the system operator specifies otherwise. In order to operate at the power factors defined in Figure 2-6, DGs must have reactive power control functions that are capable of controlling the reactive power at the PCC.

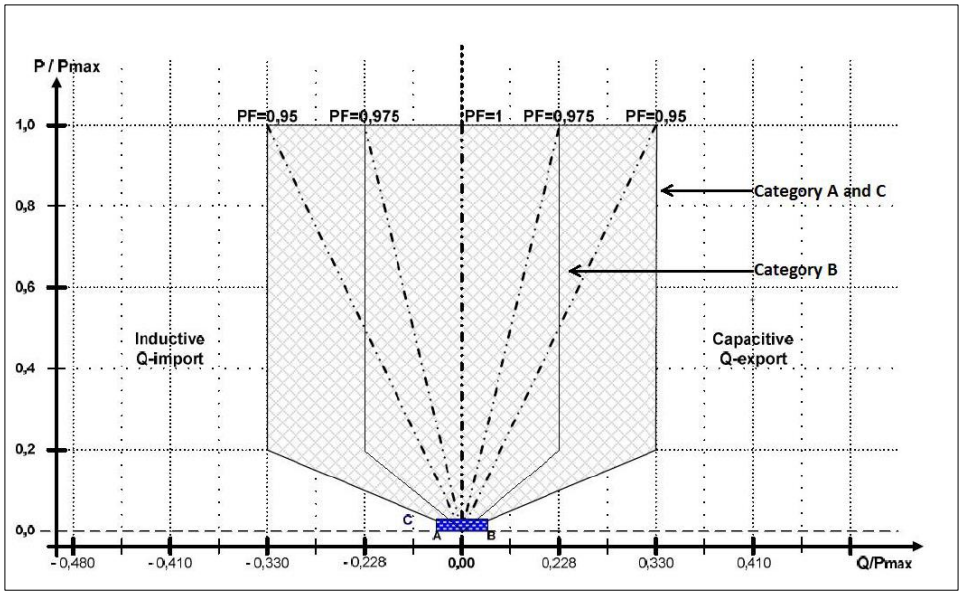

Figure 2-6: The requirements for reactive power for DGs of categories A and C (power factor of 0.95) and category B (power factor of 0.975) **[22]**

In addition to reactive power control, DGs should also be equipped with voltage control functions which must be agreed upon by the network service provider (NSP) and the system operator (SO). The accuracy of the voltage set point at the PCC is expected to be within ±0.5% of the nominal voltage while the accuracy of performed control should not vary by more ±2% of the required reactive power. The voltage control characteristics for DGs are presented in Figure 2-7 below. The voltage change (p.u) which is a result of a change in reactive power (p.u.) is configured as droop in Figure 2-7 below.

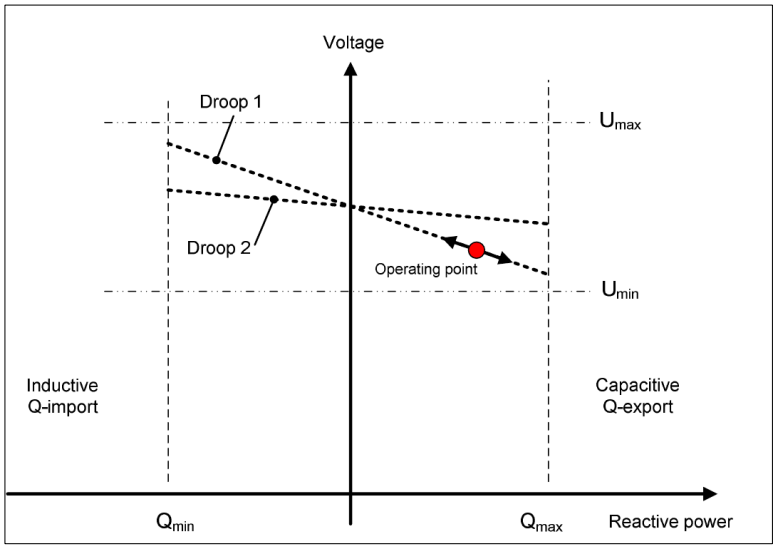

Figure 2-7: Voltage control requirements for grid integrated DGs **[22]**

2.4 Utilization of DGs for PQ Enhancement

DG technologies, particularly wind and solar PV can effectively be utilized to improve PQ in electricity networks. A number of approaches must however be employed in their integration and operation to ensure improved system's PQ. This calls for a need to strictly design grid integrated DGs

systems such that enhancement of PQ at the PCC becomes a priority. While the generation of sustainable power into the grid should be the primary objective of DG deployment, they should have the ability to mitigate the negative effects they pose on the network [11]. The primary parameters of concern in power systems with DG integration include voltage and frequency deviating from permissible limits.

Various PQ enhancement techniques have been developed and tested in grid-integrated DGs, particularly in networks with wind and solar PV integration. Wind and solar based DGs are preferred over most DG technologies and currently the paramount choice for distribution grid operators. The higher availability of their resources and the present strict environmental regulations has drawn attention to deployment of wind and solar PV based DGs. [37]. Voltage fluctuations at the PCC is however one of their drawbacks as it has negative impacts on system's PQ. Over voltage (OV) instances have been recorded at the PCC during low local load conditions and various OV prevention methods have been developed [27].

Different methods of OV prevention employs different techniques to ensure that the PCC voltage is maintained within acceptable limits. One such technique is reactive power control during conditions of OV such that voltage is maintained within acceptable levels [11] [27]. Reactive power control (RPC) also allows increased DG penetration level since generators with RPC can supply or absorb reactive power depending on voltage conditions at the PCC [33]. Another method of improving the system's PQ is to incorporate energy storage systems in DG integration [27]. There are several other methods which had been proposed for PQ improvement in grid-connected DG and will be discussed in the next sections.

2.4.1 *Incorporating energy storage systems*

Using energy storage devices in grid-connected DGs has been found to be an effective method to mitigate voltage deviations in distribution networks. Energy storage systems (ESSs) are more helpful in applications when the grid is unable to accommodate electrical power generated from RES at the PCC [38]. As mentioned earlier, during low local load conditions, the electrical power generated by DG may result in over-voltages at PCC and consequently cause reverse power flows. However if each DG unit is coupled with energy storage devices, any surplus power produced by DG resources can be stored, thus reducing the risk of OV caused by injecting more power than is locally absorbed. [27]. Dependency of RE resources on weather conditions makes them to non-dispatchable, thus if their energy is not stored, it must be consumed as soon as it is generated [38]. ESSs have been found to have the ability to absorb the variability of RE sources, thus allowing RE power to be dispatched [38].

Most importantly, ESSs can be used in every section of renewable power systems including in wind and PV resources integrated in electricity networks. Utilization of ESS technologies is improtant since storage devices can always be charged during periods of maximum generation and low demands conditions. When the ESS is fully charged and DG generation is still at peak, DG should be able to disconnect to allow ESS to discharge. The energy can then be used later to support the voltage by supplying the local load during periods of peak demands [39]. Some of the fundamental imperatives of utilizing ESSs in grid connected DGs include meeting demand and reliability during the grid's peak hours, energy arbitrage, balance and reserve, as well as frequency regulation at the transmission level [38] [40]. Furthermore, EESs can also be employed for voltage control as well as for grid capacity support at distribution level [38]. A number of ESS technologies have been developed and their effective incorporation in DG integration to the grid will be beneficial in future during widespread deployment of DG technologies.

A wide number of energy storage mediums with the ability to mitigate PQ problems in grid-connected DG have been deployed in most renewable energy projects. These include battery storage, compressed air energy storage (CAES), capacitor storage (SC) or super capacitor energy storage (SCES), flywheel energy storage (FES), pumped hydro storage (PHS), superconducting magnetic energy storage (SMES) and thermal energy storage (TES) [38]. Some of these storage technologies are matured and have gained commercial acceptance whereas some are still at an early stage of development or conceptualization. Battery storage is more popular in solar PV based DGs, but it can still be effective when utilized in other forms of DG applications such WECS. The main components that make up a storage system are storage mediums as mentioned above, charging and discharging schemes and control that governs the entire ESS [38]. The ongoing research for utilizing electric vehicles as the form of energy storage will also contribute to efficient energy storage in the future.

2.4.2 *Using Power electronics devices to enhance PQ of the power system*

The power electronic converters used to interface DG sources to the grid can also play a significant role in enhancing the system's PQ. Some grid-connected power converters have additional functionalities, such as control reactive power, harmonics minimization, unbalanced power correction, thus contributing to improvement of the network's PQ [41]. The Multi-Functional Distributed Generation Unit (MFDGU) is one of the power electronics devices with the ability to improve PQ performance of DGs which also upgrading DGs themselves [41]. It consists of a combination of power electronic components such as filters and intelligent control schemes essential to mitigating PQ

issues at the PCC. The schematic showing an MFDGU topology used to enhance the PQ on a three phase, 4 wire LV distribution network is presented in Figure 2-8 below.

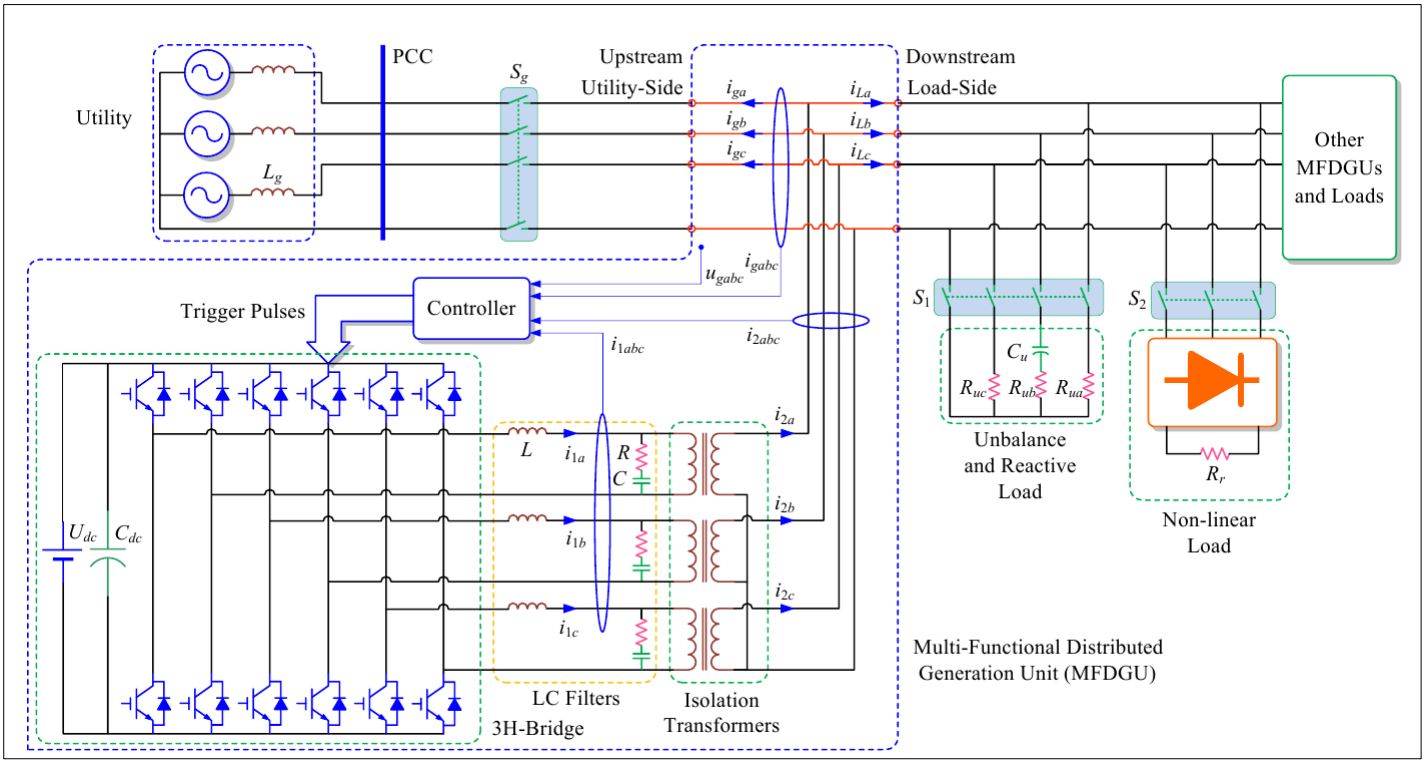

Figure 2-8: The configuration of the MFDGU topology used to enhance the PQ of grid integrated DG **[41]**

Another control strategy with the ability to enhance voltage quality in grid integrated DG uses versatile power electronic interface as well as intelligently controlled ESSs [42]. This technology allows multiple connection of DG systems together with ESSs and is considered to be the future application of grid-interfacing converters. A basic structure showing multiple DG systems with energy storage and local loads interconnected to form a micro grid is presented in Figure 2-9. Grid integration of DGs employing the technology depicted in Figure 2-9 have been proved to be suitable for PQ improvement and enable efficient power transfer in power systems [42]. When required, DG systems will be disconnected from and re-connected back to the grid when conditions at the PCC have reverted to normal conditions. Islanding is made possible by a series of coordinated control strategies and communication system employed in the design of the system below.

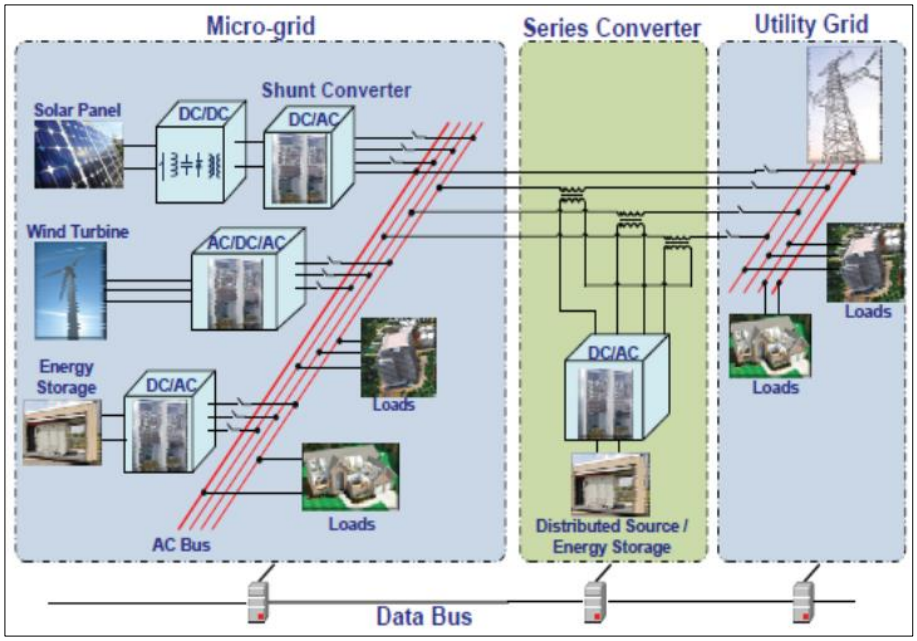

Figure 2-9: An example of a future application of grid-integrating converters for integrating multiple DG systems with improved PQ **[42]**

2.4.3 *Using DGs to enhance PQ*

In addition to supplying electrical power to the grid, a strategic operation of a multiple DGs such as wind and solar PV can also contribute to PQ enhancement while supplying electrical power to the grid. DGs make a deliberate attempt through their capabilities such low voltage ride through (LVRT) to regulate the voltage on the power system while continuing real power generation [17]. Voltage level at the PCC increases as the real power output of the DG increases and this causes DG to respond by trying to maintain the voltage at the constant magnitude. Voltage regulation at the PCC can be achieved by adjusting the reactive power output of the DG. The reactive power can either be increased or absorbed to increase or lower the voltage to offset any increase or decrease due to the real power component [43].

Voltage regulation by DG is however preferred in stand-alone DG applications where DG supplies electrical power to the entire load [17]. In grid-connected DG applications, voltage regulation is achieved by intelligently interacting DG units with the utility system's voltage regulation equipment. A number of factors such as the capacity and location of the DG and impedance characteristics of the line should be considered in analysis of the impact of DG units on improving the distribution system's voltage [17]. DG technologies can however be effectively used in enhancing the PQ in terms of the PCC voltage profile improvement and power loss reduction in both grid connected and islanding mode of operation.

PQ improvement techniques using some of DG features have been found to be effective and economical. For instance, power smoothing in WECS can be achieved by controlling the kinetic energy of the turbine's inertia to generate a smooth output power [44]. Power smoothing can also be achieved by pitch angle control system in WECS which is the most common method for smoothing power fluctuations during below rated wind incidents [44]. This method uses a fuzzy logic pitch angle control to generate a smooth output power for all the operating regions of the wind turbine. Controlling the DC-link voltage of the DC-link capacitor can also make a significant contribution to smoothing the output power in grid integrated WECS [45].

2.5 Impacts of Wind and Solar PV on PQ Enhancement

Wind and PV based DGs have grown significantly over the past years due to higher availability of their resources. Their integration to power systems can however pose adverse impacts to the grid thus deteriorating the PQ of the system. Appropriate mix of wind and PV based DGs can however increase the efficiency and reliability of the system by mitigating the problems resulting from their intermittent nature [37]. In order to determine how wind and solar-based DGs differ in their capacity to improve the PQ, it is important to understand the contribution of each individual technology on PQ problems and the degree at which they can contribute to system's PQ enhancement.

Wind energy is harvested using blades which then drive the electrical generator to covert the kinetic energy of the flowing air masses to useful electrical energy. The three competing technologies used for connecting WECS to the power system are the directly connected induction generator, the doubly-fed induction generator (DFIG) and the permanent magnet synchronous generator (PMSG) [46]. However wind power has intermittent character whereby the wind speed and thus the generated power vary randomly with time. An erratic nature of generated power is one of the major causes of PQ problems in power systems with wind energy integration [18] [32]. WECS can however be utilized effectively to enhance the PQ in power systems as will be discussed in the sections to follow.

Solar energy on the other hand is converted to useful electrical energy by using semiconductor cells that produce photo current when exposed to the sun. The current output of the cell varies with the amount of radiation that reaches the panel with higher irradiation levels resulting in higher currents [46]. The output power of the solar PV is therefore highly dependent on the level of solar irradiation thus making the energy harvest from the sun variable with seasons. Also, an inverter used to convert the DC output current of PV to AC current can also contribute to harmonic emissions in the power system. Variations in solar irradiation has been found to be the cause of power fluctuations and voltage flicker thus resulting in PQ problems in high penetrated PV systems in the power system [47].

2.5.1 *Impacts on power system voltage profiles*

Electricity supply from WECS is subject to the risk of voltage profile disturbances at the PCC due to the operation of the WECS. The negative voltage profile problems resulting from grid-integration of WECS include fluctuations in voltage profile, voltage rises at the PCC as well as voltage dips. Fluctuations in the system voltage profile negatively affect the voltage sensitive loads connected to the network. This is because voltage fluctuations causes flicker, which can further be classified into flicker emissions during continuous operation and flicker emissions due to wind generator and capacitor switching [18]. Voltage variation is the main problem associated with wind power at the local level and is the result of variations in generated power [48].

The impact on the system's voltage profile, of connecting wind turbines to the grid also has a direct relationship to the short circuit level of the power system which also indicates the strength of the electrical system [48]. The voltage profile at the PCC is related to the short circuit impedance and the apparent power of the wind power generation unit by Equation (2-6) [49]. From the equation, it can be observed that if the impedance is small, voltage variations will also be minimum, indicating a stronger grid. Larger impedance on the other hand results in larger voltage variations and shows that the grid is weak.

$$\Delta U = S_{max}(Rcos\emptyset - Xsin\emptyset)/U^2 \quad (2\text{-}6)$$

where ΔU represents the voltage change at PCC in volts, S_{max} is the maximum apparent power in MVA, $\emptyset$ is the phase difference in degrees and U is the nominal voltage of the grid in p.u. If the voltage change exceeds that specified in the grid codes, the effect may be severe on the power systems and call for the WECS to be disconnected from the grid. Since most South African networks consist of weak grids, an assessment of PQ improvement by installation of DG is essential.

The start-up of wind turbines can also cause a sudden reduction in voltage magnitude at the PCC, resulting in voltage dips. Voltage dips can occur as a result of faults on the main grid where the dip magnitude at the PCC is dependent on the fault type, impedance and distance from the wind turbine' PCC [50]. Fixed speed wind generators have been proved to be more sensitive to voltage dips since they are directly connected to the main grid [32]. The voltage dips are represented as a percentage of voltage change as depicted by Equation (2-7). It was established in [49] that the accepted voltage dip limiting value must be less than or equal to 3%.

$$d = K_u S_n / S_k \quad (2\text{-}7)$$

where d is a relative voltage drop, S_n is a rated apparent power in MVA, S_k is a short circuit apparent power in MVA and K_u is a sudden voltage reduction factor.

It is established in existing literature that WECSs have the capability of making a significant contribution to the system's voltage profile improvement. Different wind energy technologies differ in their capacity to improve voltage profile. The DFIG is however the widely used WECS technology due its ability to absorb reactive power during its operation. The voltage profile at the PCC is maintained within acceptable limits by properly controlling the reactive power in the network. Since WECS power generation can be highly intermittent during unstable wind conditions, the resulting voltage variations can be controlled by using fast dynamic control of the reactive power in the distribution network [51]. Flexible AC Transmission Systems (FACTS) such as Static Var Compensator (SVC) and STATCOM are effective solutions capable of providing voltage control in distribution networks. The optimal location and number of installed SVC devices is however important in achieving effective voltage control, particularly in complex network's with larger number of dispersed sources [51].

PV systems connected to electricity networks also impact the voltage profile at the PCC. High penetration of PV systems in distribution systems affects the systems PQ by introducing voltage variations, power fluctuations and low voltage stability in the grid [52]. These challenges are brought about by the fluctuations in solar radiation due changing density of clouds and other factors such as the temperature of the solar cells [53]. Lower penetration level of PV systems however have minimum impacts on the voltage profile at the PCC compared to larger penetrations.

PVs located close to distribution system loads can play a significant role in voltage profile enhancement and power flow reduction [52]. Their combined usage with battery energy storage also contributes to the voltage profile enhancement in the distribution systems and improves the reliability of a power system supply. Nonetheless, PV systems compared to other renewable energy technologies such as wind energy and are costly. However, the expectation is that grid-connected solar PV-based DGs will continue growing and play a vital role in PQ enhancement [54].

Instances of over voltage also occur at the PCC when solar PV systems are connected to the LV networks due to reverse power flows during low load periods and high PV penetration [55]. Voltage rise problem at the PCC where PV systems are integrated can be prevented by employing various techniques. One of the approaches of avoiding voltage rise challenge without limiting the capacity of PV systems is the use of inverters with active power curtailment (APC) schemes [55]. When the AC

bus voltage is below a particular value, the APC scheme enables the inverter to inject maximum power available from the DC source and to also reduce the injected power when the bus voltage rises above this value [55]. This method of over-voltage prevention is very attractive since it only needs minor modification in the DG's inverter control logic and also for the fact that it is activated only when needed.

Variations in active power have more effects on voltage regulation as compared to reactive power variation in low voltage grids. But in terms of economic reasons, voltage profile regulation via reactive power is more preferred over active power curtailment. A proposed method of preventing voltage rise problem in grid-integrated PV systems without grid reinforcement is reactive power contribution by PV systems developed in [56]. There are different ways of controlling reactive power for the purpose of supporting the voltage profile in PV integrated grids such as using STATCOM. The methods used for reactive power control in order to improve the voltage profile at PCC should however contribute to reactive power only in instances when voltage profile at the PCC violates the grid code requirements [56] [47].

2.5.2 *Impacts on power system losses*

Power losses in power system are one of the fundamental indicators of the economic operation of the power system and hence cannot be ignored in PQ improvement analysis. Grid-integration of WECS has a direct impact on network's power losses. While the integration of WECS at optimal locations can significantly reduce the total active power losses of the system, integration at non-optimal locations can result in increased power losses [57]. Power losses in WECS can also occur as a result of operation of semiconductor devices and other connected equipment such as power transformers [58]. In the assessment of electrical losses associated with WECS, it was revealed that wind turbine topologies with MV-DC output have lower percentages of losses than those with MV AC output [58]. It was however found that the average power losses decreases with the increase in wind turbine's rated power as well as the increase in the mean wind speed in all wind turbine topologies.

Apart from the conduction and switching losses associated with operation of semiconductor devices, WECS with ESSs can also experience losses due to the internal resistor of the battery and are highly dependent on the type of battery technology used [59]. The losses associated with both the battery resistor and semiconductor devices are also strongly dependent on the voltage and current waveform, thus why the presence of harmonics in their waveforms contribute to power losses. In the analysis aimed at determining the efficiency and reliability of converters used in WECS application, the intermediate boost converter was found to offer high efficiency and reliability as compared to the

intermediate buck-boost converter, back-to-back converter and matrix converter [60]. The choice of a converter used in WECS applications is therefore important if power losses are to be minimized.

Electricity networks with PV penetration can also face the risk of power losses associated with the operation of the PV system. The power losses incurred in PV systems are associated mainly with operation of an inverter used for DC to AC conversion as well as the battery operation in applications where ESS is involved. As mentioned the internal resistance of the battery may also contribute to power losses in PV systems. PV systems also face the risk of low energy-conversion efficiency caused by their non-linear and temperature-dependent voltage and current characteristics [61]. The low electrical efficiency in PV systems can be overcome by tracking the maximum power point (MPP) using a number of online of offline algorithms such that the system's operating point is forced towards the optimal conditions of maximum power generation [47] [61].

In [37], a mixed solar-wind hybrid system was optimally placed in a distribution network using an objective function that considers active power loss reduction while taking the line capacities as constraints. An optimal combination of wind and PV based DG significantly reduce the systems losses while improving the PQ in the power system. The components of the wind solar hybrid must be strategically chosen such that not only their efficiency is optimized but also their reliability. With the application of maximum power point tracking technologies as well as optimization algorithms in design of wind and PV based DGs, an overall efficiency and performance of the power system can be improved.

2.5.3 *Impacts on power system frequency*

The output power of DGs has a direct impact on the system's frequency since in the event of frequency event, the generators need to inject or absorb kinetic energy into or from the grid to counteract the frequency deviation. As mentioned earlier, the output power of WECS varies continuously with time due to fluctuations in wind speed. Fast variation in generated power leads to voltage variations and this may consequently impact the system frequency. Frequency changes in a power system may be as a result of unbalance between generation and consumption in the whole system [46]. The presence of larger amounts of DG in the power system may cause frequency disturbances and in WECS, the smaller system inertia may cause larger frequency variations during normal system operation [46]. The loss of large generation unit can also result in larger frequency drops and consequently result in unwanted operation of the under frequency protection.

Several approaches have been employed to mitigate frequency disturbances in WECS integrated to the utility grid. For instance, the Nordic and European synchronous systems are equipped with emergency control that changes the active power setting of the HVDC link when one of the systems experiences large frequency drops [46]. In order to return the frequency to a value close to the system's nominal frequency, the generation should be higher than consumption for a while so that the kinetic energy that was initially used to limit frequency drop can be supplied back [46].

Some wind inertia methods capable of improving the power system frequency response are developed using different approaches such as time series sampling of wind speed, wind turbine de-loading, linear control, short-term over-production and tuning of tip speed ratio [62]. In DFIG based wind farms, a satisfactory frequency support can be achieved by employing dynamic reserve allocation like governors [30]. Furthermore, it was noted in [62] that a comprehensive frequency response can be achieved by considering detailed model of load frequency relief, wind active power generation and synchronous machine dynamics in frequency response analysis.

High penetration of solar PV based DG can also have an adverse impacts on the power system's frequency. As mentioned earlier, smaller system inertia can cause frequency instability problem in the power system. PV based DGs have zero inertia as opposed to conventional generators and their high penetration level could adversely affect the frequency stability of the power system [63]. In cases of low inertial to high PV penetration, the conventional generators co-existing with PV based DG will be forced to provide torque and inertia to prevent frequency instability. The effect of reduced system inertia due to high PV penetration does not only impact the system frequency stability but can also impact system's voltage stability [63].

Several investigations aimed at analysing the impact of high PV penetration on the system's frequency profile have been conducted. One of the analysis that took into account the rapid variation in power injection caused by factors such as change in irradiance, temperature and tripping out of the grid connected converter is presented in [63]. The authors found that at 20% PV penetration level, a system experienced frequency instability, thus confirming that high penetration of PV based DG has adverse impacts on frequency stability.

A number of frequency regulation methods have been proposed and implemented in electrical networks with high PV penetration. The research work proposed in [63] forces the grid integrator to inherit frequency support feature of conventional generators in PV such as inertial response, primary and secondary frequency control and active power reserves provision. Another strategy found capable

of providing frequency control in PV systems is droop based frequency control which comprise of primary frequency support and emergency frequency support [64]. Using this control method, it was found that PV can provide primary frequency support similar to that provided by the synchronous generator. In this method, the system can always switch to the emergency mode of frequency support during severe disturbance to prevent frequency overshoot.

2.5.4 *Impact on harmonics*

Power electronic converters used in modern wind turbines inject harmonics into the power system and consequently produce waveform distortions [65]. The problem of voltage and current harmonic distortion in grid-connected WECS is common in wind generators with variable speed operation since they use power electronics converters for grid interface. The converters are responsible for waveform conversion from AC to DC, and then from DC to AC and the continuous switching of converters results in waveform distortion in the system's output power. The variable speed wind turbines do not only produce harmonics but also produce inter-harmonic because of the variable switching frequency of the converters [66]. A number of standards provide the limits of harmonics injection at the PCC level and this has called for electrical systems operators to develop harmonic mitigation techniques in power systems. The harmonics injected by power electronics converters can however be smoothed by using harmonic filters.

Inverter technology used in PV systems is an important technology for reliable grid interconnection operation of PV systems. The increasing deployment of solar PV systems will require a large number of inverters to be integrated to the same feeder so that electrical power can effectively be injected in the grid. The non-linearity of voltages and currents associated with inverter applications can result in harmonic injection into the grid and can consequently cause the inverter to reject the grid [47]. The presence of harmonics in power systems can contribute to unbalanced line voltages as well as ac voltage variations, thus affecting the system's PQ [54]. The investigation on using multiple inverters in a single feeder indicated that the parallel and series resonance between the grid and inverters are responsible for high values of total harmonic distortion [67].

A method aimed at characterizing the total current harmonic distortion based on the performance of inverters operating also showed that electrical power supplied by inverters is highly dependent on the total harmonic distortions (THDs) in the system [68]. The two most important characteristics of an inverter are its efficiency and quality of electricity supply where the latter can be analysed from the current THD. This means that a significant increase in THD levels will impact the quality of electricity

supply. This will consequently present the challenge to electricity networks operators attempting to follow the regulatory standards and also for customers with sensitive equipment connected to the network [68].

The problem of voltage and current THDs in PV based DG can however be minimized by installing limited amounts of PV generation at strategically-sited points in the network. THD can also be minimized by utilizing advanced control options offered by modern power electronic converters [46]. The converters may be capable of compensating for the downstream harmonic injection and provide damping of harmonic resonances, thus limiting the voltage distortion at the resonance frequency [46]. If a wide range of possible algorithms proposed for THD mitigation is employed, a satisfying level of power system's operation with improved PQ can be achieved.

2.6 Optimal placement and sizing of DGs for PQ improvement

It has been shown through research that connecting DG at non-optimal locations in the network may deteriorate the network's PQ. The respective sizes of integrated DGs also play a significant role in determination of the system's PQ. For a proper planning of grid integration of DGs, it is important to determine the optimal location and size of DGs such that the overall PQ of the network is enhanced. DG placement problem formulation is done by defining the parameters to be optimized in an objective function and the constraints. A significant voltage profile improvement and active power loss reduction were achieved in [69] by using GA based approach under line loading and voltage constraints. The optimal allocation of DGs in electricity networks is vital in planning of grids with DGs. This is because DG location and capacity can be pre-determined from the knowledge of network characteristics such as loading conditions and line parameters. A number of optimization techniques were successfully utilized to obtain the optimal locations and sizes of DGs in different networks. The objective function in most DG optimization problems is based on the minimization of total active power losses and system's voltage profile improvement.

A number of optimization techniques have successfully been used in power systems to obtain optimal solution to an optimization problem. Some of the optimization techniques capable of identifying optimal solutions in DG grid integration problems include Particle Swarm Optimization (PSO), Genetic Algorithm (GA), Artificial Bee Colony (ABC), fuzzy optimization, etc. The optimization techniques are applied to optimize certain network parameters such as voltage profile improvement, active power loss reduction, reliability improvement, etc. Voltage quality is one of the major indicators of system's PQ, voltage profile improvement is therefore crucial in the optimal DG placement and sizing problems. It was established in [25] that power injections by DG units placed close to load

centres provides an opportunity for system's voltage support, reduction in total power losses and improvement in system's reliability.

2.6.1 *Voltage profile improvement and active power loss minimization*

A number of techniques have been employed to improve the network voltage profile in optimal DG allocation problems. In addition to voltage profile improvement, the reduction of the total active power losses is also considered in most DG placement problems. For instance, the method for optimal DG placement and sizing proposed by Prasad et al. in [70] indicated that a significant improvement in the system voltage profile and active power reduction were achieved. Voltage profile improvement and active power loss reduction in their work was achieved by employing a hybrid technique of genetic algorithm and neural network. The study also considered optimal DG allocation under different loading conditions and identified that a better voltage profile improvement and power loss reduction are achieved by placing multiple DGs at optimal locations.

The study in [57] introduced voltage sensitivity analysis to determine the optimal sitting and sizing of DG units using a methodology based on Particle Swarm optimization (PSO). A two staged methodology based on PSO algorithm is employed for allocation of DG units in a radial distribution systems to reduce network active power losses and improve voltage profiles. The results obtained in this work indicated that proper size and location of DG can significantly improve the system's performance by reducing losses and improving the system's voltage profiles. The determination of optimal solutions pertaining to grid integration of DGs for PQ improvement is dependent on a number of factors which include type of DG, network type, loading, etc.

In addition to voltage profile improvement and active power loss reduction, the study performed in [71] considered minimization of voltage sag problem in determination of optimal solutions for proper grid integration of DG. The optimization technique employed in this analysis is based on Genetic Algorithm (GA). Voltage sag mitigation capability of the developed algorithm is evaluated by investigating the voltage at voltage sensitive buses of the distribution system. The simulations performed on a 20kV distribution network showed the efficiency of the proposed algorithm in improving voltage profiles, reducing power losses and minimizing voltage sags in voltage sensitive buses.

A number of studies have been conducted pertaining to optimal sizing and sitting of different DG technologies for PQ improvement and loss reduction. It is crucial to investigate the role of wind and

solar PV based DGs on system's overall PQ improvement in order to observe the degree of improvement achieved for each technology. The optimal mix of solar PV and wind based DGs for PQ improvement is also essential to investigate so that combinational performance of the two can be evaluated. The study conducted by Kayal et al. [37] proposed an efficient approach for optimal placement and sizing of solar and wind DGs in distribution network by considering the system's total power loss reduction, voltage stability and network security improvement. In this study, a weighted PSO technique was successfully employed to optimize the objective function which considers bus voltage limits, line loading capacity and penetration constraints of DGs.

2.6.2 *System's reliability improvement*

In addition to voltage improvement and power loss reduction capabilities, grid-integration of DG units also contributes to system's reliability improvement. The reliability improvement of the power system is achieved by introducing the reliability indices in the objective function of the optimization problem. A number of studies aimed at improving the reliability of the system by optimal sitting and sizing of DG units in distribution systems have been done. In order to successfully improve system's reliability, certain reliability improvement indices are defined in the objective function of the problem, in addition to indices such as PQ improvement.

The new methodology for optimization of grid-connected DG units based on PQ and reliability improvement of the system is discussed in [72]. The authors in [72] considered the multi-objective function that relies of power quality and reliability improvement of the distribution system using PSO technique. The objective function in [72] considers power loss reduction and voltage stability improvement as indices that define system's PQ. The system reliability index is a combination of several reliability indices which include Average Energy Not Supplied (AENS), Customer's Average Interruption Duration Index (CAIDI) and System's Average Interruption Duration Index (SAIDI). The results indicated that voltage profiles and system reliability are improved by the optimal placement and sizing of DGs in distribution systems.

2.6.3 *Enhancement of system's economic performance*

The placement and sizing of DG units in a distribution system also impacts the economic performance of the power system. In addition to voltage profile improvement, power loss reduction and maximization of supply reliability, maximization of profit for distribution companies is also considered in identification of optimal DG location and size [73]. The investment costs and benefits in PQ and reliability equipment are evaluated on the basis of expected frequency and type of PQ

events, economic cost of PQ events to the utility, and the capital and operating costs of PQ mitigation facilities.

Some of the economic benefits of installing DGs in distribution networks include reduction in on-peak operating cost, shorter construction time, reduction in transmission costs and lower capital costs comparatively to small generators [74]. The reduction in transmission costs is the result of close proximity of DGs to the system load centres, hence shorter transmission distances. The active power loss reduction as a result of optimal DG allocation also contributes to the economic performance of networks with DG integration.

2.7 Research focus

The focus of this research will be on identifying the impacts of DG grid integration on system's power quality by observing the voltage quality as well as total system losses for different grid integration scenarios. After investigating their impacts on system's PQ, the methods essential for improving the system's PQ in utility grids with DG are explored and the degree of PQ improvement between solar PV and wind power based DGs is observed. For the purpose of facilitating proper planning of DG grid integration, PQ enhancement in networks with DG will be done through a number of approaches which include, optimal DG placement and sizing under different scenarios, utilization of voltage control techniques, application of energy storage systems, etc.

Voltage quality has been identified as one of the major indicators of system's PQ. The system's PQ improvement techniques and approaches applied in this study will focus on improving the voltage profiles of the network while also reducing the total active power losses in the system. The reliability of the system is also a significant aspect which grid integration of DGs should be able to enhance. In addition to PQ improvement, the enhancement of system's reliability through grid integration of DGs will also be investigated by applying appropriate methods. The investigations in all the case studies will focus on a comparative analysis between solar PV and wind power based DGs in terms of PQ improvement, line loss reduction and reliability improvement.

2.7.1 *Summary of Literature Review*

The review indicated that poor planning of the network with DG can result in negative impacts on network's PQ. The grid-codes governing the integration of DGs in South African networks have also been reviewed to provide clarity on permissible voltage and frequency ranges, reactive power requirements as well as voltage through capabilities of DGs. The review of grid-integration of wind and solar PV-based DGs on PQ enhancement also indicated that grid-integration of DGs have an impact on network's voltage profiles, power losses, frequency and harmonics. It was also revealed by

the review that DGs can strategically be utilized for PQ enhancement in electricity networks by employing appropriate measures during grid planning. Some of the additional findings of the review is that the optimal placement and sizing of DGs can result in contribute positively to voltage profile and reliability improvements as well as enhancement in system's economic performance.

3. Theory of power quality enhancement with grid-connected DGs

3.1 Introduction

As stated in the previous sections, PQ in electrical networks with DG integration is a crucial aspect that needs a particular attention, considering the detrimental impacts of poor PQ on customer loads. Several parameters such as voltage profile, frequency profile, injected harmonics, etc. are significant in determining the effect of DG integration on power system's PQ. The types of PQ improvement to be investigated, as well as several approaches of measuring the improvement are presented in this section. For reliability and security purposes, the power system is expected to operate within the set boundaries under both normal operating conditions and during system disturbances. PQ improvement analysis in this work therefore focuses on these two operating conditions of the power system. The performance of the power system with DG integration will be observed and analysed with reference to the South African grid codes and international standards governing the integration of DG systems to electricity networks.

It was highlighted in Chapter 2 that the performance of the power system might be highly affected by the presence of DG technologies in the electrical grid, especially if DG integration is poorly planned. Voltage quality is one of the major challenges that utilities face upon integration of DG units to electricity networks. In majority of the existing research work, the improvement of voltage profile in electricity networks upon DG integration still remains a challenge, particularly when it comes to utilizing DG technologies effectively for the purpose of improving the system's PQ. Kayal et al. [36] however confirmed that appropriate combination of solar and wind based DGs can significantly improve the efficiency and reliability of the system by mitigating the problems caused by their variable nature. This chapter therefore reviews the performance of grid-integrated DG systems under normal operation conditions and during disturbances. The techniques employed in grid-connected DG systems for the purpose of PQ improvement are also covered.

3.2 Voltage profile during normal operation

The variation in voltage profile at the PCC due to intermitted nature of DG technologies is of paramount concern in electricity networks with DG integration. The magnitude of the supply voltage is highly influenced by voltage variations due to alterations in the real and reactive power drawn by the loads in network with DG integration. Several international standards provide a series of PQ requirements for electricity networks with DG integration, in terms of voltage fluctuations at the PCC. It is a significant requirement that the acceptable range of voltage variations at the PCC in distribution

systems is maintained under all system's operating conditions. Variations in voltage profiles in electrical networks with DG depend on voltage level, grid type, grid strength, DG location and penetration level on the grid [75]. It is therefore crucial to fully understand the impacts of the above factors on the system's voltage profile for efficient network planning.

3.2.1 *Voltage rise due to DG*

Before the introduction of DG, over-voltages were less of a concern in electricity networks due to the traditional design of electricity networks. Large penetration of DG in distribution networks however results in voltage rise at the PCC as well as the terminals of the generator and this consequently affects all customers connected downstream of the DG unit. Voltage rise due to high DG penetration levels within sub-transmission and distribution networks is the key factor limiting large scale deployment of DG [76]. The generator should operate at a higher voltage as compared to the other nodes so that it can be able to export power to the grid. Voltage rise issue in distribution networks, as a result of DG integration, can easily be described by making reference to a two-bus distribution system shown in Figure 3-1 and the equations that follow.

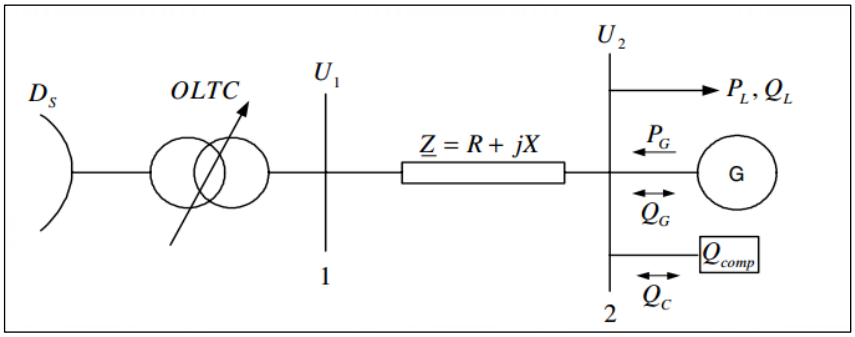

Figure 3-1: A two-bus distribution system with DG integration illustrating voltage rise effect compensation **[77]**

The distribution system shown in Fig. 3-1 comprises a line with the impedance of $+jX$, an on-load tap changer (OLTC), reactive power compensator (Q_C) and DG unit (P_G, Q_G) together with a local load (P_L, Q_L). The voltage rise along the network is described using Equation (3-1) below which also considers the parameters of other connected equipment such as those providing reactive power compensation, as illustrated in Figure 3-1.

$$\Delta U = U_1 - U_2 = \frac{R(-P_G+P_L)+X((\mp Q_C+Q_L \pm Q_G)}{U_2} \qquad (3\text{-}1)$$

Most voltage control schemes in distribution networks cannot effectively respond to voltage rise problem upon integration of large amounts of DG due to power flow inversion. One of the simplest approaches to prevent OV in distribution networks is restricting the maximum capacity and location

of DG within the grid planning phases [27]. This approach requires a predictive analysis of voltage profiles for a particular DG size and location in the network. This method however is time intensive and may result in errors due to changing network loading. Several approaches are however effective in mitigating the voltage rise issue and will be discussed under classical voltage control section. One of the simplest but unfavourable approaches to mitigate voltage rise and keep it within a permissible range is the implementation of power curtailment.

i. Overvoltage Curtailment

During instances when the system's voltage gets closer or above the prescribed magnitude, a curtailment scheme in which production is reduced is employed [45]. The overvoltage limit is pre-set such that the maximum possible production at any time would result in a voltage that does not exceed the limit. To illustrate the principle of overvoltage curtailment, a graphical representation shown in Figure 3-2 is used. As observed in the illustration, the dotted line in Figure 3-2 is the overvoltage limit while the solid curve represents the voltage magnitude without tripping. The dashed curve resembles the voltage magnitude when production is reduced. The algorithms applied for over voltage curtailment must ensure that the voltage is kept exactly at the dotted line to ensure maximum and efficient delivery of DG generated power [45].

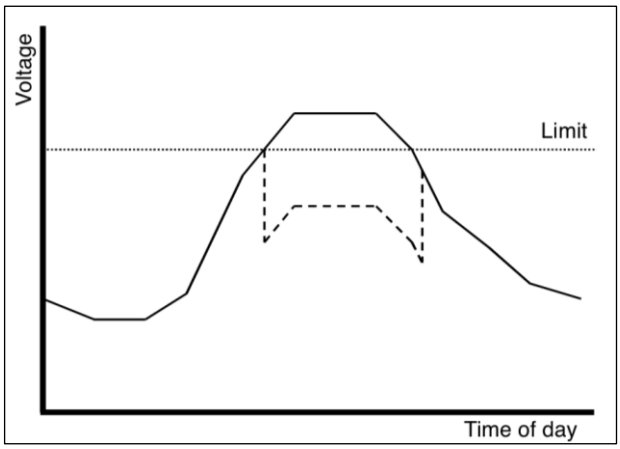

Figure 3-2: Impact of overvoltage tripping on voltage variations **[46]**

3.2.2 *Voltage drop*

Although voltage drop is not a common problem in electricity networks with high penetration of DG's, there are instances when voltage magnitude will drop below the prescribed voltage magnitude. The level of voltage in the network is dependent on a number of parameters that include load demands, feeder parameters such as length and diameter as well as several other equipment. Voltage drops may result in under-voltages which are defined in IEEE STD 1159-1995 as drop in voltage for a period greater than 1 min and typical values 0.8-0.9 p.u. Under voltages mainly occur as a result of the opposite of events that cause over-voltages such as switching on large loads or under overloaded

circuit conditions [78]. Under voltage condition may also arise as a result of switching off of a capacitor bank.

3.2.3 *Influence of DG on voltage control*

As discussed earlier, with DG-integration, distribution systems are no longer passively supplying loads, but become active with power flows and voltages that are determined by generation and loads. High penetration levels of DG affect the operation of conventional voltage control schemes used in electricity networks. This is due to voltage variations such as voltage rise at the PCC which can consequently result in reverse power flows.

3.2.4 *DG impact on feeder voltage and current*

The voltage along the feeder is one of the fundamental parameters that integration of DG units affects and it is important to consider this in the design of distribution systems. Prior to introduction of DG, the design of distribution system would be primarily focused on prevention of excessive voltage drops [46]. The parameters of the feeder such as maximum length, as well as other methods had therefore been implemented for the purpose of preventing voltage drops along the feeder. The introduction of high penetration level of DGs may however result in voltage rises on the feeders. The current along the feeders may also increase as a result of high penetration level of DGs and this might result in feeder current carrying capacity exceeding its maximum limit.

3.3 Voltage profile during system disturbances

Electrical sub-transmission and distribution systems are dynamic systems which are continually affected by disturbances due their close proximity to loads. Faults in electrical networks are cleared by the protection system whose primary goal is to detect and isolate the fault while minimizing the fault's duration and the number of affected customers [79]. For reliability and security of supply purposes, the system is expected to remain stable following a disturbance which can be either as a result of connected loads or integrated DG units. To achieve this, certain requirements regarding the performance of the power system during fault occurrence and post fault state are imposed to DG units integrated to the distribution system [80].

The grid codes reviewed in Chapter 2 require that integrated DG units continue operating during the fault even in cases when the voltage drops below permissible values or even zero. Faults in electrical systems can cause temporary voltage swell, voltage dips/ sag, or a complete loss of voltage which

consequently result in complete interruptions. The fault characteristics as well as the protection technology employed determine the duration and magnitude of the fault; whereas the ability of the system to recover from fault depends on the interconnection strength and the available reactive power support [81].

3.3.1 *Voltage Dips*

Voltage dip in electricity networks is defined as the sudden reduction of the voltage magnitude to a value in the ranges of 10% to 90% of the nominal voltage magnitude with the duration of 10ms to one minute [50]. Some research literatures define voltage dip as a reduction in voltage magnitude below a dip magnitude threshold with duration usually from several cycles to several seconds [13] [82]. As described in Chapter 2, voltage dips are caused by several factors including the switching of electrical machines such as motors, generators and transformers. The voltage dip also occurs as a result of short circuit faults in the power transmission and distribution systems. Voltage dip is defined by its duration and magnitude in the form of lost and retained voltage. Lost voltage is the reduction in voltage at a bus following a fault or any abnormal incident while retained voltage is the reduced voltage still available at the busbar. The dip magnitude is defined by the fault types, source and fault impedances whereas the duration is defined by the fault clearing time [82]. The voltage dip in this work will be measured by the level of voltage drop during the dip as well as the time taken by the voltage to recover to its nominal value after the voltage dip.

The severity of the voltage dip occurrence varies according to network configuration of the network, fault location, fault type, etc. [83]. Voltage dip phenomenon is illustrated in Figure 3-3. It can be observed that the voltage dip starts when the voltage drops to the value lower than the nominal voltage magnitude at the time T1. The voltage dip continues up to T2, after which the voltage recovers to a value over the threshold value. Both the magnitude and the duration of the voltage dip have been indicated in the diagram. The duration of the voltage dip in this scenario is T2-T1.

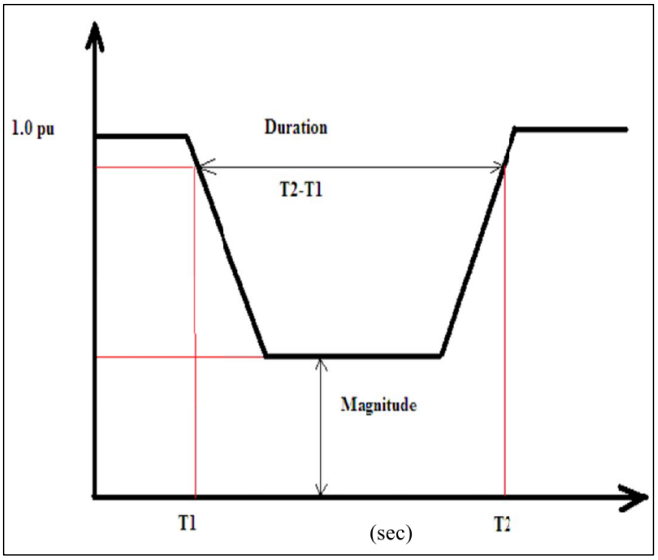

Figure 3-3: Voltage dip with magnitude and duration marked **[82]**

The impacts of grid-connected DGs on voltage dip differ according to the characteristics of both DG and network types. For example, Ipinnimo et al. found that the wind generator has the capability of mitigating multiple voltage dips sufficiently on the DG bus-bar when compared to the transmission bus bar due to the fact that WTG provides support to the PCC voltage [81]. Weak grids are also vulnerable to voltage dips because they are usually designed for relatively small loads, which cause the voltage to drop below the allowed minimum when the design load is exceeded [80]. Several approaches to mitigate voltage dip problems on the network have been proposed by a number of researchers. A large number of proposed methods utilize DG to improve the system's PQ, particularly the voltage dips challenges. Some techniques include the use of series compensation to transfer to micro grid operation during dips and utilization of converter-based DG such as DFIG [80].

3.3.2 *Fault ride through (FRT) capabilities*

Various DG regulating standards regarding the power system's operation during fault conditions have proposed certain operational requirements. Integration of DG units to MV and LV networks is usually limited to a certain percentage of the substation installed kVA such that DG effect in distribution network operation is minimized [84]. However, in order to increase DG installed capacity, certain operational characteristics are imposed on DG systems such that their operation can resemble that of conventional generating units. The interconnection of DG sources such as wind and solar with the existing power system is also subject to compliance with rules regarding power system operation during grid disturbances. The Fault Ride through (FRT) or Low Voltage Ride through (LVRT) requirements for their grid integration has thus been developed.

The FRT criterion is basically the defined reactive and voltage requirements which DG units are expected to meet in the case of faults in the system. Integrated DGs must be able to ride-through faults and low voltage conditions to avoid failure of the system and their ability to do this is referred to as LVRT capability [85]. The connected DG sources must therefore be able to remain connected to the grid during voltage dips, thus the LVRT capability ensure system's post fault stability and fast discovery. The system's acceptable voltage ranges as well as the time period in which the system must remain online must be well defined so that LVRT requirements can be met. An example showing the LVRT requirement for a solar PV plant is shown in Figure 3-4 below:

:

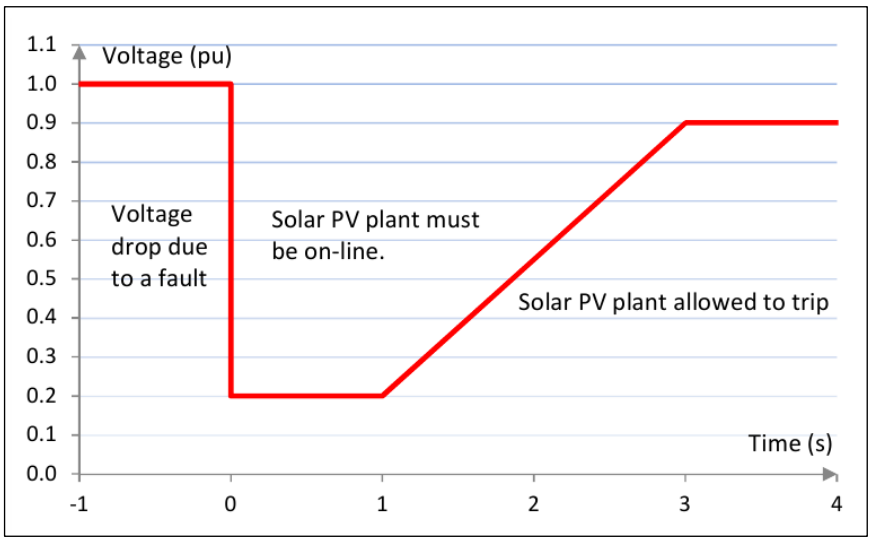

Figure 3-4: LVRT requirement for a solar PV plant integrated to the power grid **[86]**

In Figure 3-4, the LVRT requirement depicts that when the voltage at the PCC drops to 20% of the nominal magnitude, the PV plant should remain connected for 1 second. The solar plant should also stay connected when voltage can recover above 90% within the period of 3 minutes as depicted by Figure 3-4. Disconnection or transition to island mode is permitted in the cases of prolonged voltage dips and persistent grid faults. Similar LVRT requirements apply to grid-integrated WECS with the exception that the online time is shorter. The support to system voltage must be provided using compensation devises whereas certain WECS inject reactive current to support voltage recovery [31].

The LVRT capability was initially applied to large scale WECS such that operational characteristics similar to those of conventional generators can be achieved during fault conditions [85]. The trend has however been expanded to solar PVs due to their large scale deployment and technical improvements. Various energy markets have imposed new regulations regarding the behaviour of DGs during system disturbances and may differ according to specific network requirements. For

instance, the LVRT requirements for different country's grid codes are depicted by Figure 3-5 below. These schemes are applicable to a wide range of DG sources including wind and solar PV generators.

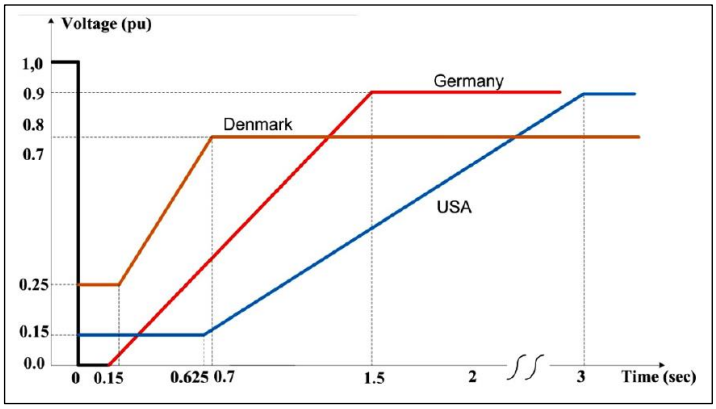

Figure 3-5: FRTC schemes of several energy markets **[87]**

Contrary to temporary under-voltages, there are instances when temporary over-voltages may occur as a result of load shedding, faults or variations in generation and loading. Over-voltages in electricity networks may also occur as a result of high transmission line capacities coupled with generation tripping or unbalanced faults [88]. An over-voltage can also occur during the recovery of system's voltage after the fault clearance. The resulting over-voltages have different durations and magnitudes depending on the cause of disturbance. The grid codes governing DG integration into electricity network specify the minimum time that DG should remain connected to the grid during an overvoltage. The High Voltage Ride Through (HVRT) requirements for wind and solar PV based DGs have this been developed.

The recent grid codes specify specific HVRT requirements for DG systems connected to utility networks. The requirements on system's over voltages consider over-voltages resulting from DG operation as well as those originating from the grid. The international grid code requirements pertaining to HVRT differ according to countries and local requirements. For instance, the Australian grid code for wind turbines requires wind turbines to withstand even an over voltage of 1.3 p.u. for 60ms as depicted in Figure 3-6 below:

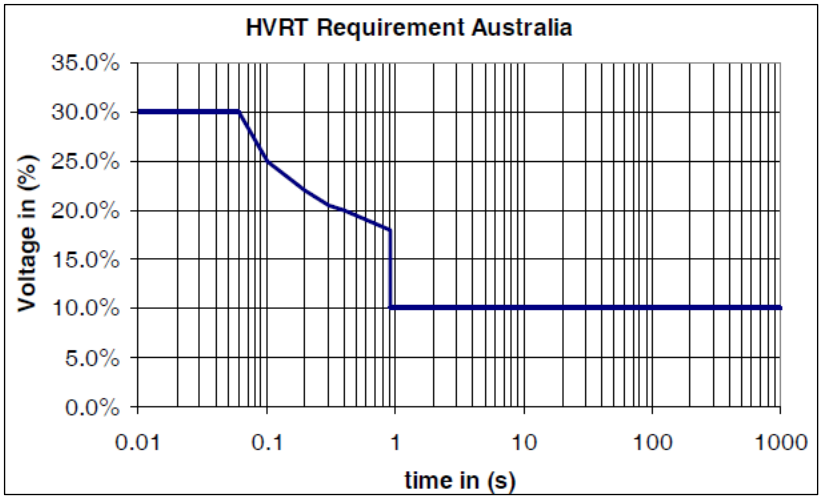

Figure 3-6: HVRT Requirements in the Australian Grid Code **[89]**

3.4 Voltage control in grid-connected DG systems

The increasing penetration level of DG in distribution networks requires implementation of a system that is capable of functioning under dynamic operating conditions in order to improve the system's PQ. Voltage is one of the most crucial parameters for the control of power system upon integration of DG. The challenge faced by active networks to maintain voltage within permissible limits has initiated development of several control mechanisms essential for mitigating voltage issues. These approaches include the use of coordinated or central and decentralized or distributed methods, both of which have been proven capable of alleviating the voltage rise issues in electrical networks with DGs [90]. Centralized approaches have been found capable of increasing DG installed capacity through use of wide area voltage control and reactive power management while distributed voltage approaches limit voltage rise in feeders where load and generation are considered continuously distributed [91]. Their effectiveness however differs according to network characteristics, network strength, point of connection and active and reactive power exported from the PCC into the grid.

The control of voltage in electricity networks with DG integration is classified into three hierarchical levels viz. primary, secondary and tertiary levels [92]. The primary control is performed by Automatic Voltage regulator (AVR), secondary control by on-load tap changers while tertiary control coordinates the action of primary and secondary control equipment such that secure operation of the power system is maintained. Different approaches to mitigate voltage issues such as excessive voltage rise in electricity networks include reduction of the primary substation voltage, increasing the conductor size, limiting the active power injected by DG into the network, installation of auto transformers, etc. [93] Several other effective voltage control mechanisms include reactive power compensation, Load Drop Compensation (LDC) as well as installing specialized voltage regulation equipment.

3.4.1 *Reactive power control*

Reactive power control approach for voltage dip mitigation in DG-integrated networks can be implemented using either centralized control or decentralized control approach of which the latter allows each integrated DG unit to control its reactive power production [89]. Centralized control of reactive power requires the use of a centralized Power Control Unit (PCU) for the exchange of data such as voltage levels among all controlled buses for both generation and load as illustrated by Figure 3-7(a). In the case of decentralized control, each generator controls its reactive power generation on the bases of local measurement as illustrated in Figure 3-7(b). Decentralized control is advantageous in that it is able to provide voltage support controlling locally its operating modes while being cost effective due to limited need for large investments on communication systems [86].

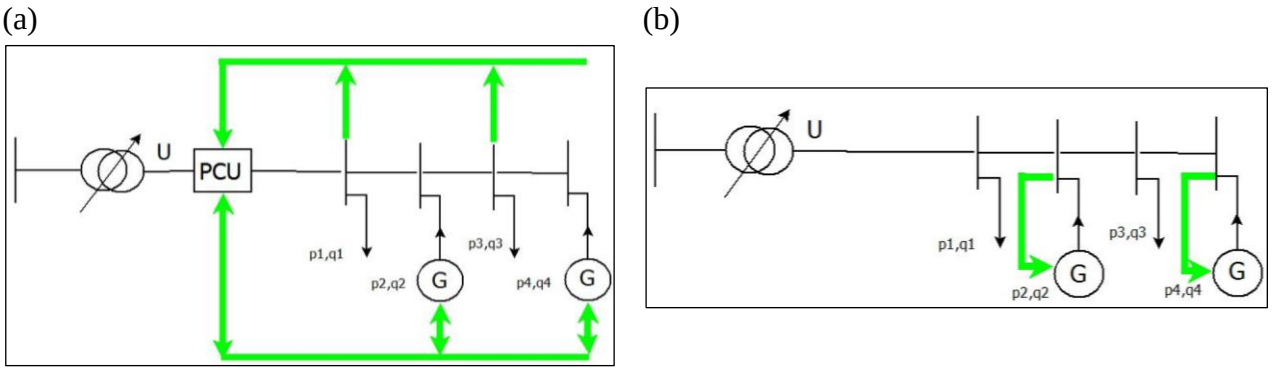

Figure 3-7: **(a)** Centralized reactive power control (b) Local or decentralised reactive power control **[93]**

Reactive power control approach in DG-integrated systems can also be applied for controlling the power factor by maintaining the ratio of active power to reactive power constant. The feeder voltage rise caused by excessive generation of active power has been identified from the previous section as a challenge that distribution network operators (DNOs) face. This is because in order for reactive power, Q to compensate the feeder voltage rise caused by generated active power, P the expression $Q = -RP/X$ must be true [91]. This is often impossible since high loads require an amount of reactive power that the generator capacity does not support. Furthermore, the generator power generation settings would have to be altered whenever the load changes such that the power factor is kept constant at the PCC. Due to these challenges, most DNOs prefer maintaining the power factor constant rather than regulating it.

The principle of voltage regulation by DG reactive power control is illustrated in Figure 3-7 below. The voltage at the output of DG is regulated using the linear slope with a dead-band, ε as shown in

Figure 3-8. The DG reactive power boundary values can either be fixed or can fluctuate as function of DG active power generation such that the voltage at PCC is kept within the acceptable values.

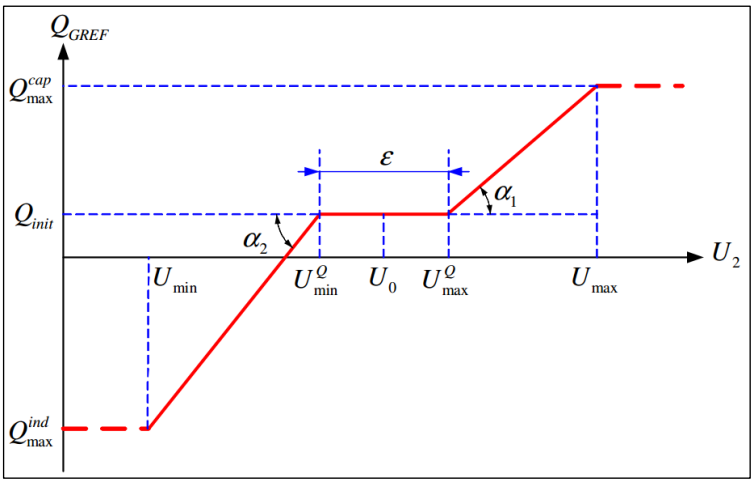

Figure 3-8: DG reactive power control low in respect with PCC voltage value **[94]**

An alternative approach proposed by Carvalho et al. [91] is based on finding the magnitude of generator's reactive power, Q_G which will be capable of minimizing the voltage rise caused by the generated active power, P_G. The value of the generator reactive power, Q_G, which mitigates the voltage rise problem induced by P_G is given by Equation (3-2) below.

$$Q_G{}^{*} \approx \frac{X}{R^2+X^2} - \sqrt{\left(\frac{X}{R^2+X^2}\right)^2 - P_G{}^2 + \frac{2RP_G}{R^2+X^2}} \qquad (3\text{-}2)$$

where X and R are the reactance and resistance of the line between DG connection point and the transformer stepping up the voltage at DG terminals to that of the PCC bus; P_G is the active power generated by a DG unit.

When a synchronous generator is used, reactive power control is realized by an excitation system consisting of an AC or DC excitation controller and voltage measurement components. Synchronous generators however have limitations on voltage and reactive power control in distribution systems; additional compensating devices are therefore required to maintain the voltage within acceptable levels [90]. Several equipment have been proven to be a promising solution and are used by DNOs to provide reactive power support to the grid. The equipment capable of delivering or absorbing the reactive power include capacitor banks, SVCs, STATCOM, etc.

i. Capacitor banks

Capacitors in a power system can be used as compensating devices due to their capability to provide reactive power control functionality. They are also installed on the distribution network feeder so that

the power factor of the system can be improved. Capacitors installed for the purpose of voltage control in a power system can either be of shunt or series type and can also be permanently connected or be switchable. The capacitors connected permanently are designed as part of the utility grid to be controlled whereas switchable capacitors are part of control devices are responsible for providing grid support by recovering voltage variations [95]. In addition to switchable shunt capacitors, local reactive power compensation can also be achieved by using mechanically switched capacitors which are connected to the power system either directly by a circuit breaker or via a transformer.

In order to ensure local compensation of reactive power which is utilized by consumers, capacitor banks are either connected directly to the bus bar or to the tertiary winding of the local transformer throughout the system. The shunt capacitors are particularly applied in distribution grids so that reactive power can be supplied as close as possible to the point of consumption. In transmission systems, shunt capacitors are used to compensate for inductive losses defined by $I^2\omega L$ and they also ensure acceptable voltage levels during heavy load conditions. The output of the shunt capacitor is however unfavourable during system disturbances due to the linear relationship of its current and voltage which results in much reduced reactive power output at reduced voltage.

ii. Static var compensator

The static Var Compensator (SVC) is part of the family of flexible alternating current transmission systems (FACTS). It is used in power networks to regulate and control the voltage to the desired set point during normal system operation and in instances of system disturbances. The advantage of SVC over most voltage regulating devices is that is supplies a fast-acting, precise and adjustable amount of reactive power to the network to which they are connected [96]. In addition to voltage control, SVCs can also be employed for dynamic power factor correction through properly controlled reactive power compensation.

iii. Static Synchronous Compensator

The static synchronous Compensator (STATCOM) also falls under the family of FACTS. The STATCOM operation is based on power electronic voltage-source converter and can either absorb or inject reactive power. The controlled reactive power compensation in electricity networks can be successfully achieved by using the STATCOM due to its fast response to voltage changes [97]. In transmission networks, the STATCOM facilitates the fundamental reactive power exchange and provides voltage support to buses which suffer poor voltage profiles due to faults and disturbances in the network.

3.4.2 *On-load tap changer*

The commonly used principle of voltage control in distribution networks is based on a transformer with different turn's ratios that keeps the voltage on the secondary of the transformer within a certain dead band by means of automatic tap changer [46]. Transformers equipped with OLTC are employed in electricity networks so that they control voltage variations due to loading. HV/MV transformers installed in South African networks are equipped with OLTC that are responsible for maintaining the network voltage magnitudes within permitted limits. These transformers are configured to regulate and maintain the secondary voltage supplied to customers within statutory limits. The required voltage is basically achieved by altering the number of turns in one winding of the transformer such that the transformer's turn's ratio is physically changed [98].

The tap position of the transformer is controlled by a relay which sends a command to the tap changer when the secondary voltage is no longer within the permissible range. The schematic of a tap changer placed in the primary winding and an equivalent circuit of a two-winding transformer equipped with the tap changer located in the secondary winding are shown in Figure 3-9. The basic control loop of OLTC is also illustrated in Figure 3-10.

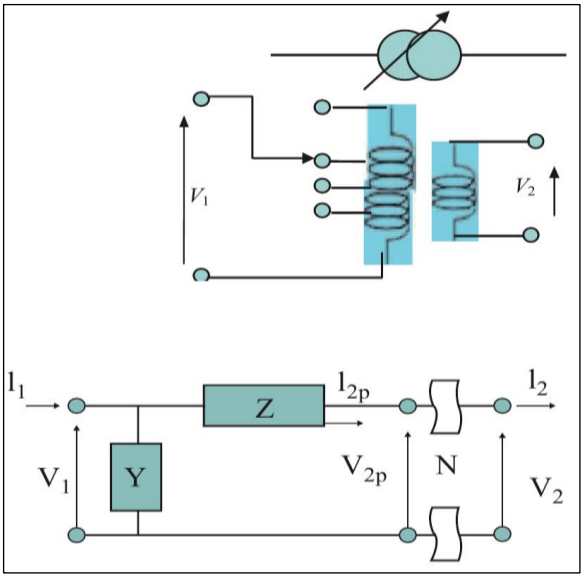

Figure 3-9: Single phase OLTC and its equivalent circuit **[95]**

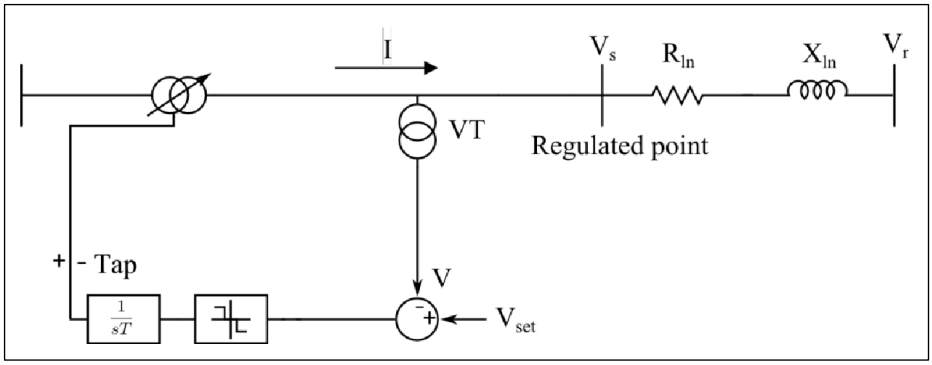

Figure 3-10: The control loop of an OLTC **[33]**

The success of an OLTC to perform voltage control at each voltage level depends on the voltage solidity of the next higher level. The control of OLTC is based on a local measurement of several parameters that include the transformer's secondary current, MV bus-bar voltage and feeder sending-end current [94]. The parameters that are regulated by an OLTC are assessed based on forecast of the voltage profiles during maximum and minimum load conditions of the feeders. The OLTC control attempts to modify the MV bus-bar voltage according to the following equation;

$$V_i = V_P + RI_T \tag{3-3}$$

where V_P is the reference voltage that is chosen by the distribution operator, R is the compensation parameter, I_T is the transformer's secondary current and V_i is the MV bus-bar voltage that is being modified.

3.4.3 *Voltage regulation*

DG voltage regulation can be achieved by using the combination of several control approaches which will be capable of controlling both the DG voltage and the voltage of the feeders. The use of OLTC transformers for voltage reduction on the feeder where the generator is connected may result in extremely low voltages on adjacent feeders supplying the load [94] . In this case, Voltage Regulators (VRs) are employed to separate the control of feeders supplying the loads from the control of a feeder to which DG is connected. VRs can either be passive or active where passive regulator is for example an autotransformer with a transformation ratio of 1 and variable taps whereas active regulators based on power semiconductors [99]. VRs are therefore installed when the feeder voltage needs boosting either because the line is too long or the low voltage limits are not met due to increasing feeder load.

A typical VR transformer and the corresponding tap changer have a configuration as depicted in Figure 3-11. VRs usually have a total of 16 steps, with a reversing tap to buck or boost the voltage, giving $\mp 10\%$ single phase regulation at 0.6525% per step [33]. They are therefore designed to

provide rated regulation of voltage, at rated current with a PF determined by the network requirements at the connection point.

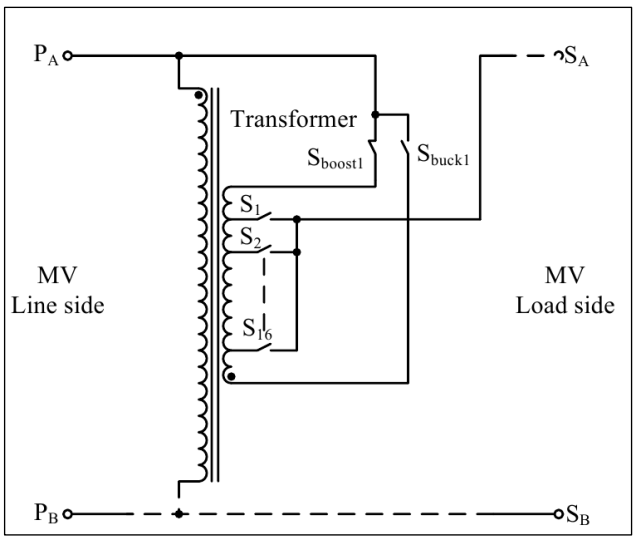

Figure 3-11: A Typical VR with a single phase autotransformer with a tap changer **[33]**

3.4.4 *Line drop compensator*

Line drop compensation (LDC) is one of the control features associated with OLTC, particularly in cases where OLTC does not provide adequate regulation along a feeder. LDC uses a measure of secondary current to track the voltage at the secondary side of the transformer and simulates the voltage drop across the feeder between transformer and the load [100]. In most electricity networks, voltage regulation is usually performed at a distance from the network's load centre and this may result in a load being supplied at unacceptable voltage level due to voltage drops across the line between the load and a substation. LDC is therefore installed to offset these voltage drops. The regulator's desired voltage can be adjusted such that the load is supplied at the desired voltage level. The use of LDC is crucial in cases where DG units such wind turbines are integrated into a distribution network at remote locations where voltage level is uncontrolled.

LDCs are rarely used on the South African network because of the high complexity when a single LDC is used to regulate several feeders [101] [102]. The major challenge with LDC is that when the loads are distributed among many feeders and are spread along the entire length of the feeder, it becomes difficult to adjust the line-drop compensation to suit all network points [99]. Figure 3-12 shows an Automatic Voltage Control (AVC) relay scheme with LDC which, instead of providing voltage control at the transformer terminals, controls it at a nominal load point. The DNOs define the maximum and minimum voltage limits within which LDC must ensure that the system operates at.

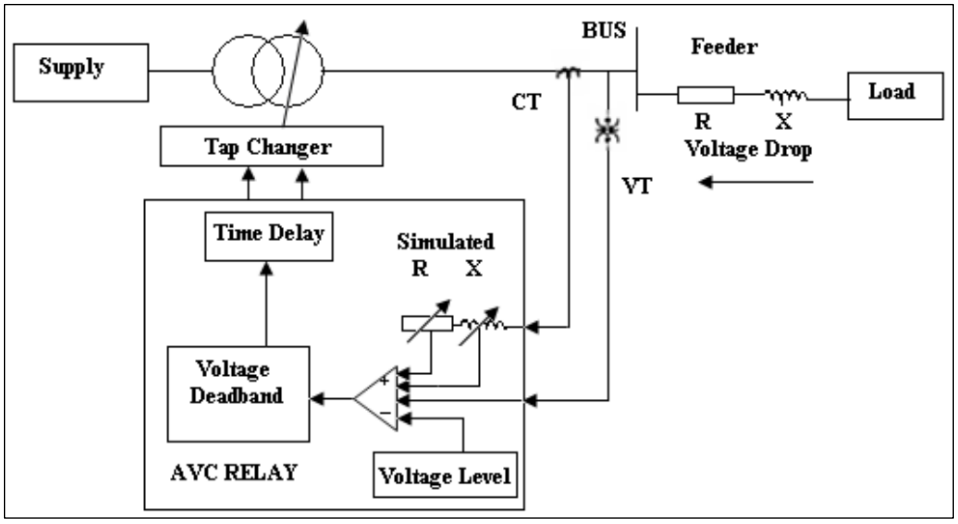

Figure 3-12: AVC relay scheme equipped with LDC **[100]**

Network parameters that LDC utilizes to regulate the voltage at the regulation point include the feeder current, the supply voltage and the impedance of the line. The voltage at the point of regulation of a LDC is calculated using Equation (3-4).

$$V_r = V_s - I(R_{Ln}\cos\emptyset + X_{Ln}\cos\emptyset) \qquad (3\text{-}4)$$

where, V_s is the voltage at the supply point, I is the current through a line of impedance$R_{Ln} + jX_{Ln}$.

Equations (3-5) and (3-6) are used to estimate the voltage at the regulating point for maximum and minimum load, respectively.

$$V_{r.Lmax} = V_{s.max} - I_{L.max}(R_{Ln}\cos\emptyset + X_{Ln}\cos\emptyset) \qquad (3\text{-}5)$$

$$V_{r.Lmin} = V_{s.min} - I_{L.min}(R_{Ln}\cos\emptyset + X_{Ln}\cos\emptyset) \qquad (3\text{-}6)$$

The maximum and minimum sending end voltages are $V_{s.max}$ and $V_{s.min}$, respectively. $I_{L.max}$ and $I_{L.min}$ are the line current at maximum and minimum load while the PF at tap changers is represented by $\cos\emptyset$.

It was highlighted in [100] that without the application of LDC, the load current can be delivered outside the voltage limits due to voltage drops along the feeder, assuming the loads are connected at the end of the feeder. The LDC will control the voltage from the source to be low during low load and high during high load, accounting for the feeder voltage drop [103]. Equation (3-7) is used to estimate

the feeder voltage profile when OLTC is equipped with a LDC. Ideally, the voltage calculated with LDC is the equivalent to the voltage at the load connection point.

$$V(\lambda) \approx V_{set} + \frac{R_{set}P_L - X_{set}Q_L}{V_{nom}} - \frac{R_{Ln.\lambda}P_L - X_{Ln.\lambda}Q_L}{V_{nom}}(1 - 0.5\lambda) \qquad (3\text{-}7)$$

The parameters $V(\lambda)$ and V_{set} are the regulated voltage and the voltage set point, respectively. R_{set} and X_{set} form the set impedance of the LDC while $R_{Ln.\lambda}$ and $X_{Ln.\lambda}$ form the impedance of the line as a function of distance from the regulating point. V_{nom} is the nominal voltage of the system under consideration.

The comparison of the voltage profiles along the feeder with and without application of LDC is illustrated in Figure 3-13. It can be observed that upon application of LDC, the loads may be supplied within voltage limits.

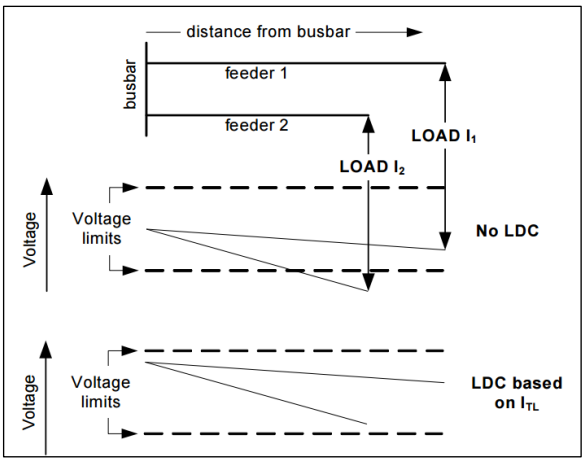

Figure 3-13: Voltage profile along the feeders with and without application of LDC **[104]**

3.5 Mitigating DG impacts for maximum penetration

The impacts of DGs on power quality are the major limitations to their large scale deployment. The increasing interest in large scale deployment of DG requires that the system's performance is not deteriorated by their high penetration levels but is rather enhanced in terms of the quality of power. The security and reliability of electricity supply is the primary priority for utilities, certain measures should therefore be taken into account to mitigate the issues affecting the system's PQ. Some approaches include improvement of the distribution network to allow safe integration of high DG penetration levels. The fundamental goal of DG integration is to increase their penetration levels without adversely impacting the system's operation and performance.

Some of the advantages of integrating DG units into electricity networks include feeder demand reduction and more importantly, their ability to support local voltage [79]. Voltage support offered by DG helps to improve voltage profile in distribution networks that initially suffered poor voltage levels prior to installation of DG during peak loading conditions. DG integration however impacts effective operation of some of the network equipment including capacitors, tap changer settings and protection disruptions. A number of strategic approaches necessary to increase the distribution network's ability to accommodate an increase in DG have been proposed, some of which alter the network's infrastructure and may be expensive to implement. Effective solutions include upgrading of existing conductors, voltage control, redesigning the network, installation of fault current limiting devices, etc.

3.5.1 *Optimal placement planning*

The well planned DG placement is fundamental in reducing the adverse impacts of DGs on utility networks. The optimal placement of DG can be successfully achieved by taking into account the characteristics of the network in which DG will be connected. The optimal DG placement and sizing requires use of optimization techniques in grid integration planning stages to ensure enhanced operation of the system. Some of the widely used optimization techniques capable of determining the optimal location and size of DGs include Particle Swarm Optimization (PSO) and Genetic Algorithm (GA). The allocation of DG for improvement of network voltage profiles and reduction of power losses in distribution networks will be discussed in detail in the next chapter.

As discussed in Chapter 2, optimal DG placement and sizing in different distribution networks was successfully done in a number of researches. For instance in [105], a significant reduction in total active power losses of the system and voltage profile improvement was achieved by the optimal sizing and placement of DG using PSO algorithm. The significant improvement in network's voltage profile and power loss reduction were also achieved in [106] using GA technique to determine the optimal placement and size of DGs.

3.5.2 *Upgrading conductors*

The problems associated with DG integration range from excessive voltage rises at PCC to feeders being over-loaded. This is due to a traditional design of feeders which is based on unidirectional power flow from high voltage busbars to lower voltage busbars. Weak grids such as most South African grids are more vulnerable to power quality disturbances due to their high impedance and low mechanical inertia. The strength of the network is defined by its short circuit power S_{SC} as seen from the PCC and is dependent on the Thevenin's equivalent impedance of the grid. Upgrading of feeder conductors either through reinforcement or extension is therefore considered as a solutions to enhance power transfer capability of the distribution network upon large scale integration of DG units [79].

The other method of improving the power transfer capability of the network would be to put each DG on its own and connected through adequately sized radial feeder to serve the HV/MV substations. However this solution is more expensive and is likely to put limitations on utilization of DG in remote locations where RES such as wind and solar are usually found in abundance. In the case where DG is integrated to a weak network, and is unable to perform to its optimal during low local consumption, the feeders connecting the DG and the substation will require reinforcement or upgrading to increase DN's capacity to accommodate more DG [79]. Considering the cost of upgrading feeder conductors, the cost of the DG may outweigh the gain in feeder capacity increase, it is therefore not an attractive approach.

3.5.3 *Voltage control*

As discussed in the previous sections, the principle of voltage control in grid-connected DG systems is crucial in mitigating the adverse impacts brought about by DG-integration. A number of electrical equipment used for voltage control in electricity networks have been proposed and tested for their effectiveness and efficiency. These include the use of tap changing transformers, capacitors, SVCs, STATCOMS, etc. Research has shown that with a combination of certain algorithms, fuzzy logic systems and proper modelling, the existing voltage control equipment may be capable of accommodating the increasing penetration of intermitted DG as well as a rising load level [79]. Based on the broad and widely studied research in the area of voltage control in grid-connected DG systems, only two cost effective techniques will be studied.

Specific case studies conducted on local voltage rise mitigation have showed that among inexpensive voltage control approaches, installation of reactive power compensation devices at the DG's PCC may be attractive solutions [79] [99] [107]. Studies also identified that lowering the voltage of the upstream sub-stations facilitates efficient network transfer capacity upon integration of DG units. Using devices such as STATCOMs and SVCs for voltage control purposes in electricity networks has also proved to be cost effective solution. Voltage control in this study will be investigated using STATCOM and SVC to observe the degree of PQ improvement upon integration solar PV and DFIGs.

3.5.4 *Network redesign to a mesh system*

Redesigning the network such that it is operated meshed will ensure that disconnection of one component does not cause an interruption for the rest of the customers [108]. High penetration level of DG in utility grids makes the power flow bidirectional, similar to the mesh networks of the HV

power grid [79]. The complete redesign of the network however has its own drawbacks which can make the solution less attractive. In a radial network, addition of DG reduces the loading in the network, given that the amount of DG is less than the hosting capacity [46] . Mesh operated transmission and distribution networks have their busbars paralleled as illustrated in Figure 3-14 below. This will consequently result in large power flow between certain regions and consequently increase the short circuit responsibilities on the system.

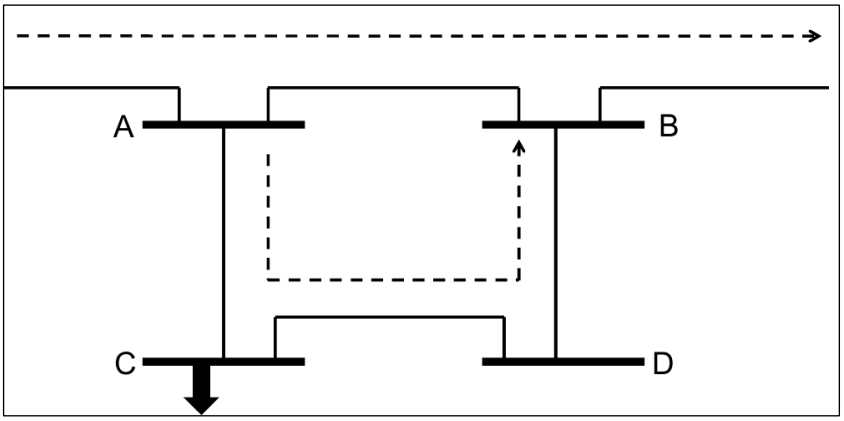

Figure 3-14: A large power flow scenarios in a meshed network **[46]**

In a mesh operated network shown above, a large power flow occurs in connection A-B compared with the loop A-C-D-B. Connecting the load to Bus C will result power flow increase in A-C while reducing it in the connection D-B. Connecting a DG unit to node C will reduce the loading and thus increase flow between D and B, resulting in overloading. A mesh operated network therefore increases the fault currents levels and protection equipment with higher rating should be used. This may urge the fault current to consequently go beyond the limits of some of the distribution network equipment [79] . Strategic operation of meshed network however has the potential to allow DG integration to the network.

An alternative option may be designing balanced looped secondary sub-feeders connection customers and producers. This allows for fault isolation such that a greater portion of the system remains energized even in cases when the fault occurs on the main feeder. In situations when the fault occurs inside one of the feeders, the fault is localized such that other loops remain affected. To increase the capability of the network to accommodate more DG in a meshed network, an intertrip scheme may be used [46]. The scheme involves equipping the loop with fault locating relays such that the loop can be split into two radial sub-feeders upon fault isolation [79]. An example of an intertrip scheme with protection relays placed in some lines and a DG integrated to one of the buses is depicted in Figure 3-15. Intertrip scheme is however preferred in larger DG units such as wind parks, connected to sub

transmission systems, where the (N-1) principle could otherwise restrict the capacity of DG that can be integrated [46].

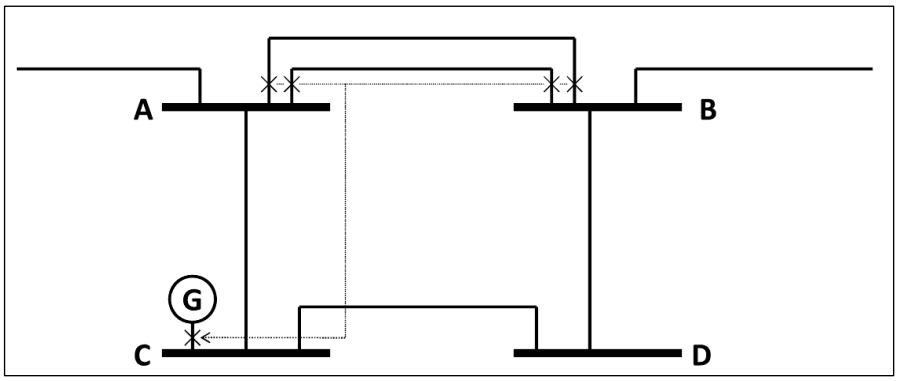

Figure 3-15: An intertrip scheme applied in a meshed network **[46]**

3.5.5 *Fault current limiting devices*

Besides voltage regulation and power quality constraints, the total fault level is one of the important requirements for connection of DG units to the network as is often the main limiting factor for the interconnection of DG units to the grid [109]. One of the significant parameters that characterize the distribution system is the maximum acceptable fault current which is related to the thermal and mechanical withstands capability of networks equipment. Larger penetration levels of DG contribute to an increase in short circuit current in the distribution networks and may adversely impact the operation of the system [79] [33]. The requirements set out in international standards pertaining to short-circuit capacity in the network should be satisfied at every point of the distribution system under maximum fault current conditions [109].

The increasing short circuit current in distribution networks due to DG integration can be mitigated by the use of Super-conducting Fault Current Limiting Devices (SFCL) [79]. Two types of SFCL viz. resistive type and inductive superconductors are used in electricity networks. In the case of resistive types, the resistance remains significantly small until the fault creates sufficient heat to quench the superconductor, making the SFCL more resistive and thus limiting the fault. An inductive type SFCL is similar to a transformer with the secondary winding made of a closed superconductor ring whose resistance is also negligible during normal operating conditions. The superconductor is however quenched in the event of fault since the resistance of the primary rises sharply. Their usage in networks allows more DG to be integrated in to the distribution network while limiting the negative impacts.

3.6 Conclusion

The chapter highlighted the detailed impacts of DGs on power quality in terms of voltage quality during normal system operation as well as during instances of disturbances. It is evident that grid integration of DGs impacts the PQ of the networks and therefore proper planning of their integration is essential for enhanced network performance. Several power quality measures which include voltage control are capable of mitigating some of the detrimental impacts of grid integration of DGs. The planning of maximum penetration of DGs in electricity networks requires a number of approaches which include upgrading of conductors, network redesign, optimal placement and sizing planning, etc. The optimal planning of DG allocation is an important factor as some vital parameters such as size and location can be identified such that the improvement in overall PQ of the network as well as reduction in system's power losses can be achieved. This will require a proper formulation of the optimization problem and the right choice of optimization techniques depending on the problem solved.

4. The optimal allocation of DGs in utility grids for PQ improvement

4.1 Introduction

For determining optimal solutions pertaining to power quality issues in utility grids with DG, a number of optimization algorithms are employed. This chapter presents the selection of optimization technique to be employed in determination of optimal DG sizes and locations in electricity networks, taking into consideration, the power quality improvement and power loss reduction. Research has shown that placement of DG sources in non-optimal locations in the network results in a number of power quality issues which include over-voltage as well as increased power losses among others [24] [71]. Voltage profile quality is the major concern for PQ issues in utility grids with DG integration. The primary objective for the optimal placement and sizing of DG is therefore the improvement of system's voltage profiles and reduction of active power losses. The application of the techniques to finding optimal siting and sizing of DGs in utility grids will also be highlighted in this chapter. Finally the algorithms which will be applied for finding the optimal solutions in this work will be identified.

The application of optimization algorithms requires modelling the system as an optimization problem such that the best suitable value for the objective function can be obtained. The objective function is subject to a number of constraints that define operational or design constraints [110]. The size and location of DG in the network are some of the design constraints which will be defined for the problem. The voltage limit is one of the operational constraints which will also be defined to ensure that a proper system's PQ is maintained during the entire optimization process. The purpose of applying optimization techniques is to obtain the best locations and sizes of DG units to be integrated to the distribution network, such that the overall power quality of the system is improved in terms of the resulting bus voltage profiles. Some of the popular optimization techniques used in DG placement and sizing problems include Genetic Algorithm (GA), Particle Swarm Optimization (PSO), ant colony optimization, Artificial Bee Colony (ABC), etc.

4.2 Optimization technique selection

Planning of electricity networks involving DG requires application of optimization techniques such that several factors can optimally be determined. The significant aspects whose optimal solutions may be determined for proper planning of DG integration include the best DG technology to be utilized, number and capacity of DG, best location, type of network connection, etc. [23]. The impact of DG integration on network's power quality, power losses, stability and reliability is one of the primary factors to consider for optimal planning of electricity networks with DG integration. Among the

popular optimization techniques in DG allocation problem, GA will be considered and employed in this work because of its faster convergence capabilities and ability to solve non-linear problems. GA also has the ability to avoid being trapped in local minima and can be combined with local search methods increase its exploitation search.

4.3 Genetic Algorithm

Genetic algorithm (GA) is a search and optimization algorithm which is motivated by the principle of natural selection; a biological process whereby stronger organisms are likely to be winners in a competitive environment. GA was introduced by John Holland in 1970 and has been applied in numerous engineering problems requiring optimization of certain parameters. GA is one of the common artificial intelligence, optimization tools which have successfully been used for optimal DG placement and sizing in a number of literatures. The two processes involved in GA are that of individual selection for the production of next generation and that of handling of the selected individual for formation of the next generation [111]. The processes applied to manipulate the selected individual include crossover and mutation. The outcome of the applied selection mechanism is determined by the chosen individual for reproduction as well as the number of offspring's each selected individual produce. The selection strategy in GA therefore employs the principle that the better an individual is; the better chances of being a parent [112].

The GA consists of three different search phases [106]; the first phase creates an initial population; the second phase evaluates the fitness function while the third one produces a new population. The fitness function is used to evaluate each individual from the randomly generated initial population. The individuals are either duplicated or discarded based on their fitness values. The duplicated individuals possess a high fitness value and are generated by the production operator of the GA. Discarded individuals are those with low fitness values [69].

The crossover operator selects two individuals within the generation and a crossover site and synthesizes bits of knowledge obtained from both parents showing excellent performance, thus enhancing the chances of a better offspring. The mutation operator is used to explore some of the invested points in the search space by random flipping of a 'bit' in population of strings [106]. The optimization mechanism of a GA can be adopted and applied in electrical power systems to find optimal solutions for a number of problems. To ensure proper grid planning including DG, GA will be used to determine the optimal location and capacity of DG in electricity networks such that the overall PQ of the system is improved [70].

The brief description of the basic components and processes involved in GA technique is provided below:

a) Initialization of population:

The first step in implementing GA is to create an initial population. This is done after the type of chromosome representation is made. The random number generator that distributes numbers within the specified lower and upper bounds of GA is used to generate the required number of individuals. The initial population is important in GA because it is a basis for the set of possible solutions of a genetic problem.

b) Objective and fitness functions

The objective or fitness function is what the algorithm is trying to optimize. The objective function should be defined to allow for the optimal solutions to be obtained. It provides a measure of how individuals have performed in the problem domain, is used. The parameters to be optimized are defined in an objective function to be evaluated by GA. The fitness function will be defined as a mathematical equation which takes into account all the parameters to be optimized in a problem.

c) Crossover

The crossover operator resembles the biological crossing over and recombination of chromosomes in cell meiosis. The process of obtaining new chromosome from two existing chromosomes employs crossover operation. The crossover operation takes into account the rate of crossover and based on this, the genes are selected and a new child chromosome is generated. The fitness function is then applied to the new child chromosomes after which mutation occurs. The mathematical representation of the crossover is explained using Schema theorem [113] which specifies the expected number of chromosomes $N(s, t+1)$ carrying schema, s in the next generation. The simplified representation is shown by Equation 4-1 below:

$$N(s, t+1) = u(s, t)[1 - e]N(s, t) \quad (4\text{-}1)$$

where $u(s, t)$ is the average fitness of the chromosome carrying schema s at time t, and e is the overal probability that the cluster s will be destroyed or created by mutation or crossover.

The above formula can be rewritten in terms of the probabilities, $P(s, t)$ as shown by Equation 4-2:

$$P(s, t) = \frac{N(s,t)}{N(t)} \quad (4\text{-}2)$$

where $N(t)$ is the size of the population at time t.

d) Mutation

In mutation, gene values in a chromosome are changed from their initial state such that genetic diversity is maintained from one generation to the next. The operation of mutation is also performed on the basis of the rate of mutation. The genes are randomly mutated based on the mutation rate, after which termination occurs. The mutation stage may be represented a constant linear operator on probability vectors as depicted in Equation 4-3 below:

$$M(p)_j = P_{ij}p_1 + \cdots + P_{nj}p_n \quad (4\text{-}3)$$

Where P_{ij} is the probability of i mutating into j.

e) GA termination

The termination stage is where the best chromosome is selected on the basis of the defined fitness function. The process explained above is repeated until the maximum number of iterations is reached. In the context of DG placement and sizing problem, their location and capacity parameters are obtained after the completion of the termination process.

The advantages of using Genetic Algorithm as an optimization technique are listed below:

- GA has the ability to avoid being trapped in local minima;
- GA can be combined with local search methods to increase its exploitation search;
- GA is easy to understand and implement in a number of engineering problems including planning of grid integration of DGs;

4.4 Conclusion

The GA optimization technique discussed above have the capability to obtain the optimal solutions pertaining to PQ improvement in utility networks with DG integration. The GA is selected as an optimization technique to be employed in optimization section of this study. The other motivating factor for the choice of GA is its success in the studies performed in a number of optimization problems in power systems. The detailed GA parameter settings and its application on DG placement and sizing will be discussed on the optimization procedure and problem formulation in the next chapter.

5. Modelling of networks and DG systems

5.1 Introduction

In order to analyse and demonstrate the plausibility of power quality enhancement in electrical networks with DG integration, a discussion of different system models at component level is essential for understanding their effect on the overall accuracy of the system. This will not only help improve the accuracy of the simulation results but will also enhance understanding on the overall operation of the system. The crucial components in a typical electrical network at both the transmission and distribution levels include transformers, transmission lines, busbars, loads as well as the integrated DG systems. Additional components such as voltage regulators and power electronics devices also form part of the power system network; their models are also discussed in this chapter. It is worth noting that the models of certain devices involved in the operation of the distribution system are not included in this chapter. These include protection system, telecommunications and metering systems as they are not the focus of this work.

The description of the optimization procedure and problem formulation for case studies aimed at improving the system's PQ by optimal allocation of DG are also included in this chapter. These include the formulation of the multi-objective function which takes into account voltage profile improvement and total active power loss minimization in the network. The chapter also details the parameter settings of the applied optimization techniques and the methodology followed for the determination of optimal solutions essential for PQ improvement in electricity networks. The necessary coding of the formulated optimization problem as well the applied algorithm is done in MATLAB 2014a environment using the data of the test networks to be discussed.

The work pertaining to PQ enhancement in utility grids using DGs will be executed according to the following outline below:

- The studies of impacts of DG location and penetration levels on network's PQ are carried out on both the transmission and distribution networks by considering two test systems, the IEEE 9-bus and IEEE 33-bus systems.
- PQ improvement using DG is explored on IEEE 9-bus as well as the IEEE 33-bus systems by employing techniques such as reactive power compensation, energy storage installation and optimal DG placement and sizing.
- The optimal allocation of DG for PQ enhancement in electricity networks is executed by employing GA technique. DG ability to improve network's voltage profiles as well as reducing

power losses in the network is investigated through optimization on both the sub-transmission and distribution networks.

5.2 Test networks models

5.2.1 *The IEEE 9-bus system*

One of the test systems used for the purpose of analysing the role of grid integration of DG on PQ enhancement is a standard IEEE 9-bus system which is a built-in test network in DIgSILENT Powerfactory and is represented by a single line diagram of Figure 5-1. The system consists of three synchronous machines which represent conventional generators supplying the network. The synchronous generator at Bus 1 is used as a reference machine and hence Bus 1 is set to slack bus type. The network will be slightly modified by adding busbars from which DG systems will be integrated. The network has different voltage levels as follows; 13.8 kV at generator Bus 1, 18 kV at generator Bus 8, 11 kV at generator Bus 3 and 230 kV at the remaining buses. The part of the network with the loads represents the sub-transmission network. The detailed data showing the values of the respective components of the 9-bus system are presented in Section 10, Appendix A.

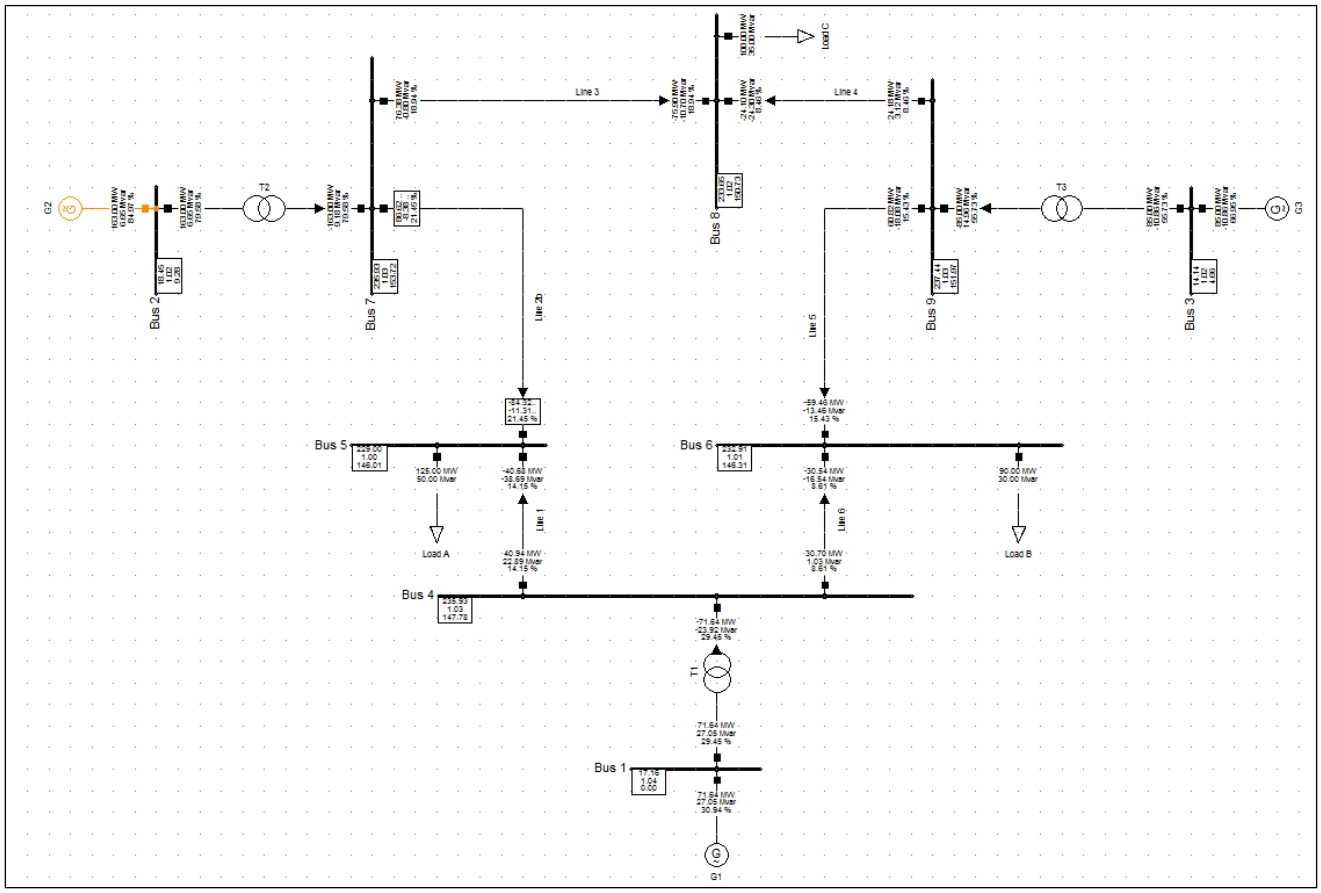

Figure 5-1: The single line diagram of a standard IEEE 9-bus system modelled in Powerfactory

5.2.2 *The IEEE 33-bus system*

The IEEE 33-bus system is employed in this work to represent the distribution network. In this system, Bus 1 is considered as a slack bus at the base voltage of 12kV and base apparent power of 10MVA. The rest of the network's busbars are load buses and potential candidates for DG integration. The system is radial in nature with power flowing from the main substation to the respective load buses. The respective sizes of the loads connected to the system's buses are presented in the Table A-5 in Appendix A. The lines and bus data of the 33-bus distribution system shown in Figure 5-2 are also presented in Table A-4 in Appendix A. The total installed peak demand of the system is 3.69 MW at a power factor of 0.9 lagging. The total active and reactive power losses observed after power flow is executed are 0.2107MW and 0.048MVAr, respectively. The single line diagram of the radial 33-bus distribution system is shown in Figure 5-2 below.

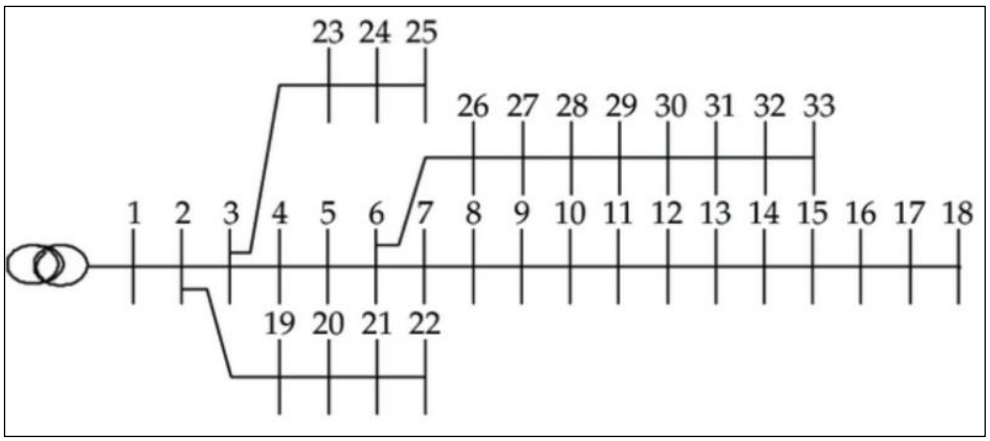

Figure 5-2: The single line diagram of a standard IEEE 33-bus radial distribution system

5.3 Software selection

The simulations of the networks and DG models are done in DIgSILENT Powerfactory version 14.1. DIgSILENT PowerFactory is chosen to execute the case studies in this work because of its embedded functionalities and ability to execute transient analysis of power systems. DIgSILENT also offers a platform for modelling and simulation of generation, transmission, distribution and a comprehensive analysis of DG grid integration [112]. Successful simulations using DIgSILENT had been done by researchers and industrial experts for quite some time and its performance had been satisfactory thus far.

Additionally, DIgSILENT offers the platform to model complex power systems components which are not included in its library. Some of the crucial components which can be modelled in power factory include FACTS devices such as STATCOMs. Power factory allows for the user to define these models through DIgSILENT Simulation Language (DSL). In DIgSILENT PowerFactory, the relevant model

is built in a graphic window of the program by selecting and connecting the components provided in its library.

The case studies involving application of GA optimization technique for PQ improvement are executed by running the relevant codes in MATLAB 2014a. The employed optimization algorithm is written as a code and applied to the test power systems to determine the optimal solutions such as optimal locations and size of DGs in the network. Newton Raphson (NR) power flow method is run in conjunction with GA optimization algorithm by writing the code in MATLAB such that power flow results before and after DG integration are obtained.

Modelling assumptions

Several assumptions are required prior to simulations of the above models of test systems as well as that of DGs. The assumptions considered in this study are aimed at simplifying some of the complexities associated with obtaining accurate results pertaining to PQ improvements in this work. The assumptions made for the purpose of this work are as follows:

- The demand for load is less than the total installed capacity.
- The configuration of the distribution system is radial and is fed by the high-voltage/medium-voltage (HV/MV) substations. The addition of DG to the distribution network structure will therefore maintain the radial configuration of the network.
- All buses in the test networks are considered as potential locations for DG installation with a slack bus being an exception.
- In reality, planning of intermittent DG sources such as wind turbines and PVs is highly dependent on the availability of their resources. It is therefore assumed that the resources capable of generating the desired electrical power as per a particular case study are available.
- From the protection point of view, the circuit breakers equipped with relays exist at the beginning and end of each line for protection of loads at the respective nodes

5.4 DG systems modelling

As stated in the previous sections, two types of technologies, viz. wind and solar PV based DGs will be considered in the study. Their detailed models must be developed and understood for their successful implementation as well as grid integration. The main purpose of integrating DGs to electricity networks is to inject power into the grid for network support and to meet the ever-growing demand. Ideally DG control mechanisms should be able to maximize the amount of generated active

power while maintaining good power quality and enhanced grid stability. The models of several control mechanisms of DGs are also incorporated in this section.

5.4.1 *Solar PV modelling*

A number of PV generator models have been developed and discussed in literatures [52] [54] [68] which have a number of similar components and control strategies. In grid-connected PV systems, the main components include a set of PV arrays that convert the solar energy directly into DC electricity. Hence, the DC-to-AC conversion mechanism is employed prior to grid integration. For grid-connected PV systems with power rating above 1MW, power-conditioning unit is used to convert DC power to AC power because of its ability to keep the PVs operating at maximum efficiency [47]. In some cases, the boost converter with maximum power point tracking (MPPT) controller and a voltage source inverter with hysteresis controller are used so that maximum power can be extracted from the PV source. The discussion of detailed models of the main components of the PV generator system follows.

i. PV array model

A solar panel uses solar photovoltaic semiconductor cells (also referred to as wafers) which produce photocurrent upon exposure to the sun. The PV cell is a building block of PV array and is made of a photosensitive p-n junction diode that produces the photo current I_L as a result of the light falling on it [46]. The direct current output of the cell is a function of solar irradiance and cell temperature. The simplified equivalent electrical circuit of a crystalline PV module is shown in Figure 5-3. In this model, I_L is the current generated by the sunlight, I_d is output terminal DC current. The resistances R_{sh} and R_S are the shunt resistance and internal resistance, respectively.

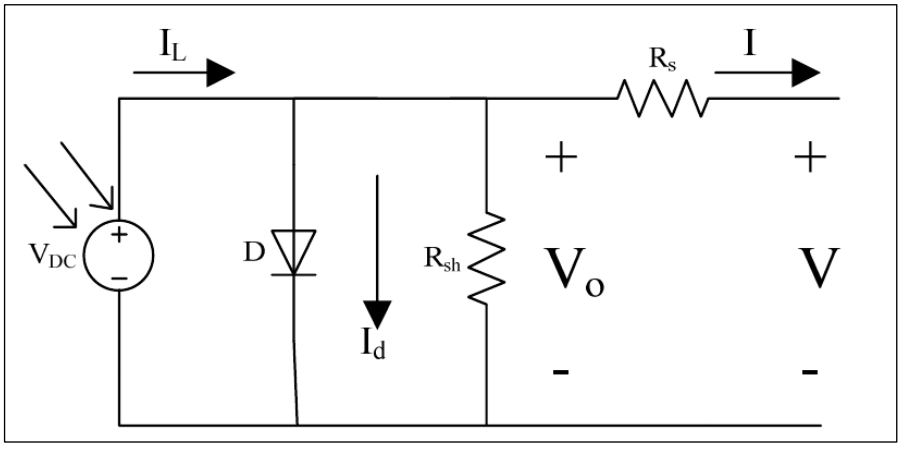

Figure 5-3: Equivalent circuit of the crystalline silicon PV module **[47]**

The output current of a PV module is expressed as a function of photo current I_L, diode current I_d and the voltage V_o across the shunt resistance R_{sh}. Equation (5-1) below is an expression of the output current, I of the PV module shown above.

$$I = I_L - I_d - \frac{V_o}{R_{sh}} \quad (5\text{-}1)$$

The diode current, I_d is obtained using equation (5-2) below:

$$I_d = I_o \left[e^{\frac{qV_{oc}}{nKT_r}} - 1 \right] \quad (5\text{-}2)$$

where I_o is the reverse saturation current of the diode, V_{oc} is the open circuit voltage, q is the charge on an electron ($1.6 \times 10^{-19} C$), k is Boltzmann constant (1.38×10^{-19}), T_r is the temperature on the absolute scale, and n is a factor whose value is between 1 and 2.

The PV array output current, designated as I in Figure 5-3 above is also dependent on several other variables which include electron charge as depicted by the diode current expression in equation 5-2 above. The exponential function used to model a PV cell is derived from the physics of p-n junction so that the PV array output current can be expressed as a function of additional parameters such as cell short circuit current and number of connected PV cells. The detailed expression of PV array output current with relevant parameters included is depicted in equation (5-3) below:

$$I_{PV} = I_{SCA}(G) - N_P \times I_o \left[e^{\frac{(V_A + I_{PV} R_S) q}{n N_S k T}} - 1 \right] \quad (5\text{-}3)$$

where I_{PV} is the array current (A), V_A is array voltage (V), $N_s = N_{CS} N_{SM}$ and $N_P = N_{SP}$ where N_{CS} is the number of series-connected cells in the module, and N_{SM} and N_{SP} are the number of modules connected in series and parallel in the PV array, respectively. R_s is an array series resistance, G represents solar insolation and $I_{SCA} = N_P I_{SC}$ where I_{SC} is the cell short circuit current.

Practical arrays are composed of a number of connected PV cells which can be connected either in parallel or series depending on the requirements of the PV system. The authors in [114] indicated that cells connected in parallel increase the current output of the PV array whereas cells connected in series provide greater output voltages. This is due to the fact that in serial connection of PV modules, the resulting voltages are additive while in a case of parallel connection of modules, the currents become additive. Equation (5-4) is a simplified expression of the array output current with additional parameters included so that the characteristics at the terminals of the PV array can easily be observed [114] .

$$I = I_{pv} - I_o\left[e^{\frac{(V+R_SI)}{V_t a}} - 1\right] - \frac{V+R_SI}{R_p} \quad (5\text{-}4)$$

where I_{pv} and I_o are the PV and saturation currents of the array, respectively and $V_t = \frac{N_s kT}{q}$ is the thermal voltage of the array with N_s cells connected in series. In a case where the array is composed of parallel connected cells, the PV and reverse saturation currents are expressed as I_{pv} and I_o, respectively. Equation (5-4) give rise to the I-V curve shown in Figure 5-4 below with three significant points marked; short circuit current $(0, I_{sc})$, MPP (V_{mp}, I_{mp}) and open circuit voltage $(V_{oc}, 0)$.

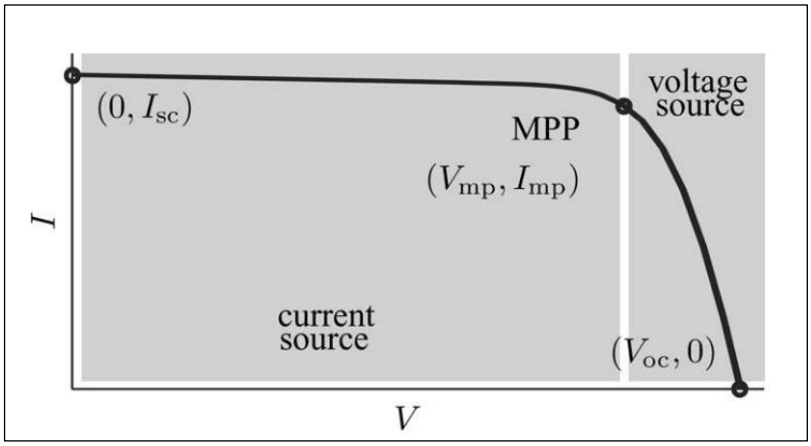

Figure 5-4: Characteristics I-V curve of a practical PV device with three significant points: short circuit, MPP and open circuit **[114]**

The net output current of the cell is computed by subtracting the diode current from the current generated by the incident light as shown in Figure 5-5. The photo-current of the cell is modelled as a constant value whereas that of the diode increases exponentially with the cell voltage.

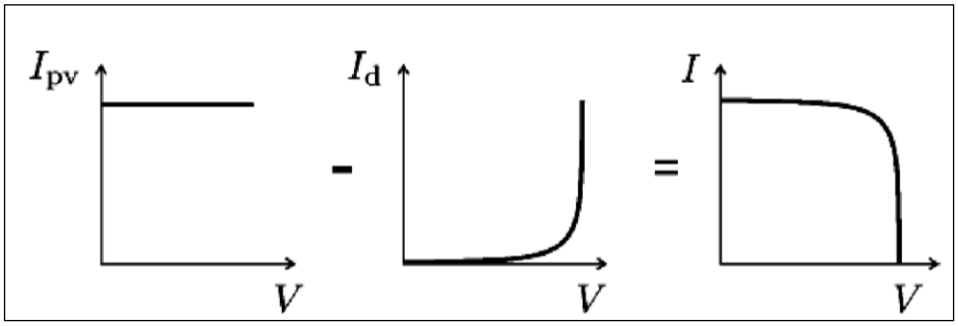

Figure 5-5: Current-Voltage characteristics curve of a PV cell. The total output current is calculated from the light-generated current, I_{PV} and the diode current, I_d **[114]**

The graphical representation of the current output of the cell for different values of output voltages at two different cell temperatures, T_1 and T_2 where $T_1 < T_2$ shown in Figure 5-6 demonstrates that that an increase in cell temperature results in increased current output.

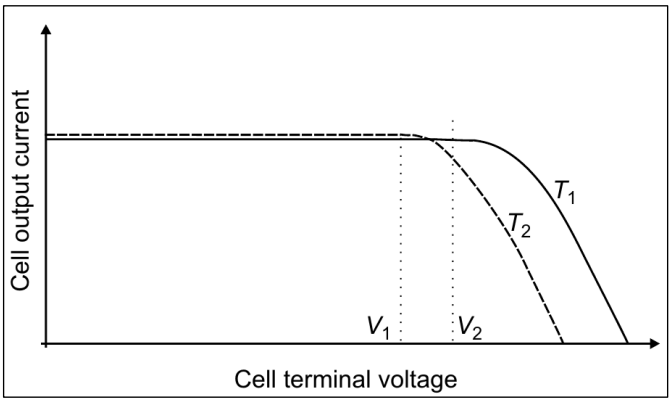

Figure 5-6: The current- voltage characteristics of a PV cell at two temperatures T_1 and T_2 ($T_1 < T_2$) **[46]**

The current generated by the PV device is also highly dependent on the amount of the incident light since the generation of charge carriers is directly affected by the amount of incident light. It is quite difficult to determine the value of the light-generated current without the influence of series and parallel resistances [114]. The assumption $I_{sc} \approx I_{pv}$ was therefore adopted in several texts and is generally used to model PV devices because in practice, the series resistance is low and the parallel resistance is high. The light-generated current of the PV cell is a linear function of the solar irradiation and is also influenced by temperature according equation (5-5) below [114].

$$I_{pv} = (I_{pv,n} + K_1 \Delta T) \frac{G}{G_n} \tag{5-5}$$

where $I_{pv,n}$ is the generated current at nominal condition (25^0C and 1000W/m^2), ΔT is temperature change in Kelvin, G in the irradiation on the cell surface in watts per meters and G_n is the nominal irradiation.

PV cells are either connected in parallel or in series depending on the required output power as the authors in [114] indicated. The choice of connection type also depends on the control strategy and inverter topology employed in grid-integrated PV systems. A number of power inverter topologies and control structures for grid-connected PV systems have been developed and the models are discussed in the next sections. Most control strategies applied to grid-connected PV systems are based on voltage oriented control which is capable of controlling the DC-link voltage as well as regulating the current injected into the grid [115]. The models of converter topologies employed in both the PV-side and grid-side control of grid-connected PV systems and discussed in details below.

A. DC-DC converter model

The main function of a DC-DC converter is to convert a DC input voltage to a DC output voltage with the magnitude higher or lower than that of the input voltage [116] . DC-DC converters are therefore required to produce a regulated output voltage from the PV array, by temporarily storing the input energy and releasing it to the output at the different voltage. Typical MPP voltage range of a PV panel is from 15V to 40 V. Hence DC-DC converters should be designed such that the required voltage is fed in to the AC module for high efficiency operation [117]. The model of the DC-DC converter is already incorporated in solar PV generator model in DIgSILENT and its parameter values are listed in Table B-2 of Appendix B.

B. Inverter model

As described earlier, the function of an inverter is to convert DC power from the PV module into AC power that can be utilized directly by local loads or injected into the grid via a transformer. In grid-connected applications both single-phase and three phase inverters can be employed depending on maximum power output of the system as well as conditions at the PCC. It was however reported in [118] that single-phase inverters inject current into only one phase of the grid, resulting in an imbalance between the phases. Different inverter topologies have been developed and utilized in grid-connected PV systems and each topology has its own pros and cons. For enhanced performance of power networks with grid-connected PV applications, the inverters have vital features such as MPPT, anti-islanding, high conversion efficiency, automatic synchronization with the grid and more importantly, they must have low level of harmonic distortions [118]. The inverter is already incorporated in solar PV generator model built in DIgSILENT and its parameters are listed in Table B-2 of Appendix B.

ii. The model of a grid connected PV system model

The major two sections that form a complete model of a grid connected PV system are the solar power conversion unit and the interfacing unit. The solar power conversion unit consists of the solar panels and mounting equipment while the latter have converters designed for interfacing the PV system to the grid. The main components of a general model of a grid connected PV system with no battery storage are PV array, a DC link capacitor and an inverter as depicted in Figure 5-7 below.

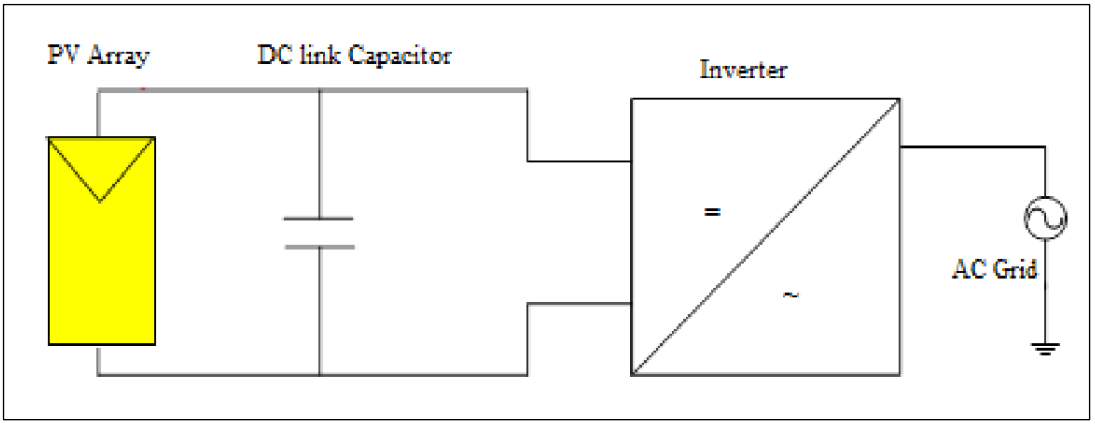

Figure 5-7 Power factory model of a PV system integrated to the grid **[119]**

The generic model of a PV system is already developed and available in the library of DIgSILENT PowerFactory, with some basic control and design features included. PV system is modelled as a static generator due to the absence of any rotating machinery in the system. The static generator template used to represent the PV system in this study has the required control functions and converters incorporated in its design. It is connected directly to a solar busbar from which the transformer can be used to integrate the whole system to the PCC. The compete model of a PV system as simulated in DIgSILENT is shown in Figure 5-8 below.

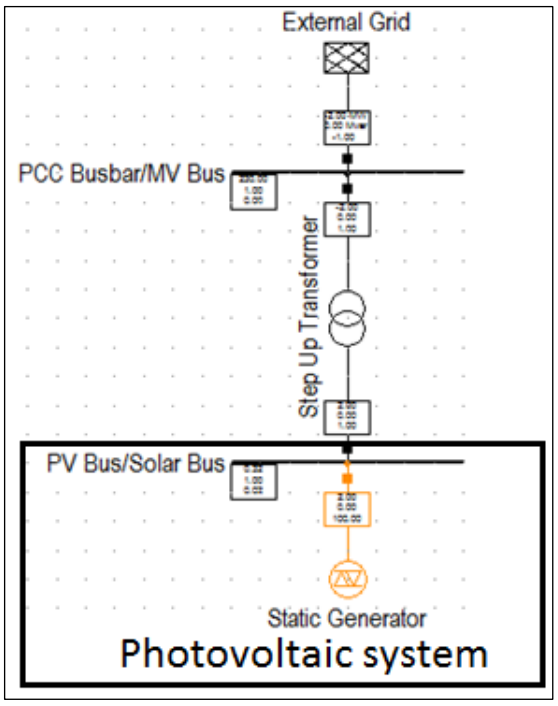

Figure 5-8: Grid-connected PV system modelled as a static generator in DIgSILENT

The static generator in the above model is set to "photovoltaic generator" by selecting a "photovoltaic" module in category list as shown by the typical interface window of the static generator in Figure 5-9 below. As discussed earlier, PV system is operated at unity power factor since it does not inject any reactive power into the grid. The new requirements for grid tied generators outlined in [120], however

show that the operating power factor of a PV system is dependent on the voltage level at the PCC. For instance, the power factor for a PV plant integrated on the medium voltage level should be in the range of 0.95 lagging to 0.95 leading whereas for LV it should be in the range 0.9 lagging to 0.9 leading. The static generator's parameter settings are therefore chosen such that the system operates at a power factor determined by the voltage level at the PCC. The reactive power of the static generator is however maintained at zero since there is no reactive current injection from a PV system.

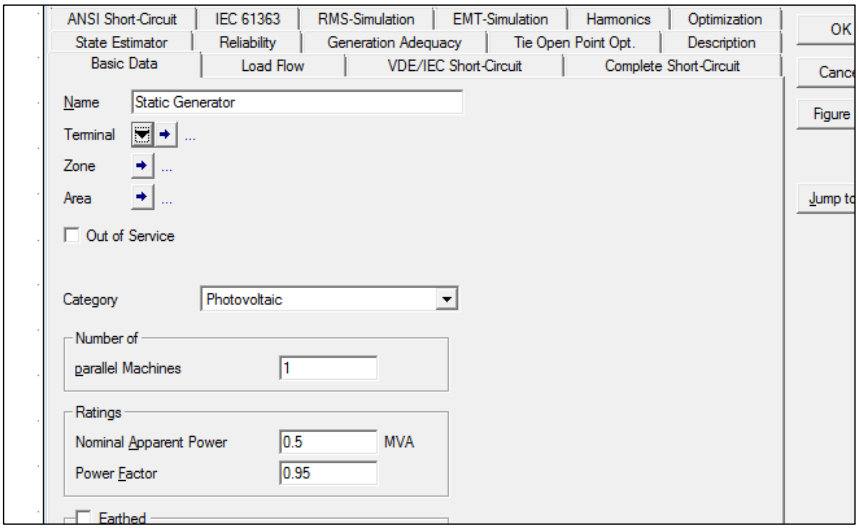

Figure 5-9: The basic data window for static generator in DIgSILENT

The parameter values of a static generator used in PV system model are presented in detail in **Appendix B.** In order to execute the power flow in DIgSILENT PowerFactory, the active power generation of the generator as well as other parameters are initially defined. The parameter settings of the PV module can be altered in accordance with the requirements of the system and case studies conducted. The static generator model is equipped with the local voltage controller, whose control mode is set to power factor control as can be seen in Figure 5-10. The capacity of the PV plant is altered by changing the number of parallel machines in the data input window of DIgSILENT. The reactive power limits of the PV system on the other hand are based on the capability curve of the static generator depicted in Figure 5-10 or can be defined manually.

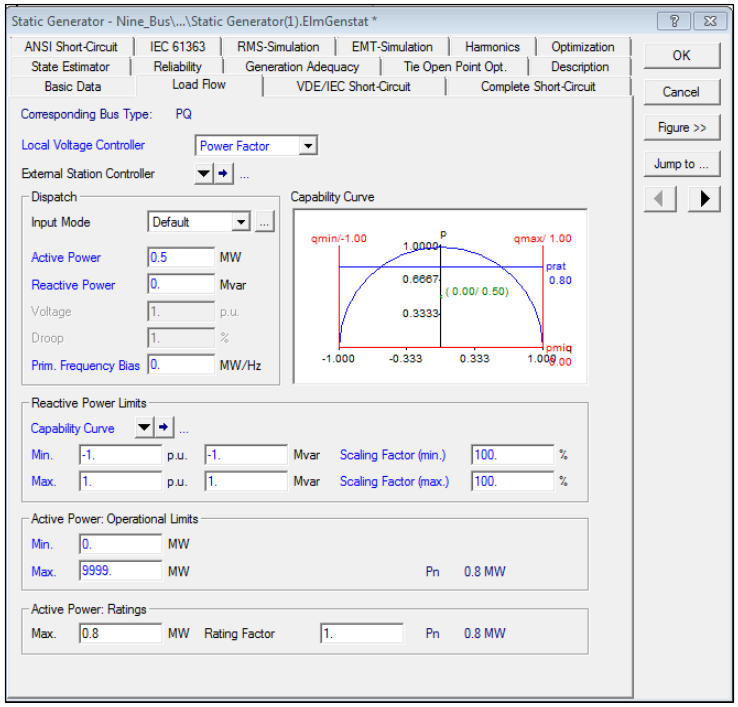

Figure 5-10: Parameter input window of a static generator with the inverters capability curve

5.4.2 *Wind energy conversion systems modelling*

Wind energy conversion systems (WECS) generate electrical energy by harnessing the kinetic energy of the flowing air masses using the blades. In order to understand electricity generation in WECS, it is important to consider the aerodynamic models of the wind turbine. This model used to determine the characteristics of the wind turbine. The kinetic energy of the air masses is used to drive the wind turbine. The power in the wind is thus represented as the rate of change of kinetic energy. Equation (5-6) is used to define the mechanical power, P_W extracted by the rotor blades takes into account the difference between the upstream and downstream wind velocities as shown below [121]:

$$P_W = \frac{1}{2}\rho A V_W (V_u - V_d) \qquad (5\text{-}6)$$

where:

A : is area swept by rotor blades in m^2

ρ : Represents the density of the wind in W/m^2

V_W : Average velocity of rotor blades in m/s

V_u : Downstream wind velocity in m/s

V_d : Upstream wind velocity in m/s

The simplified version of the above equation is the following equation (5-7) which includes the power coefficient of the rotor, C_p.

$$P_m = \frac{1}{2} C_p \rho A V^2 \quad (5\text{-}7)$$

The output power of the wind turbine is dependent on the area of the swept rotor blades, power coefficient of the rotor and the wind speed. Varying the power coefficient of the rotor as well as the areas of the blades will change the turbines output power. Wind speed however, is a natural phenomenon and there is no direct control in its dynamics. There are several wind turbine types in the market including the Permanent Magnet Synchronous Generator (PMSG), Squirrel-Cage Induction Generator (SCIG) and a Doubly Fed-Induction Generator (DFIG). The popular generator technology used in the market today is a DFIG wind turbine due its performance abilities. The DFIG turbine model is considered in this study.

i. DFIG wind turbine model

The DFIG in a wind turbine model is an induction machine operated at speed greater than its synchronous speed. The DFIG operates on similar principles as the wound-rotor induction generator equipped with external power electronic circuits on the rotor and stator windings [122]. In A DFIG, both the stator and rotor are connected to the grid and the latter is connected via power electronics converter. The three phase stator winding of the DFIG system is fed directly from the three phase supply voltage which is usually less than 1 kV. The rotor excitation is done through AC voltage from the back-to-back AC-DC-AC power convertor connected to the rotor windings. The schematic of a DFIG model with the relevant components indicated is presented in Figure 5-11 below.

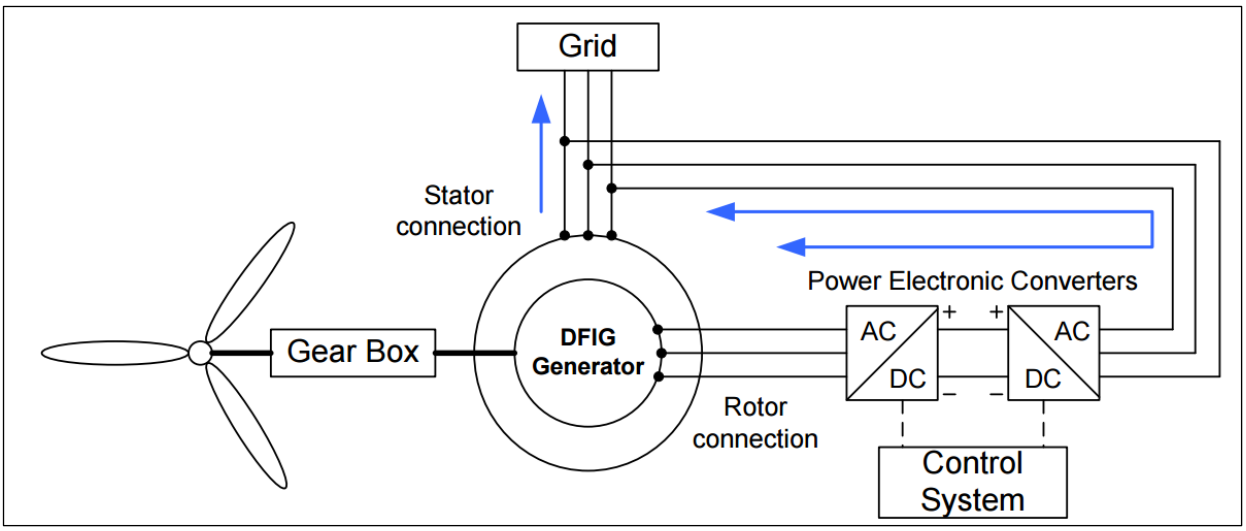

Figure 5-11: The schematic of a DFIG wind turbine based system **[122]**

The DFIG wind turbine system is equipped with a gearbox for control of wind speed between the rotating blades and DFIG generator. As depicted by Figure 5-11 above, the generator is connected to the grid on both the stator and rotor sides. Due to the difference of stator and rotor side voltages, the

three-winding transformer will be used to model grid connected DFIG as will be shown in DFIG model in PowerFactory. The control mechanism of the machine is via converters connected between the rotor and the grid. The controlled quantities in a DFIG generator are either total active and reactive powers or the total active power and voltage of the stator. Since only a small part of the total active power is exchanged with the grid via the rotor, the stator active power can be controlled to control the total active power of the machine.

As indicated in Figure 5-11 above, the model of DFIG system consists of a drive drain system consisting of a gearbox and shaft capable of increasing the rotational speed of the shaft [123]. The stator winding of the DFIG system is corrected directly to the grid while the rotor winding is connected via the AC-DC-AC power electronics converter. Equation (5-8) below is used to model the shaft torque of the drive drain system of DFIG.

$$\frac{dT_{tw}}{dt} = K_s N_m \omega_t - K_s \omega_g \left[\frac{N_m^2 B_s}{J_t} - \frac{B_s}{J_g}\right] T_{tw} + \frac{N_m B_s}{J_t} T_t + \frac{B_s}{J_g} T_g \qquad (5\text{-}8)$$

where the individual parameters represent:

dT_{tw}, T_t and T_g : Drive train torque, Turbine and generator torques respectively

K_s: Shaft stiffness

N_m : Ratio of gear

ω_t and ω_g : Turbine and generator rotational speeds respectively

J_t and J_g : Turbine and generator inertias respectively.

B_s: Damping coefficient

The equations demonstrating the electrical characteristics of the DFIG model are derived by considering the equivalent circuits of the stator and rotor in a rotating frame as depicted in Figures 5-12 (a) and 5-12 (b) below.

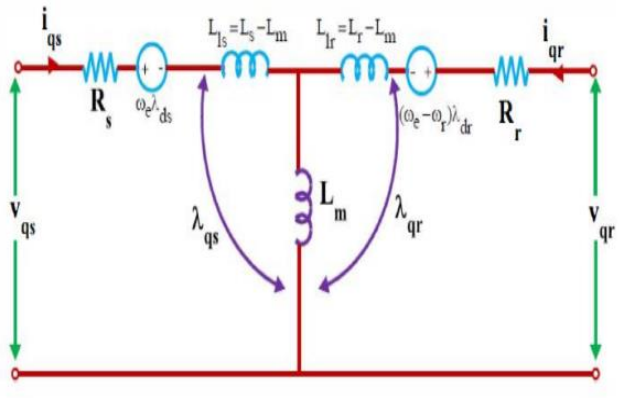

Figure 5-12 (a): DFIG equivalent circuit in the q-axis reference frame **[124]**

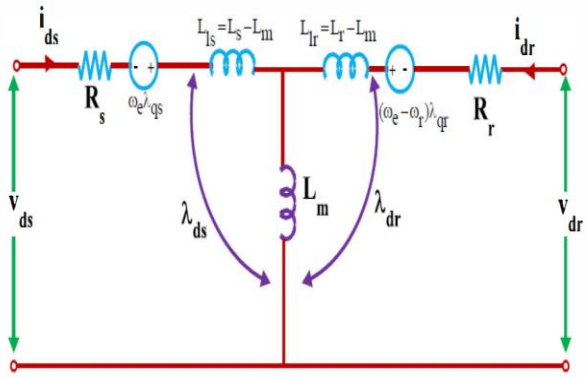

Figure 5-12 (b): DFIG equivalent circuit in the d-axis reference frame [124]

The stator and rotor equations are as listed below:

$$V_{qs} = P\gamma_{qs} + \omega\gamma_{ds} + r_s i_{qs} \quad (5\text{-}9)$$

$$V_{ds} = P\gamma_{ds} + \omega\gamma_{qs} + r_s i_{ds} \quad (5\text{-}10)$$

$$V_{qr} = P\gamma_{qr} + (\omega - \omega_r)\gamma_{dr} + r_r i_{qr} \quad (5\text{-}11)$$

$$V_{dr} = P\gamma_{dr} + (\omega - \omega_r)\gamma_{qr} + r_r i_{dr} \quad (5\text{-}12)$$

where V_{qs} and V_{ds} are the stator voltages in the q and d frames respectively, V_{qr} and V_{dr} are rotor voltages in the q and d frames respectively, γ_{qs} and γ_{ds} are stator flux linkages in the q and d frames respectively, γ_{qr} and γ_{dr} are rotor flux linkages in the q and d frames respectively,r_s and r_r are resistances of stator and rotor respectively, ω is the rotational speed of the rotor and P is the constant.

The model of the DFIG wind turbine as modelled in DIgSILENT PowerFactory is depicted in Figure 5-13 below. The main components of the model include a DFIG machine, back-to-back PWM converter which includes the DC link, the three winding transformer and the shunt filter. DFIG machine is the main power source and the PWM converter acts as a control system for the DFIG system. The shunt filter is included in the model for mitigation of harmonics. The stator voltage is set to 3.3 kV and that of the rotor at 1.15kV. The grid voltage will depend on the voltage level at the PCC. The three windings transformer is therefore included to interface the stator and rotor outputs to the grid. The initial settings of the individual components included in the DFIG model are presented in Table B-8 in appendix B.

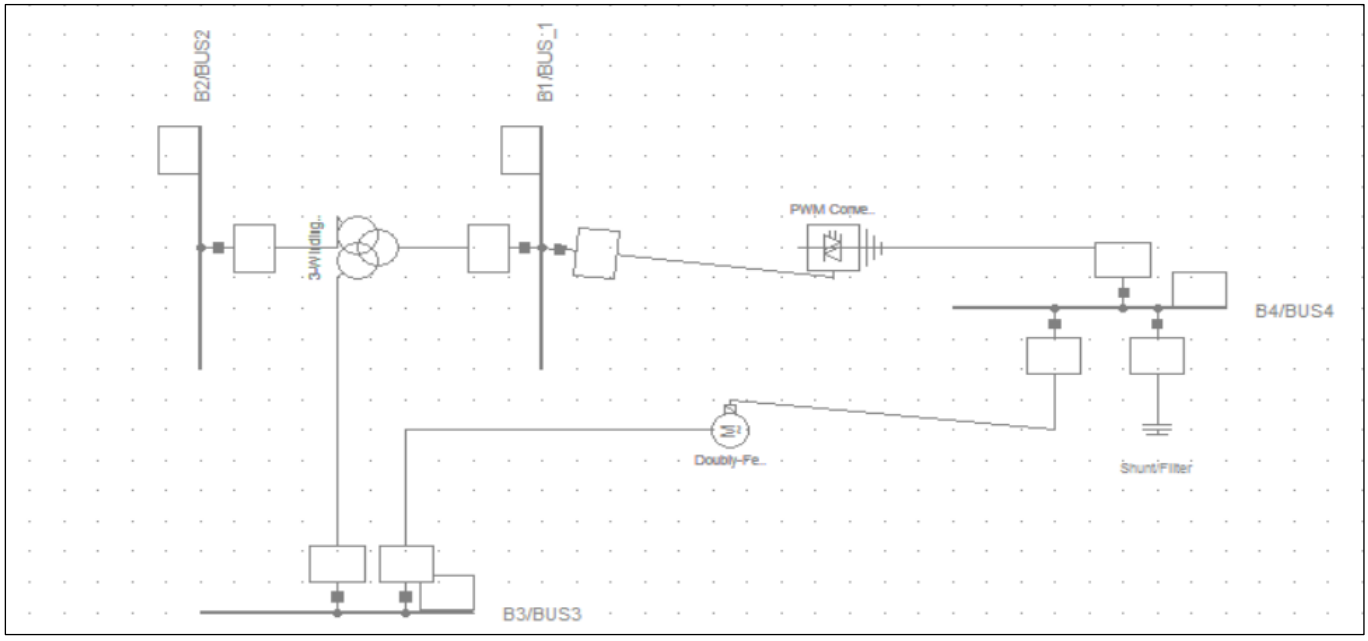

Figure 5-13: The model of grid-integrated DFIG wind turbine

ii. DFIG converter model

The converter in a DFIG wind turbine models is an interface between the rotor and the grid. The DFIG converter model consists of a rotor side converter which controls the torque production of the DFIG and the grid side converter which regulates the voltage of the DC link between the two converters [125]. The DC link capacitor is connected between the two converters to smoothen output voltage. The back-to-back PWM converters employed in a DFIG turbine model in this work are as depicted in Figure 5-14 below. The values of the parameters assigned to the converter are detailed in Table B-6 in Appendix B.

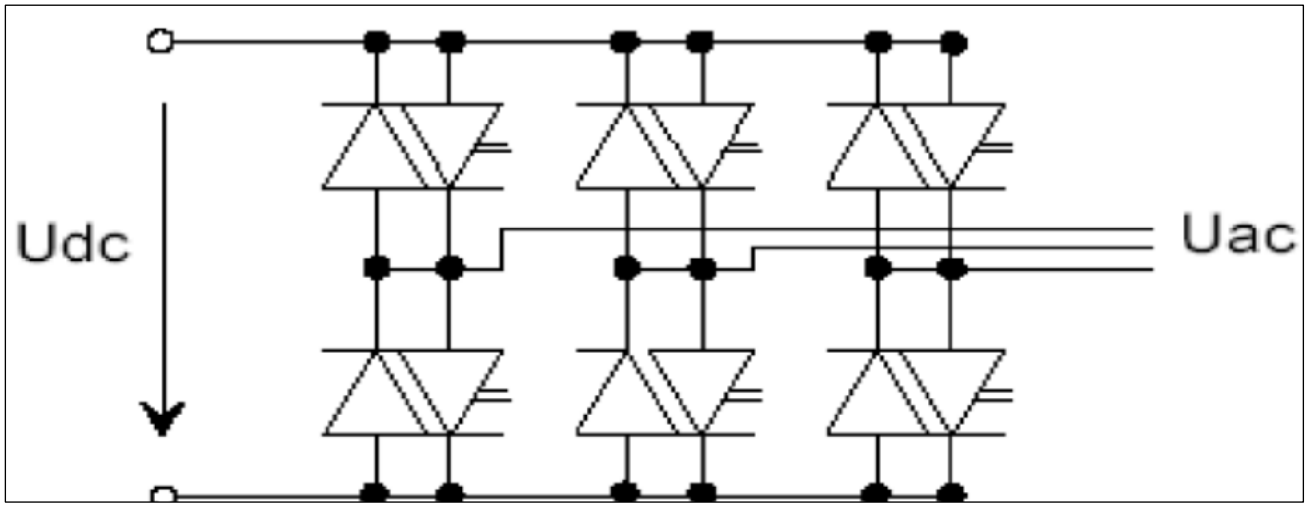

Figure 5-14: The PWM model for DFIG **[126]**

The converter's input DC voltage and the corresponding AC output voltage are related by equations (5-13) and (5-14) below:

$$U_{ACr} = K_0 \times PWM_r U_{DC} \quad (5\text{-}13)$$

$$U_{ACi} = K_0 \times PWM_i U_{DC} \quad (5\text{-}14)$$

where U_{ACr} and U_{ACi} are real and imaginary components of the AC voltage, respectively; PWM_r and PWM_i are real and imaginary components of the modulation factor, respectively; U_{DC} is the DC voltage and K_0 is a constant dependant on the nature of PWM wave form.

5.4.3 *Energy storage modelling*

Energy storage will also be employed as PQ improvement measure in grid connected DGs so that it contributes to voltage regulation. As discussed earlier, incorporating a form of energy storage system (ESS) at PCC of DGs can also smooth out power fluctuations by charging and discharging process. The type of ESS considered in this study is battery energy storage system (BESS) due to its popular application in renewable energy systems and availability of its model in DIgSILENT PowerFactory. The dynamic model of the BESS implemented in DIgSILENT comprises converter, frequency control, PQ-measurement, charger control as depicted in Figure 5-15 below: The significant parameters of the BESS components as well as its ratings are presented in Appendix B.

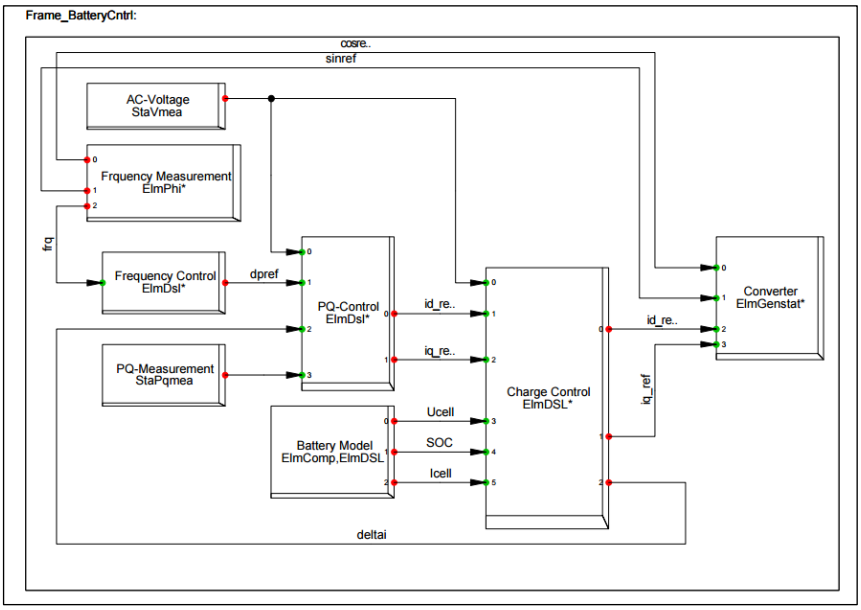

Figure 5-15: The composite model of the BESS in power factory

5.5 Model of voltage control schemes

It was established that DFIG-wind farm may not be able to provide adequate reactive power for voltage support, particularly during instances of grid side disturbances such as three phase faults. This is due to limited reactive power capacity of DFIG wind farms connected to distributions and sub-transmission networks. For the purpose of maintaining the transmission line voltage and decreasing the voltage sags due to insufficient reactive power, the devices capable of injecting or absorbing reactive power are employed. The Static Synchronous Compensator (STATCOM) and Static Var Compensator (SVC) will be employed as voltage control mechanisms for the purpose of improving PQ in grid connected solar PV and DFIG systems.

DIgSILENT offers a platform to model different FACTS devices used for voltage control. The STATCOM is modelled in DIgSILENT Powerfactory using the library element called static generator. The static generator can be utilized in a number of applications including PV generators, fuel cells, reactive power compensator and wind generator. The static generator is set to operate as STATCOM by operating it in reactive power compensation category. The static generator is then set to resemble the behaviour of STATCOM by defining a set of equations in DIgSILENT Simulation Language (DSL). The control block of STATCOM responsible for controlling the absorbed or injected reactive power is also defined in DSL as depicted in composite frame model of DIgSILENT shown in Figure 5-16.

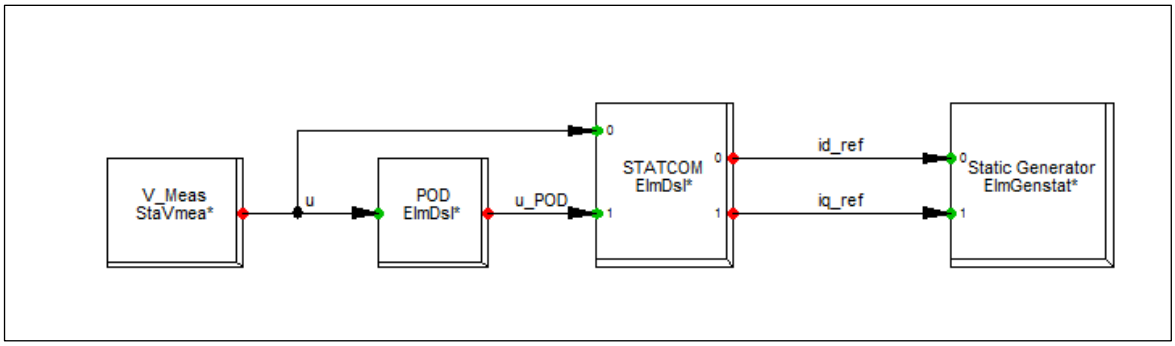

Figure 5-16: Implementation of STATCOM control block diagram in Power factory's composite frame

DSL allows programming of control modes of power systems elements such as STATCOM. The DSL model of STATCOM is developed by defining its composite model and relating it to the power system such it runs inside the time domain simulation. The composite model is represented using a block diagram referred to as composite frame as depicted in Figure 5-16. The STATCOM model is first initialized to link its controller to the grid. The output of the STATCOM is linked to the input of the static generator *ElmGenstat* object. The *Static generator ElmGenstat* is a library used to model the

STATCOM in PowerFactory. The parameters of the STATCOM controllers such as controller gain are left at default values and only rated apparent power is specified.

The SVC is a built-in model in DIgSILENT power factory and has the ability to be set in two different reactive control modes viz. reactive power control mode and voltage control mode. The SVC parameter setting window in PowerFactory offers an option to either select reactive power control or voltage control mode of operation in control tab. In reactive power control mode, the reactive power production or consumption to the system is constant, while voltage control mode seeks to keep the voltage at the specified voltage set point by reactive power contribution. The SVC will be operated in voltage control mode with the voltage set point set at 1.1 p.u. in distribution network and 1.05 in sub-transmission network for the purpose of controlling the voltage locally. Voltage set point is chosen based on voltage operating range for LV, MV and HV networks specified by the SA renewable energy grid code [22]. The respective choice of operating mode is done in power factory by double clicking on the SVC model as depicted in Figure 5-17 below.

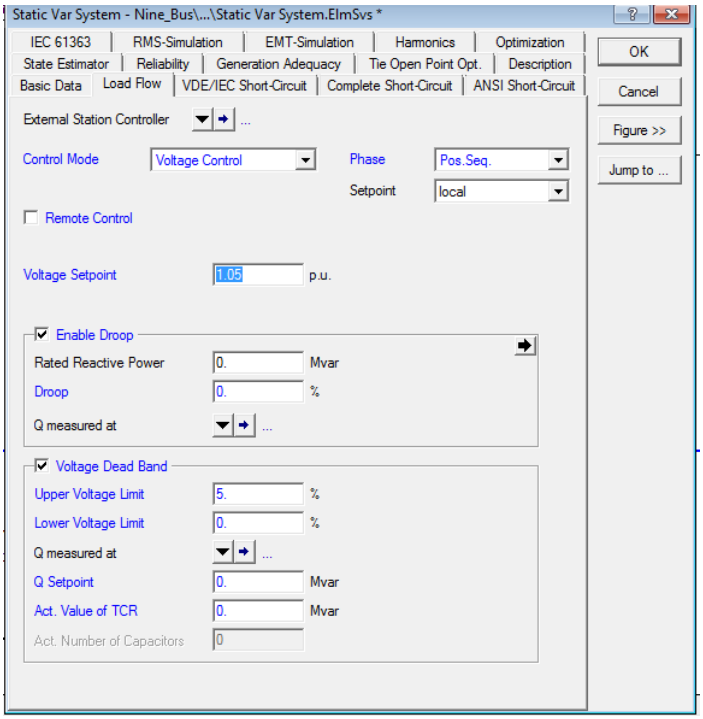

Figure 5-17: SVC model settings in DIgSILENT PowerFactory

5.6 Optimization procedure and problem formulation

In order to effectively determine the optimal solutions pertaining to a proper grid integration of DGs, their optimal location and sizing must be determined to ensure the improvement of the overall PQ of the network. Genetic Algorithm (GA) technique is used to obtain the optimal size and location of integrated wind and solar PV systems on IEEE 9-bus and IEEE 33 bus test networks previously

described. Research has established that the optimal penetration levels of DGs in electricity networks result in improved voltage profiles and reduced active power losses. The objective function for the optimal allocation of DGs therefore seeks to minimize the total active power losses of the system while improving the voltage profiles subject to defined constraints.

5.6.1 *Objective function*

The main objective of the proposed optimization procedure is to minimize the total active power losses and improve the voltage profile of the system. The multi-objective function for the problem in this study is adopted from [71] and modified such that voltage profile improvement is incorporated. The objective function in [71] is formulated only to maximize power loss reduction in the network. Voltage profile improvement is therefore included by adding an expression that provides voltage values at network buses. The mathematically formulated objective function applied in an optimization procedure is given by equation (5-15):

$$f = Min((f_1 + k_1 f_2) + \beta_1 \sum_{i \in N_{DG}} [\max(V_{ni} - V_{ni}^{max}, 0) + \max(V_{ni}^{min} - V_{ni}, 0)]) \quad (5\text{-}15)$$

The functions f_1 and f_2 are the objective functions for the total active power loss and voltage profile improvement, respectively. The penalty coefficients k_1 and β_1 are random numbers in the range of [0, 1] and are set to 0.5 and 0.3, respectively for this problem. The bus number where DG is installed is represented by N_{DG}. V_{ni} is the voltage magnitude at bus, ni. The maximum and minimum voltages at the particular bus are denoted as V_{ni}^{max} and V_{ni}^{min}, respectively. The mathematical formulation of the functions f_1 and f_2 are as expressed by Equations (5-16) and (5-17) below:

$$f_1 = P_{Loss} = \sum_{(i,j)=1}^{N} P_{L(i,j)} \quad (5\text{-}16)$$

$$f_2 = \sum_{ni=1}^{n_n} (V_{ni} - V_{rated}) \quad (5\text{-}17)$$

where P_{Loss} is the active power losses of the line and N is the number of branches in the network. V_{rated} is the rated voltage of the network and is chosen as 1 p.u in this work. The individual system's active power losses are calculated using line resistance, R and the respective branch current by applying the following equation:

$$P_{Loss\,i} = I^2 R \quad (5\text{-}18)$$

The main constraints to this problem are the capacity of DG and the voltage range specified by the grid codes governing grid integration of DG into utility networks. The voltage limits are decided based

on the grid integration of DG which allows the maximum voltage variation of $\mp 5\%$ and $\mp 10\%$ in sub-transmission and distribution networks, respectively. The bus voltage and DG capacity ranges considered in this work are defined in equations (5-19), (5-20) , (5-21)and (5-22) below.

$$0.9\ p.u\ \leq V_i\ \leq 1.1\ p.u\ (For\ IEEE\ 33-bus\ network) \quad (5\text{-}19)$$

$$0.95\ p.u\ \leq V_i\ \leq 1.05\ p.u\ (For\ IEEE\ 9-bus\ network) \quad (5\text{-}20)$$

$$0.1MW \leq P_{DG} \leq 6.5MW \quad (5\text{-}21)$$

$$-5MVar \leq Q_{DG} \leq 5MVar \quad (5\text{-}22)$$

The results obtained when the above objective function is solved in MATLAB are the total power losses in MVA of the system before and after DG placement and sizing, the voltage magnitudes in p.u at system's buses before and after optimal DG placement. The size and locations of DGs on the network also form part of the results of the optimization process. The optimal size and location of DG are printed on the output window after each generation until the optimal solution is found.

5.6.2 *Load flow*

The purpose of executing the load flow in power systems analysis studies is to obtain information regarding magnitudes and phase angles of bus voltages, real and reactive powers on the transmission lines and generator buses as well as other variables. There are a number of numerical methods essential for load flow analysis in power systems. These include Gauss-Seidel, Newton-Raphson and fast decoupled methods. As explained earlier, the load flow in DIgSILENT PowerFactory is executed by clicking the load flow calculation button in the software. The load flow in solving the optimization problems in MATLAB is executed by employing the conventional Newton Raphson method to calculate the relevant variables. This method is the practical method of obtaining load flow solutions in bigger power networks. The flow of power between system's buses is computed using NR because it takes less number of iterations to complete the power flow.

The conventional Newton Raphson (NR) method is defined by writing the relevant power flow calculation equations in MATLAB code. Equations (5-23) and (5-24) are used to compute the real and reactive power between the buses. Load flow method is appropriately combined with GA technique to achieve the optimal solution to the problem.

$$P_i = P_{DGi} - P_{Di} = |V_i| \sum |V_k| \left(G_{ik} \cos(\theta_i - \theta_k) + B_{ik} \sin(\theta_i - \theta_k)\right) \quad (5\text{-}23)$$

$$Q_i = Q_{DGi} - Q_{Di} = |V_i| \sum |V_k| \left(G_{ik} \sin(\theta_i - \theta_k) + B_{ik} \cos(\theta_i - \theta_k)\right) \quad (5\text{-}24)$$

where P_i and Q_i are net active and reactive powers in MW and MVAR, respectively at bus i, respectively. P_{DGi} and Q_{DGi} are the active and reactive powers of DG in MW and MVAR, respectively at bus i while P_{Di} and Q_{Di} are the active and reactive loads MW and MVAR, respectively at bus i. V_k and V_i are voltage magnitudes in p.u. at bus k and bus i. G_{ik} and B_{ik} are real and imaginary parts of the element in the bus admittance matrix corresponding to the ith row and kth column. θ_i and θ_k are the voltage angles at bus i and bus k, respectively.

The NR load flow is run in conjunction with GA technique by first defining the Equations (5-23) and (5-24) after the network's line and load data has been entered in Matrix format on MATLAB. The voltage magnitudes at each node as well as the power losses are then calculated and displayed. The GA then uses the results of the power flow to determine the optimal locations based on the nodes voltage magnitudes and total active power losses after power flow is executed. After GA determines the optimal DG placement, NR load flow is executed again to obtain the voltage magnitudes as well as the power losses across the lines of the network to observe the improvement.

5.6.3 *Optimal DG placement and sizing using Genetic Algorithm (GA)*

As discussed in Chapter 4, GA is implemented by specifying the settings of a number of parameters essential for its execution. GA op106erates on a set called 'population', and a number of possible solutions, referred to as 'individuals' of a genetic problem [127]. The population size is different depending on the type of network considered. For example, the population size is set to 5 for the IEEE 9-bus system and 32 for the 33-bus system. It was highlighted in [112] that the best results are achieved when the population size is equal to the dimension of the problem, i.e. the number of network's nodes. There are 32 nodes which are candidates for DG integration for the 33-bus system while for the 9-bus system, there are only 5. The number of generations is set to 10, which indicates that the optimal solution is obtained after 10 generations.

The initial population is set up before executing each case study depending on the number of variables being optimized. For instance, when determining the optimal location and size of a single solar PV on a 33-bus system, the initial population will have two variables representing the initial location and size of DG. In this case, the initial population can be set as bus 30 and 2MW in MATLAB code. It is important to define the initial population because GA starts with a randomly generated initial population within which each individual is evaluated by means of an objective function defined by equation (5-15). The individuals in the starting and next generations are copied or discarded based on

their fitness values. GA operators are then employed to identify the generation with high performing individuals.

The objective function defined by equation (5-15), together with other parameters such as the upper and lower bounds of DG location and capacity are taken as inputs to the main GA function programmed in MATLAB. The test systems used in the determination of the optimal sitting and sizing of DGs are IEEE 9-bus system which represent the sub-transmission network and IEEE 33-bus system which represents a distribution network. The lower and upper bounds of DG locations are therefore set to bus 4 and bus 9 for a 9-bus system and bus 2 and bus 33 for a 33 bus system, respectively. In the case of a 9-bus system, bus 1, 2 and 3 are excluded because the conventional generators are connected at these buses. For the 33-bus network, bus 1 is excluded in the range because it is a slack bus and considered a non-ideal location for DGs. The lower and upper bounds for DG capacity are set to 0.1 MW and 6.5 MW in the case of solar PV integration. For the DFIG, the lower and upper bounds of real and reactive powers of DG are set in the range, 0.1MW to 6.5 MW and -5 MVar to 5 MVar, respectively.

The inputs essential for the computation of GA function in MATLAB code include the objective function, linear equality and inequality constraints, the bounds discussed above as well as GA parameters such as population size. Some of the outputs of this function include the optimal location and size of DG unit which had been initialized as a vector whose size depends on expected solutions. The program therefore outputs the DG size and its corresponding location. The procedure of GA employed to find the optimal solution as per defined fitness function involves a random generation of an initial population of possible solutions by following the procedure outlined below:

- For each solution, the bus number of DG location as well DG capacity are selected between the lower and upper bounds specified above.
- The objective function defined by equation (5-15) is used to provide the measure of individual's performance in the problem domain.
- A number of DG sizes are randomly chosen until the assigned size is reached while ensuring that the constraints specified are maintained.
- DG units are then randomly located among the different buses of the network except for bus1 which is a slack bus.
- The objective function is used to evaluate and scale the fitness of each solution
- New solutions are then produced by application of genetic operators whose implementation details consist of *selection*, *crossover*, *mutation* and *reinsertion* processes explained in section 4.3.

- After the specified number of iterations is reached, GA is terminated and the optimal solution is displayed.

5.7 Conclusion

This necessary modelling of the test networks and DG for the purpose of enhancing PQ in electricity networks have been presented in this chapter. The models of the techniques capable of improving PQ such as reactive power compensation and their implementation is Powerfactory have also been explained. The problem formulation for the optimal placement of DG is executed to demonstrate the capability of DGs in enhancing PQ in sub transmission and distribution networks.

6. Planning case studies

This chapter explains the case studies conducted for the purpose of investigating the role of grid integration of wind and solar farms on power quality enhancement. The simulation set-up of network models discussed in chapter 5 is presented in detail. The case studies conducted are aimed at investigating the enhancement of the network's PQ when wind and PV based DGs are integrated. The simulation process seeks to investigate the behaviour of crucial parameters such as network voltage profile which is essential in identifying the network PQ. Some case studies seek to determine the optimal solutions pertaining to grid-integration of DGs such as size and location of DGs in the network. The system's power losses are also significant for the efficient and economic operation of the power system. In addition to voltage profile, the total active power losses of the system losses will be investigated in different case studies. In all case studies conducted, the comparative analysis is made between grid-integration of solar PV plants and DFIG-based wind farms on the basis of PQ improvement and active power loss reduction of each DG type.

6.1 Case 1: Networks operation without DG integration (Base case)

The base case seeks to investigate the performance of the IEEE 9-bus (please see Figure 5-1) and IEEE 33-bus (please see Figure 5-2) networks in terms of the bus voltage profiles and the overall active power losses of the network when no DGs are integrated. The networks are built in DIgSILENT PowerFactory and the voltage magnitudes at different buses of the network are observed after the power flow is executed. The analysis is done firstly when no faults are occurring in the network and secondly when faults occur in the network. The three phase fault is applied at line 2 of the 9-bus system and between bus 4 and bus 5 of the 33-bus distribution system as shown in Figure 6-2 and Figure 6-3. The simulation is run for 20 seconds and the fault is set to occur at t=1s and is cleared after 0.1 second at t=1.1s.

6.2 Case 2: Effect of DG placement on PQ enhancement

This case study investigates the performance electricity networks when DGs are integrated at different buses of the network. The idea is to observe the impacts of DG location on voltage profiles at the PCC and overall active power losses of the networks. In this case study, the size of DG is kept fixed while its location is varied in terms of the bus at which it is integrated. The system's performance is analysed on the basis of the resulting voltage profiles and power losses when DGs are integrated at different buses of the network. The study seeks to observe whether the placement of DGs in a network will improve voltage profile and reduce system's power losses. The buses of the network which result in

better voltage profiles after DGs are integrated are identified. All bus bars of the test network are considered as the potential candidates for DG integration except bus 1 which is a slack bus to which the external grid is connected. The investigation is done on both the IEEE 9-bus sub-transmission network and IEEE 33-bus network shown in Figure 6-1 and 6-2, respectively.

The impact of grid-integration of DGs on PQ is investigated during the normal operation of the power system firstly when there are no faults in the network and secondly when a fault occurs in the network. The voltage profiles and the overall active power losses resulting from DG-integration at a particular bus are observed and compared to that of the base case. The difference between the impacts of integration of solar PV and DFIG-based DGs on PQ and their capacity to improve the system's PQ are investigated by comparing the results obtained for each technology.

6.2.1 *DG placement on IEEE 9-bus sub-transmission network*

The impact of DG location is investigated on the IEEE 9-bus system by observing the PCC voltage profiles and overall active power losses after DG integration at different network buses. The results of the base case without DG-integration are used as reference for comparison. For this network, the buses used for DG integration are bus 2 to bus 9. The size of DG is kept fixed at 10MVA. PQ is investigated for both solar PV and DFIG-based DGs integrated at different times, such that the performance of each DG type can be independently analysed. The analysis of the impacts of DG location on the network's PQ is performed on the 9-bus system through the following sub-cases:

- The performance of the network in the absence of faults in the system is investigated for integration of DFIG and solar PV at different buses. The simulation is run for t=20s and no short circuit or switching event is set to occur after t=0.
- DG ability to support the system's voltage profile is investigated by applying a three phase fault at line 7 of the test system. The simulation is run for 20 seconds and the three phase fault is set to occur during the first second (t=1s) and is cleared after 0.1 seconds (t=1.1s). From t=1.1s to t=20s the system is simulated to operate normally.
- The comparative analysis of grid integration of solar PV and DFIG-based DGs is done in terms of the resulting voltage profiles and system's active power losses for both normal (without fault) and abnormal (with fault) network operating conditions.

6.2.2 *DG placement on IEEE 33-bus distribution network*

The impact of DG location in distribution networks is investigated on IEEE 33-bus distribution system. The 33-bus distribution network as depicted in Figure 6-2 consists of 4 branches identified by bus numbers from which loads are connected. The effect of DG location is investigated by observing

the bus voltage profiles and overall active power losses of the network as DG is integrated at different branches. Table 6-1 lists bus bars corresponding to each of the branches of the 33-bus system. The total load capacity supplied by each branch is also listed in Table 6-1. Solar PV and DFIG-based DGs are independently connected to the first bus of each branch which is bus 23 (Branch 1), bus 26 (Branch 2), bus 7 (Branch 3) and finally bus 19 (Branch 4). The size of DG used for this network is fixed at 5 MVA, due to the load size of this network.

Table 6-1: The branches with the corresponding buses and total load size of the 33-bus distribution network

Branch name	Bus number	Total load
Branch 1	23-25	930 kW, 450 kVar
Branch 2	26-33	920 kW, 410 kVar
Branch 3	7-18	1075 kW, 510 kVar
Branch 4	19-22	360 kW, 160 kVar

For the 33-bus distribution network, the impacts of DG location on PQ are investigated by executing the following sub-cases:

- The network bus voltage profiles are observed at the PCC when the simulation is run in the absence of faults in the system. The simulation is run for t=20s and no short circuit or switching event is set to occur after t=0.
- DG ability to support the system's voltage profile is investigated by applying a three phase fault at line between bus 6 and bus 7 of network. The simulation is run for 20 seconds and the three phase fault is set to occur during the first second (t=1s) and is cleared after 0.1 seconds (t=1.1s). From t=1.1s to t=20s the system is simulated to operate normally.
- The comparative analysis of grid integration of solar PV and DFIG-based DGs is done in terms of the resulting voltage profiles and system's active power losses for both network operating conditions.

6.3 Case 3: Effect of DG sizing on PQ enhancement

This case study investigates the impact of DG sizing on the network's PQ. For this case study, the location of DG remains fixed while its capacity is altered. The bus identified in terms of the resulting voltage profiles as the best PCC from Case 2 is chosen as the location of DG for the analysis in this case study. The penetration level of both solar PV and DFIG-based DGs is increased in steps of 10% from 1 MVA to a maximum value and the voltage profiles and power losses resulting from integration of each source are investigated. Penetration level of DG in the network can be calculated using

Equation 6-1 below which relates the total system loading with the capacity of integrated DG. The primary contribution of this case study is to manually determine the maximum size of DG that the chosen network can withstand without violating voltage limits or unexpected load disconnections due to over-voltages.

$$\%DG_{penetration\_level} = \frac{P_{DG}}{P_{L,\max}} x100 \quad (6\text{-}1)$$

The voltage profiles at the PCC and the total active power losses are observed and recorded for each penetration level and the results are compared with that of the base case. It is expected that that as DG penetration level is increased, the voltage profile at the PCC will also increase and show significant improvement in comparison with that of the base case. The total active power losses in the network are also expected to reduce due to rising capacity of integrated DG. In this case the DG capacity will be increased to a maximum value. The value that will be considered to be optimal will be the one to result in significant improvement in voltage profile with the magnitude not exceeding the maximum voltage limits. The overall active power losses associated with the optimal DG capacity are also recorded to observe the reduction level from that of the base case.

6.3.1 *Scenario 1: Impact of DG sizing in sub-transmission networks*

The impact of DG capacity on network's PQ is investigated in the sub-transmission level by considering the 9-bus sub-transmission network of Figure 6-1. For this system, DG penetration level is increased up to 47%, which is equivalent to DG capacity of 150MVA. The optimal capacity of DG is considered to be the maximum DG capacity whose resulting voltage profiles are within limits specified by the grid codes but PQ improvement is significant. For the purposes of observing the effect of DG sizing on PQ, the simulations are conducted as follows:

- The voltage profiles at the PCC and total active power losses are recorded as the capacity of solar PV and DFIG is increased in the absence of faults in the network.
- The above approach is repeated with the three phase fault occurring at line 7. The simulation is run for 20 seconds and the three phase fault is set to occur at t=1s and is cleared after 0.1 seconds (t=1.1s). From t=1.1s to t=20s the system is simulated to operate normally.

6.3.2 *Scenario 2: Effect of DG sizing in distribution networks*

For the 33-bus distribution network, the capacity of DFIG and solar PV is increased in steps from 0.5MVA to 30 MVA. The PCC is chosen as Bus 7, which was identified as the best location based on the resulting voltage profile at the PCC upon DG integration. The comparative analysis between solar PV and DFIG integration is made by observing the DG type that will achieve higher penetration level without violating the voltage limits at network buses. The active power losses resulting from each

DG penetration level are also observed such that a comparative analysis of the performance of solar PV and DFIG-based DGs can be made. The DG technology which will be beneficial during periods of high power demands will be the one found to attain higher penetration levels without violating voltage limits while also keeping active power losses at minimum.

6.4 Case 4: Effect of voltage control schemes for PQ enhancement in utility grid with DG integration

As discussed earlier, one of the variables that manifest power quality problem is a non-standard voltage profile which may result in failure or mal-operation of customer's equipment. The grid code for integration of renewable energy plants in South African networks requires DGs to have the capability of varying reactive power support at the PCC within the reactive power ranges defined in Figure 2-5 in Chapter 2. DGs must therefore be equipped with reactive power control functions that are capable of controlling reactive power at the PCC. A number of voltage control schemes play a significant role in improving the quality of power in utility grids with DG integration. This case investigates the impacts of applying voltage control schemes with the capability of generating or absorbing reactive power on network's PQ in the presence of DGs. The goal is to enhance the system's PQ by controlling the voltage at the PCC such that its magnitude is within limits of tolerance as per South African grid code. The effect of voltage control mechanisms based on reactive power compensation will be explored on IEEE 9-bus and IEEE 33-bus network with DG integrated at bus 8. The investigation is performed in the presence of solar PV and DFIG-based DGs and the degree of PQ improvement for each DG technology is observed.

In order to maintain the system's PQ, the applied voltage control schemes will absorb or supply reactive power to mitigate the voltage dips, voltage interruption and improve the power factor at the PCC. Voltage dip is simulated by introducing a three phase fault on the networks. Solar PV and DFIG-based DGs will be connected at the PCC at different times and the transient behaviour of the system will be explored with and without voltage control at the PCC. Voltage control scheme capable of offering reactive power compensation for voltage support will also be integrated at the PCC to offer voltage support during the fault. The voltage profile at the PCC will be observed before and after fault occurrence in the presence of voltage control device. Voltage control devices employed in this case will be a Static Compensator (STATCOM) and a Static Var Compensator (SVC) which are both capable of accomplishing reactive power compensation. The impact of each control mechanism on power quality improvement is evaluated for grid integration of solar PV as well as DFIG-based DGs.

Table 6-2: The parameter settings of the STATCOM and SVC for the IEEE 9-bus and IEEE 33-bus networks

Parameter	IEEE 9-bus system	IEEE 33-bus system
Reactive power	22.8 MVAr	5.7 MVAr
Voltage rating	230 kV	12kV
Reference voltage	1.05 p.u.	1.1 p.u.
Regulator time constant	10 seconds	10 seconds
Regulator gain	100	100

The SVC and STATCOM are as modelled in Chapter 5 and their parameters are presented in Table 6-3. Their voltage reference is set to 1.05 p.u. and 1.1 p.u. for the 9-bus and 33-bus networks, respectively. The reference voltage is chosen based on the maximum allowed voltage limit for sub-transmission and distribution networks as specified by the South African grid code. Their reactive power rating is based on the reactive power requirements for DGs connected in South African grids as presented in Figure 2-6, which is dependent on the size of DG and operating power factor. For instance, if DG operating at the power factor of 0.95 is rated at 100MW, the requirement of the production of reactive power is 33 MVAr (0.33 p.u.) capacitive and 33MVAr (-0.35 p.u.) inductive. DGs in this analysis have the capacity of 20MVA and fall under category A, as referred to by the grid code governing grid integration of DGs into South African networks. Therefore the requirement for production of reactive power is 22.8 MVAr, both inductive and capacitive. The South African grid codes do not specify the required reactive power for DGs operating at the power factor of 1, therefore in the case of solar PV integration, the default is also set at 22.8 MVAr.

The analysis of PQ improvement in electricity networks by using DG coupled with voltage control schemes is executed as follows:

- The DFIG and solar PV with the capacity of 20MVA are integrated at Bus 8 of the 9-bus network and the three phase fault is set to occur on line 7 at t=1s and cleared at t=1.1s. The simulation is run for 20 sec and the resulting voltage profiles at the PCC and total active power losses are observed.
- For the 33-bus distribution network, the size of DG is fixed at 5 MVA and the fault is set to occur on the line between bus 4 and bus 5 at t = 1s and is cleared at t =1.1s.
- The simulations are then run with the STATCOM and SVC connected at the PCC of the two networks.

- For each voltage control device, voltage profile at the PCC and the total active power losses are observed.
- The comparative analysis is made between DFIG and solar PV based on the results obtained for each control device.

6.5 Case 5: Power quality improvement by installation of energy storage system

It was established that the integration of variable DGs such as wind turbines and solar PV may result in power grid frequency variations. This may have detrimental impacts to connected loads, particularly the critical loads which are sensitive to poor PQ levels. In order to resolve the problems posed by the intermittency of RES, there is a need to support the grid integrated DGs with some form of conventional power source. It was established in [128] that for every 10% wind penetration, a balancing power equivalent to 2-4% of the installed wind capacity is essential for a system to maintain stability. Energy storage has been identified as one component with the capability to play a vital role in power quality management of the grid without presenting the complexities posed by the use of conventional power plants. The PQ in networks with DG integration can therefore be enhanced by coupling DG with a form of energy storage at the PCC.

Several ESSs effectively used in power systems were discussed in Chapter 2. The type of energy storage to be employed in this study is battery energy storage (BES) whose model is discussed in Chapter 5. This case study investigates whether connecting BES at the PCC of DGs will contribute to system's PQ improvement in the network and to what extent the PQ will improve. The impact of ESS on the improvement of dynamic behaviour of the DG is also investigated in terms of the voltage support offered by its integration. The capability of BES to provide voltage support during instances when a nearby grid fault causes a reduction in a grid voltage profile is also investigated. It is expected that BES will reduce the voltage recovery time following the fault occurrence and will also smoothen the voltage profile at the PCC. In addition to PQ improvement, the ability of BES to reduce the power losses in the system is also investigated. The impact of coupling DG with BES together with DG on voltage profiles and total system losses is investigated for solar PV and DFIG-based DGS through the following sub-cases:

6.5.1 *IEEE 9-bus sub-transmission network*

For the 9-bus sub-transmission network, the capacity of DG is fixed at 10MVA while that of the BES is kept at 2MW with the Amp-hour rating of 115Ah. The current drawn by the load connected at the PCC (Bus 8) is 460A, it is assumed that the battery will contribute one quarter of the total current

which is equivalent to 115Ah. This is because 25% of the load is considered as priority load and this will be supplied for an hour. The behaviour of voltage profiles at the PCC (Bus 8) with DG integration is observed in the presence and absence of BESS. The impact of including BES on active power losses of the network is also observed for each DG type. The analysis is conducted during the normal operation of the network with not fault occurrence and in instances of faults in the network. The three phase fault applied similar to the above case studies.

6.5.2 *IEEE 33-bus distribution network*

For the analysis of BES impact on PQ enhancement in distribution networks, the capacities of DG and BES are fixed at 1 MVA and 0.4 MW, respectively. The total current drawn from the grid by the distribution network's load is 341.6 A, the battery is thus rated at 90A-h such that it can contribute one quarter of the current for an hour. DG and BES ratings are determined on the basis of the total loading of the 33-bus distribution network. The PCC is chosen as Bus 5 which was identified as the best PCC from case 2 based on the resulting voltage profiles. The analysis is conducted during the normal operation of the network without any fault occurrence and then with fault occurrence in the network. The fault is simulated as a three phase fault similar to the earlier case studies.

The comprehensive analysis of the impact of coupling BES with DG on PQ enhancement is executed as outlined below:

- The comparative analysis is done between grid integration of solar PV and DFIG-based DGs on the basis of the resulting voltage profiles at the PCC and total active power losses for each network.
- The first scenario involves the comparison of the PCC voltage profile obtained when BES is included with that obtained when DG only is integrated.
- The comparison of the level of PQ improvement obtained when BES is connected with solar PV and DFIG-based DGs is conducted during the normal operation of the system and during an instant of fault occurrence in the system.
- The type of DG technology that results in more improvement in system's PQ is identified between solar PV and DFIG-based DGs.

6.6 Case 6: PQ improvement in weak networks with DG integration

Most South African networks are characterised by long and weak grids which may pose adverse impacts upon integration of DGs. Renewable energy resources such as wind and solar are usually available in abundance at location far from end users and the PCC will consequently be far from power consumption points. At these locations, weak grids are often found and are characterized by high grid

impedance [129]. It is therefore imperative to observe the impacts of integration of DGs to networks with different grid strengths in order to facilitate proper planning of their grid integration. This is particularly vital because high penetration levels of fast, acting renewable energy sources such as wind and solar into weak grid requires comprehensive planning studies essential to ensure enhanced system's PQ and operation. High penetration levels of renewable energy sources will alter the strength of the grid, and therefore make the grid weaker.

The strength of an electrical grid can be characterized by the ratio of resistance to reactance of the line or short circuit ratio (SCR) of the utility grid. The SCR is the measure of the system strength at a particular point and is an understood as an accepted approximation of the grid's strength. In this case study, the strength of the 9-bus and 33-bus networks is changed by altering the short circuit capacity of the external grid while DGs rated at 10% of the system's load are connected. The respective DG sizes and their PCC for two networks considered in this study are presented in Table 6-4 below. The aim is to investigate the relationship between system's voltage profiles and grid strength upon integration of DG. Equation (6-3) below is used to calculate the SCR of the grid at different short circuit capacity (SCC) values which are manually specified in DIgSILENT depending on the grid strength required. The grid is considered weak if the SCR value is smaller than 10.

$$SCR = \frac{SCC}{S_{N,DG}} = \frac{U_G^2}{Z_{weak} \times S_{N,DG}} \tag{6-3}$$

In equation (6-3) above, SCC is the short circuit capacity of the grid in kVA, which is the amount of power flowing at a given point in an instance of short circuit. $S_{N,DG}$ is the rated capacity of an active component such as DG in MVA. U_G is the voltage magnitude in kV at the PCC while Z_{weak} is the absolute value of the grid impedance in kΩ.

Table 6-3: Parameter specification for significant components for Case 7

Variable	IEEE 9-bus network	IEEE 33-bus network
DG capacity	33.5 MVA	410 kVA
Integration point	Bus 8	Bus 5
Total base load	335.34 MVA	4.1

The comparative analysis is done between solar PV and DFIG-based DGs integration at each grid strength on the basis of the resulting voltage profiles at the PCC. The active power losses of the system do not change as the short circuit capacity is altered, they are therefore not considered for performance

comparison between solar PV and DFIG. The strength of the grid is varied from the weak grid (SCR <10) to strong grid (SCR>10) and the voltage profiles are observed for both solar PV and DFIG integration. In order to observe DG ability in assisting system's voltage recovery, the three phase fault is applied on Line 7 and between bus 4 and 5 for the 9-bus and 33-bus networks, respectively. The fault occurs at 1 second and is cleared after 0.1 second.

6.7 Case 7: The optimal allocation and sizing of DG for PQ improvement

The strategic placement and sizing of DGs at their optimum can be vital as they help reduce network losses and improve system performance by enhancing its overall PQ, efficiency and reliability [110]. Proper planning of grid integration of DG into electricity networks therefore requires determination of optimal parameters such as location and size of DG in the network. This scenario determines the optimal size and location of DGs on a 9-bus sub-transmission and 33-bus distribution networks using GA technique. The primary objective is to improve the system's voltage profiles and minimize the total system's active power losses. The objective function therefore considers voltage profile improvement and total real power loss reduction as defined by Equation (5-17). As discussed in the problem formulation of the optimal DG placement, the minimization of the objective function is subject to the defined operational constraints which are the voltage limits and DG sizes.

In this analysis, the loads of the two networks are considered constant throughout the optimization procedure and are as depicted in Table A-1 and Table A-5 in Appendix A. For the 33-bus distribution network, all system's busbars are considered as the potential candidates for DG integration except for bus 1 which is modelled as a slack bus from where the external grid is connected. For the 9-bus sub-transmission network on the hand, the potential candidate buses for DG integration are Bus 4 to Bus 9. The data of the test networks is defined in code written for calculation of the optimal solutions essential for PQ improvement. Some of the calculations defined in MATLAB code involve load flow calculation by Newton Raphson method and application of an optimization technique to obtain the optimal solution.

Power quality improvement by optimal placement and sizing of single and multiple DG units will be investigated using GA. The parameter settings of the GA algorithm used for the determination of the optimal solutions in this case study were discussed in section 5.7.3 of Chapter 5. The types of DGs considered in this analysis are solar PV and DFIG whose models were discussed in Chapter 5. The solar PV generator is modelled as an active power generator operating at unity power factor while the DFIG is modelled as the active and real power generator. The reactive power setting of the DFIG is

however made negative because DFIG-based DG draws reactive power in its operation. The comparative analysis will be made between optimal integration of solar PV and DFIG on the basis of the resulting voltage profiles and total active power losses. Furthermore, the comparison will also be made by observing which DG technology has the highest capacity after the optimal placement.

6.8 Case 8: PQ improvement by optimal placement of DG considering different load models

Most studies pertaining to optimal DG placement and sizing assume constant power load models. Constant load models have however been proved to show insensitivity to variations of voltage profile as well as frequency of the system [130]. In practice, electricity networks are composed of residential, commercial and industrial loads which are all dependent on the respective bus voltages. The load models have a significant effect on the optimal placement and sizing of DG units in distribution networks. The load models used in this case therefore varying with voltage levels at their connection points.

Equations (C-1) and (C-2) in Appendix C, representing the load model equations are incorporated in load flow program to calculate the bus power for each load model. The impact of different load models on the optimal placement and sizing of DG is investigated by observing the resulting voltage profile and total power losses after the application of GA optimization algorithm. The multi objective function considered in this study is that defined by Equation (5-15) which takes into consideration, total active power loss reduction and improvement of voltage profile. The resulting power losses and voltage profiles will be compared to those of constant load models to observe the impact of taking into account the different load models.

In this case study, the active and reactive load exponents are defined for both summer and winter days to represent the seasonal load models for most South African distribution networks. The exponent values for load models are different for residential, commercial and industrial loads. It must be noted that the value for real and active power exponents is zero for all types of constants load models. The load models chosen for this case study are presented in Table 6-4. In practice, the load models of electricity networks vary with different seasons of the year. The load condition is therefore considered as low level for summer nights, medium level for summer days and winter nights and peak level for winter days. The values of the load models for both summer and winter days and nights are extracted from [69] and modified to adopt the seasonal load models of South African networks. The load exponents extracted from [69] are defined for both active and reactive powers of residential, commercial and industrial load models as depicted in Table 6-4.

Table 6-4: The seasonal daily active and reactive power exponent values for different load types

Season and time	Load type	α	β
Summer day	Residential	0.73	2.96
	Commercial	1.26	3.50
	Industrial	0.17	6.0
Summer night	Residential	0.92	4.12
	Commercial	0.99	3.95
	Industrial	0.18	6.01
Winter day	Residential	1.02	4.18
	Commercial	1.50	3.23
	Industrial	0.17	6.01
Winter night	Residential	1.30	4.26
	Commercial	1.51	3.95
	Industrial	0.18	6.01

This case study is executed by writing the relevant code in MATLAB and the 9-bus sub-transmission and 33-bus distribution networks are considered for the analysis. The loads of the 9-bus system are considered to be industrial loads. Therefore the loads exponents used are that of industrial load type. The 33-bus distribution system on the other hand consists of the combination of all the load models defined in Table 6-5 above. The load type of the 33-bus distribution network is depicted in Table 6-5 below.

Table 6-5: The load types and corresponding bus numbers for a 33-bus distribution network

Load type	Load connected to Bus number
Residential	5,6,9,10,11,12,15,16,17,18,26,27,28
Commercial	2,3,4,13,14,19,20,21,22,23,29,31,33
Industrial	7,8,24,25,30,32

In this case study, the system voltage profile is observed considering an average of the seasonal load models for the whole year as well as for each seasonal daily period. For seasonal daily periods, voltage profile improvement before and after DG installation is observed for typical summer day and night load levels as well as for typical winter day and night. The type of day such as weekend days and holiday are not independently considered in the analysis due to their significantly smaller number in comparison to the weekdays for both annual and seasonal periods. The impact of both solar PV and DFIG-based DGs on PQ improvement is observed and compared.

The sub-cases conducted for comprehensive analysis in this case study are as listed below:

- The voltage profiles and total active power losses before and after optimal integration of single DG and multiple DGs are observed for the two networks considered when annual load models are considered.
- The comparative analysis between integration of solar PV and DFIG-based DGs is done on the basis of the resulting voltage profiles at load points as well as the total active power losses.
- The investigation of the performance of the two networks in terms of bus voltage profiles and total active power losses is conducted during each load period, namely; summer days, summer nights, winter days and winter nights.
- The comparative analysis between integration of solar PV and DFIG-based DGs is then done for DG integration on the two networks considered.

7. Results and discussion

This chapter presents the results obtained from the simulations of the case studies discussed in Chapter 6. The models of the test networks and that of solar PV and DFIG discussed in Chapter 5 are built and simulated in DIgSILENT PowerFactory. The impact of grid-integration of DGs on PQ enhancement is investigated on both the sub-transmission (IEEE 9-bus system) and distribution (IEEE 33-bus system) networks. The impacts of DG integration are identified and discussed with particular emphasis made on the resulting voltage profiles at the PCC and the overall active power losses in the networks. The comparative analysis is made between grid-integration of solar PV and DFIG based DGs in terms of PQ improvement capabilities of each. The grid codes governing integration of DG units in South African electricity networks are used as indicators of the quality of power in the system.

7.1 Case 1: Networks operation without DG (Base case)

The results of the voltage profiles and overall active power losses of the test networks without DG-integration are presented in this section. The voltage magnitudes at different buses of both the IEEE 9-bus and IEEE 33-bus networks are observed and presented.

7.1.1 *Operation of the 9-bus sub-transmission network*

The voltage profiles at different buses of the 9-bus sub-transmission network after the load flow is executed are shown in Table 7-1 below. It can be seen that the voltage magnitude at Bus 1 is highest at 1 p.u since this bus is assumed to be the slack bus with reference voltage set to 1 p.u. Voltage magnitude is lowest at Bus 2 with the magnitude of 0.932 p.u. The buses whose voltage magnitudes are outside the range of 0.95 p.u. to 1.05 p.u. are Bus 2, Bus 5, Bus 7, Bus 8 and Bus 9 as shown in Table 7-1.The voltage magnitudes at other buses of the network are within the limits specified by the grid codes.

Table 7-1: Voltage magnitude at different buses of the 9-bus network without DG-integration (Base Case)

Bus number	Voltage magnitude (p.u.)
1	1.025
2	0.932
3	0.979
4	0.976
5	0.935
6	0.958
7	0.935
8	0.936
9	0.94

The transient behaviour of the network is also investigated by applying the fault as described in Chapter 6. The voltage profiles at the load buses of the 9-bus system are observed and are shown in Figure 7-1. It can be seen that during the instant of fault occurrence, a reduction in voltage magnitude occurs at the load buses, with Bus 5, experiencing the largest drop in voltage. It can be seen that after the fault is cleared, the voltage attempts to increase towards the nominal. The voltage settles at the highest magnitude of 1.01 p.u. at Bus 8 as shown in Figure 7-1. The LVRT requirements are not applicable in this scenario since no DG is connected. It is however expected that DG integration will result in improvement in voltage profiles while meeting the LVRT capabilities required by the grid code. The overall active power losses of the 9-bus network without DG integration are also observed after the load flow is executed are amount to 2.18MW.

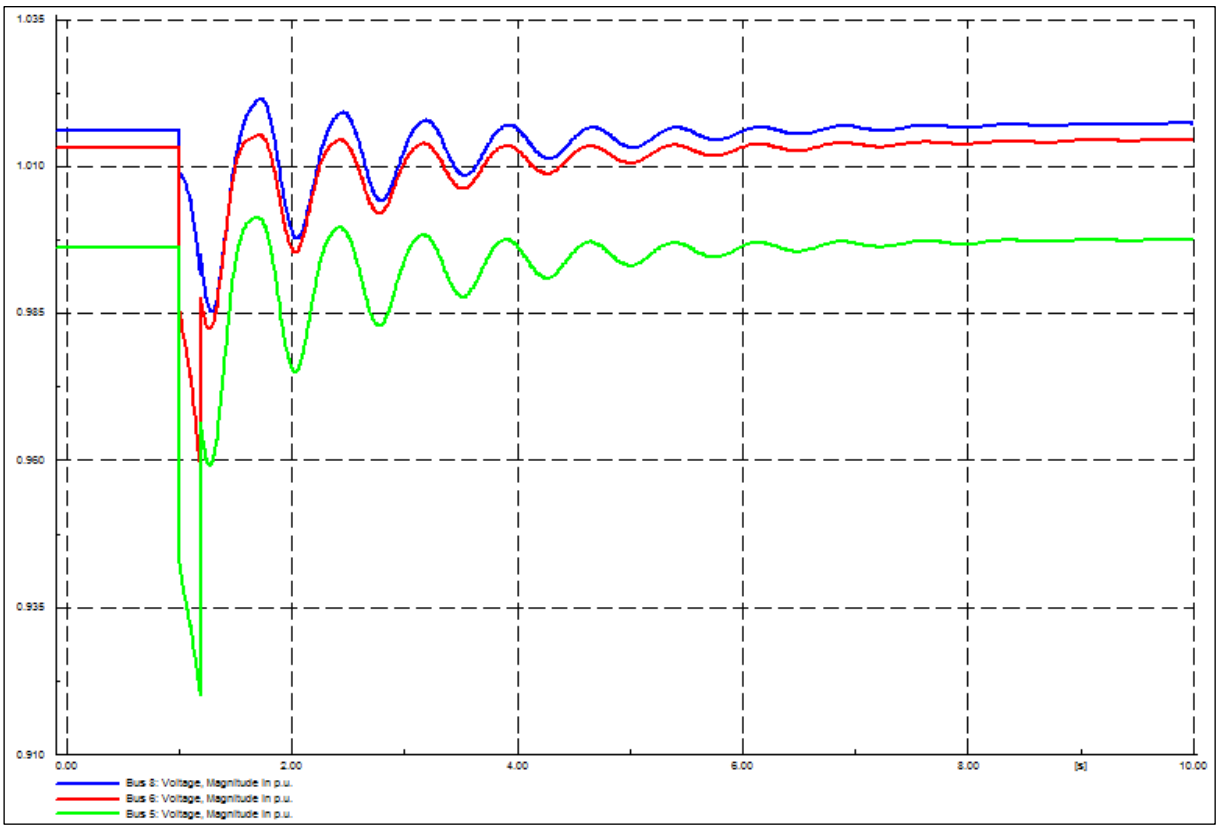

Figure 7-1: The voltage profiles at load buses (Bus 5, 6 and 8) of the 9-bus network during fault occurrence (Base Case)

7.1.2 *Operation of the 33-bus distribution network*

The results of voltage magnitudes at different buses of the 33-bus distribution network obtained after the execution of the power flow are presented in Figure 7-2 below. It can be seen that the lowest voltage magnitude of 0.917 p.u. occurs at Bus 17, Bus 18 and Buses 31 – 33. The voltage magnitude at Bus 1 remains constant at 1.p.u. since it has been set as the slack bus with the voltage set-point of 1.p.u. Except for the slack bus, the voltage magnitudes are highest at Bus 18, which is located at the

end of branch 3 as labelled in Table 6-1 of Chapter 6. The overall active power losses of the network after the load flow in executed are found to be 0.236MW.

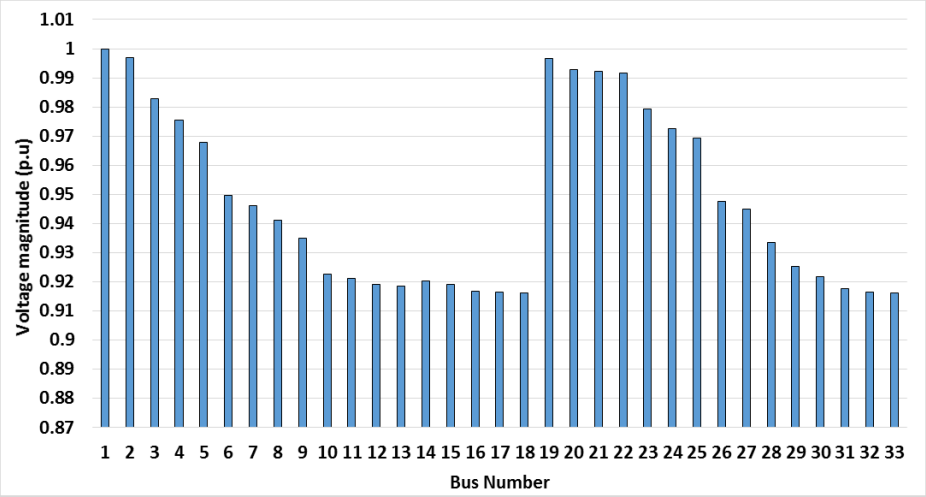

Figure 7-2: The voltage magnitudes at different buses of the 33-bus network without DG integration (Base Case)

The voltage profiles are also observed upon the simulation of the fault as discussed in Chapter 6. The voltage profiles are observed at the last buses of four branches of the network and are shown in Figure 7-3. It can be seen that the voltage magnitude momentarily drops to a lower value after fault occurrence and returns to nominal voltage when the fault is cleared. Bus 7 experiences the largest voltage drop of 0 p.u. while Bus 19 experiences the lowest drop in voltage during the fault. The voltage profiles at other buses of the network follow the pattern similar to that shown in Figure 7-3. Similar to the 9-bus system scenario, the LVRT requirements are not considered since no DG is connected. The voltage profiles at different network buses however differ by value of voltage drop and final settling voltage magnitude after the fault.

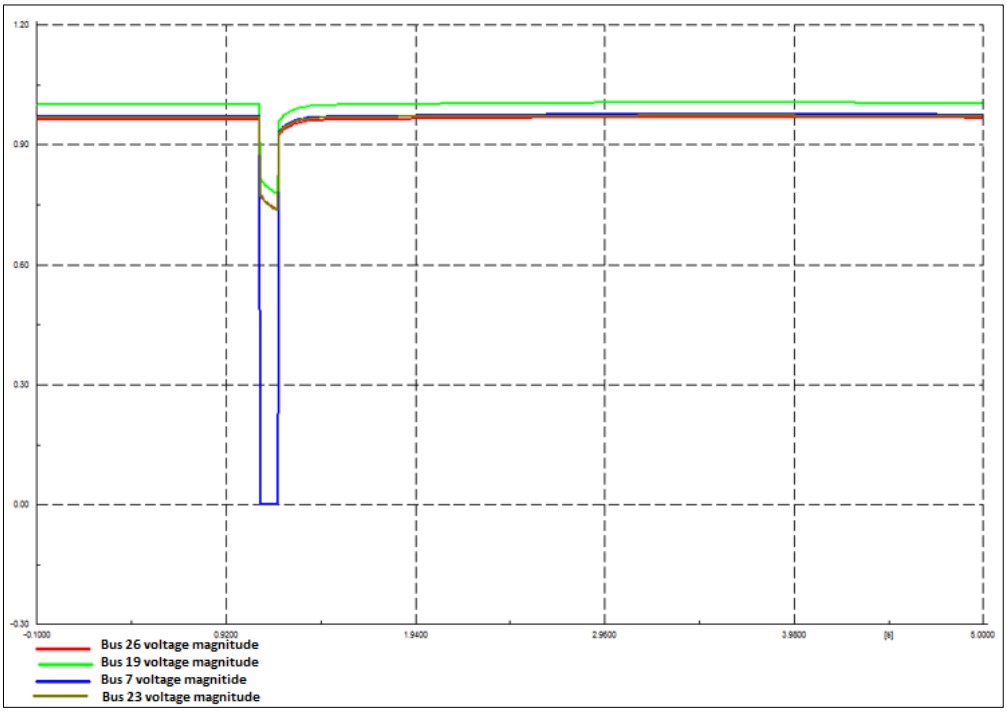

Figure 7-3: The voltage profiles at the buses of the 33-bus network in the event of fault (Base Case)

7.2 Case 2: Impact of DG placement on PQ enhancement

The results of the impacts of DG location in electricity networks are presented in this section. The impacts of DG location are investigated during the normal network operation and in the event of fault occurrence as described on Section 6-2. The analysis is performed on both the 9-bus sub-transmission and 33-bus distribution networks.

7.2.1 *DG placement on IEEE 9-bus sub-transmission network*

i. Impact on voltage profile in the absence of faults

The results of the voltage profiles obtained after the integration of solar PV and DFIG based-DGs with the capacity if 10MVA at different buses of the 9-bus system in the absence of faults are presented in Table 7-2 below. The results show that integration of solar PV and DFIG based DGs affects voltage profiles at their PCC depending on the point of integration. In order to observe how solar PV and DFIG-based DGs differ in their impacts in improving the voltage profile, the percentage deviation from the base case voltage profile is calculated using Equation (7-1) after integration of each DG type.

$$\%\, Deviation = \frac{(V_{After_{DG}\_integration} - V_{base\_case})}{V_{base\_case}} \times 100\% \qquad (7\text{-}1)$$

where V_{base_case} and $V_{After_{DG}\_integration}$ are bus voltage magnitudes in p.u. before and after DG integration respectively.

The PCC voltage magnitudes change upon DG-integration depending on the chosen bus. DG integration at some network buses either increases or decreases the voltage magnitude at the PCC. For instance integrating a DFIG at Bus 2, results in reduction of the base case voltage by 5.6% whereas integrating an equal capacity of solar PV at the same bus results in voltage reduction of only 0.5%.

Table 7-2: Voltage profiles at the PCC before and after integration of Solar PV and DFIG on a 9-bus system during normal system operation (Case 2)

Integration point	Type of DG	Base voltage magnitude (p.u)	Average voltage after DG integration (p.u)	Deviation from base voltage
BUS 2	Solar PV	0.932	0.927	-0.54%
	DFIG		0.883	-5.26%
BUS 3	Solar PV	0.979	0.977	-0.2%
	DFIG		-	-
BUS 4	Solar PV	0.976	0.976	0%
	DFIG		0.975	-0.1%
	Solar PV		0.936	0.1%

BUS 5	DFIG	0.935	0.939	0.43%
BUS 6	Solar PV	0.958	0.962	0.42%
	DFIG		0.961	0.31%
BUS 7	Solar PV	0.935	0.936	0.11%
	DFIG		0.938	0.32%
BUS 8	Solar PV	0.936	0.973	3.95%
	DFIG		0.982	4.91%
BUS 9	Solar PV	0.94	0.975	3.72%
	DFIG		0.979	4.15%

DG integration at Bus 8 results in a significant improvement of the voltage at the PCC as can be seen in Table 2. Solar PV integration at Bus 8 results in voltage magnitude increase of 3.95%, integration of DFIG at the same bus results in an increase of 4.91%. DFIG results in a higher increase in voltage magnitude because of its reactive power support capabilities, as opposed to solar PV. Integration of solar PV and DFIG-based DGs at Bus 9 also shows improvement in PCC voltage profile. The graphical comparison of the voltage profiles at the PCC resulting from integration of solar PV and DFIG at Bus 8 are presented in Figure 7-4. It is observed that solar PV and DFIG integration at different network buses differ in their ability to improve voltage at the PCC depending on the integration point. For instance, the voltage profiles depicted in Figure 7-4 show a higher increase in bus voltage profile after DFIG integration in comparison to integration of solar PV of the same capacity.

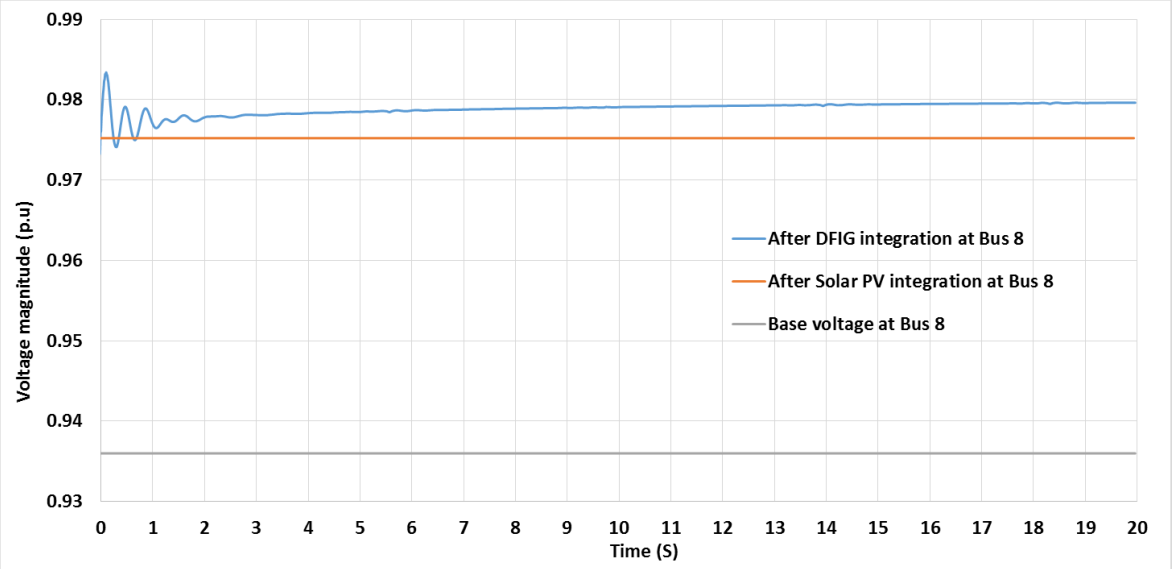

Figure 7-4: Comparison of PCC voltage profiles after integration of solar PV and DFIG-based DGs at Bus 8 in 9-bus network (Case 2)

ii. Impact on voltage profiles during fault conditions

A. DFIG integration

The results of voltage profiles at the PCC after the three phase fault is introduced at Line 2 of the 9-bus network are also presented. It was observed that DG-integration at some of the network's busbars results in voltage magnitudes at the PCC fluctuating outside the acceptable limits. The worst voltage

profiles were observed when DFIG was integrated at Buses 2, 3, 4, 5 and 6. DFIG integration at Buses 2 and 5 in particular results in voltage magnitude dropping towards zero after the fault is cleared whereas voltage magnitude drops to 0.45 p.u. when Bus 6 is used as PCC. DFIG integration at all other buses, except for Bus 7, Bus 8 and Bus 9 results in worst voltage profiles at the PCC.

In order to identify the PCC that results in improved voltage profiles, the voltage profiles at three buses are plotted on the same axes for better comparison. Figure 7-5 shows the comparison of the voltage profiles when DFIG-based DG is integrated at Buses 7, 8 and 9 at different times. The best location for DG placement is defined as the PCC whose voltage profile depicts a significant improvement in comparison to that of the base case. In addition to improving the base voltage profile, the voltage magnitudes should also be within the acceptable limits of $\mp 5\%$ of the nominal voltage.

It can be seen that after the fault is cleared, the voltage profile when DFIG is connected at Bus 9 fluctuates outside the prescribed limits for about 10 seconds before settling to a constant value of 1.0 p.u. Bus 9 is interfaced with the generating Bus 3 by a transformer stepping up the voltage from Bus 3 where the synchronous generator, G3 is connected. DFIG integration therefore contributes to the delay in settling of Bus 9 voltage profile due to the two generating sources attempting to be in synchronism with each other. When DFIG is integrated at Bus 7 and Bus 8, the voltage fluctuations are relatively small and the constant voltage magnitude is attained 3 seconds after the fault clearance. It is also observed that after the fault is cleared, DFIG attempts to support the voltage towards the constant voltage magnitude of 1.0 p.u. The voltage rise after the fault occurrence is due to active and reactive power injection by DFIG at the PCC. The significant voltage support is particularly observed when DFIG is connected at bus 7 and bus 8. DFIG integration at Bus 7 and Bus 8 increases the voltage magnitude towards 1.05 p.u. after the fault is cleared. When Bus 7 and Bus 8 are chosen as PCC, the voltage magnitudes assume a constant value of 1.05 p.u. following a series of small variations lasting for about 1.5 seconds. Buses 7 and 8 are therefore identified as the best PCC for DFIG integration to the 9-bus sub-transmission network.

DGs are connected at the HV portion of the 9-bus network and according to the LVRT requirements set out by the SA grid code, DGs of category A3 (100-1000 KVA) should be able to withstand voltage drops to zero, measured at the PCC for a minimum period of 0.15 seconds without disconnecting. In terms of the LVRT capabilities, DG integration only at Bus 8 complies with LVRT requirements set out by the grid code. The HVRT requirements are however not met for DG integration at the three buses since the voltage profiles contradict with the grid code that DGs should withstand voltage peaks up to 120% of the nominal for a minimum of 2 seconds without disconnecting.

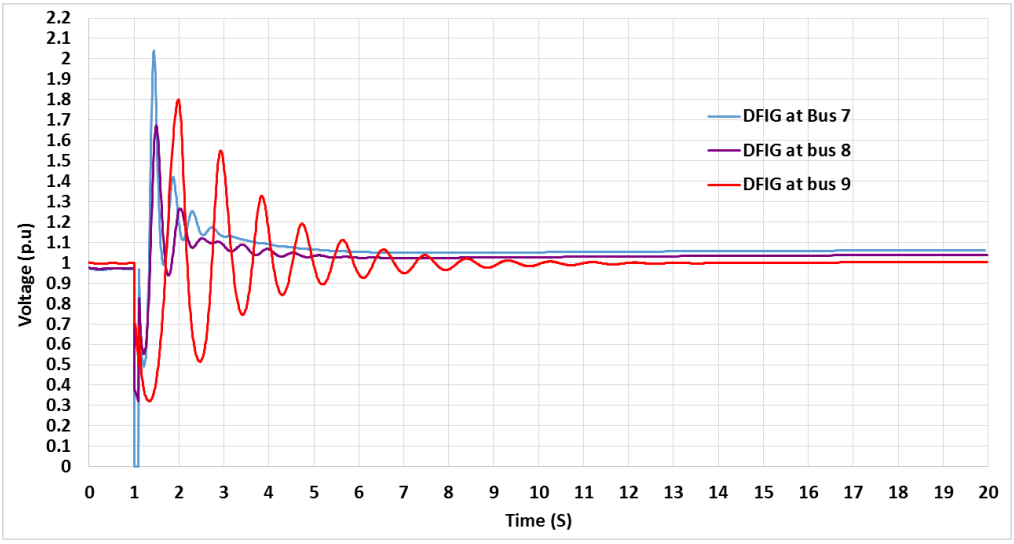

Figure 7-5: Voltage profiles at the PCC when DFIG based DG is integrated at Bus 7, 8 and 9 of 9-bus network

It is crucial to also observe voltage profiles at load buses because this is where voltage sensitive loads are connected. Selecting Bus 8 as the PCC for DFIG integration, voltage profiles at Bus 5, Bus 6 and Bus 8 load centres are observed for compliance with the specified voltage limits. Figure 7-6 shows that a brief voltage spike occurs at all load buses after the fault is cleared. The voltage profile thereafter settles to constant magnitudes throughout the simulation. The voltage magnitudes at Bus 5, Bus 6 and Bus 8 settle to constant values of 0.85 p.u., 0.93 p.u. and 1.04 p.u, respectively. In order to bring the voltage magnitudes at load buses 5 and 6 within the acceptable range, appropriate sizing of integrated DG is essential. The LVRT and HVRT requirements for the load buses are not considered since these are not the PCC where DG is connected.

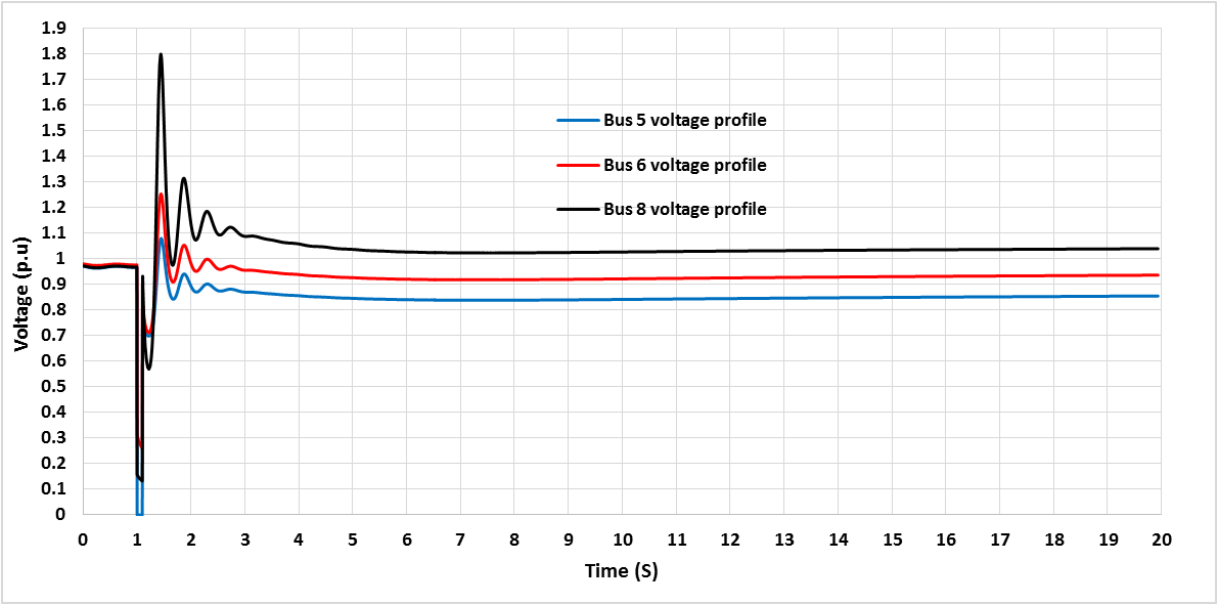

Figure 7-6: Voltage profiles at load buses when DFIG is integrated at Bus 8 of 9-bus network (Case 2)

B. Solar PV integration

The results of the voltage profiles at different PCC after solar PV integration to the 9-bus network are presented in Figure 7-7 below. It can be seen that solar PV integration at some buses results in a relatively shorter voltage recovery time after the fault is cleared. Choosing some buses as the PCC for solar PV integration demonstrated less support to the bus voltage profile since the voltage magnitude settles below the lower limit of 0.95 p.u. The PCC which resulted in voltage profiles below the lower limit are Bus 4 and Bus 5 with the magnitudes of 0.89 p.u. and 0.88 p.u. respectively. The connected Solar PV has no reactive power exchange capabilities with the grid and hence offers minimum support to the PCC voltage profile. Coupling solar PV with a device with reactive power support capabilities (such as FACTS) would bring the voltage magnitudes within acceptable limits.

Figure 7-7 also shows that solar PV-integration at most system buses results in significant improvement in PCC voltage profile. The PCCs whose voltage profiles are within the range of 0.95 p.u. to 1.05 p.u. are as follows; Bus 6 (0.95 p.u.), Bus 9 (1.04 p.u.), Bus 3 (1.05 p.u.) and Bus 8 (1.05 p.u.). The voltage profiles however rise above the limit of 1.05 p.u. when solar PV is integrated at Bus 2 seen in Figure 7-7. This is due to the fact that a conventional utility generator is connected at Bus 2 and hence additional generation results in voltage rise at this bus. Appropriate sizing of solar PV could ensure that voltage profiles are brought within the required limits at the PCC. In comparison with the case of DFIG integration, solar PV integration in most system buses results in fewer voltage fluctuations and a shorter voltage recovery time after fault clearance. This is because solar PV generates active power in constant DC form while DFIG generates AC power which fluctuates according to the input air masses.

The integration of solar PV-based DGs on all the buses of the 9-bus network complies with the LVRT requirements as per the South African grid code since the voltage drops last for only 0.1 seconds (contrary to specified 0.15 seconds) after which the voltage rises and settles as shown in Figure 7-7. In terms of the HVRT capabilities, the resulting voltage profiles have no peaks and do not rise above the limits specified for HVRT requirements.

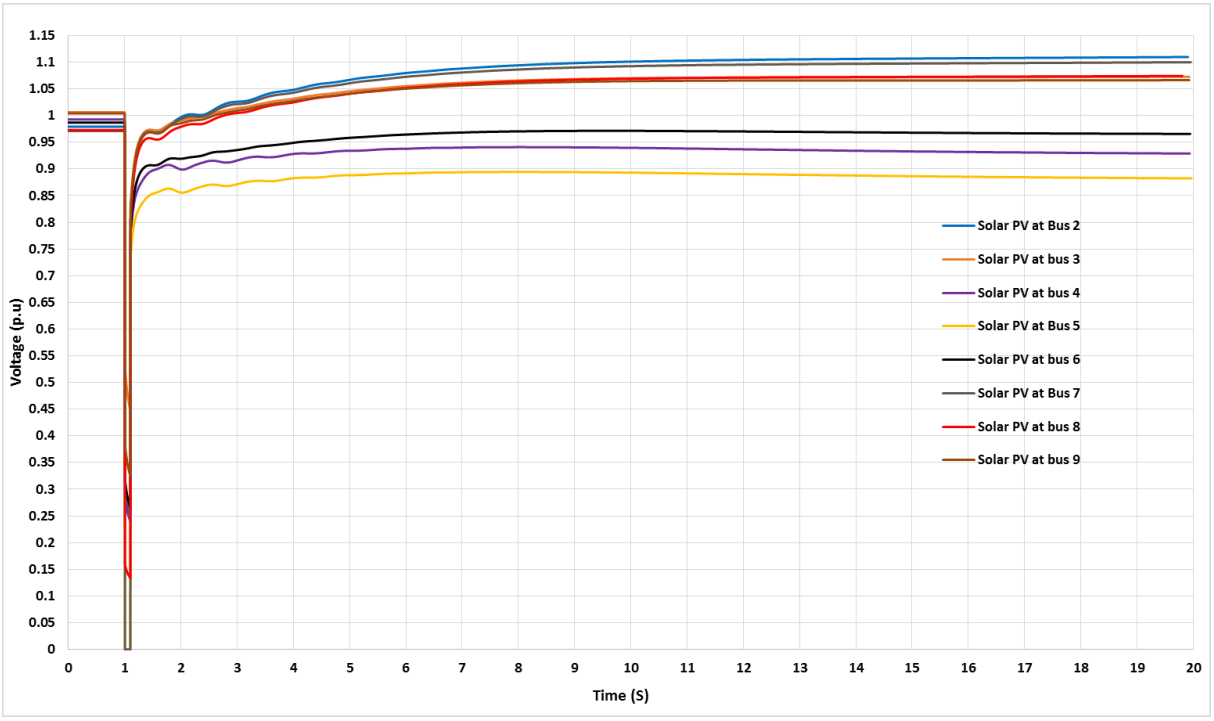

Figure 7-7: Voltage profiles at the PCC after integration of solar PV at different buses of the 9-bus system (Case 2)

The comparison of the voltage profiles resulting from integration of DFIG and solar PV at Bus 8 is shown in Figure 7-8. Using the voltage profile at Bus 8 when no DG is integrated as reference, it can be seen that DFIG and solar PV impact the PCC voltage profile differently. The voltage profile, when DFIG is integrated, exhibits a brief voltage rise after the fault and decaying oscillations until the constant voltage magnitude of 1.0 p.u. is attained. Solar PV-integration on the other hand, results in voltage profile at the PCC settling to a constant value of 1.04 p.u. immediately after fault clearance. The oscillations observed in the PCC voltage profile before DG integration are also mitigated upon solar PV integration. From the voltage profiles presented in Figure 7-8, it is seen that that solar PV integration results in a better improvement of the PCC voltage profile in comparison with DFIG-based DG of the same capacity integrated at the same PCC.

The comparison of the resulting voltage profiles when solar PV and DFIG-based DGs are connected also indicate that both LVRT and LVRT requirements are met after integration of solar PV-based DGs only. The DFIG-based DGs only meets the LVRT requirements specified for HV networks. The HVRT requirement is not met by DG since the voltage peak at the PCC rises higher than 120% of the nominal for the specified minimum time, as required by the grid code.

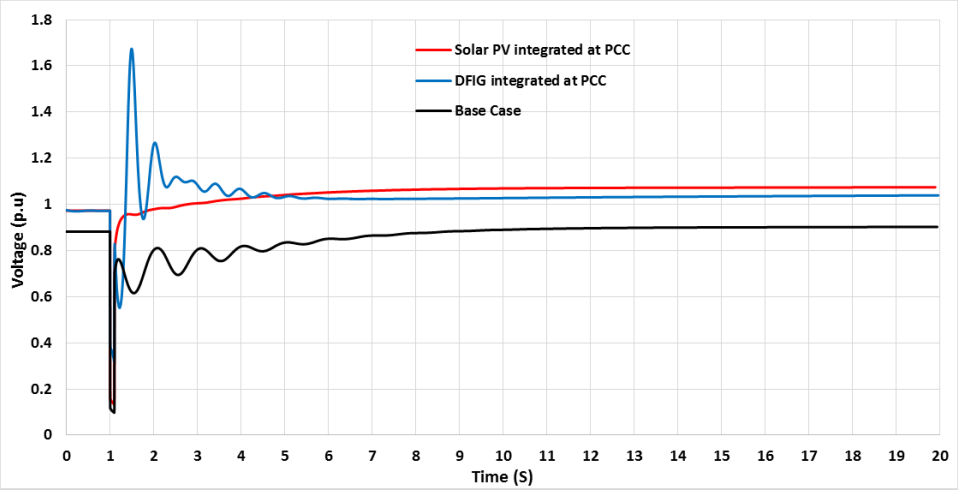

Figure 7-8: Comparison of voltage profiles at the PCC for solar PV and DFIG integration at Bus 8 of 9-bus network (Case 2)

iii. Impact of DG location on total active power losses

The overall active power losses of the network are also observed when solar PV and DFIG are integrated at different buses of the 9-bus network. The total active power losses are observed for each integration scenario and are compared with that of the base case when no DG is integrated. It is observed that the overall active power losses in the absence of DGs amount to 2.18 MW and tend to decrease with DG integration at different buses as depicted in Figure 7-9. The overall active power losses are lowest with the value of 1.9 MW when DFIG is integrated at Bus 5. The resulting active power losses for solar PV integration at the same bus amount to 2.04 MW. The smallest active power losses in the case of solar PV integration are obtained when solar PV is integrated at Bus 6, followed by Bus 8. The reduction in active power losses is more for DFIG integration at most system buses in comparison to that resulting from solar PV integration at the same buses.

The PCC which resulted in better voltage profiles after integration of DFIG and solar PV-based DGs is Bus 8. The total active power losses after DFIG and solar PV integration at bus 8 are reduced to 2.01MW and 1.97 MW, respectively. The total reduction in active power losses from that of the base for DFIG and solar PV integration at Bus 8 is 9.67% and 7.8%, respectively. It is observed that in addition to providing better voltage profile improvement at the PCC, solar PV integration at bus 8 also results in more reduction in total active power losses in the system. The resulting active power losses are more for DFIG due to a series of converters used to interface the DFIG rotor and the grid.

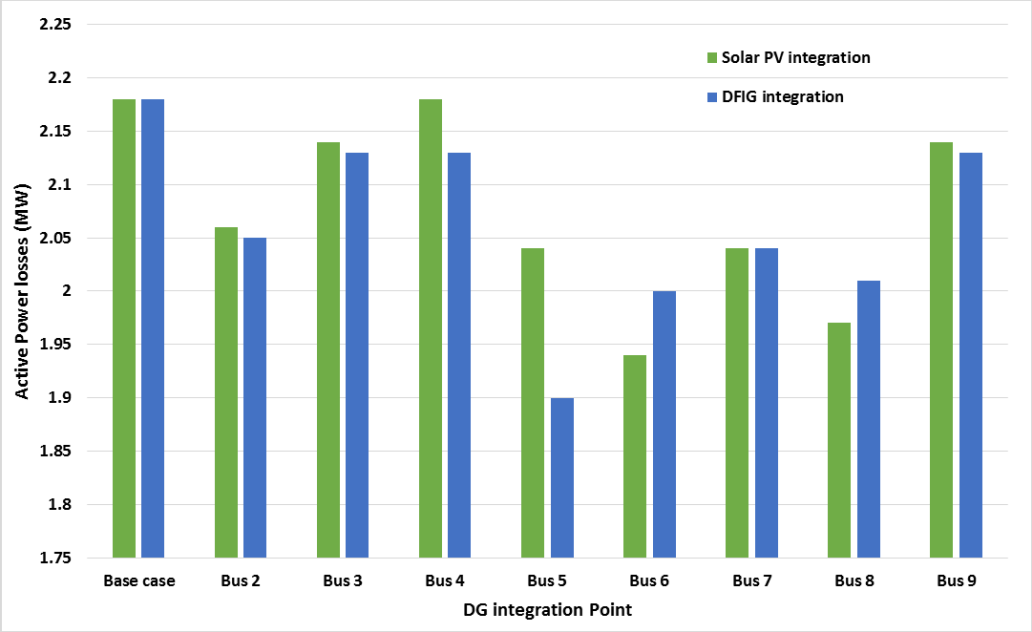

Figure 7-9: Comparison of the total active power losses when Solar PV and DFIG-based DGs are integrated at different buses of 9-bus network (Base Case and Case 2)

7.2.2 *DG placement on IEEE 33-bus distribution system*

The results of the impacts of DG location on PQ in 33-bus distribution network are presented in this section. The voltage profiles resulting from DG location at the four buses, Bus 23, Bus 26, Bus 7 and Bus 19, of the network as described in section 6.2 are presented during the normal system operation and in the event of fault occurrence in the network. The resulting total active power losses as result of DFIG and solar PV integration at selected bus bars are also presented in this section.

i. Effect of DG placement in the absence of faults

The voltage magnitudes at different buses of the 33-bus network when DFIG-based DG is connected at the buses specified are presented in Figure 7-10. It can be seen that upon integration of DFIG, momentary oscillations occur on the PCC voltage profiles before settling to a constant magnitude. The highest voltage magnitude is experienced when DFIG is connected at Bus 7, as depicted in Figure 7-10 below. The PCC voltage profile is lowest at 0.976 p.u. for DFIG integration at Bus 19 of the network. As much as DFIG-integration alters the voltage magnitudes at the PCC, the resulting voltage profiles at the chosen PCCs of the 33-bus network are within the limits specified for distribution grids.

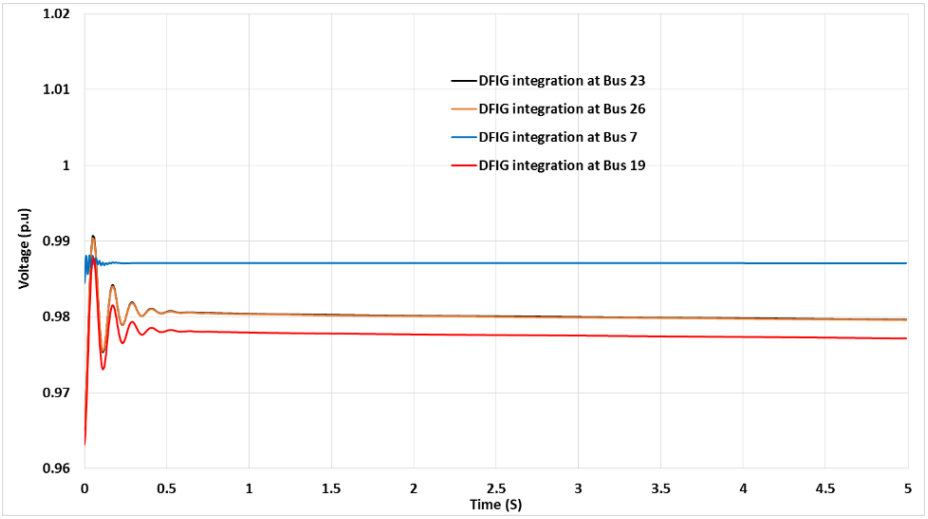

Figure 7-10: Voltage profiles at the PCC after DFIG-integration at selected buses in 33-bus network in the absence of fault in the network (Case 2)

The voltage profiles are also observed after integration of the similar capacity of solar PV-based DG in the absence of faults. Figure 7-11 shows the voltage profiles at Bus 23, Bus 26, Bus 7 and Bus 19 of the 33-bus distribution network after integration of Solar PV. It can be seen that the highest voltage magnitude is obtained when Solar PV is connected at Bus 7 with the magnitude of 0.971 p.u. The voltage magnitude at Bus 7 before any DG integration is 0.948 p.u. Solar PV-integration at Bus 7 therefore results in voltage improvement of 2.23% in comparison to that of the base case. The voltage is lowest at Bus 19 with magnitude of 0.964 p.u. The voltage profiles at the chosen PCCs are however within the limits specified by the grid codes for distribution networks. It is also observed that voltage profile improvement is more for integration of DFIG in comparison to the same capacity of Solar PV connected at the same bus.

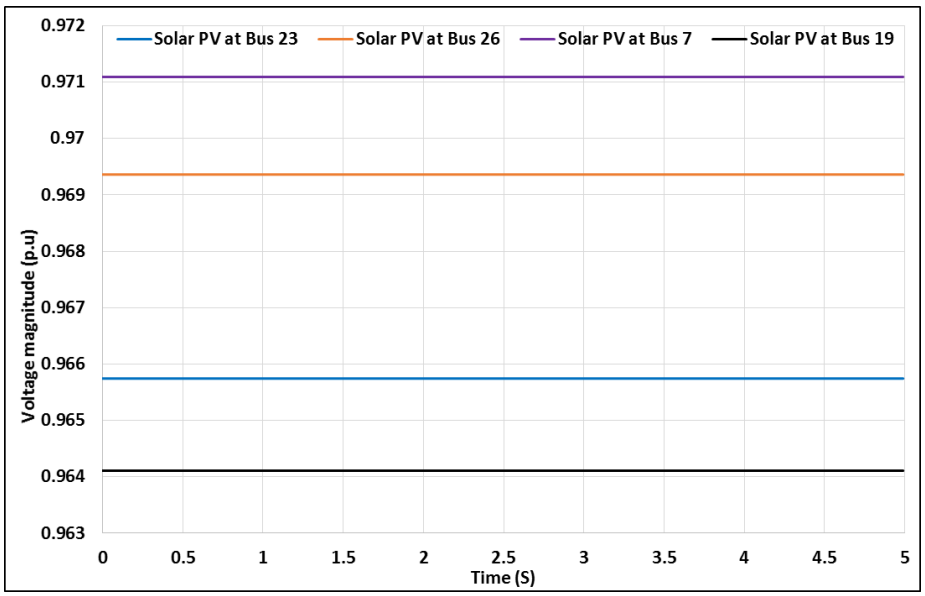

Figure 7-11: Voltage magnitudes at the PCC after Solar PV-integration at selected buses in the absence of fault in the 33-bus network (Case 2)

ii. Effect of DG placement during fault conditions

The effect of DG location in distribution networks is also observed during instances of fault occurrence as explained in Chapter 6. Figure 7-12 shows the resulting voltage profiles after 1 MVA DFIG is integrated at the selected buses of the 33-bus network. It can be seen that during an instant of fault occurrence (t=1 second), the voltage magnitude rises or drops depending on the chosen PCC. The voltage is observed to drop to 0.71 p.u. when DFIG is integrated at Bus 7. Since Bus 7 is located on the branch of the faulted line, it is momentarily disconnected during fault occurrence and re-connects to the rest of the network after the fault is cleared. The DFIG remains the sole power source for the disconnected network portion, thus boosting the voltage from 0 p.u of the base case to 0.7 p.u. The resulting voltage magnitudes at the PCC when DFIG is connected to Bus 23, Bus 26 and Bus 19 rise during fault occurrence because a larger portion of the network loads are momentarily disconnected during the fault thus resulting in over-voltages as a result of more active power injection. The voltage profiles at the PCC however return to the nominal value of 1 p.u. after the fault is cleared.

The 33-bus distribution network is at 12 kV and considered as LV network. The SA grid code for connection of DGs to LV requires that DGs remain connected for 0.15 seconds when the voltage drops to 60% of the nominal voltage. DFIG integration at the buses shown in Figure 7-12 complies with LVRT requirements since the minimum voltage attained is 0.71 p.u. at Bus 7. The HVRT requirements are also met because the grid code specifies that DGs should continue operation when the voltage is between 85% and 110% of the nominal.

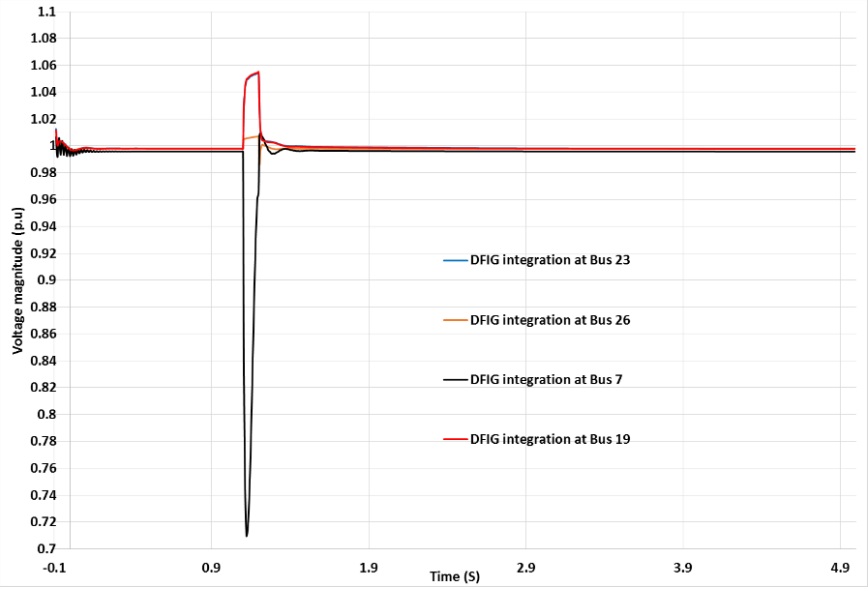

Figure 7-12: Voltage profiles at the PCC after DFIG integration at different buses the 33-bus network in the event of fault (Case 2)

The resulting voltage profiles at the PCC after integration of 1 MW solar PV at the selected buses of the 33-bus distribution network are shown in Figure 7-13. It can be seen that during an instant of fault occurrence (t=1 second), the PCC voltage drops or rises depending on the chosen PCC. The voltage

drops to 0. 74 p.u. when solar PV is connected at Bus 7 and again rises towards 1 p.u. when solar PV is connected at other buses as shown in Figure 7-13. More improvement in PCC voltage profile is obtained when DFIG is integrated in comparison with when solar PV is integrated at the same buses. The voltage profiles however follow similar patterns with the exception that brief voltage fluctuations occur during the beginning of the simulation in the case of DFIG integration. The LVRT and HVRT requirements are also met for solar PV integration at different network buses as specified by the SA grid code requirement for DG integration.

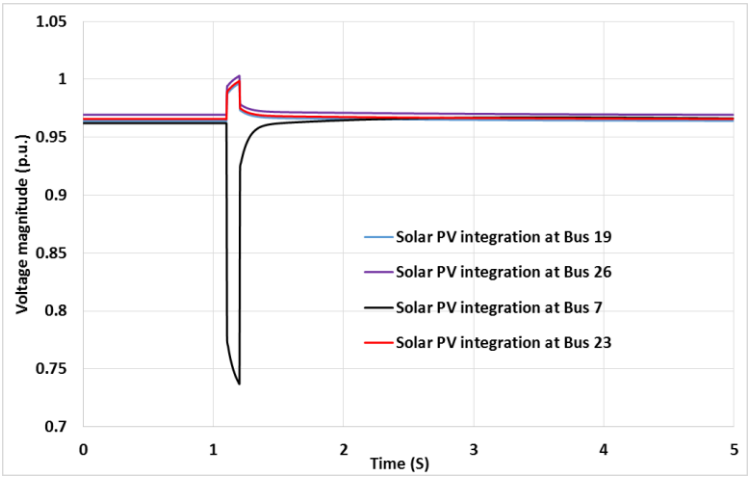

Figure 7-13: The voltage profiles after Solar PV-integration at different buses of the 33-bus network in the event of fault (Case 2)

The loads at the 4 branches of the 33-bus distribution network differ in capacity as depicted in Table 6-1. Branch 3, where Bus 7 is located, is a heavily loaded branch with the combined load power of 1.19MVA. Integration of DFIG and solar PV with the capacity of 1 MVA at Bus 7 therefore offers minimum support to voltage support during the fault since the branch's power demand is higher than the injected power by DG. The voltage magnitude rises to a value higher than the nominal voltage magnitude during the instant of fault occurrence upon DG integration at Bus 19, Bus 26 and Bus 23 because the combined electrical power demand of the corresponding branches is lower than 1 MVA. The reverse power flows which will likely result in increased active power losses on the lines are likely to occur upon integration of 1 MVA DG at Bus 19, Bus 26, and Bus 23.

iii. Impact on overall active power losses

The overall active power losses resulting from integration of solar PV and DFIG-based DGs at selected buses of the 33-bus distribution network are presented in Figure 7-14. In comparison with total active power losses of the base case, a significant reduction is observed when DFIG-based DG is integrated at all the selected buses. The overall active power losses of the network are lowest when DFIG is integrated at Bus 7. Integration of solar PV at different buses results in insignificant change in active power losses as can be seen in Figure 7-14. DFIG-based DG therefore results in a greater

reduction in overall active power losses on the 33-bus distribution network in comparison with solar PV integrated at the same bus.

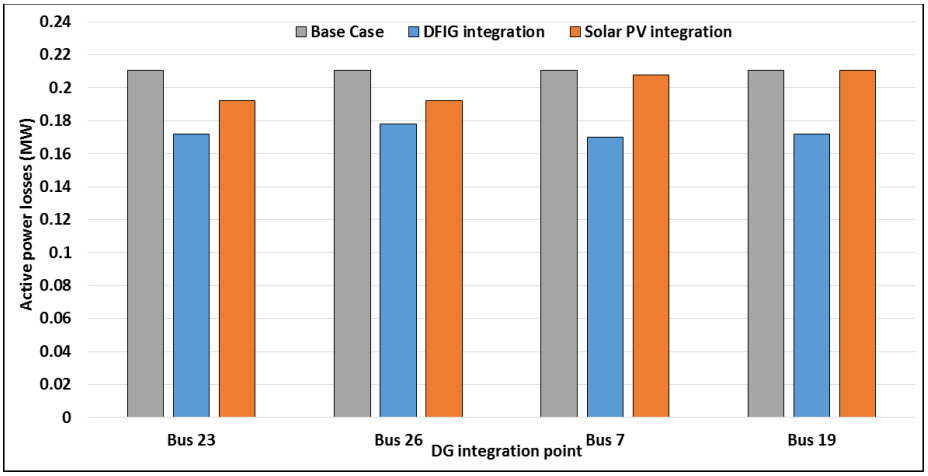

Figure 7-14: Impact of DG location on 33-bus network's overall active power losses (Case 2)

A greater reduction in overall active power losses occurs after DFIG integration because of its reactive power exchange capability, a feature that enhances the line power transfer capabilities transfer of apparent power through the lines, hence reducing the current due to improved voltage support. The possibility of reverse power flow is therefore reduced in the case of DFIG integration in comparison to solar PV integration which injects only active power in to the grid.

7.3 Case 3: Effect of DG sizing on PQ enhancement

The effect of altering the capacity of solar PV and DFIG-based DGs on PCC voltage profiles and overall active power losses is investigated in this case. As discussed in Chapter 6, the analysis of the impact of DG sizing is performed on both sub-transmission and distribution networks.

7.3.1 *Impact of DG sizing in 9-bus sub-transmission networks*

The voltage profiles resulting from changing the capacity of integrated solar PV and DFIG-based DGs on a 9-bus sub-transmission network are presented in this section. As described in section 6.3, the analysis is conducted first during the normal network operation in the absence of faults and then during instances of fault occurrence.

i. Impact of DG sizing in the absence of faults

A. Impact on voltage profiles

From Case 2 observations, Bus 8 was proven to be the best PCC of the 9-bus network based on the resulting voltage profiles after DG integration. DGs are therefore connected to Bus 8 in this case. The voltage profiles at Bus 8 are observed as the capacity of DGs is increased. The comparative analysis is made between DFIG and solar PV-based DGs on the basis of the PCC voltage profiles as result of increasing the penetration level of each. The system's overall active power losses resulting from increasing the penetration level of DFIG and Solar PV are also observed.

The voltage profiles as a result of increasing the penetration level of solar PV at Bus 8 are shown in Figure 7-15. It is observed that the voltage magnitude at the PCC increases as the capacity of solar PV is increased. The capacity of solar PV was increased up to 100MW which is equivalent to 31.7% of the total loading of the network. This was to observe whether the system can handle large penetration levels. The active power losses were however observed to increase at higher capacities hence limiting solar PV capacity to 100MW. It can be seen that at 31.7% of solar PV penetration level, the voltage rises to 0.974 p.u. which is an 1.64% increase from that of the base case.

The resulting voltage profiles depict that increasing the penetration level of solar PV results in a significant improvement of the PQ in the system. It is however worth noting that very high penetration levels of solar PV may result in excessive voltage rises at the PCC and violate the grid code requirements. This was manifested by the voltage profiles resulting from the integration of penetration levels higher than 40% which in addition to resulting in voltages magnitudes rising above the pre-defined limits, also resulted in increased overall active power losses in the network.

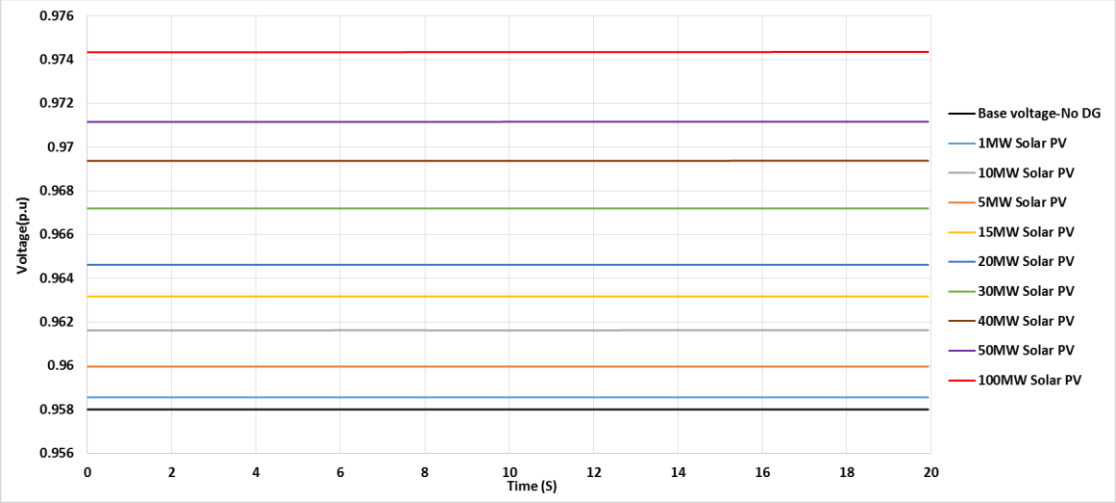

Figure 7-15: The voltage profiles resulting from increasing the penetration level of integrated solar PVs at Bus 8 at 9-bus network (Case 3)

The voltage profiles resulting from increasing the penetration level of DFIG-based DGs at the same bus are shown in Figure 7-16. It can be seen from this figure that at very low penetration levels (1 MVA to 5 MVA), the voltage profile at the PCC drops slightly below that of the base case, as depicted in Figure 7-8. The voltage profile at the PCC is however observed to increase with the increasing capacity of DFIG at the PCC. At DFIG capacity of 100MVA, which is equivalent to 31.7% of the total loading of the network, the voltage profile increases to 0.985 p.u. and is 3.6% higher than that of the base case. In addition to voltage rise at the PCC, it can be seen that brief voltage fluctuations are introduced upon DFIG integration.

In comparison with the case of solar PV integration, the voltage profiles resulting from increasing the penetration level of DFIG are relatively higher for the same penetration level. The comparison of the voltage profiles resulting from integration of the same capacities of solar PV and DFIG based DGs are presented in Figure 7-17. Using the base case voltage profile as reference, it can be seen that the PCC voltage rises upon integration of both solar PV and DFIG, but higher voltage magnitudes are attained in the case of DFIG integration. For instance, as depicted in Figure 7-17, at 70MW penetration level, the voltage profile as a result of solar PV integration rises to a constant value of 0.974 p.u. At the same penetration level of DFIG, the voltage profile settles to a value of 0.983 p.u. after brief oscillations. The overall voltage profile results obtained as the penetration level of solar PV and DFIG are increased in the absence of faults indicate that a significant voltage support is offered by DFIG integration than Solar PV integration. This is due to the fact that DFIG has the capability of injecting and absorbing reactive power as per its voltage control settings. The quality of the voltage profile is however better in the case of solar PV integration due to absence of voltage fluctuations, as manifested by the resulting voltage profiles.

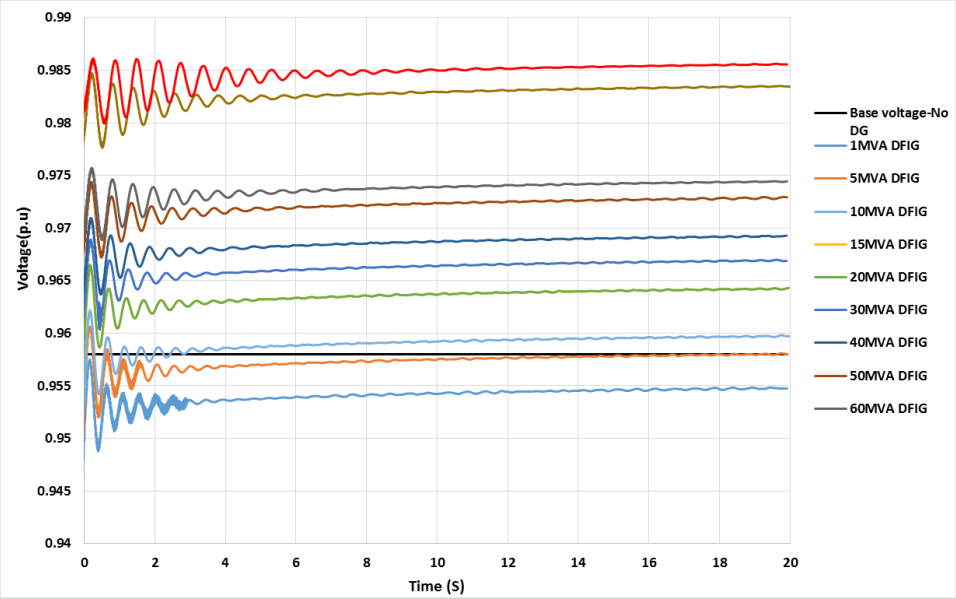

Figure 7-16: The voltage profiles resulting from increasing the capacity of integrated DFIG at the Bus 8 PCC of 9-bus network (Case 3)

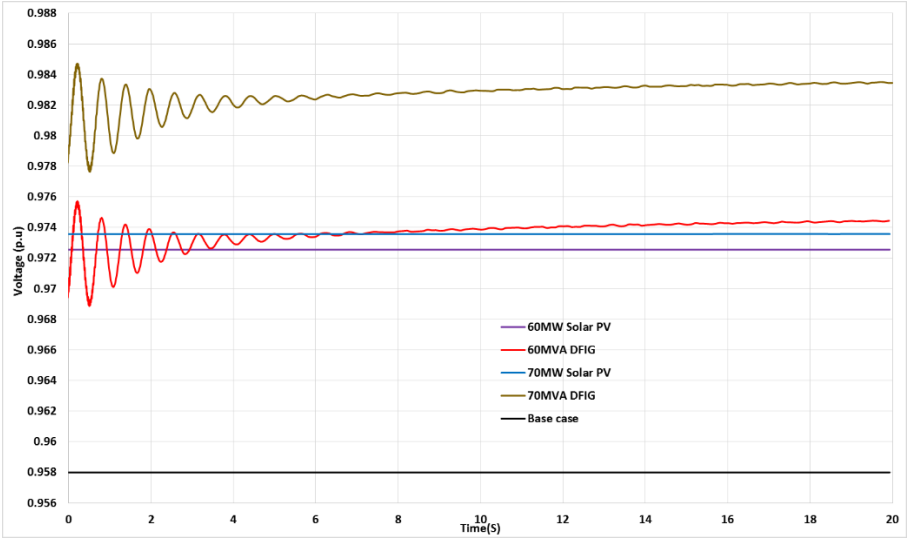

Figure 7-17: The comparison of the voltage profile at the Bus 8 PCC of 9-bus network for the same penetration levels of solar PV and DFIG based DGs (Base Case and Case 3)

B. Impact of DG sizing on total active power losses

The overall active power losses as a result of altering the penetration levels of solar PV and DFIG based DGs in the absence of faults are also observed for comparison. The results illustrating how the overall active power losses of the network change with altering the capacity of DGs are shown in Figure 7-18. It can be seen that as the penetration level of DGs is increased, the total active power losses decrease as depicted in Figure 7-10. The active power losses however decrease up to certain penetration level of DGs, after which they start to increase. The total power losses due to solar PV integration are relatively lower than that resulting from DFIG integration from DG capacities of 5MVA to 70MVA. The total losses however start to increase as the capacity of DGs is increased beyond 80MVA as depicted in Figure 7-10. The penetration level of DGs was increased up to 47.62% which is equivalent 150MVA. The total power losses as a result of large penetration levels of solar PV integration are higher than that of the base case and that of DFIG integration case as depicted in Figure 7-18. At DG capacities higher than 70 MVA, DFIG results in lower active power losses because of an enhanced electrical power transfer as a result of reactive power support offered by DFIG. The reason for an increase in active power losses due to very high DG penetration level is the reverse power flow which occurs when the total supplied electrical power exceeds that of the network loads.

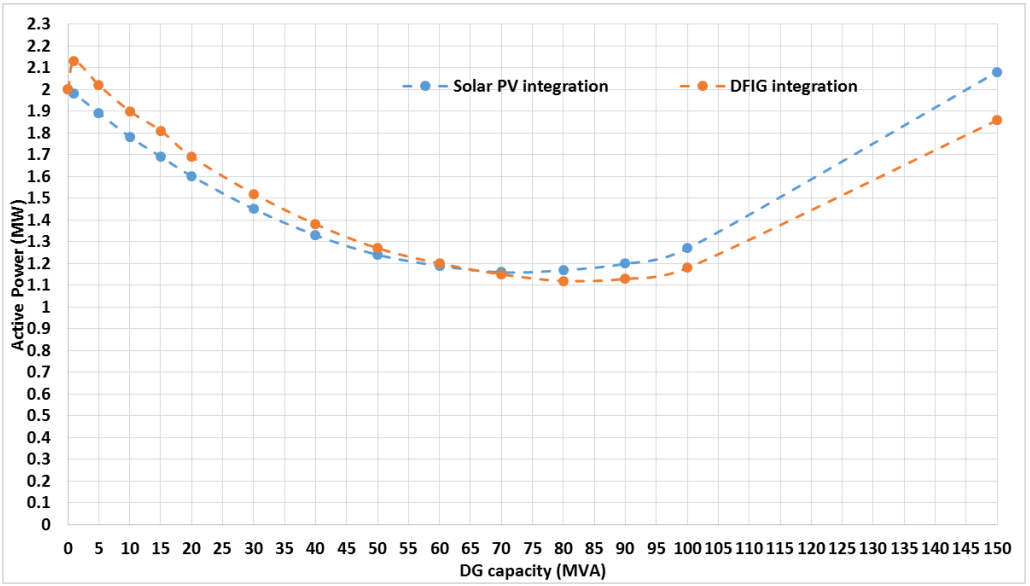

Figure 7-18: The total active power losses of the 9-bus network as a result of increasing the penetration level of solar PV and DFIG at the PCC

ii. Impact of DG sizing in the presence of faults

A. Impact on voltage profiles

The results of increasing the capacity of integrated DGs during the fault in the network are also presented in this section. Figure 7-19 shows the resulting voltage profiles when the capacity of DFIG integrated at Bus 8 PCC of the 9-bus test system is increased in the same manner. In comparison with the voltage profile of the base case, increasing the DFIG capacity at the PCC results in increasing voltage magnitude at the PCC. The voltage recovery time after the fault also reduces as DFIG capacity is increased. It can be seen from Figure 7-19 that once the capacity of DG reaches 20 MVA, a brief voltage spike occurs during the fault after which voltage settles to a constant value of 1.30 p.u. The voltage spike occurs as a result of DFIG responding to bus voltage drop by injecting reactive power in to the grid. It is therefore evident that during fault condition in the network, DFIG capacity as high as 20MVA will result in over-voltages at the PCC which may result in reverse power flows. The maximum capacity of DFIG which results in voltage limits not exceeding the prescribed limits is obtained to be 18MVA. The power flow calculation in DIgSILENT could not converge and hence results could not be obtained at capacities of DFIG greater than 20MVA.

The DFIG capacities considered are that falling under category B as per the SA grid code and should abide by the LVRT and HVRT requirements specified for DGs of this category. Since the 9-bus network is a HV system, the LVRT requirements are met because the voltage drop is above 0% for all DFIF capacities. The HVRT requirements are however violated at DFIG capacity of 20 MW since the voltage rises above 120% of the nominal voltage for over 2 seconds.

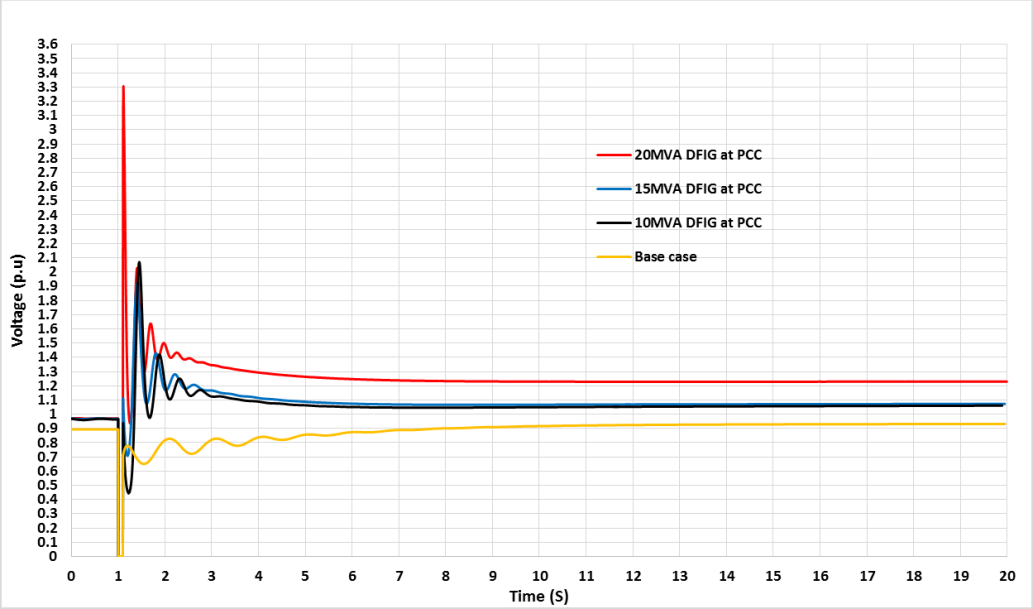

Figure 7-19: Voltage profiles at the Bus 8 PCC of 9-bus network for different capacity levels of DFIG-based DG (Case 3)

The results of the voltage profiles obtained from increasing the capacity of solar PV at the PCC are depicted in Figure 7-20 below. It is observed that increasing the capacity of solar PV at the PCC has a minimum impact on the post fault voltage profile but only up to a capacity of 25MW. As the capacity of solar PV reaches 30MW, the distortions in the PCC voltage profile are experienced as indicated in Figure 7-20 below. This is the result of increased harmonics in the output voltage of the inverter of the solar PV system. The PV system is operated at unity power factor and injects only active power into the grid, large penetration levels therefore result in lack of reactive power in the network. The voltage magnitudes at the PCC and nearby buses are consequently increased. In addition to multiple voltage fluctuations, the magnitude of the voltage after fault clearance reaches 0.75 p.u., which is below the lower limit specified by the grid codes. The solar PV capacity of 30MW is equivalent to the penetration level of 8.95%, as calculated using Equation 6-1. In the case of solar PV integration, both the LVRT and HVRT requirements are met at the capacities investigated.

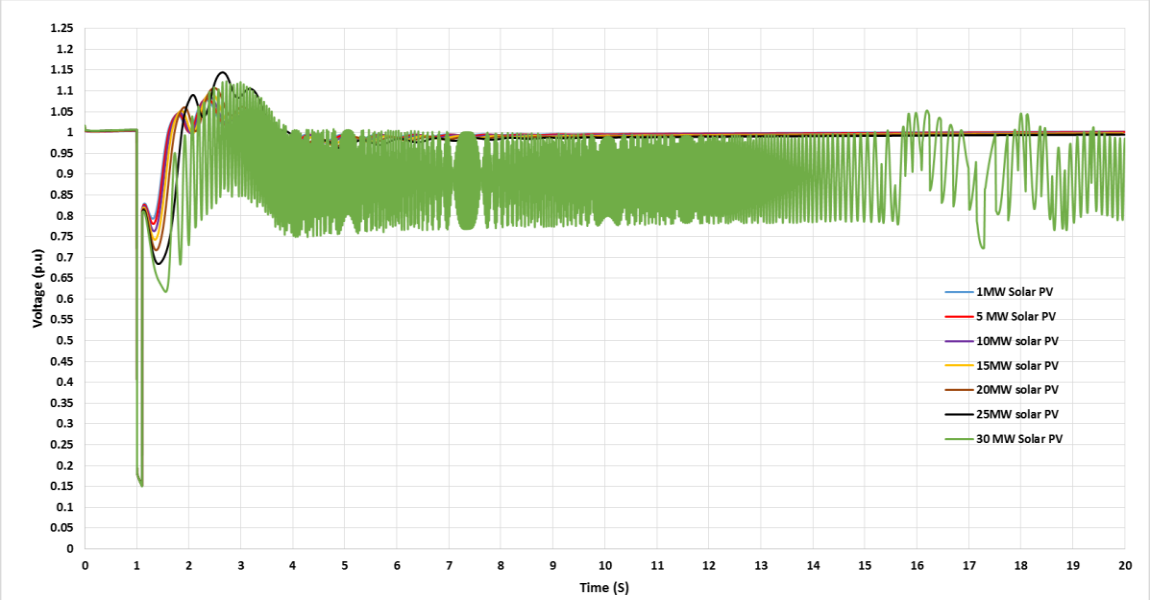

Figure 7-20: Voltage profiles at the Bus 8 PCC of 9-bus network for different capacity levels of Solar PV based DG (Case 3)

The voltage profiles at the PCC resulting from integration of solar PV with capacities below 30MW are presented in Figure 7-21 below. It is observed after the fault is cleared, the voltage rises briefly followed by small fluctuations before settling to a constant magnitude of 1.0 p.u. As the penetration level of solar PV is increased, the post fault PCC voltage attains a higher value before assuming the nominal value of 1.0 p.u. The solar PV capacity of 25MW results in voltage briefly rising to 1.15 p.u. before returning to 1.0 p.u. after the fault occurrence. From the results obtained, it is observed that in comparison with DFIG integration, larger capacities of solar PV can be integrated at the PCC without violating voltage limits in the event of fault in the network.

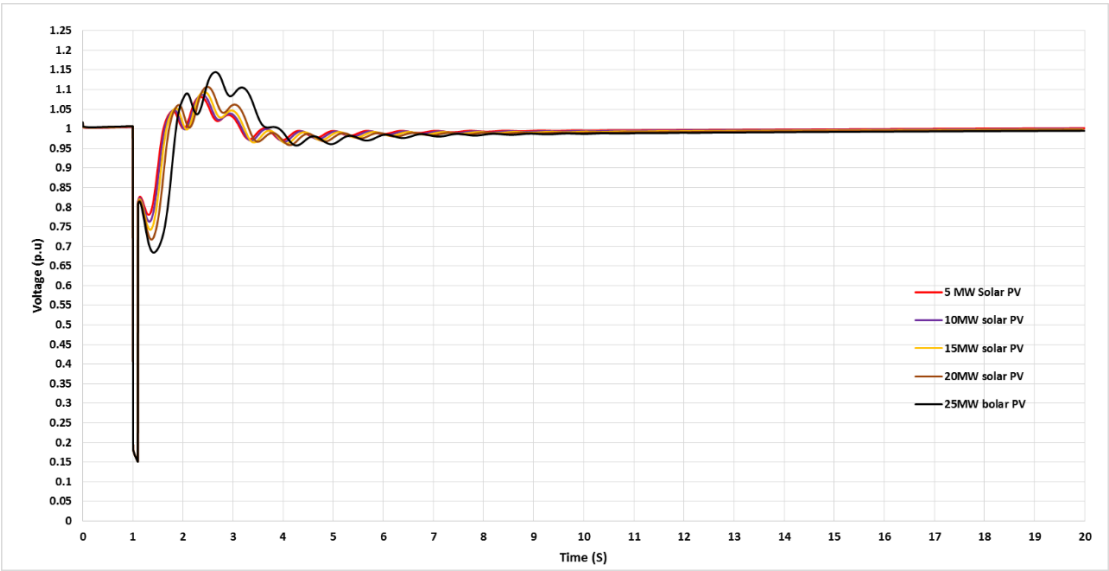

Figure 7-21: Improvement in voltage profile at the Bus 8 PCC of 9-bus network for increasing capacities of solar PV (Case 3)

B. Impact on total active power losses

The total active power losses obtained as the capacities of solar PV and DFIG-based DGs at the PCC are increased are presented in Figure 7-22 below. It can be seen that the overall active power losses when a 1 MW solar PV is integrated at the PCC amounts to 2.15MW, which is 29.5% lower than that obtained for the same capacity of DFIG. It can be seen that the total active power losses are lower for solar PV as compared to DFIG integration at the same capacity levels. As can be seen, the difference in total active power losses is higher at lower capacity levels and starts narrowing as the capacities of solar PV and DFIG are increased. The higher decrease is due to enhanced transfer of apparent power through the lines which consequently lower the current magnitude at higher DFIG capacities. The overall active power losses are approximately equal at the capacity of 20MA indicating that higher DFIG penetration levels may result in more reduction in power losses relative to solar PV integration.

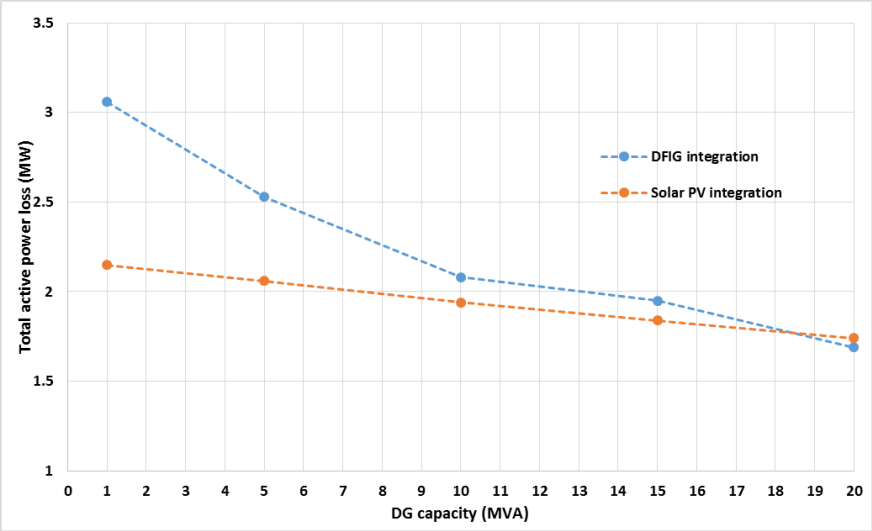

Figure 7-22: Comparison of the total active power losses for the increasing capacity of DFIG and Solar PV integrated at the Bus 8 PCC of 9-bus network (Case 3)

The DFIG-based DG has the least positive impact on the overall active power losses because the injected power is intermittent, presenting high time variability, and does not match well with the load pattern of the nodes. Additionally, DFIG exchanges power through both the rotor and stator. The majority of the power is passes through the stator and only a small fraction is passed through the rotor and the PWM converter. More active power is therefore lost from the DFIG system as power is injected into the grid, in comparison with the solar PV-based DG.

7.3.2 *Impact of DG sizing in 33-bus distribution network*

The impact of DG sizing in distribution networks is investigated on the IEEE 33-bus distribution network as discussed in Chapter 6. As discussed, the capacity of DGs in distribution network is limited to 5MVA. The analysis is performed in the absence of faults and during an instance of fault occurrence.

i. Impact of DG sizing in the absence of faults

The resulting voltage profile after DGs were integrated at Bus 7 in Case 2 indicated that Bus 7 is the best PCC for DG integration. The voltage profiles at the PCC resulting from increasing the capacity of DFIG-based DGs connected at Bus 7 of the 33-bus distribution network are shown in Figure 7-25. It can be see that upon integration of DFIG, momentary oscillations occur on the PCC voltage profile before settling at the constant value. Larger fluctuations in the PCC voltage profile are observed at the highest DFIG capacity of 5 MVA. A more improved PCC voltage profile occurs at DFIG capacities less than 5 MVA due to reduced fluctuations in bus voltage profile as depicted in Figure 7-23. The voltage magnitude at the PCC is observed to increase as the capacity of DFIG is increased. In comparison to the base voltage profile, a significant improvement in PCC voltage profile is observed as the DFIG capacity is increased.

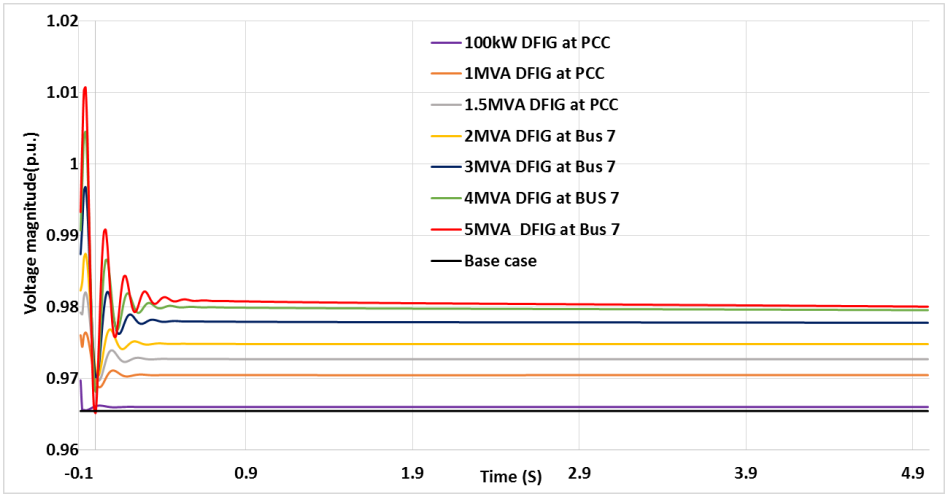

Figure 7-23: Voltage profiles at the Bus 7 PCC of 33-bus network for increasing the capacity of DFIG-based DGs (Case 3)

The voltage profiles at the PCC resulting from increasing the capacity of solar PV at Bus 7 during normal network operation are shown in Figure 7-24. It can be seen that similar to the case of DFIG integration, increasing the capacity of solar PV-based DGs results in an increase in voltage magnitude at the PCC.

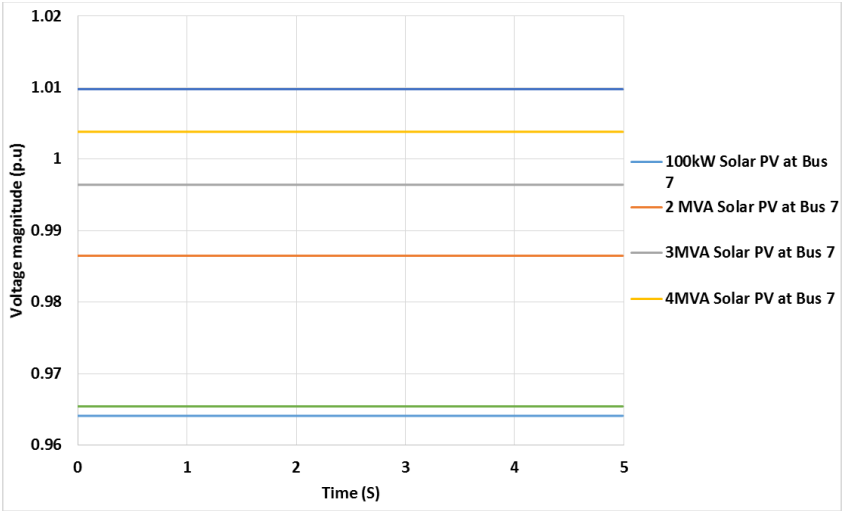

Figure 7-24: Voltage profiles at the PCC for increasing the capacity of Solar PV-based DGs at the Bus 7

ii. Impact of DG sizing during fault condition

The voltage profiles at the PCC resulting from increasing the capacity of DFIG-based DGs during fault condition are shown in Figure 7-25. The voltage at the PCC when DGs are not connected, instantly drops to 0 when the fault is applied before returning to 0.97 p.u. after the fault clearance. The voltage magnitude during the fault is seen to increase on increasing capacity of DFIG. From the DFIG capacity of 2MVA, the voltage rises to values outside a limit of 1.1 p.u., for 33-bus distribution network during fault occurrence. The optimum capacity of DFIG that offers a significant support to the PCC voltage profile without violating the limits during the fault is 1 MVA as shown in Figure 7-25.

The LVRT requirements are met at DFIG capacities of 1 MVA since the voltage drop is at 60% of the nominal for the duration of the fault (0.1seconds). This is within the requirements of 60% for 0.15 seconds as required by the SA renewable plants grid code. The HVRT requirements on the other hand are violated when DFIG capacities exceed 1 MVA since the voltage rises over 120 % for over 0.16 seconds as required by the grid code for DG integration in LV networks.

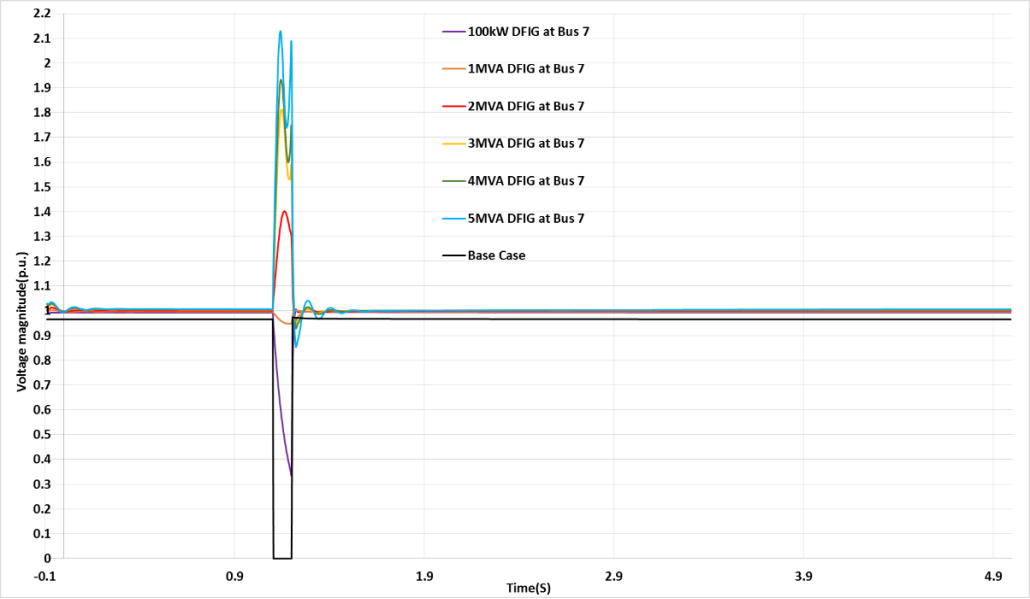

Figure 7-25: Voltage profiles at the Bus 7 PCC in 33-bus network for different capacities of DFIG-based DGs (Case 3)

Increasing the penetration level of solar PV, during the fault on a 33-bus distribution network, results in a voltage transient behaviour as shown in Figure 7-26. It can be seen that during an instant of fault occurrence, the voltage drops to lower magnitudes before returning to a constant value after the fault is cleared. Unlike the case of DFIG integration, the magnitude of the voltage during the fault is lower for the same capacity of solar PV due to insufficient reactive power support from the solar PV system. The final settling voltage after the fault is cleared however increases with the increasing solar PV capacity. The fault voltage however show a significant improvement at Solar PV capacity of 100kW,

where both the fault voltage magnitude as well as post voltage magnitudes lie within the specified limits 0.9 – 1.1 p.u. for the distribution network. The LVRT requirements for solar PV integration are only met at solar PV capacities of 100 kW up to 2 MVA. Higher solar PV capacities violate the LVRT requirements for LV networks since the voltage drops below 60% of the nominal as required by the grid code.

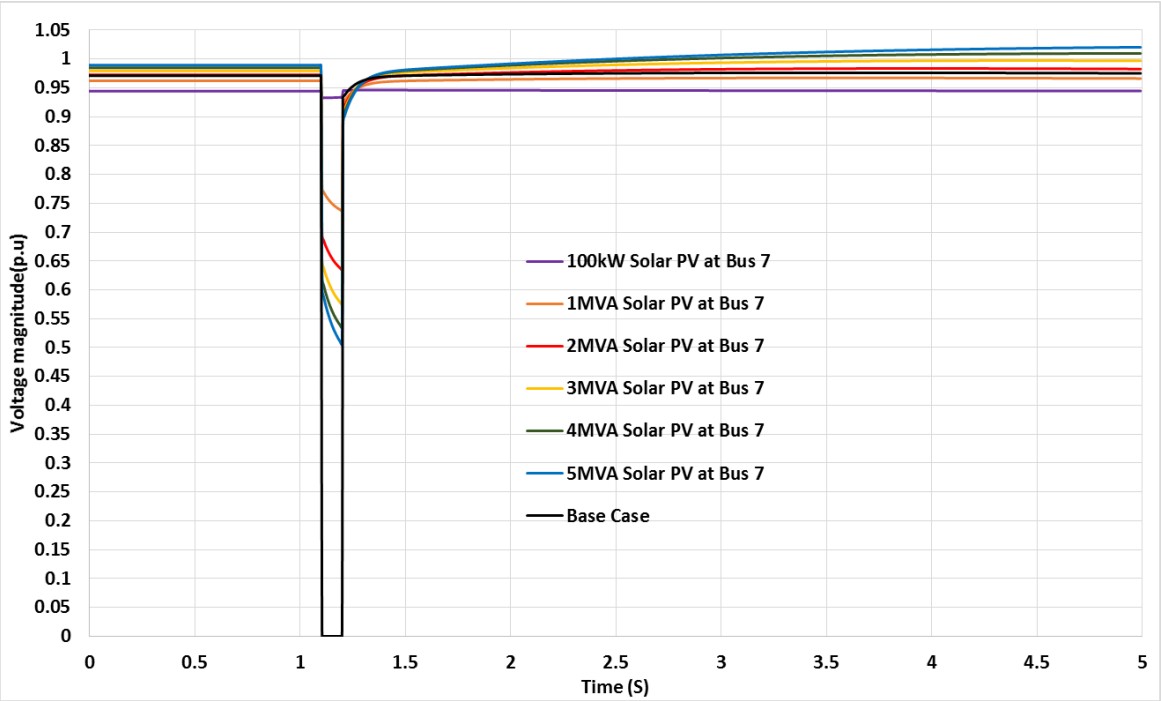

Figure 7-26: Voltage profiles at Bus 7 PCC in 33-bus network after integration of different Solar PV capacities (Case 3)

iii. Impact on active power losses

The overall active power losses of the 33-bus distribution system in the absence of faults are also observed before DG integration and while the capacities of solar PV and DFIG-based DGs are increased. Figure 7-27 below shows the comparison of the impacts of DG capacity on the overall active power losses of the network. It is observed that increasing the capacity of both Solar PV and DFIG-based DGs results in reduction of active power losses. The overall active power losses however start increasing at solar PV capacity of 3MW and continue increasing up to 0.23 MW at solar PV capacity of 5MW. The cause of an increase in active power losses at high penetration level is the reverse power flow that occurs because the supplied load upstream of the PCC is small relative to solar PV capacity. The lack of reactive power support capabilities of the solar PV system also contributes to increased active power losses because of poor power flow transfer. A linear reduction in overall active power losses is however observed when the capacity of DFIG is increased. DFIG on the other hand has reactive power exchange capability with the grid which offers a proper voltage control and hence less chance of reverse power flow.

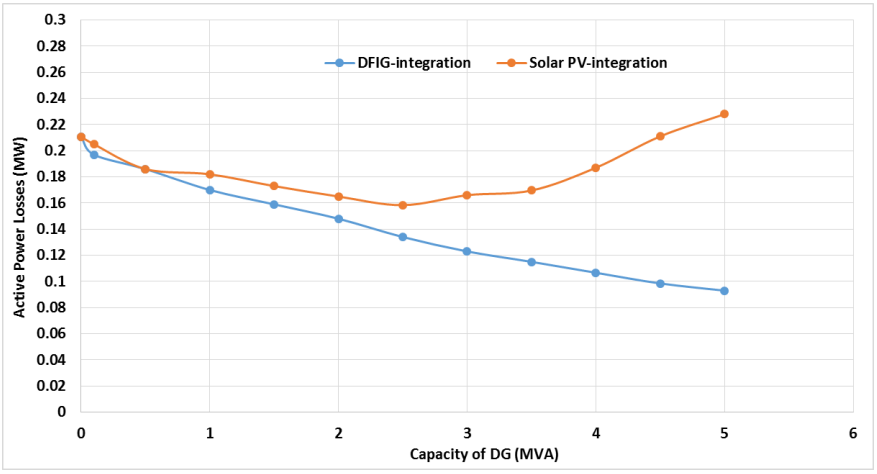

Figure 7-27: Comparison of the overall active power losses in the 33-bus network as DG capacity is increased (Case 3)

7.4 Case 4: PQ enhancement in grid-connected DGs by application of voltage control schemes

The results obtained when voltage control schemes are included at the PCC are presented below. PQ improvement by application of STATCOM and SVC for reactive power compensation is investigated on the IEEE 9-bus sub-transmission and IEEE 33-bus distribution networks discussed in Chapter 5. The resulting voltage profiles and overall active power losses of the networks are observed under the three-phase fault condition. The models of STATCOM and SVC are as discussed in section 5.6 and their parameters for the two networks are presented in Table 6-3.

7.4.1 *Effect of voltage control in 9-bus sub-transmission network*

The impacts of voltage control in sub-transmission networks is performed on the 9-bus network discussed in Chapter 5. The PCC is chosen as Bus 8 and the transient behaviour of the system is observed in terms of the resulting PCC voltage profiles when STATCOM and SVC are connected at the PCC of solar PV and DFIG-based DGs.

i. Reactive power compensation by STATCOM

The voltage profiles showing the impact of including the STATCOM at the Bus 8 PCC of the network with solar PV and DFIG-based DGs are shown in Figure 7-28 and Figure 7-29 respectively. The voltage profiles at the PCC are compared after integration of DGs only and that when STATCOM is connected at the PCC. Figure 7-28 shows that including a STATCOM at the connection point of Solar PV results in a significant improvement in voltage profile at PCC before and after the fault. The voltage magnitude before connecting the STATCOM is 0.9 p.u. and it rises to 1 p.u. after the STATCOM is included at the PCC. In comparison to the base case, and Case 2 when Solar PV alone is connected at Bus 8, the fluctuations in voltage profile after the fault clearance are significantly reduced upon the connection of the STATCOM. Voltage control offered by STATCOM in solar PV-

integrated system leads to improved and smoothened PCC voltage profile due to STATCOM's ability to absorb and inject reactive power thus stabilizing voltage excursions. For this case, both the LVRT and HVRT requirements are met since the PCC voltage drop and duration are within the required limits.

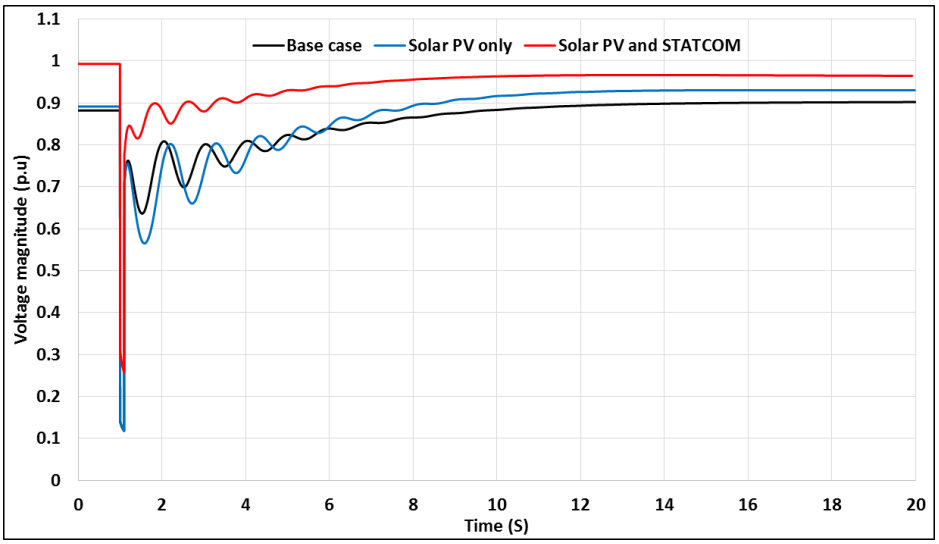

Figure 7-28: Voltage profiles at PCC to illustrate the impact of STATCOM when solar PV is connected at Bus 8 PCC of the 9-bus network (Case 4)

Figure 7-29 presents the voltage profiles at the PCC when DFIG and STATCOM are connected at the same PCC. It is observed that in the absence of STATCOM, voltage momentarily rises to higher values during an instant of fault occurrence when DFIG is connected. The voltage then fluctuates for 7 seconds before settling to a constant magnitude of 1 p.u. When STATCOM is included, the voltage fluctuations are significantly reduced as the voltage fluctuates only for 2 seconds before settling to constant magnitude of 1.05 p.u. The brief voltage spike during fault occurrence however exceeds the maximum voltage limit of 1.05. It would therefore be necessary to develop a proper control mechanism that will limit the amount of reactive power that STATCOM injects into the grid for voltage support. The amplitude of the fluctuations is also significantly reduced in comparison to that of when DFIG is connected alone. Voltage control by STATCOM is therefore observed to be more effective in the case of solar PV integration in comparison to DFIG integration. The DFIG system's capability of injecting or absorbing reactive power in its operation contributes to the voltage behaviour depicted in Figure 7-29.

The LVRT requirements are met for all scenarios depicted in Figure 7-29. The HVRT requirements are however violated when DFIG alone is integrated since the voltage rises over 120% for over 2 seconds before settling at a constant value. Including the STATCOM at the PCC limits voltage rise to only 1.8 seconds during an instant of fault occurrence.

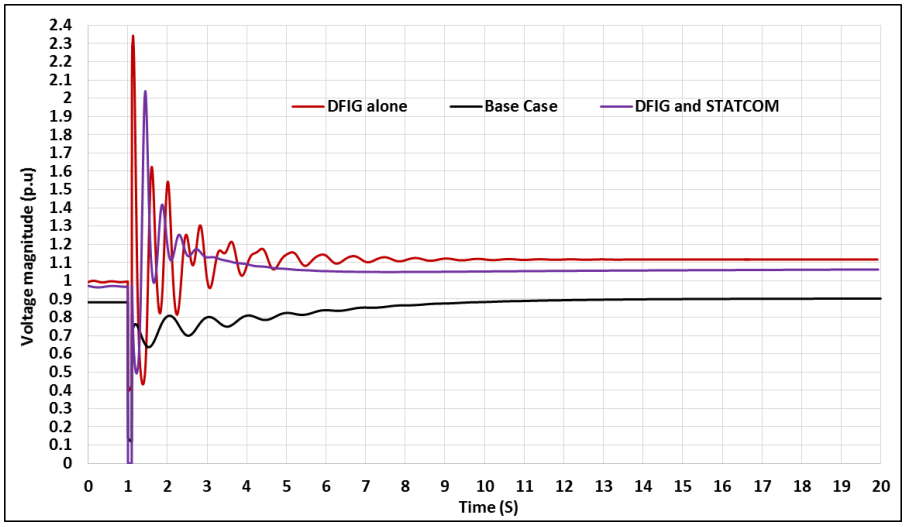

Figure 7-29: Voltage profiles at PCC to illustrate the impact of STATCOM when DFIG is integrated at Bus 8 PCC of the 9-bus system (Case 4)

ii. Reactive power compensation by SVC

The results illustrating the transient response of the system after connecting the Static Var Compensator (SVC) at the PCC of the grid with solar PV integration are presented in Figure 7-30. It is observed that during the integration of solar PV only, after the fault is cleared, voltage oscillates briefly below lower limit of 0.95 p.u., before attaining the constant voltage magnitude of 0.92 p.u. It can be seen that upon the integration of an SVC at the PCC, the voltage rises to a higher magnitude and recovers within a relatively shorter time after fault occurrence. The PCC voltage attains the constant value of 1.01 p.u. after the fault occurrence, which is significantly higher than that resulting from integration of solar PV only and that of the base case. In this case, the LVRT requirements are met for solar PV only integration and when SVC is included.

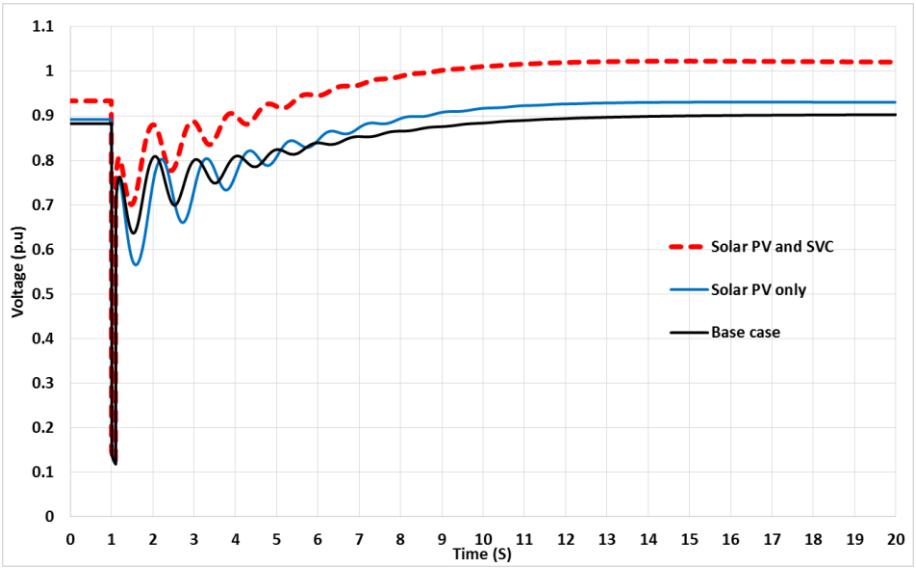

Figure 7-30: Voltage profiles at PCC to illustrate the impact of SVC when solar PV is integrated at Bus 8 PCC of the 9 bus system (Case 4)

The resulting voltage profiles are also observed in the case when DFIG integration is coupled with SVC for voltage control at the same PCC as shown in Figure 7-31. It is observed that a brief voltage spike occurs upon fault occurrence followed by oscillations lasting for 7 seconds when DFIG is connected without SVC at the PCC. The voltage then settles to a constant magnitude of 1 p.u. After the SVC is introduced at the PCC, the brief voltage spike's magnitude as well as the voltage fluctuations is significantly reduced. The voltage also rises and settles at a constant value of 1.1 p.u. A rapid voltage rise is the result of the SVC responding to the voltage drop through reactive power injection. The voltage oscillations die sooner when SVC is included and the voltage settles to a higher value in comparison to the case when DFIG is integrated without an SVC. The LVRT requirements are satisfied for integration of both DFIG only and when SVC is included. The HVRT requirements are however violated when DFIG alone is connected as the voltage rises above 120% of the nominal for over 2 seconds. Including the STATCOM at the PCC ensures compliance with the HVRT requirements as shown in Figure 7-31.

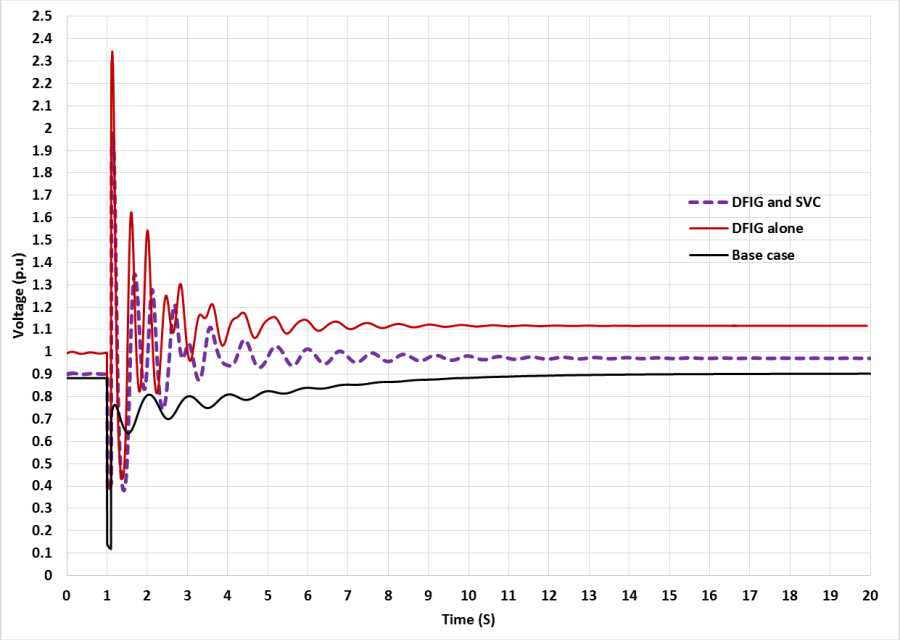

Figure 7-31: Voltage profiles at PCC to illustrate the impacts of SVC when DFIG is integrated at Bus 8 of the 9-bus system (Case 4)

From the results of the PCC voltage profiles above, it can be seen the STATCOM performs better than an SVC in both grid-connected solar PV and DFIG-based DGs. The resulting voltage profiles at the PCC also reveals that the STATCOM results in a relatively better improvement in voltage profile when coupled with solar PV. This is because of the solar PV is initially designed to operate at unity power factor and the inclusion of STATCOM helps meet the reactive power demand on the grid. The DFIG on the other hand has the capability of injecting reactive power into the grid; the presence of

STATCOM could result in excessive reactive power being injected at the PCC during the fault occurrence and consequently affects voltage quality.

iii. Impact on overall active power losses during fault condition

The overall active power losses resulting from the introduction of STATCOM and SVC at the PCC when solar PV and DFIG-based DGs are integrated are presented in Figure 7-32. The overall line losses when STATCOM and SVC are used for voltage control at the PCC are 1.84 MW and 1.9 MW, respectively in the case of Solar PV integration. In the case of DFIG integration, the overall active power losses of the network are reduced to 1.86 MW and 1.96MW after connection of STATCOM and SVC, respectively. In comparison with the case when DGs are connected without voltage control devices, a maximum reduction in overall active power losses is observed when STATCOM is connected for both Solar PV and DFIG-based DGs. Based on the obtained results, the STATCOM and SVC achieve a significant reduction in line losses in addition to improving the voltage profile in networks with DG integration.

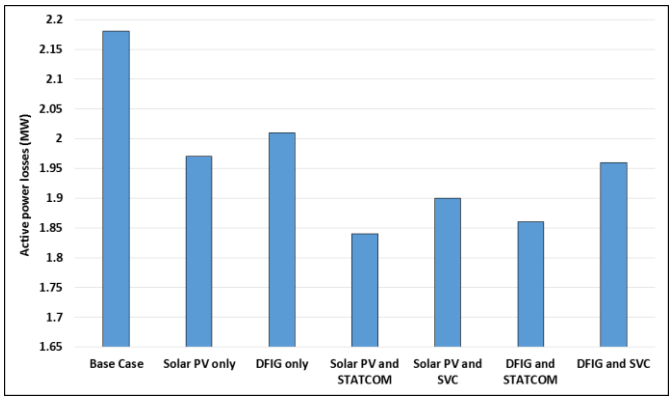

Figure 7-32: Overall active power losses in the 9-bus network for different DG-integration scenarios

The reactive power compensation provided by STATCOM and SVC helps to improve the power factor and allows for an increase in transfer of apparent power through the transmission line, hence reducing current loss in the network. The overall active power loss reduction is however more for STATCOM compared to SVC in both grid-integrated solar PV and DFIG-based DGs. Though SVC is still effective in voltage control, its bulky passive components increases the active power losses compared to that of STATCOM.

7.4.2 *Effect of voltage control in 33-bus distribution network*

The results of the effects of applying STATCOM and SVC based voltage control in grid-connected solar PV and DFIG-based DGs in the distribution network are presented in this section. The transient behaviour of the system is investigated on the basis of the resulting voltage profiles at the PCC when solar PV and DFIG-based DGs are connected at Bus 7 of the 33-bus distribution network.

i. Reactive power compensation by STATCOM

The voltage profiles resulting from connecting the STATCOM at the PCC of DFIG and solar-based DGs are presented in Figure 7-33 and Figure 7-34 respectively. It is observed that during the instant of fault occurrence (t=1 second), the voltage drops to 0 p.u. when DGs are not connected and to 0.95 p.u. and 0.45 p.u. when DFIG and solar PV are integrated, respectively. During the instant of fault occurrence in the network, incorporating the STATCOM at the PCC offers a significant support to the PCC voltage when both solar PV and DFIG -based DGs are connected. Figures 7-33 and 7-34 show that voltage settles to the values of 1.1 p.u. and 1.2 p.u. in the case of DFIG and solar PV integration, respectively. The settings of a STATCOM controller are required to be adjusted to bring the voltage magnitude within acceptable limits in the case of solar PV-integration.

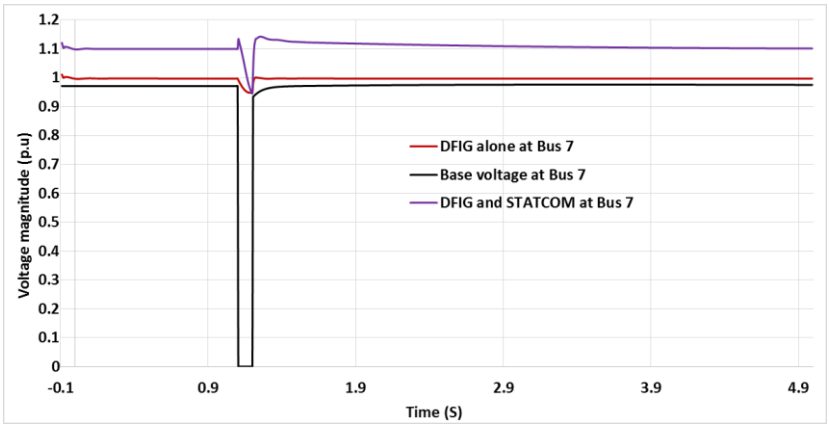

Figure 7-33: Voltage profiles at the Bus 7 PCC showing the impacts of connecting STATCOM at DFIG integration point in the 33-bus network (Case 4)

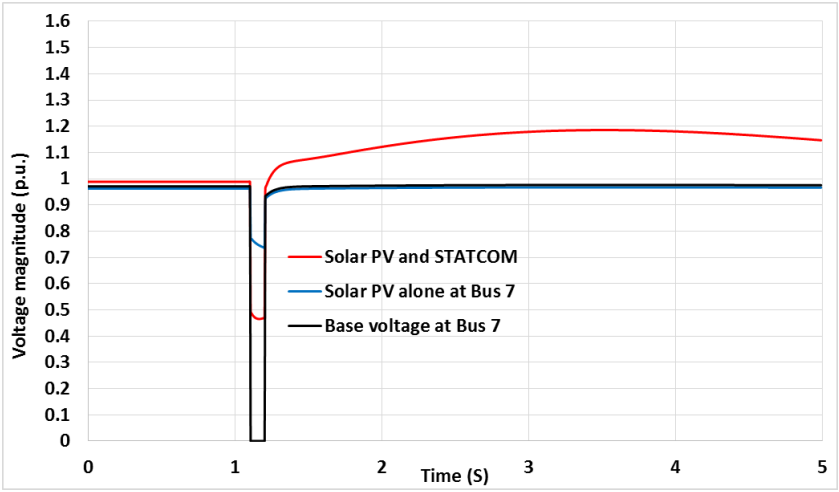

Figure 7-34: Voltage profiles at the Bus 7 PCC showing the impacts of connecting STATCOM at solar PV integration point in 33-bus network (Case 4)

ii. Reactive power compensation by SVC

The voltage profiles resulting from connecting the SVC at the PCC of DFIG and solar PV-based DGs are presented in Figure 7-35 and Figure 7-36 respectively. It is observed that upon incorporating the SVC at the PCC, the voltage rises and settles at 1.05 p.u. and 1.1 p.u. for DFIG and solar PV-based

DGs, respectively. The voltage briefly rises to 1.6 p.u. during an instant of fault occurrence (t=1 second) when DFIG is integrated and drops only to 0.95 p.u. when solar PV is integrated. The voltage spike occurs as a result of excessive reactive power injection by DFIG and SVC in an attempt to support the PCC voltage during fault. The reactive power compensation by SVC, in addition to more power being supplied when the line is disconnected during the fault, gives rise to an increase in voltage profile at the PCC. The resulting voltage profile as result of including STATCOM at the PCC of DFIG and solar PV-based DGs integration (Figure 7-33 and Figure 7-34) show a better improvement in comparison to that when SVC is included. At low AC voltages such as 12 kV of the 33-bus distribution network, the STATCOM provides a better reactive power support than an SVC because the reactive power from the STATCOM decreases linearly with the AC voltage.

The voltage rise during the fault when SVC is included at the PCC of DFIG violates the HVRT requirements since the voltage exceeds 120% for over 0.16 seconds as required by the grid code. The HVRT requirements are however met at when solar PV is coupled with SVC as shown in Figure 7-36. The LVRT requirement is achieved during both DFIG and solar PV integration as the voltage drops is above 60% required by the grid code.

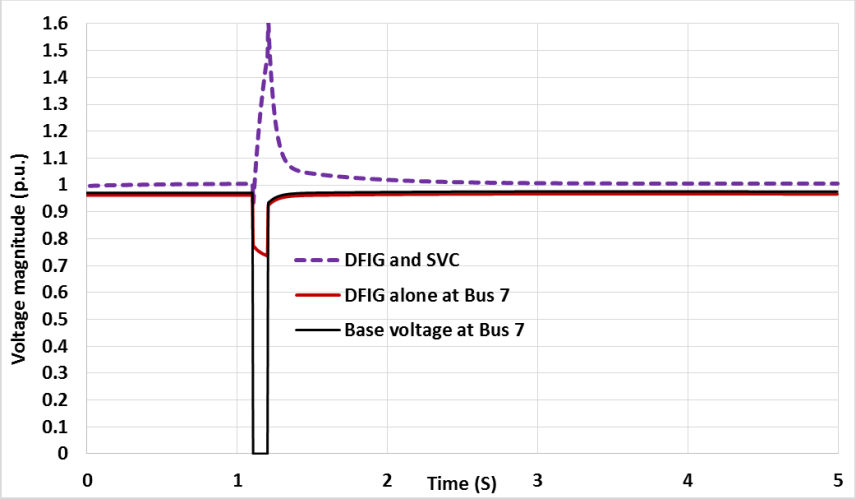

Figure 7-35: Voltage profiles at the Bus 7 PCC showing the impacts of connecting SVC at DFIG integration point in the 33-bus network (Case 4)

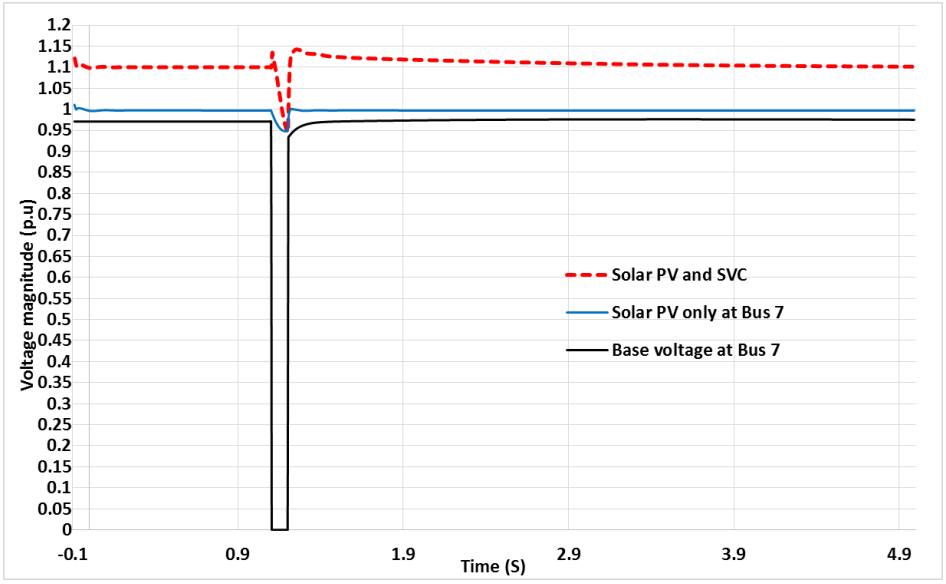

Figure 7-36: Voltage profiles at the Bus 7 PCC showing the impacts of SVC at Solar PV integration point in the 33-bus network (Case 4)

From the results of the voltage profiles obtained above, it is observed that the STATCOM and SVC are capable of improving the voltage quality in grid-connected DFIG and solar PV systems. The STATCOM however results in better voltage profiles at the PCC in comparison to that when an SVC is incorporated at the PCC for both solar PV and DFIG integration.

iii. Impact on overall active power losses during fault condition

The impact of connecting STATCOM and SVC on the overall active power losses of the 33-bus distribution network are presented in Figure 7-37. It can be observed that in comparison to the base case and Case 2 when solar PV and DFIG-based DGs are connected alone at Bus 7, the overall active power losses are reduced most upon incorporating a STATCOM at the PCC. A larger reduction in overall active power losses and better voltage profile improvement is offered by STATCOM for both solar PV and DFIG integrated in distribution network. The better voltage control offered by STATCOM decreases the risk of reverse power flow in the network feeders, hence more reduction in active power losses.

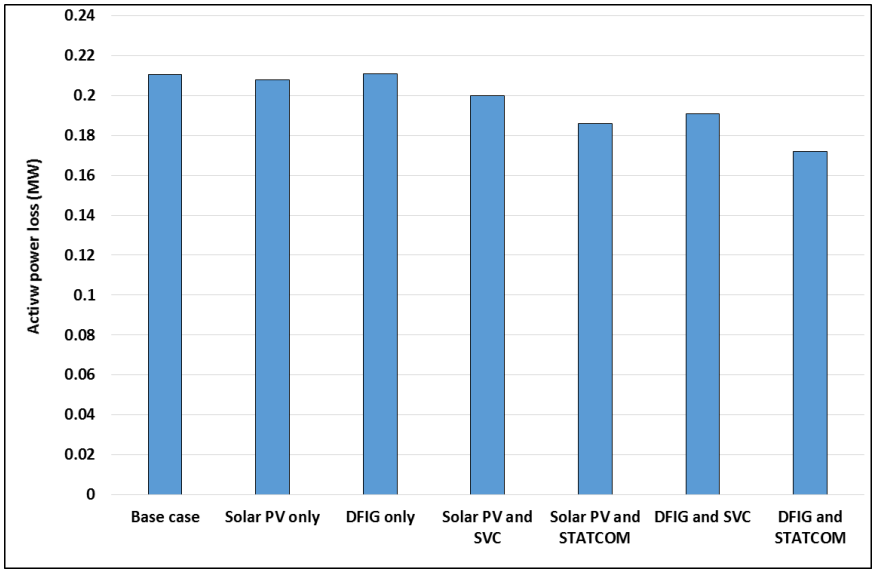

Figure 7-37: Overall active power losses as result of incorporating STATCOM and SVC at the PCC of solar PV and DFIG-based DGs

7.4.3 *Case 5: Power quality improvement by installation of battery energy storage (BES)*

7.4.4 *Installation of BES in 9-bus sub-transmission network*

The results of including BES at the PCC to improve the quality of power in sub-transmission networks with DG integration are presented in this section. The analysis is performed first in the absence and then in an event of fault occurrence as discussed in Chapter 6.

i. Impact of BES in the absence of faults

Figure 7-38 compares the voltage profiles at the Bus 8 PCC between the base case and when solar PV is integrated at the PCC with and without a 2MW BES when there is no fault in the network. It can be seen that upon integration of solar PV only, the PCC voltage profile rises from 0.958 p.u. for base case to 0.965 p.u. When BES is now introduced at the same PCC, voltage further rises to 0.966

p.u. It is thus evident that BES contributes positively to PCC voltage profile improvement after solar PV integration.

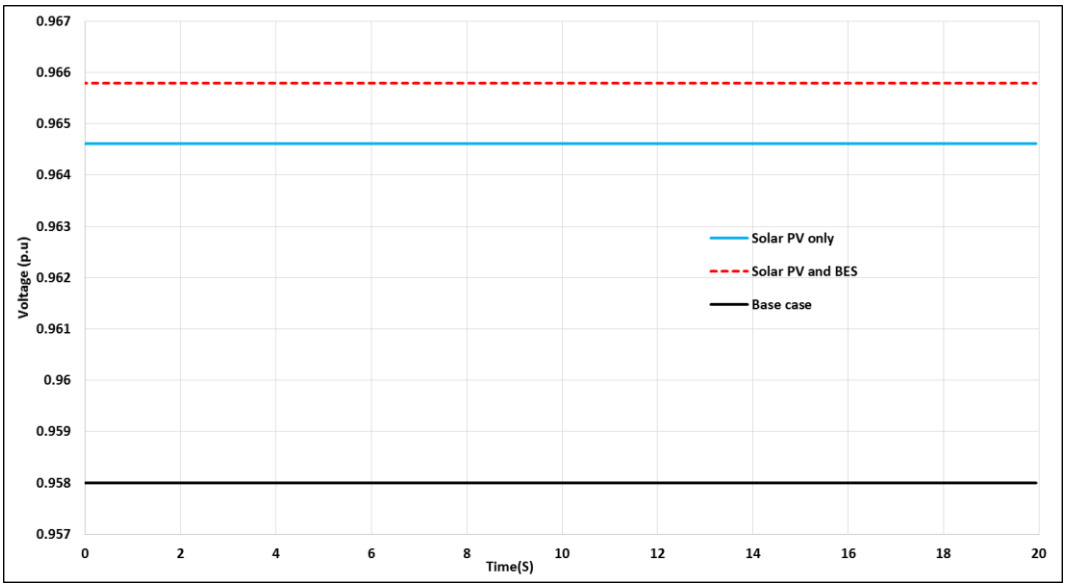

Figure 7-38: Voltage profiles for base case and with solar PV integration at the Bus 8 PCC of 9-bus network with and without BES (Case 5: without fault)

The resulting PCC voltage profiles for DFIG integration with and without BES at the Bus 8 PCC in the 9-bus network during normal system operation are presented in Figure 7-39. It is observed that integrating DFIG to the PCC results in voltage fluctuations in addition to a voltage rise as depicted in Figure 7-39. The fluctuations are dominant in the first 3 seconds of the simulation and reduce significantly afterwards. The inclusion of BES at the PCC further increases the voltage profile at the PCC though the fluctuations are still visible even after its integration. The voltage profile settles at 0.963 p.u. when only DFIG is integrated and settles to a higher value of 0.965 p.u. upon connecting the BES at the PCC. It is observed that the voltage rise due to addition of BES at the PCC is 0.21% in the case of DFIG integration and 0.1% in the case of solar PV integration. The fluctuations in the PCC voltage profile when BES is connected with DFIG settle after 12 seconds. The oscillations can be eliminated by employing reactive power control device such as STATCOM and SVC. Reducing the capacity of the BES will reduce the fluctuations. Voltage support will however be compromised by reduced BES capacity.

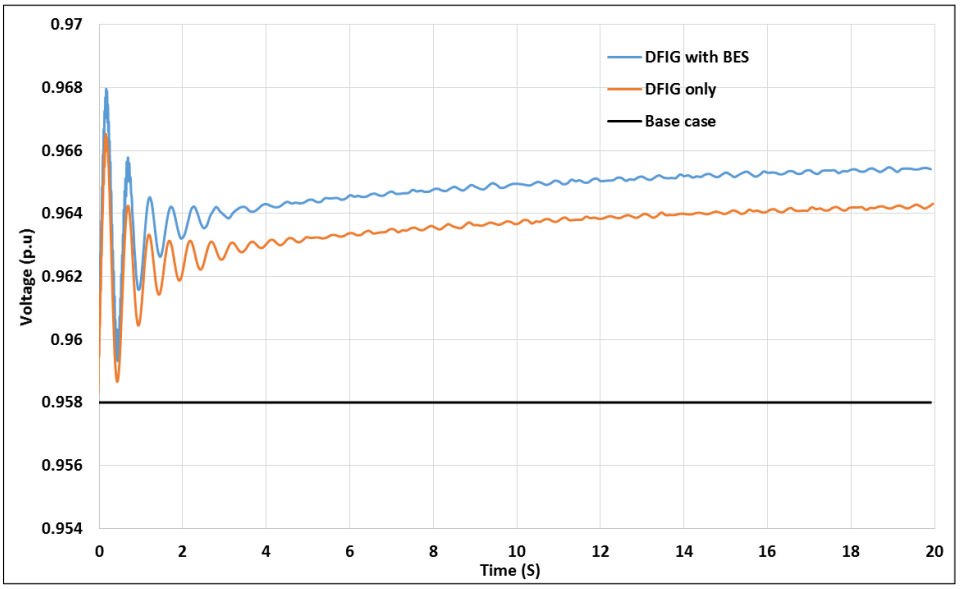

Figure 7-39: Voltage profiles for base case and with DFIG integration at the Bus 8 PCC of 9-bus network with and without BES (Case 5: without fault)

ii. Impact of BES in the presence of faults

The effect of BES is also investigated under faulted condition in the network and the transient voltage behaviour is observed during and after fault clearance when DGs are integrated with and without BES. The three-phase fault is located at Line 3 and occurs at t=1 second and is cleared at t=1.1 seconds. The PCC voltage profiles at Bus 8 for integration of solar PV with and without BES are illustrated in Figure 7-40. Figure 7-40 shows that the voltage recovery time after the fault clearance is shorter in the case when solar PV is coupled with BES, as compared to only solar PV integration and the base case. It is observed that voltage drop is lowest when solar PV and BES are both connected at the PCC. It can be seen that the post-fault voltage settles at 1.05 p.u. when solar PV is coupled with BES and to a value little lesser for only solar PV, as compared to base case voltage profile which settles at 0.9 p.u.

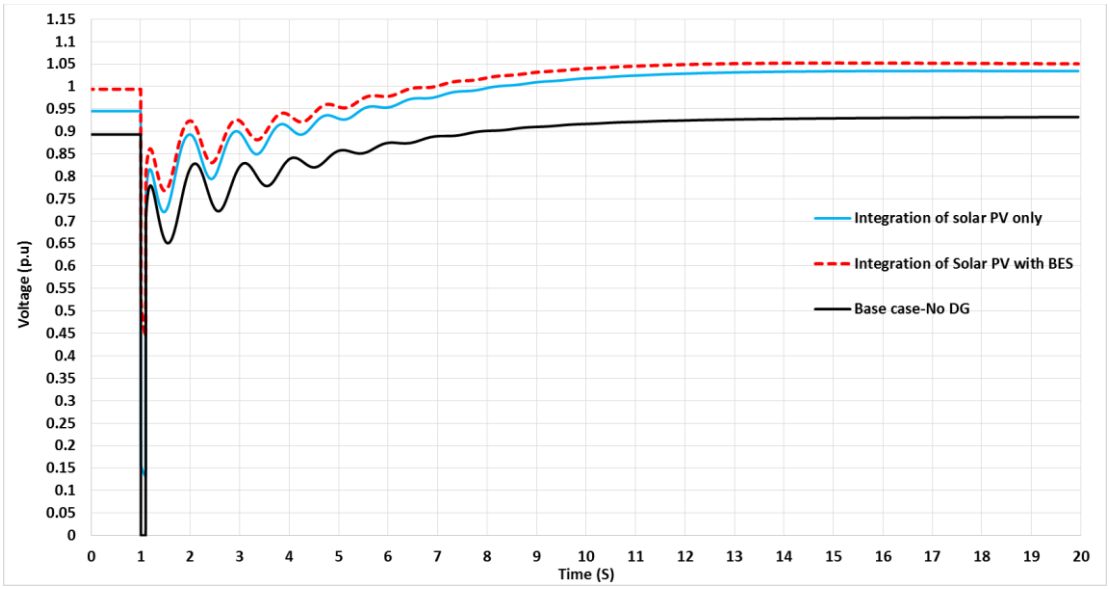

Figure 7-40: Voltage profiles for base case and with solar PV integration at the Bus 8 PCC of 9-bus network with and without BES (Case 5: with fault)

The impact of integrating DFIG with BES on the same PCC voltage profile is similarly observed for the same faulted condition and recorded in Figure 7-41. It can be seen that on incorporating both DFIG and BES at the PCC, the fluctuations in voltage profile are reduced and the voltage rises and settles at 1.2 p.u. The voltage profile after integration of DFIG and BES violates the grid code requirement since the voltage rises above the upper limit of 1 p.u. The proper sizing of the BES is essential to ensure that PCC voltages are within the required limits. In this case, it must be noted that the HVRT requirements are however violated when DFIG is integrated with and without BES.

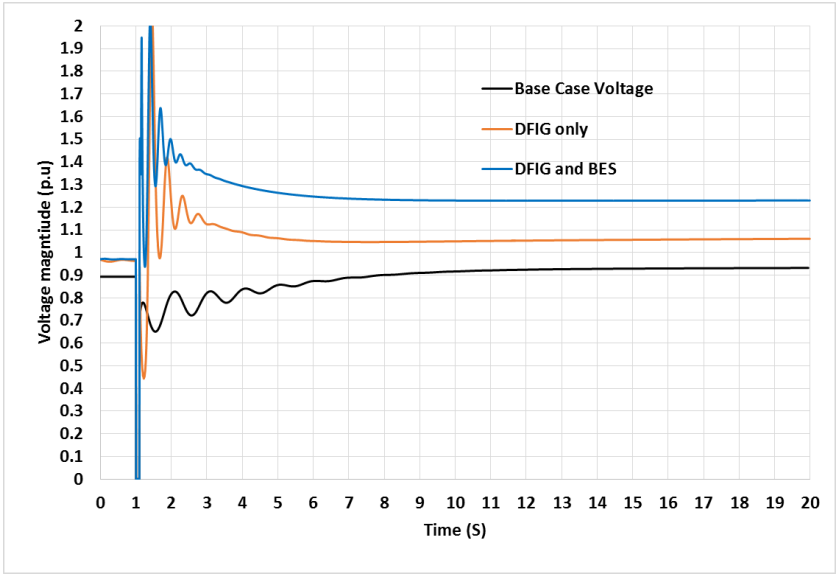

Figure 7-41: Voltage profiles for base case and with DFIG integration at the Bus 8 PCC of 9-bus network with and without BES (Case 5: with fault)

iii. Impact of BES on overall active power losses

The resulting power losses are also observed when DFIG and solar PV based DGs are coupled with BES and are compared to that of the base case as depicted in Figure 7-42. The investigation is conducted in the absence of faults in the network. The reduction in total active power losses when solar PV is integrated without BES is 20% and increases to 24% upon the inclusion of BES. The total active power loss reduction during DFIG integration on the other hand is 15.5% without BES and further increases to 19.5% upon the inclusion of BES. It is therefore observed that a more reduction in total active power losses is obtained in the case when solar PV is coupled with BES than the case of DFIG integration. Additionally, BES's capability to shift some of the current or load from peak periods to off-peak period decreases the net resistive losses in the network.

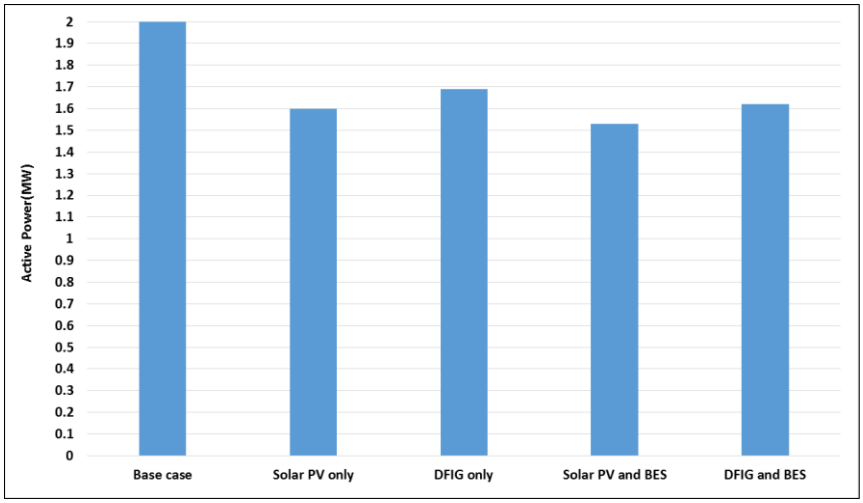

Figure 7-42: Overall active power losses resulting from inclusion of BES in solar PV and DFIG integrated 9-bus network (Case 5)

7.4.5 *Installation of BES in 33-bus distribution networks*

The impacts of incorporating BES with the capacity of 0.4 MW at the Bus 7 PCC when solar PV and DFIG-based DGs are integrated on the 33-bus distribution network are presented in this section. The capacity of DGs in this analysis is kept at 1 MVA. The analysis is performed first without fault and then with a fault condition in the network as discussed in Chapter 6. The voltage profiles at the PCC are observed in each investigated scenario.

i. Impact of BES in the absence of faults

The PCC voltage profiles are compared in Figure 7-43 amongst the base case and integration of DFIG without and with BES at Bus 7 PCC of the 33-bus distribution system when there is no fault in the network. It can be seen that upon integration of DFIG only, the voltage rises and settles at 0.95 p.u. after minor fluctuations at the beginning of the simulations. The voltage magnitude at the PCC further rises to 1.1 p.u after the BES is included at the PCC. It is however worth noting that the PCC voltage magnitude might exceed the grid code limits should the BES capacity exceed 1MVA. The BES

capacity is therefore limited to 1MVA. The BES contributes to voltage profile improvement by injecting active power as depicted by the resulting voltage profiles at the PCC.

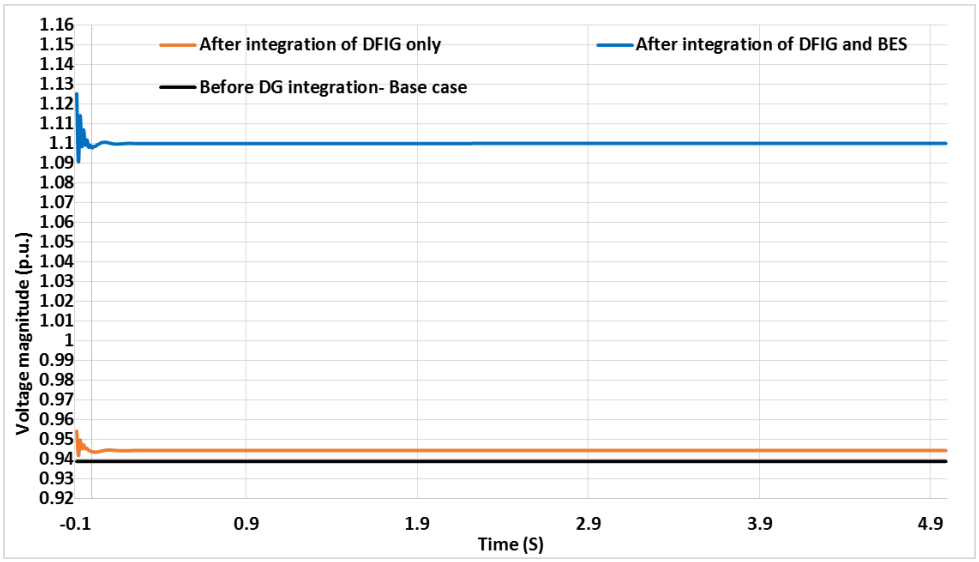

Figure 7-43: Voltage profiles for base case and with DFIG integration at the Bus 7 PCC of 33-bus network with and without BES (Case 5: without fault)

Similar comparison of PCC voltage profiles for solar PV and BES integration are presented in Figure 7-44. It can be seen that integration of only solar PV at Bus 7 results in voltage rising to 0.949 p.u. Including BES at the PCC increases the voltage further to 0.972 p.u. It is observed that coupling solar PV with BES at the PCC also results in significant improvement in PCC voltage profile. A better voltage profile improvement is however observed when BES is coupled with DFIG-based DG since the voltage settles at a higher value of 1.1 p.u for the same BES capacity.

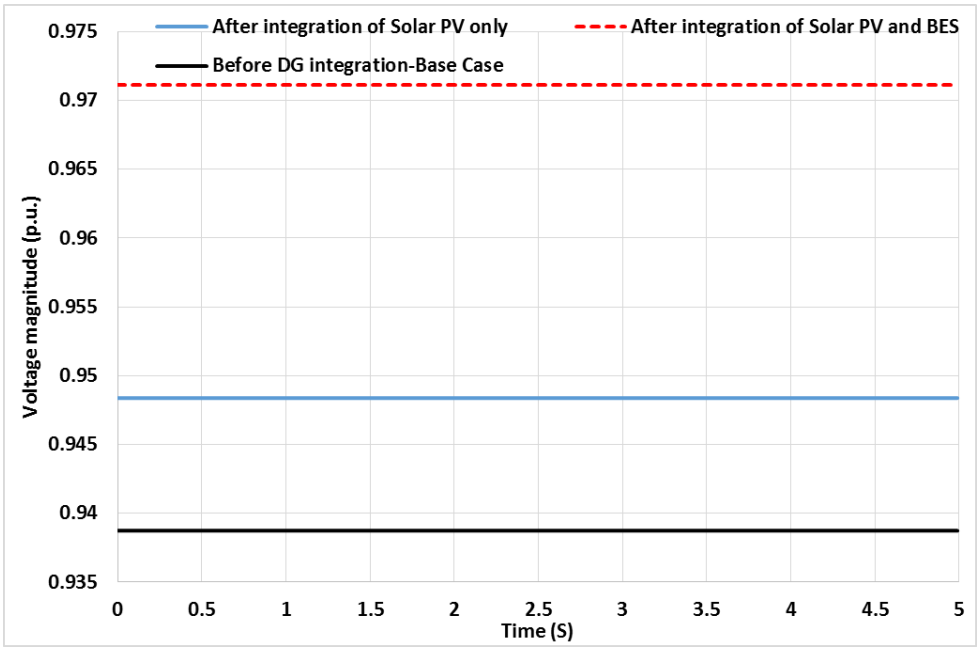

Figure 7-44: Voltage profiles for base case and with solar PV integration at the Bus 7 PCC of 33-bus network with and without BES (Case 5: without fault)

ii. Impact of BES in the presence of faults

The impact of DG integration with and without BES at the Bus 7 PCC of the 33-bus network in the event of fault are presented in this section. The fault is set to occur at t=1 second and is cleared at t=1.1 seconds. Figure 7-45 compares the voltage profiles at the PCC between the base case and cases of DFIG integration without and with BES. Figure 7-45 indicates that post fault voltage for both DFIG integration without and with BES, settles at 1.0 p.u. which is higher than the magnitude at which voltage settles for the base case (0.95 p.u.). When BES is connected the voltage during fault occurrence briefly rises to 1.2 p.u. while when DFIG is connected alone, voltage magnitude drops to 0.95 p.u. It is observed that BES contributes to voltage profile improvement only during the instant of fault occurrence, after which the final settling voltage is equal to that when DFIG is connected without BES.

When the fault occurs, the line 5 between Bus 6 and Bus 7 is momentarily disconnected the fault is cleared. The DFIG and BES therefore supply the smaller load upstream of Bus 7 and the voltage consequently rises as shown in Figure 7-45 during the instant of fault occurrence (t=1 second). After the fault is cleared (t=1.1 seconds), the line is reconnected and hence the voltage returns to the nominal magnitude of 1 p.u.

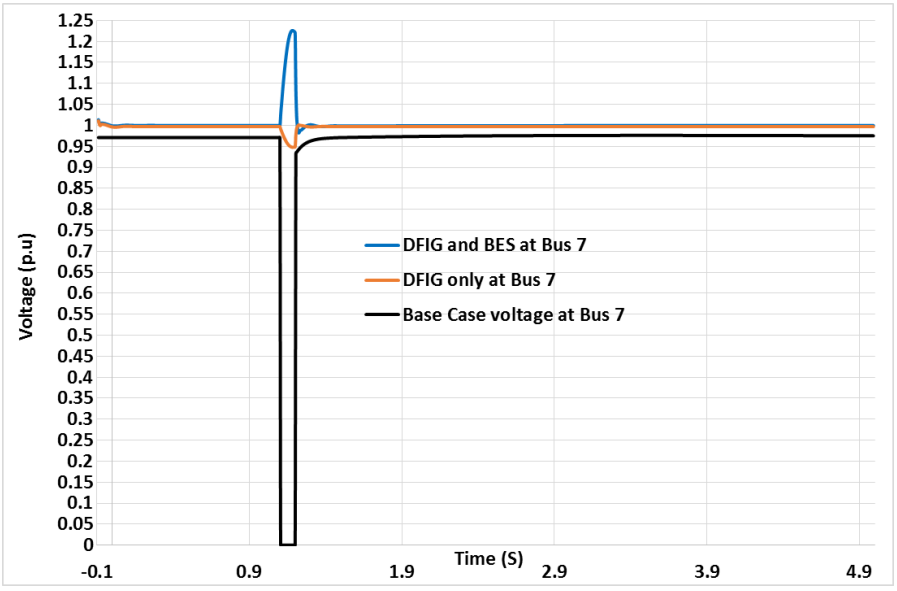

Figure 7-45: Voltage profiles for base case and with DFIG integration at the Bus 7 PCC of 33-bus network with and without BES (Case 5: with fault)

The voltage profiles at the PCC with solar PV integrated with BES are shown in Figure 7-46. The voltage magnitude of the base case (without any DG) drops to 0 p.u. during the fault. When only solar PV is connected at the PCC the voltage drops to 0.55 p.u. and after fault clearance settles to 0.95 p.u. When solar PV with BES is connected at the PCC, voltage drops to 0.65 p.u. and after fault clearance settles to 1.0 p.u. The final settling voltage magnitude as a result of incorporating BES at the PCC of a distribution network is similar for integration of solar PV and DFIG-based DGs. The impacts on

voltage differ during the instant of fault of occurrence (t=1 second), where the voltage rises to 1.2 p.u. when BES is coupled with DFIG and drops to 0.55 p.u. when BES is coupled with solar PV.

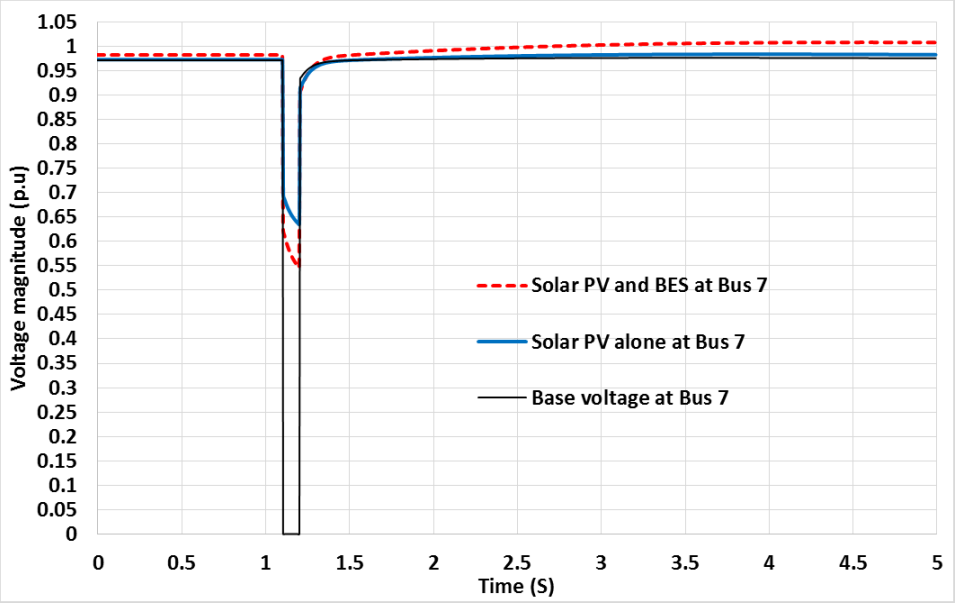

Figure 7-46: Voltage profiles for base case and with solar PV integration at the Bus 7 PCC of 33-bus network with and without BES (Case 5: with fault)

iii. Impact of BES on overall active power losses without fault

The impact of incorporating BES at the PCC on the overall active power losses of the DG-integrated 33-bus distribution network is presented in Figure 7-47. In comparison to the base case, the overall active power losses are minimum with a value of 0.158 MW when DFIG is connected with BES at the PCC. Including BES at the PCC with solar PV also results in significant reduction in overall active power losses to a value of 0.18 MW. This is a significant reduction considering that the overall active power losses of the 33-bus distribution network amount to 0.2107 MW when DGs are not connected. Connection of BES at the PCC results in significant reduction of overall active power losses for integration of both solar PV and DFIG-based DGs.

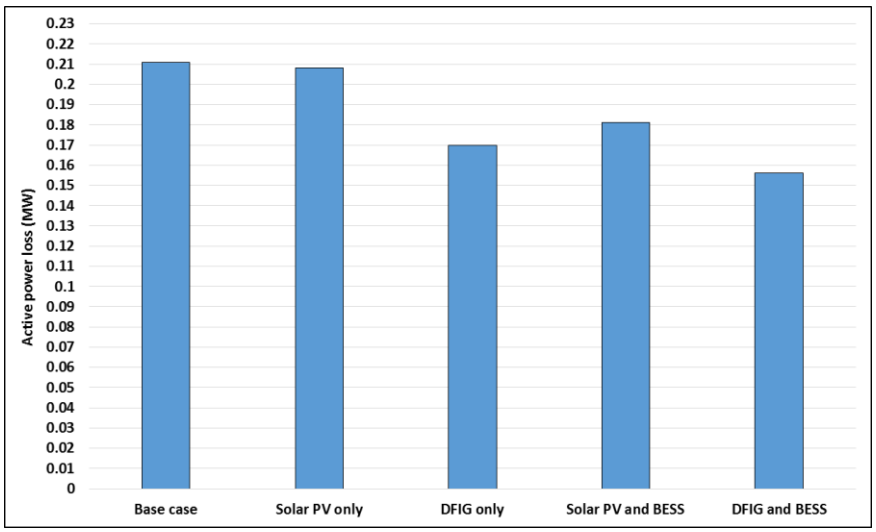

Figure 7-47**:** Overall active power losses resulting incorporating BES at the connection point of solar PV and DFIG-based DGs

7.5 Case 6: PQ improvement in weak networks with DG integration

The impact of connecting solar PV and DFIG-based DGs in weak electricity networks is investigated on the 9-bus sub-transmission and 33-bus distribution networks. As explained in section 6-9, the grid strength is altered by changing the short circuit capacity of the external grid connected to the slack Bus 1. This consequently changes the short circuit ratio of the grid as expressed by equation (6-3) and hence the strength of the entire sub-transmission and distribution networks. The voltage profiles at the PCC are observed while the strength of the grid is altered from weak grid (SCR<10) to strong grid (SCR >10). The SCR is set to 2 for weak grid and is set to 10 for strong grid. For the strongest grid, the SCR is set to 20.

7.5.1 *PQ improvement in 9-bus sub-transmission networks*

The results of the voltage profiles at different grid-strengths when solar PV is connected at Bus 8 of the 9-bus system are presented in Figure 7-48. It is observed that integration of solar PV to the weak grid (SCR=2) results in voltage at the PCC fluctuating below the limit of 0.95 p.u. for 3 seconds before settling to a constant 0.98 p.u. after the fault clearance. In addition to the weakness of the grid, another contributing factor to intense voltage fluctuations is a variable nature of solar PV and minimal voltage support due to insufficient reactive power. The voltage profile at the PCC however shows improvement at SCR=10; here the voltage only fluctuates for 1.6 seconds before settling at 0.97 p.u.

The voltage profile for integration of Solar PV at the PCC of a strong grid with SCR=20 also manifests improvement with relatively less fluctuations after the fault clearance. The post fault voltage profile settles at 1 p.u. and remains constant because the strong grid has the capability to accommodate high penetration levels of DG with minimum impact on the voltage profile and stability.

The solar PV system operates at unity power factor and therefore does not have any Low Voltage-Ride through (LVRT) capability as it does not contribute during fault or any transient condition of the system.

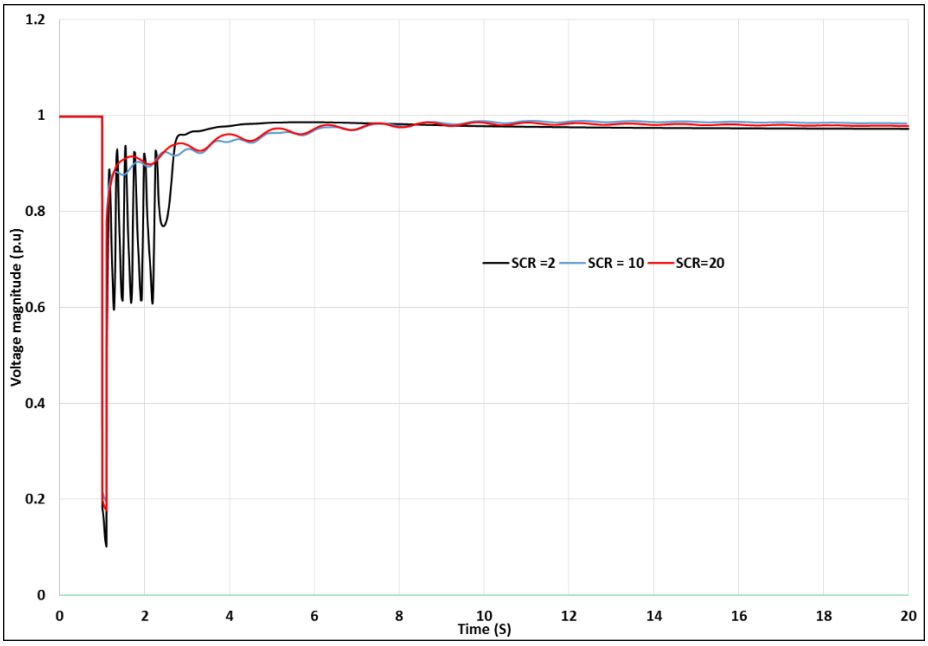

Figure 7-48: Voltage profiles at PCC for different grid strengths with 10MW Solar PV at Bus 8

Figure 7-49 presents the impacts of varying the grid strength on PCC voltage profiles when a 10MVA DFIG is integrated at the Bus 8 PCC of the 33-bus distribution network. It can be seen that when the grid is weak (SCR=2), the voltage profile at the PCC violates the grid code well outside the limits. The post-fault voltage profile for this case fluctuates between 0.2 p.u. and 0.45 p.u. indicating inability of DFIG to support the voltage profile. The poor voltage profiles when the grid is weak are the result of the stress imposed on the transmission lines and PCC bus by penetration of DFIG at the time of fault due to insufficient low FRT provided by the DFIG.

Integration of DFIG to a strong grid (SCR=10) on the other hand results in improved voltage profiles at the PCC as shown in Figure 7-49. It is seen for DFIG integration at a network of SCR=10, the improvement in PCC voltage profile is higher than that achieved for solar PV integration under the same condition. . The resulting voltage profiles for SCR=20 manifest a significant increase in the settling value with minimum voltage fluctuations and the post-fault voltage profile maintains a constant magnitude of 1.05 p.u after brief variations. The comparison of voltage profiles as a result of integration solar PV and DFIG-based DGs at different grid strengths indicates that DFIG performs better at most grid strengths due to LVRT capability of DFIG.

For DFIG integration to weak network (SCR=2), the LVRT requirements are violated as depicted in Figure 7-49. The DFIG will consequently disconnect from the grid. The HVRT requirements on the other hand are met for stronger grids (SCR=10 and SCR=20).

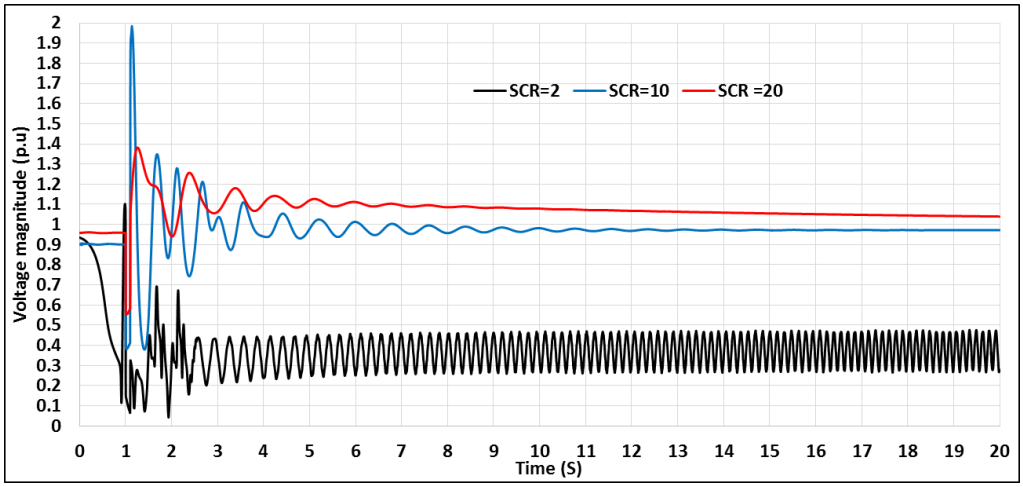

Figure 7-49: Voltage profiles at PCC for different grid strengths with 10MVA DFIG at Bus 8

7.5.2 *PQ improvement in 33-bus distribution network*

The impact of varying grid strength on PCC voltage profile for integration of DFIG-based DGs at Bus 7 on a 33-bus distribution network are presented in Figure 7-50. It can be seen that when the grid is weak (SCR=2) DFIG integration results in minimum improvement of the PCC voltage profile in terms of the voltage drop. Integrating DFIG at the network with SCR=10 however results in momentary fluctuations of the PCC voltage profile at the beginning of the simulations and immediately after the fault is cleared. The voltage profile settles at the constant magnitude of 0.97 p.u. for all grid strengths. This indicates that DFIG integration in weak distribution networks has a minimum impact on the PCC voltage profile in comparison to integration in sub-transmission networks.

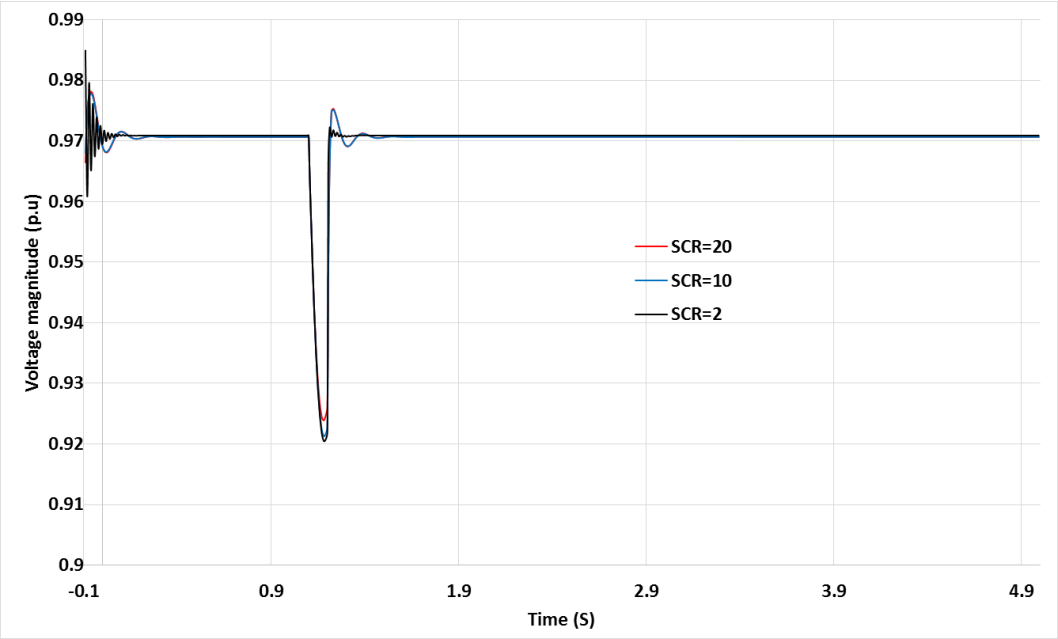

Figure 7-50: Voltage profiles at the PCC for different grid strengths with DFIG integrated at Bus7

The voltage profiles at the PCC after solar PV is connected at Bus 7 of the 33-bus distribution system at different grid strengths are shown in Figure 7-51. It is observed that before the fault, the PCC

voltage profiles follow a similar pattern for all the grid strengths. The voltage drops to 0 p.u. at the SCR of 2 and 10 and drops only to 0.9 p.u at the SCR of 20. After the fault is cleared, the voltage profile as a result of solar PV integration into weak grid (SCR = 2) settles at 1 p.u. As the grid becomes stronger (SCR = 10) the voltage briefly rises to 1.6 p.u and settles at 1.1 p.u. after the fault is cleared. The voltage profile as a result of solar PV integration into the strongest grid (SCR=20) however settles to a constant magnitude of 1.05 p.u immediately after the fault is cleared. This is an indication that solar PV integration into strong grids results in a better performance in comparison to integration into weak grid.

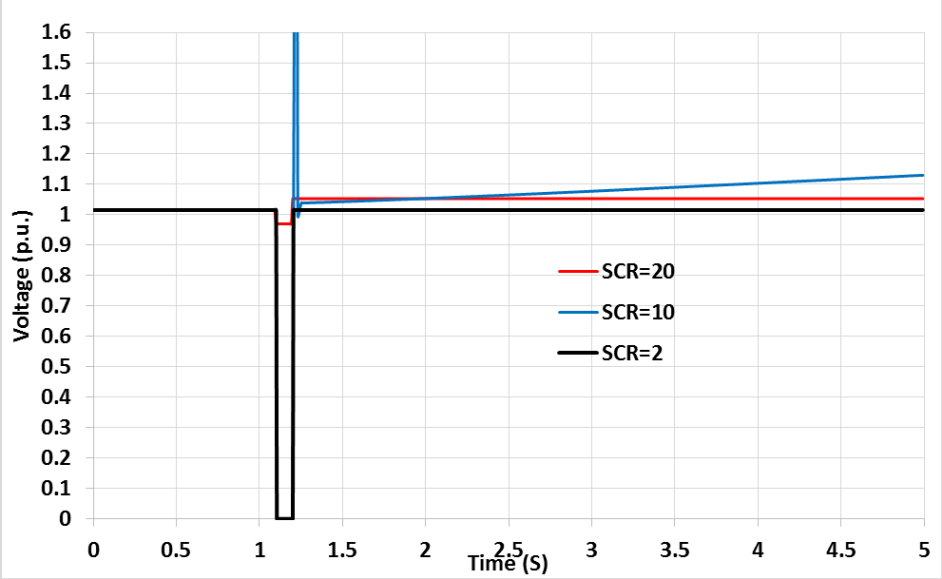

Figure 7-51: Voltage profiles at the PCC for different grid strengths with Solar PV integrated at Bus 7

7.6 Case 7: The optimal allocation and sizing of DGs for PQ improvement

As explained in section 6.8, this case seeks to determine the optimal location and size of DGs for PQ improvement and overall active power loss reduction in the network. In this case, solar PV is modelled as a unity power factor generator in MATLAB since it only injects active power into the grid. The DFIG on the other hand is modelled with a negative reactive power due to need for induction generators to absorb reactive power from the grid during operation. Power quality is enhanced by applying genetic algorithm (GA) to determine the optimal sizes and location of DGs using equation (5-17) as the multi-objective function. The equation is presented below for better reference and the symbols remain as explained in Chapter 5.

$$f = Min((f_1 + k_1 f_2) + \beta_1 \sum_{i \in N_{DG}} [\max(V_{ni} - V_{ni}^{max}, 0) + \max(V_{ni}^{min} - V_{ni}, 0)]) \quad (7\text{-}2)$$

The primary purpose is to maximize the voltage profiles (magnitudes) at system's bus bars within the specified constraints while minimizing the overall active power losses of the networks. PQ

improvement by optimal placement of solar PV is compared to that resulting from integration of DFIG based DGs by observing the resulting voltage profiles and overall active power losses after their integration. It is worth noting that in this case study, the loads of the networks are constant throughout the optimization procedure.

The optimal location of DG is determined by GA and for each location, GA determines the optimal DG size that will ensure that system voltage profile is improved while keeping the total active power losses at minimum. The parameters of the GA are as described in Chapter 6. The location and size of solar PV and DFIG are recorded and the DG type with higher capacity is observed. This case also investigates the impact of integrating multiple DGs on system's voltage profiles and active power losses.

The flow chart of a GA algorithm is presented in Figure C-1 of Appendix C. In order to define the GA algorithm such that the optimal placement of multiple DG units can be executed, the dimension of the problem is changed in the algorithm. The dimension of the problem is altered such that the number of solutions is as per the problem investigated. For instance, for determining the optimal solution for placement of a single solar PV, the number of dimensions is set to 2 in GA. The first element of the problem's dimension represents the location, while the latter represents the capacity of Solar PV. Similarly, for the optimal placement of a single DFIG-based DG, the dimension of the problem is set to 3. The first element represents the location while the other two represents the active and reactive power capacities of the DFIG. The same approach is applied throughout, depending on the number and type of DGs integrated. The GA parameters set for each scenario are presented in Appendix C.

7.6.1 *Scenario 1: Optimal siting and sizing of DGs in 9-bus sub-transmission networks*

The results obtained after executing GA algorithm to determine the optimal DG location and sizing in a 9-bus sub-transmission network are presented in this section. The optimization problem investigates the optimal placement of single and multiple DGs on a 9-bus network taking into account the constraints outlined in Section 5.7. The analysis in this case is done under normal network operation without any faults.

i. Optimal placement and sizing of single DG

The results of voltage magnitudes at each bus before and after the optimal placement and sizing of single solar PV and DFIG-based DGs are presented in Figure 7-52. The optimal bus for integration of Solar PV and DFIG based DGs is obtained by GA to be Bus 8. It can be seen that the bus voltage

magnitudes show a significant improvement after the optimal placement of solar PV and DFIG-based DGs at Bus 8. The optimal capacities of solar PV and DFIG are obtained to be 19.57 MW and 23.28 MVA, respectively. The buses which suffered poor voltage profiles before DG integration have their voltage magnitudes boosted to higher values after the optimal placement of DGs. It can be seen that before DG integration, the lowest voltage magnitude is that at Bus 9 with the value of 0.94 p.u. The voltage magnitude rises to 0.98 p.u. and 0.986 p.u. after the optimal integration of solar PV and DFIG-based DGs, respectively.

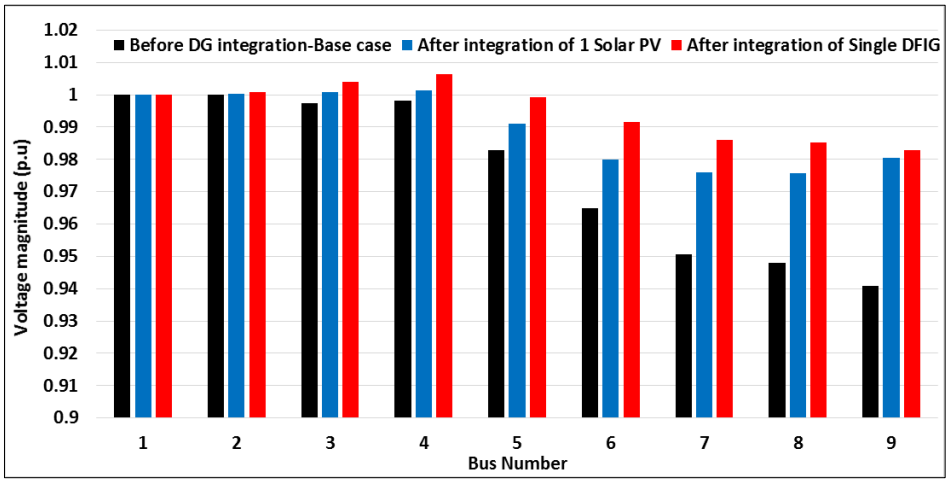

Figure 7-52: Voltage magnitudes at different buses of the 9-bus network before and after optimal integration of single Solar PV and DFIG-based DGs

The observation of the voltage magnitudes indicate that a more improvement in bus voltage profiles is experienced in the case of DFIG-integration, in comparison to that of Solar PV-integration. This is manifested by the bus voltage profiles after the optimal integration of DFIG which are predominantly higher than those resulting from the optimal placement of solar PV in most network buses.

ii. Optimal placement of multiple DGs

The GA parameters are altered as presented in appendix C while determining the optimal solution for multiple DGs. The dimension of the GA is also altered depending on the number of DGs to be optimally connected. For instance, in the case of the optimal locations of 3 solar PVs, the number of GA variable is set to 6 to cater for the 3 optimal locations and 3 optimal sizes. The upper and lower bounds of the solutions are also altered accordingly as shown in Appendix C.

The resulting voltage magnitudes at the PCC obtained before and after the optimal placement of multiple Solar PV-based DGs are presented in Figure 7-53. It can be seen that as the number of Solar PV increases, the magnitudes of the bus voltages also increase. The bus voltage magnitudes are highest after integration of 4 solar PVs. The minimum voltage magnitude at the network buses occur

at Bus 9 with value of 0.98 p.u. after the optimal placement of a single solar PV. The voltage at Bus 9 increases to 1 p.u. after integration of 1 and 2 solar PVs whereas integration of 4 solar PVs increases the voltage magnitude to 1.015 p.u.

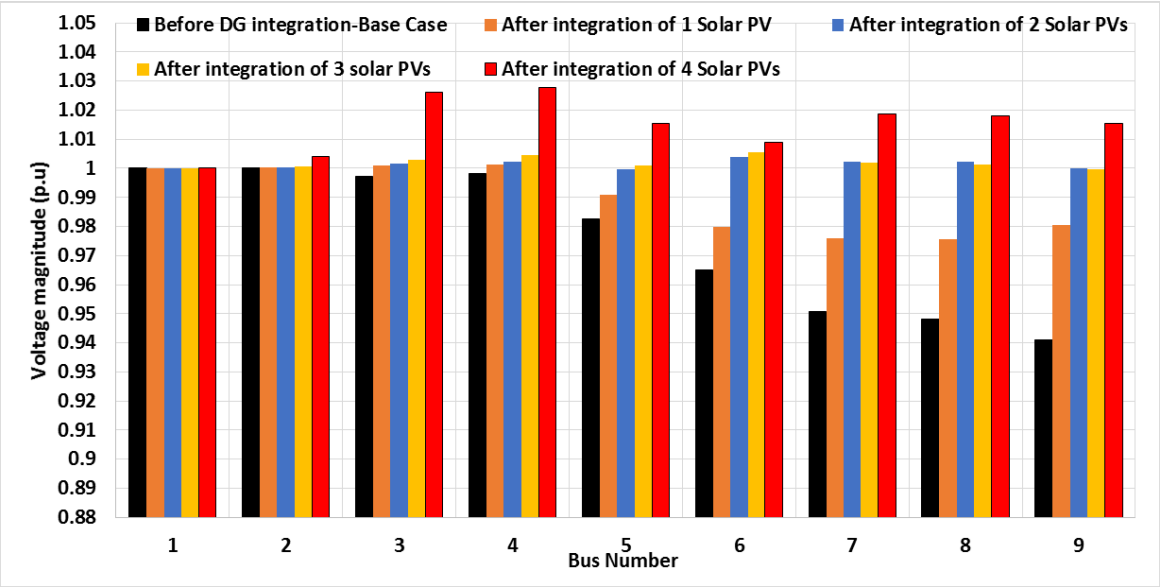

Figure 7-53: Voltage profiles at different buses of the 9-bus network before and after optimal integration of multiple Solar PV-based DGs

A larger increase in bus voltage magnitude is observed in most network buses because of the large capacity of one of the solar PVs whose optimal location and capacity are determined to be Bus 5 and 13.59MW respectively. The optimal placement of 4 solar PVs at optimal buses of the 9-bus system proves to have a significant improvement in network's bus voltages.

The number of DFIGs is increased by increasing the dimension of the GA algorithm as shown in Table C-3 of Appendix C. The bus voltage magnitudes before and after the optimal placement of multiple DFIG-based DGs are presented in Figure 7-54 below. It is observed that the bus voltage magnitudes increase with increasing the number of integrated DFIGs. The voltage magnitudes at different network buses are predominantly high when 4 DFIGs. The highest voltage magnitude after the optimal placement of 4 DFIG units occurs at Bus 4 with the magnitude of 1.038 p.u.

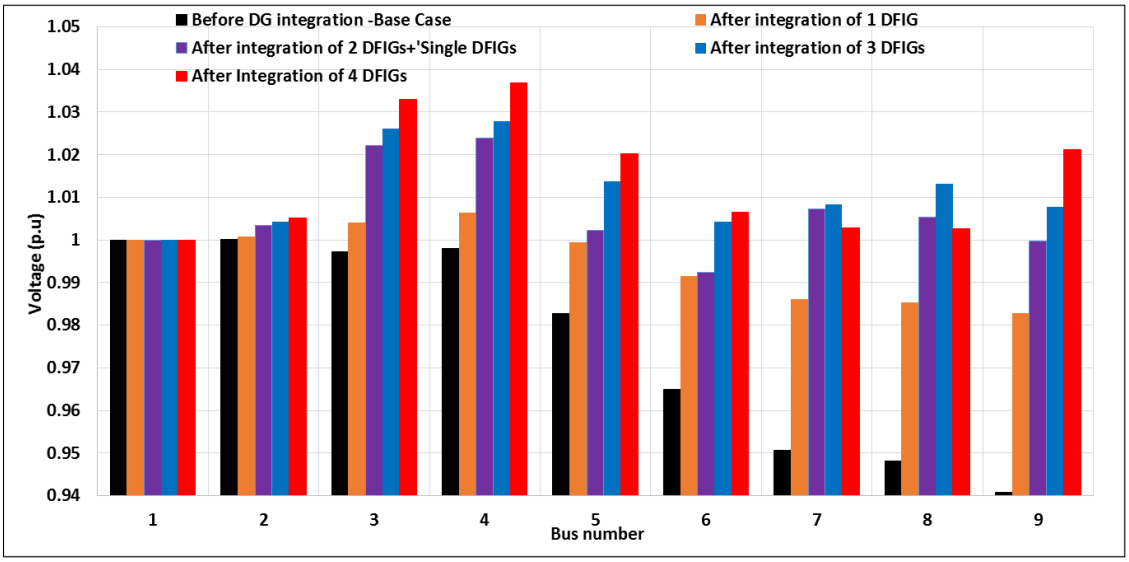

Figure 7-54: Voltage magnitudes at different buses of the 9-bus network before and after optimal integration of multiple DFIG-based DGs

The analysis of the voltage profile results obtained from integration of multiple solar PV and DFIG-based DGS indicate that a better voltage profile improvement is achieved when DFIG of integrated. For comparing the performance of multiple DG-integration, the voltage profiles obtained after the integration of 4 solar PVs and 4 DFIGs are plotted on the same graph as shown in Figure 7-55. It can be seen that the voltage magnitudes are higher at most buses when DFIG-based DG is connected. The voltage profiles as a result of Solar PV integration are only higher at Bus 6, Bus 7 and Bus 8. The voltages are higher at these buses because the combined optimal capacity of solar PV is determined to be 26.95 MW distributed between buses 5, 7, 8 and 4 as shown in Table 9. The combined optimal capacity of DFIG based DGs is determined to be 20.32 MVA distributed across buses 5, 4, 8 and 6.

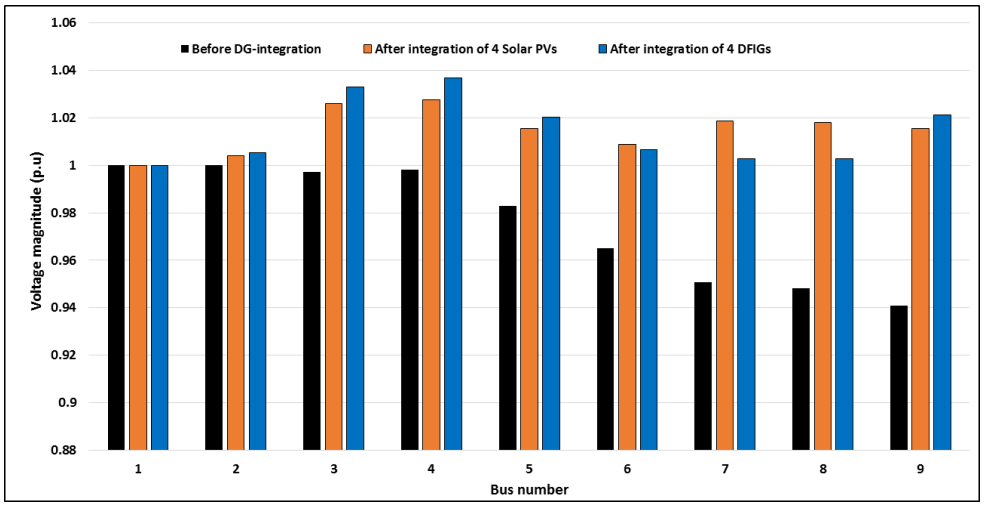

Figure 7-55: Comparison of voltage magnitudes at different buses of the 9-bus network before and after optimal integration of 4 solar PVs and DFIGs-based DGs

The summary of the results obtained from determining the optimal locations and sizes of solar PV and DFIG-based DGs are presented in Table 7-3. For each integration scenario, the location and sizes of the respective DG types are also included. The overall active power losses of the system are also

observed and recorded for each scenario to observe the impacts of DG optimal placement and sizing on power loss reduction. It can be seen that each integration scenario exhibit a different reduction in overall active power losses in the network. For the obtained results, the highest reduction of 85.7% in overall active power losses is obtained after the optimal integration of 4 Solar PVs. The lowest active power loss reduction is observed to be 61.8% after the optimal integration of 2 DFIF-based DGs at Bus 7 and Bus 4.

The overall active power losses of the network without integration of DGs amount to 2.181 MW and are referred to here as base case losses. Equation (7-4) is used to calculate the percentage active power loss reduction as the result of optimal placement of DGs.

$$Reduction\ from\ base\ case = \frac{P_{Lbasecase} - P_{LDG}}{P_{Lbasecase}} \times 100\% \qquad (7\text{-}4)$$

where $P_{Lbasecase}$ is the total active power loss in the network before integration of DGs and P_{LDG} is the overall active power losses after the optimal integration of DGs.

Table 7-3: Summary of results for the optimal placement and sizing of solar PV and DFIG-based DGs on 9-bus sub-transmission network

Number of Integrated DGs	**Type of DG**	**Optimal location (Bus no)**	**Optimal size**		**Total Power losses (MW)**	**Reduction from base case**
			Active capacity (MW)	**Reactive capacity (MVar)**		
Single DG	Solar PV	8	19.57	-	0.447	79.5%
	DFIG	8	23.28	2.57	0.443	79.69%
2 DGs	Solar PV 1	5	17.33	-	0.544	75%
	Solar PV 2	8	9.97	-		
	DFIG 1	7	11.44	7.62	0.832	61.8%
	DFIG 2	4	3.44	0.78		
3 DGs	Solar PV 1	5	4.91	-	0.311	85.7%
	Solar PV 2	4	3.45	-		
	Solar PV 3	8	7.34	-		
	DFIG 1	4	15.62	2.77	0.523	76%
	DFIG 2	8	5.58	0.34		
	DFIG 3	5	1.31	0.72		
4 DGs	Solar PV 1	5	13.59	-	0.354	83.76%
	Solar PV 2	7	1.42	-		
	Solar PV 3	8	2.05	-		
	Solar PV 4	4	8.99	-		
	DFIG 1	5	12.55	1.7	0.536	75.4%
	DFIG 2	4	2.15	0.351		
	DFIG 3	8	2.83	0.2		
	DFIG 4	6	2.76	0.51		

The overall active power losses of the network are compared for different number of integrated DGs as shown in Figure 7-56. It can be seen that in comparison with the base case, the overall active power losses are significantly reduced after the optimal integration of solar PV and DFIG-based DGs. A more reduction in active power losses is observed when solar PV-based DGs are connected, in comparison to that after DFIG-integration. The active power losses are minimum after the optimal integration of 3 solar PVs with the combined capacity of 15.7 MW. In the case of optimal integration of DFIG-based DGs, the total active power losses are minimum after integration of a single DFIG unit with the capacity of 23.28MVA.

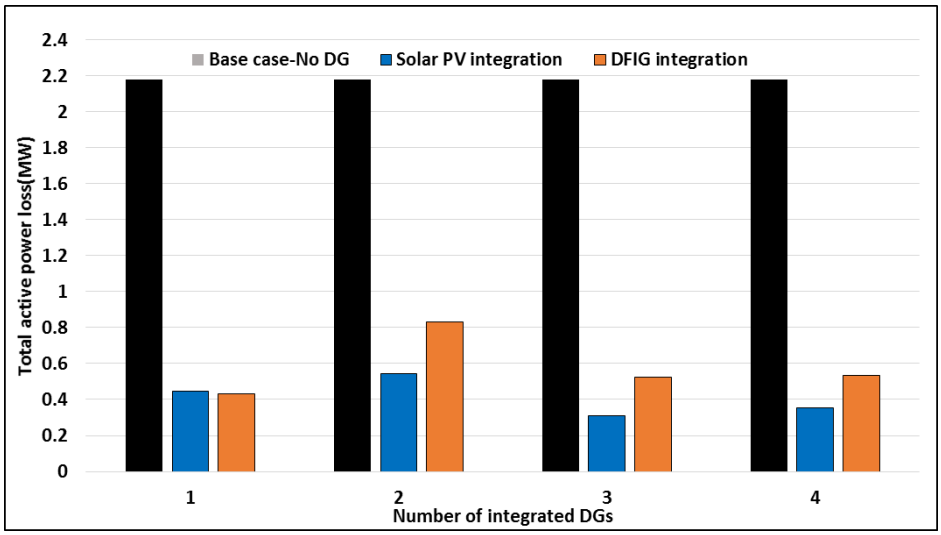

Figure 7-56: The overall active power losses before and after optimal placement of multiple Solar PV and DFIG-based DGs

7.6.2 *Scenario 2: Optimal placement and sizing of DGs in 33-bus distribution networks*

The optimal placement of DGs on a 33-bus distribution network is also performed during normal network operation without any fault occurrence in the network. Similar to the case of DG placement on the 9-bus network above, the different scenarios are achieved by changing GA parameters. The parameter settings of the GA for different scenarios are presented in Appendix C.

i. Single DG placement and sizing

The results of the voltage profiles at each bus before and after the optimal sitting and sizing of a single solar PV and DFIG-based DGs on a 33-bus distribution system are shown in Figure 7-57. The optimal buses for integration of solar PV and DFIG based DGs are determined to be Bus 25 and Bus 5, respectively. A significant improvement in bus voltage profiles is obtained after integration of solar PV and DFIG-based DGs at Bus 25 and Bus 5 respectively. The optimal capacity of Solar PV is obtained to be 2.89MW while that of DFIG is found to be 2.76 MVA. Bus voltage magnitudes which were below the acceptable minimum before integration of solar PV and DFIG-based DGs, increase to values permitted by the grid codes. It can be observed that without DG integration, the lowest

voltage magnitudes are that at bus 7 to bus 18 as well as that from bus 26 to bus 33. After integration of solar PV and DFIG, the voltage magnitudes at these busbars increase to higher values as shown in Figure 7-57. For instance, the voltage magnitude at bus 18 is 0.916 p.u. before DG integration and increases to 0.958 p.u. after the optimal integration of solar PV in the network.

The minimum voltage magnitudes after Solar PV integration occur at bus 18 and bus 19 with the magnitude of 0.958 p.u. The minimum voltage magnitude observed in the case of DFIG integration is 0.954 p.u. at bus 17 and bus 18. It is observed that more improvement in bus voltage magnitudes is experienced in the case of solar PV integration in comparison with that of DFIG integration. This is manifested by the fact that the voltage profiles resulting from solar PV integration are predominantly higher than those resulting from DFIG integration in most system buses.

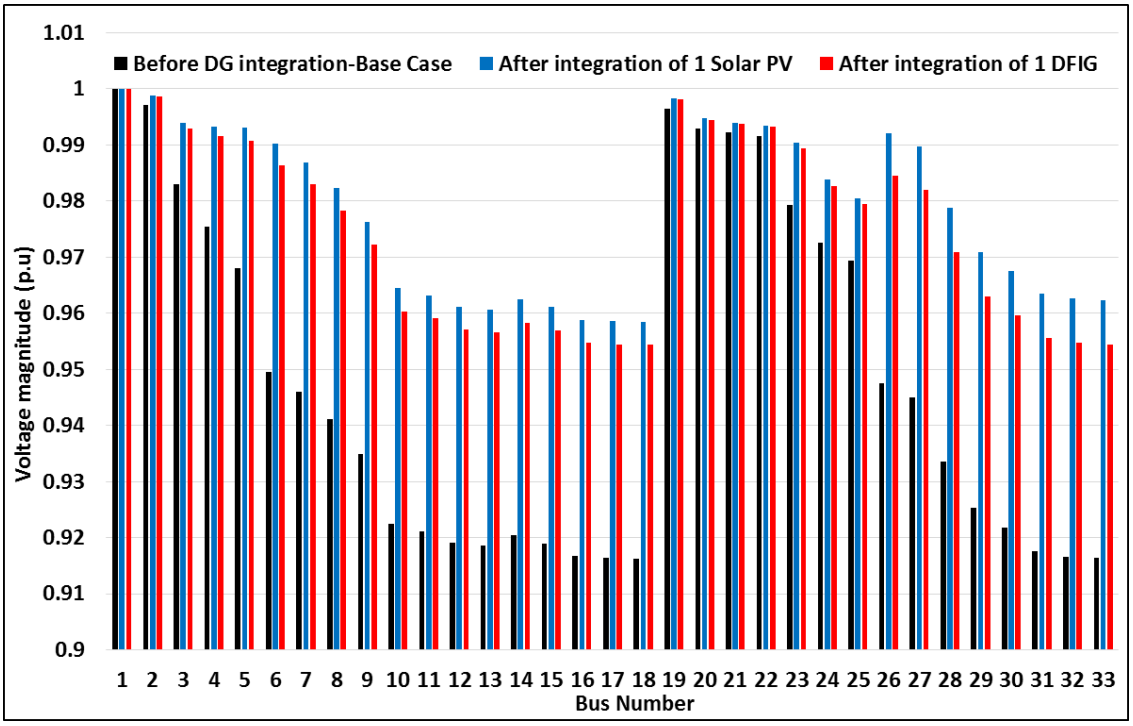

Figure 7-57: The comparison of the voltage profiles after integration of single solar PV and DFIG based DGs

ii. Effect of multiple DG optimal placement and sizing on PQ improvement

The results of bus voltage profiles after the optimal placement and sizing of multiple solar PV units on a 33-bus system are shown in Figure 7-58. As the number of integrated solar PVs is increased, the magnitudes of the bus voltage profiles also increases. The bus voltage profiles are highest when 4 solar PVs are integrated at the bus bars determined by the program. The minimum voltage magnitude when a single solar PV is integrated is 0.958 p.u. at bus 18 and is increased to 0.967 pu when 2 solar PVs are integrated. The minimum bus voltage magnitudes when 3 and 4 solar PVs are optimally allocated on the network are 0.975 p.u and 0.978 p.u., respectively.

The optimal sizes and locations of integrated solar PV units are determined for each integration scenario and the results are as presented in Table 7-3 below. The capacity of integrated solar PVs is also found to increase as the number of units is increased. For instance the combined capacity of 3 solar PVs is determined to be 3.3MW while that of 4 solar PVs is 3.7MW. The locations of the individual solar PVs together with their respective sizes are presented in Table 7-3.

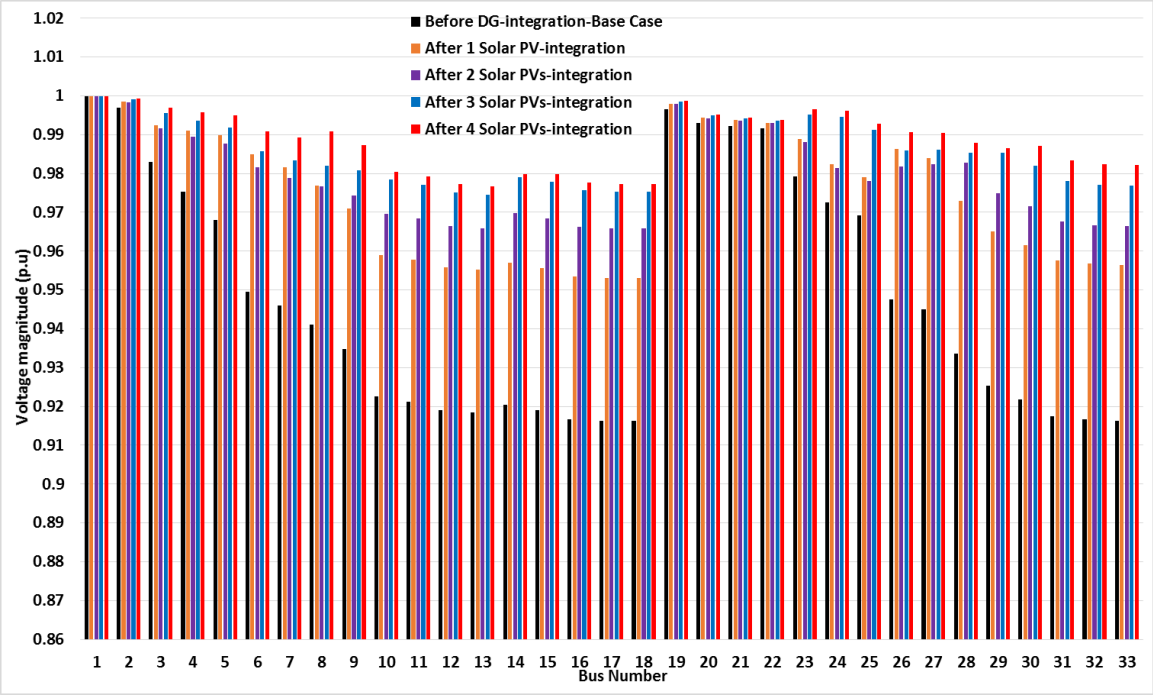

Figure 7-58: Voltage profiles before and after integration of multiple Solar PV based DGs on a 33 bus system

The voltage profile results after optimal integration of multiple DFIG units on a 33 bus system are presented in Figure 7-59. It is observed that the voltage profiles at different system buses increase with increasing the number of integrated DFIGS. The bus voltage profiles are predominantly high when 4 DFIGs are integrated. It is however observed that the voltage magnitudes at Bus 6, Bus 7 and from Bus 26 to Bus 33 are highest when 3 DFIG units are integrated. The highest voltage magnitudes after the optimal integration of 4 and 3 DFIG units are observed to be 1.0043 p.u. at Bus 11 and 1.0049 p.u. at Bus 6, respectively. The minimum voltage magnitudes after the optimal integration of 1, 2, 3, and 4 DFIG units are found to be 0.954 p.u. at bus 18, 0.964 p.u. at bus 33, 0.973 p.u. at Bus 17 and 0.97 at Bus 31, respectively.

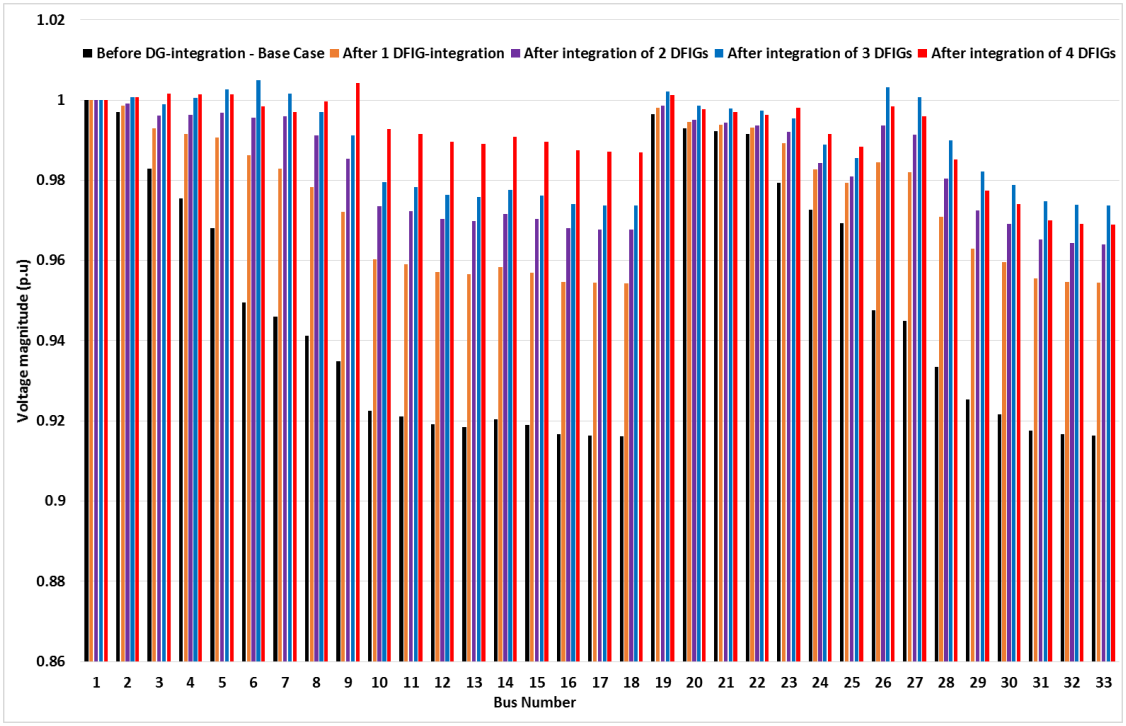

Figure 7-59: Voltage profiles obtained after the integration of multiple DFIG based DGs on a 33 bus network

The optimal locations and sizes of the integrated DFIG units are determined and recorded for each scenario and are depicted in Table 7-3. It is observed that as the number of integrated DFIG units is increased, their corresponding capacity as determined by GA also increases. The capacity of DFIG is computed by finding the equivalent apparent power from the active and reactive power ratings determined by GA. After integration of 1, 2, 3 and 4 DFIGs, their capacity is determined to be 2.76MVA, 6.96MVA, 5.16MVA and 9.93MVA, respectively. In comparison with the case of solar PV integration, it is observed that higher capacities of DFIG can be integrated without the voltage limits being exceeded.

From the analysis of the voltage profile results obtained from grid integration of multiple solar PVs and DFIG based DGs, it is observed that a better voltage profile improvement is achieved when DFIG is integrated. In order to observe the impact of solar PVs and DFIGs on voltage profile improvement, the voltage profiles obtained after integration of 4 solar PVs and 4 DFIGs are plotted on the same axes as shown in Figure 7-60. The comparison of the voltage profiles obtained indicates that voltage magnitudes are higher at most system buses after integration of DFIG based DGs. The voltage profiles as a result of solar PV integration are only higher from Bus 28 to Bus 33. It can however be seen that the overall voltage profile improvement becomes better as the number of DFIG based DGs integrated at optimal buses are improved.

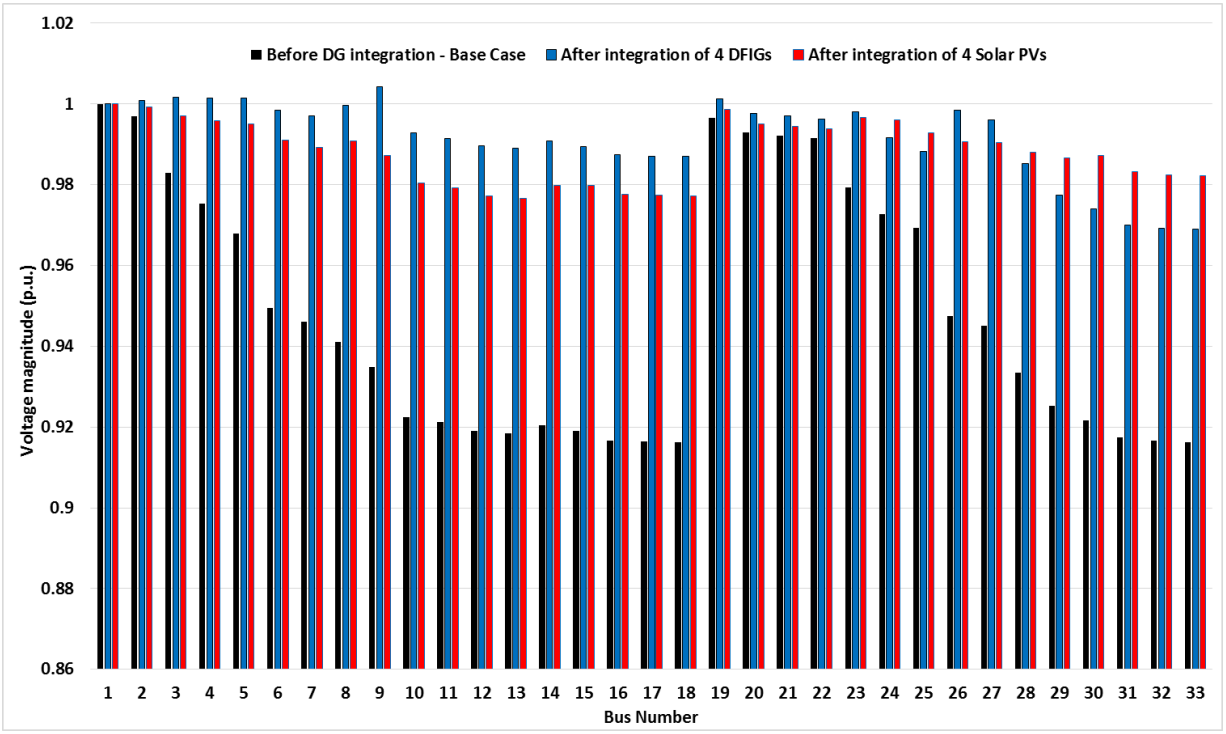

Figure 7-60: The comparison of the voltage profile after the optimal integration of 4 solar PV and 4 DFIG-based DGs

The summary of the results obtained from the determination of optimal placement of solar PV and DFIG based DGs are presented in Table 7-4. For each integration scenario, the location and sizes of the respective DG types are also included. The overall active power losses of the system are also observed and recorded for each scenario to observe the impacts of DG optimal placement and sizing on power loss reduction. The percentage power loss reduction from the base case of 0.2107MW is also recorded for each DG integration scenario. It is observed that each integration scenario exhibit different reduction in total system power losses. From the results, the highest reduction of 61.85% in total active power losses is observed after the optimal integration of 4 solar PVs. The lowest power loss reduction is observed to be 28.33% when 3 DFIGs are optimally integrated to the network. The total system losses are however found to increase from those of the base case after the optimal integration of 4 DFIGs with the combined capacity of 9.93MVA. Equation (7-4) above is used to calculate the percentage reduction from the base case losses.

Table 7-4: The summary of results for the optimal placement and sizing of solar PV and DFIG-based DGs on 33-bus distribution network

Number of Integrated DGs	**Distributed Generator**	**Optimal location (Bus no)**	**Optimal size**		**Total Power losses (MW)**	**Reduction from base case**
			Active capacity (MW)	**Reactive capacity (MVar)**		
Single DG	Solar PV	25	2.89	-	0.1124	46.65%
	DFIG	5	2.598	0.922	0.111	47.32%

2 DGs	Solar PV 1	27	1.678	-	0.0971	53.92%
	Solar PV 2	13	0.5454	-		
	DFIG 1	5	3.9	0.013	0.150	28.81%
	DFIG 2	18	2.979	1.033		
3 DGs	Solar PV 1	13	0.722	-	0.1	52.54%
	Solar PV 2	28	1.511	-		
	Solar PV 3	23	1.065	-		
	DFIG 1	18	2.477	0.387	0.151	28.33%
	DFIG 2	2	1.109	0.578		
	DFIG 3	13	1.475	0.029		
4 DGs	Solar PV 1	14	0.379	-	0.0804	61.85%
	Solar PV 2	29	1.243	-		
	Solar PV 3	7	0.992	-		
	Solar PV 4	7	1.081	-		
	DFIG 1	2	2.672	1.848	0.271	-28.62%
	DFIG 2	25	1.787	0.659		
	DFIG 3	8	1.643	0.0165		
	DFIG 4	8	2.782	1.921		

In order to compare the active power loss reduction as a result of optimal integration of different number of solar PV and DFIG based DGs, Figure 7-61 is produced. It is observed that in comparison with the base case, the total active power losses are significantly reduced after the optimal integration of both DG technologies except the case when 4 DFIGs are integrated. As depicted in Figure 7-61, more reduction in the total active power losses of the system occurs in the case of optimal integration of solar PV based DGs. Minimum active power losses occur after the optimal integration of 3 solar PVs with the combined capacity of 3.7MW. In the case of DFIG integration the total active power losses are minimum after integration of a single DFIG unit and remain the same after the optimal integration of 2 DFIGs. The total active power losses increase to 28.62% of the base case when 4 DFIGs with the combined capacity of 9.98MW are integrated at optimal buses shown in Table 7-4.

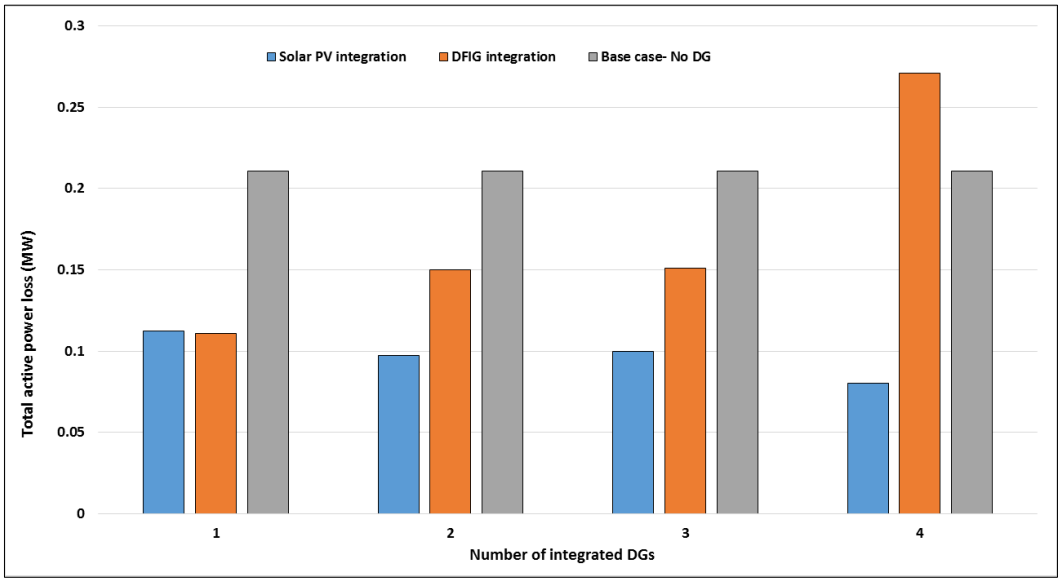

Figure 7-61: The total active power losses after the optimal placement of multiple DFIG and solar PV based DGs - Comparison with the base case total active power losses

7.7 Case 8: PQ improvement by optimal DG sizing and placement considering different load models

By applying GA optimization technique, the optimal DG locations and sizes are determined in sub-transmission and distribution networks while different load models are taken into account. As described in Section 6-8, the purpose of this case study is to determine the optimal sitting and sizing of DGs in electricity networks while different voltage dependent load models are considered. It is crucial to consider varying load models since the practical electricity networks have different types of customers such as residential, commercial and industrial loads which are considered for load modelling in this case study. Optimal location and size of both solar PV and DFIG is investigated to observe the effect on loss reduction and voltage profile improvement of each technology. The voltage profiles are presented when annual seasonal load models of the network are considered and also for each period of the day for both summer and winter seasons. The seasonal exponents values of active and reactive powers of the loads presented in Table 6-4 are used in this case.

7.7.1 *The optimal DG allocation in sub-transmission network*

The optimal placement of DG on IEEE 9-bus sub-transmission network considering voltage dependent load models are considered are presented in this section. It is worth noting that the loads of this network are classified under industrial load types, hence the load exponents corresponding to industrial load types in Table 6-4 are used. The results of the voltage profiles at different system buses when the annual load models are considered are presented in Figure 7-62. The voltage profiles when annual load models are considered are compared to that resulting from normal loading of the network when constant load models are considered. The base case normal loading Figure 7-62 was obtained from Case 6 above when voltage dependability of loads was not considered. The resulting voltage

magnitudes when no DGs are connected when voltage dependability of loads is considered use load models presented in Table 6-4 of Chapter 6. The base voltage magnitudes at different buses of the network are higher when voltage dependability of loads is considered in load flow calculations.

The results of the bus voltage magnitudes when annual load models are considered indicate that a fairly similar voltage magnitude improvement occurs for the optimal integration of solar PV and DFIG-based DGs. The voltage magnitudes are however higher at Bus 7 and Bus 8 when DFIG-based DG is optimally placed in the network. The resulting power losses after the optimal placement of DGs when the average annual load models are considered are also observed and are as presented in Table 7-5. The optimal solutions such as the size and location of DGs as determined by GA are also included in the table.

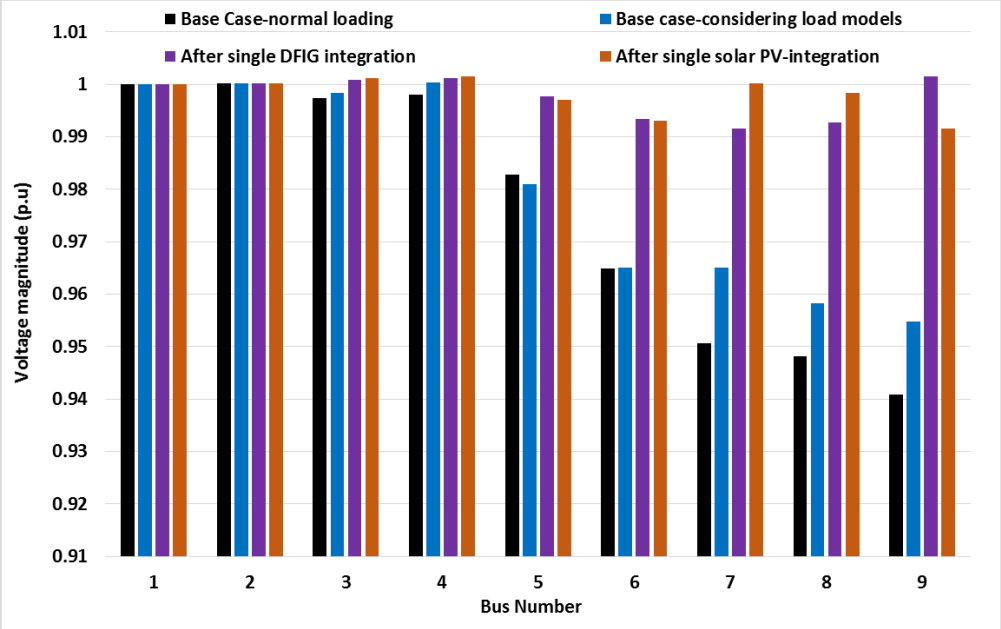

Figure 7-62: The comparison of the voltage profiles after the optimal placement of solar PV and DFIG-based DGs when average annual load models are considered

The overall active power loss of the system before DG integration is 2.18 MW. Table 7-5 presents the results of the optimal placement of solar PV and DFIG-based DGs when the annual load models of the network are considered. The optimal size of the solar PV is determined to be 25.8 MW while the optimal active and reactive capacities of DFIG-based DG are determined to be 26.64 MW and 3.95 MVar, respectively. The optimal bus for the locations of both solar PV and DFIG-based DGs is obtained to be Bus 8. A significant reduction in overall active power losses of the network is also observed after the optimal integration of both solar PV and DFIG-based DGs. It can be observed that when the annual load models of the sub-transmission network are considered, solar PV and DFIG contribute to system's active power loss reduction.

The percentage reduction in active power losses is calculated using equation (7-4) and using the overall active power losses obtained when load models are considered in the absence of DGs. The overall active power loss of the IEEE 9-bus system when load models are considered amount to 2.18 MW.

Table 7-5: The summary of results after optimal placement of solar PV and DFIG based DGs when average of the seasonal load models is considered

Number of DG	**Type of DG**	**Optimal location (Bus no)**	**Optimal size**		**Total Power losses (MW)**	**% reduction from base case**
			Active Power capacity (MW)	**Reactive Power capacity (Mvar)**		
Single DG	Solar PV	8	25.8	-	0.3648	83.27%
	DFIG	8	26.64	3.95	0.368	83.12%

In order to understand the impacts of optimal DG integration on voltage quality for each season, the impacts of the optimal grid integration of DFIG and solar PV on voltage profiles are observed during different load periods. The voltage profiles are observed before and after integration of solar PV and DFIG-based DGs in summer days and nights as well as in winter days and nights. The comparative analysis of voltage profiles and total active power losses is made between solar PV and DFIG based DGs for different load periods. The voltage profiles at different buses of the network after the optimal placement of solar PV and DFIG-based DGs during different load periods are presented in Figure 7-63, Figure 7-64 and Figure 7-65 below. The bus voltage profiles as result of the optimal placement of solar PV at nights is not included due to the absence of sunlight at nights.

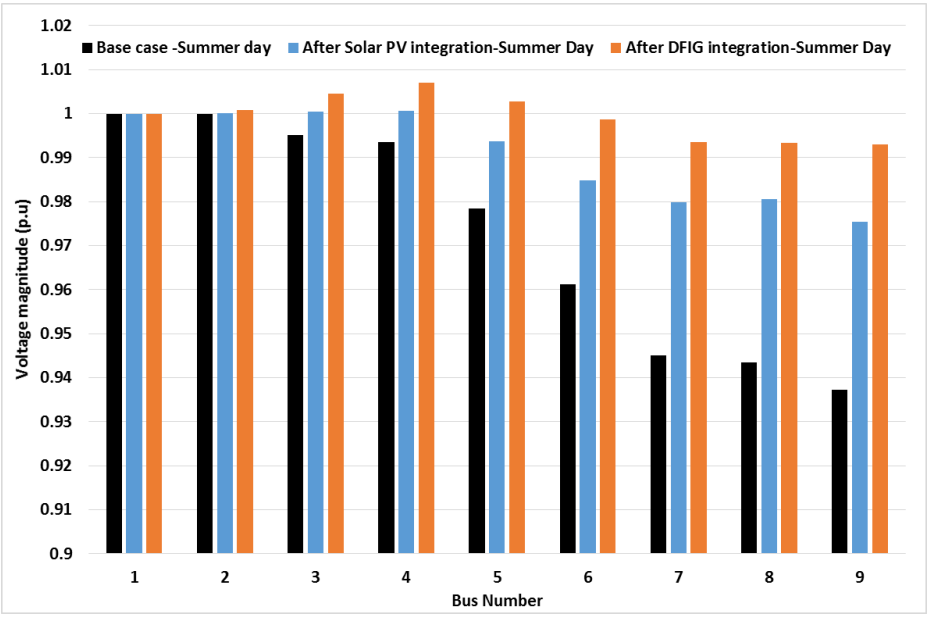

Figure 7-63: Voltage profiles after the optimal placement of DFIG and solar PV-based DGs during summer day load period – Comparison with the base case

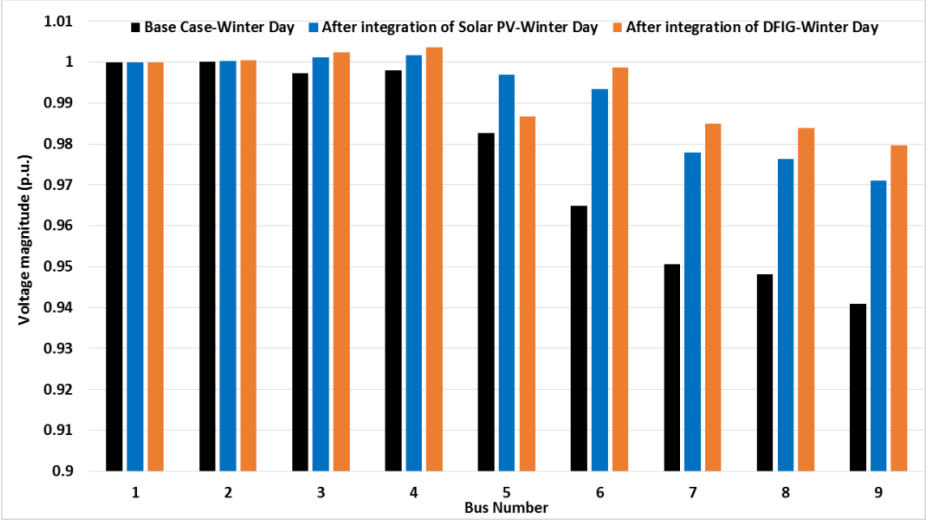

Figure 7-64: Voltage profiles after optimal placement of DFIG and solar PV during winter day load period - Comparison with the base case

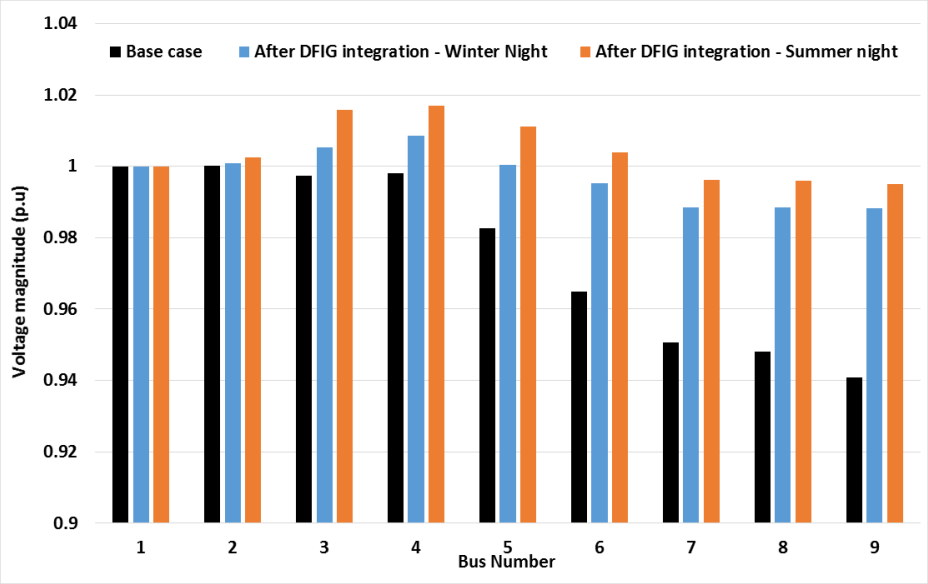

Figure 7-65: Voltage profiles after optimal placement of DFIG during winter and summer nights load periods - Comparison with the base case

The results of the bus voltage magnitudes indicate that a better voltage profile improvement is obtained after the optimal placement of DFIG based DGs for all the seasonal load periods studied. The resulting voltage profiles as a result of DFIG integration is higher than that resulting from solar PV integration for the same load periods. The highest improvement in bus voltage magnitudes occurs after the optimal placement of DFIG-based DG during summer nights as shown in Figure 7-65. The optimal bus bar for integration of solar PV and DFIG-based DGs to achieve the voltage profile improvement during different load profiles are presented in Table 7-6.

During the summer-day load period, the optimal locations of solar PV and DFIG-based DGs are obtained to be Bus 7 and Bus 4, respectively. The optimal size of solar PV is obtained to be 19.44 while DFIG-based DG is determined to have the optimal active and reactive power capacities of 16.98 MW and 2.5MVar, respectively. DG locations during winter day load period are obtained to be Bus

8 and Bus 5 for solar PV and DFIG-based DGs, respectively. The highest DG capacity of 27.13MVA is obtained during winter night load period when DFIG is connected at Bus 6. The highest reduction in overall active power losses of the network also occurs after optimal DFIG placement during this load period. The optimal DG capacity is minimum at 15.74 MVar when DFIG is connected at Bus 7, during summer day load period.

Table 7-5: The summary of results for the optimal placement of DGs on a 9-bus system during different load periods

Load period	**Distributed Generator**	**Optimal location (Bus no)**	**Optimal size**		**Total Power losses (MW)**	**% reduction from base case**
			Active Power capacity (MW)	**Reactive Power capacity (Mvar)**		
Summer day	Solar PV	7	19.44	-	0.464	78.7%
	DFIG	4	16.98	2.5	0.4	81.7%
Winter day	Solar PV	8	26.19	-	0.354	83.76%
	DFIG	5	26.82	3.42	0.356	83.67%
Summer night	DFIG	5	15.47	2.92	0.384	82.4%
Winter night	DFIG	6	26.40	6.25	0.329	84.9%

7.7.2 *The optimal DG allocation in distribution networks*

The resulting voltage profiles before and after the optimal placement of DFIG and solar PV-based DGs when considering an average of seasonal load models for the year are presented in Figure 7-66. The voltage profiles are compared to those of the normal loading of the network when constant load models are considered. It is observed that bus voltage profiles of the base case when normal network loading is considered are lower than that when the average seasonal load models are considered. The bus voltage profiles are therefore higher when voltage dependability of loads is considered in the load flow calculations.

The results of the voltage profiles when the annual load models are considered indicate that a better improvement is obtained for DFIG integration in comparison with a single solar PV integration as shown in Figure 7-66 below. The overall voltage profile has improved after the optimal allocation of DGs and the voltage profiles are within the voltage limits permitted by the grid codes. The resulting power losses after the optimal placement of DGs when the average load models are considered are also observed and are presented in Table 7-8. The optimal size and location of DGs are also included in Table 7-7.

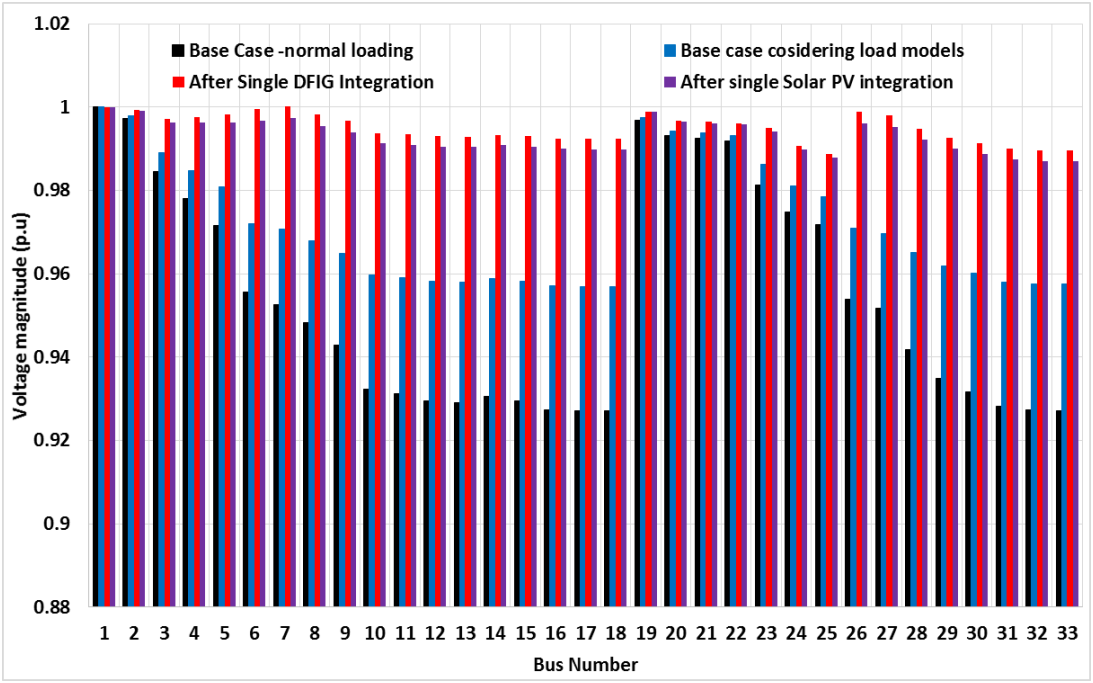

Figure 7-66: Comparison of voltage profiles after optimal placement of solar PV and DFIG-based DGs when average annual load models are considered

The optimal bus for optimal integration of both solar PV and DFIG-based DGs on a 33-bus distribution system is found to be Bus 6. The optimal size of a solar PV-based DG is determined to be 1.37MW and results in active power loss reduction of 78.9%. The optimal active and reactive power capacities of a DFIG-based DG are found to be 1.67 MW and 0.369 MVar, respectively and result in overall active power loss reduction of 78.1% which is nearly equal to that of solar PV integration. It is therefore observed that integration of single solar PV and DFIG energy sources contribute equally to system's active power loss reduction when the annual load models are considered. The results of the optimal bus bars for integration of individual DGs are as depicted in Table 7-7 . It is observed that in distribution network, the optimal integration of solar PV results in higher reduction in active power losses compared to DFIG-based DG. However, the penetration level of DGIG is higher than that of solar PV.

Table 7-6: The summary of results for the optimal placement of solar PV and DFIG based DG when the average of the seasonal load models is considered

Number of DG	**Distributed Generator**	**Optimal location (Bus no)**	**Optimal size**		**Total Power losses (MW)**	**% reduction from base case**
			Active Power capacity (MW)	**Reactive Power capacity (Mvar)**		
Single DG	Solar PV	6	1.370	-	0.01608	78.9%
	DFIG	6	1.677	0.369	0.0167	78.1%

The impacts of the optimal grid integration of DFIG and solar PV on voltage profiles are observed during different seasonal load periods. The voltage profiles are observed before and after integration of solar PV and DFIG in summer days and nights as well as in winter days and nights. The comparative analysis of voltage profiles and total active power losses is made between solar PV and DFIG based DGs for different load periods. The load models described in Section 6-8 for winter and summer days and nights are used for the analysis. The comparison of the voltage profiles resulting from grid integration of DFIG and solar PV for each load period is presented in Figure 7-67, Figure 7-68 and 7-69 below.

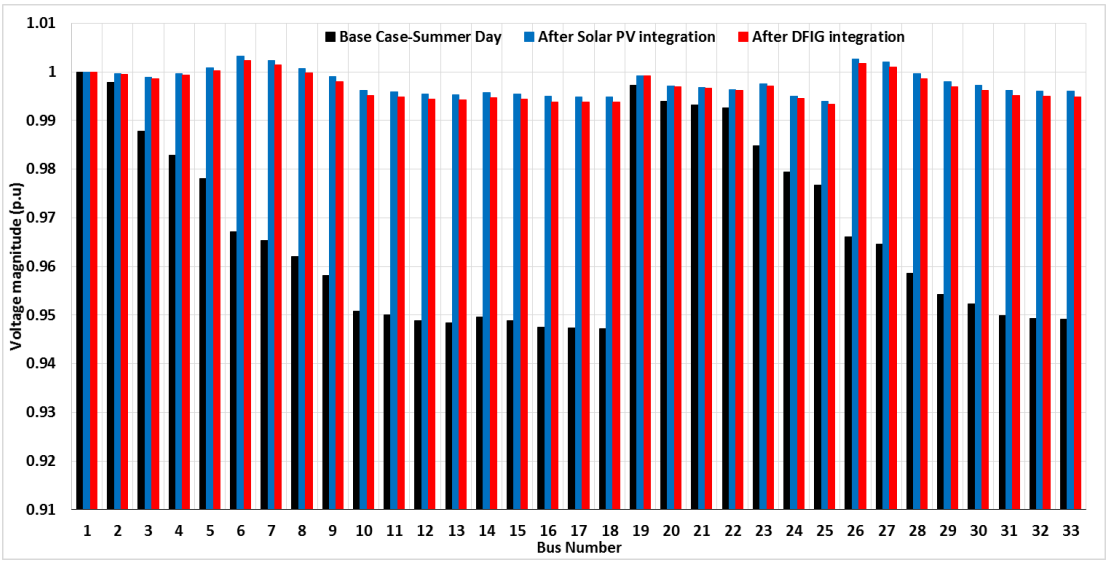

Figure 7-67: Voltage profiles after the optimal placement of DFIG and solar PV based DGs during summer day load period-Comparison with base case

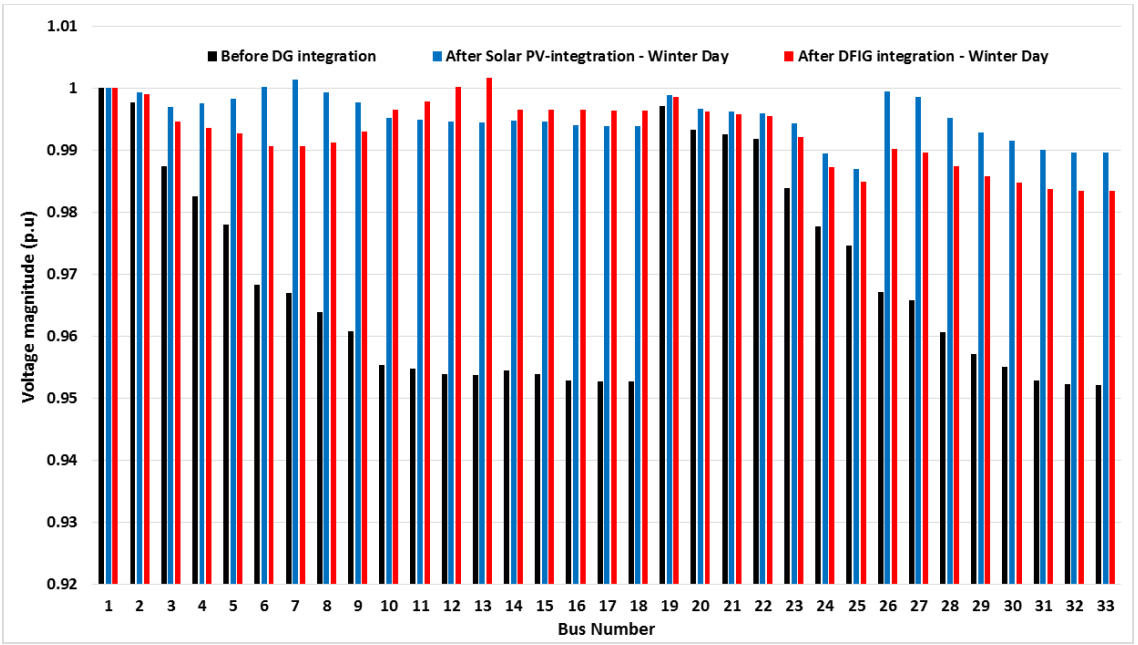

Figure 7-68: Voltage profiles after optimal placement of DFIG and solar PV during winter day load period - Comparison with the base case

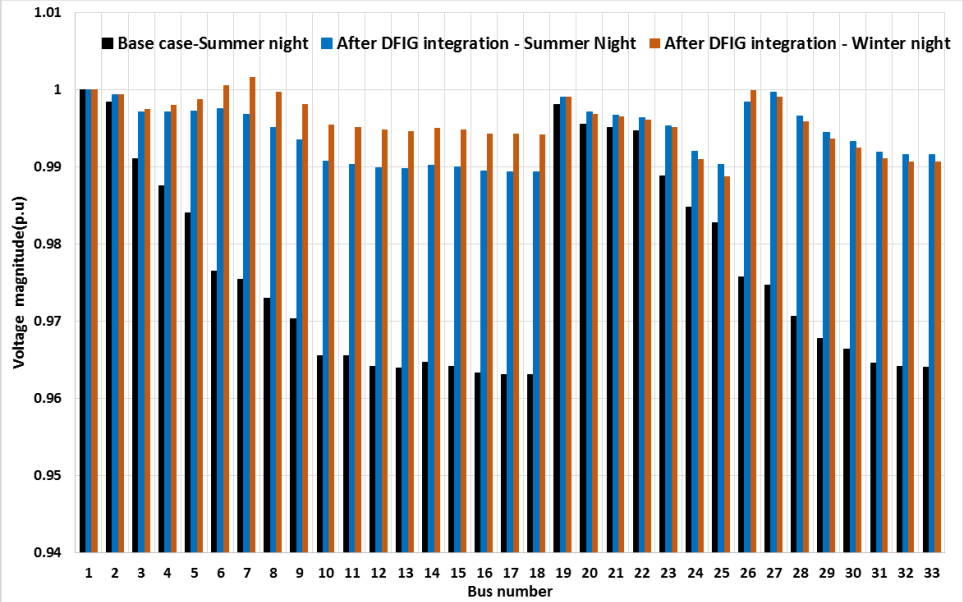

Figure 7-69: Voltage profiles after optimal placement of DFIG during winter and summer nights load periods - Comparison with the base case

It is observed that bus voltage profiles improvement is different for different load periods after the optimal DG placement. Figure 7-67 above indicates that during summer days load period, the improvement in voltage profiles at different system's buses is nearly the same for both DFIG and solar PV integration. The optimal bus bar for integration of both solar PV and DFIG to achieve voltage profile improvement depicted in Figure 7-15 for summer days is found to be bus 5 as shown in Table 7-8 below. The percentage reduction in overall power losses during summer day load period is found to be 89.32% and 88.6% for solar PV and DFIG, respectively. Therefore voltage profile improvement as well as total active power loss reduction, as a result of optimal integration of solar PV and DFIG, are the same during summer day load period. The capacity of solar PV during summer day load period is found to be 1.894MW whereas the active and reactive power capacities of DFIG-based DGs are obtained to be 1.947MW and 0.185MVar, respectively.

For winter day load period, the voltage profile improvement after the optimal placement of solar and DFIG-based DGs is as shown in Figure 7-68 above. It is observed that voltage magnitudes resulting from optimal DFIG integration are predominately higher in most system bus bars compared to that after solar PV integration except for bus 11 to bus 17. The optimal locations of solar PV and DFIG that result in voltage profile improvement shown in Figure 7-68 are 5 and 12, respectively. The capacity of DFIG is obtained to be 2.74MW and 0.213MVar and is almost twice higher than that of solar PV. As shown in Table 7-8, the percentage loss reduction is however higher for optimal solar PV integration during winter day load period.

For summer and winter nights, the impacts observed are those of the optimal placement of DFIG. Solar PV is not included for this analysis because of the absence of solar energy resource at nights. Figure 7-69 above indicates that a better voltage profile improvement is obtained after optimal DFIG integration during winter night load period in comparison with summer night load period. As depicted in Table 7-8 below, the optimal buses for DFIG integration are bus 5 and 6 for summer and winter nights, respectively. The optimal power ratings of DFIG are found to be 1.466 MW and 0.43MVar during summer nights and 1.694MW and 0.489MVar during winter night load period. Total active power loss reduction is higher during winter night load period in comparison with summer nights load period.

Table 7-7: The summary of results for the optimal placement of DG during different load periods

Load period	**Distributed Generator**	**Optimal location (Bus no)**	**Optimal size**		**Total Power losses (MW)**	**% reduction from base case**
			Active Power capacity (MW)	**Reactive Power capacity (Mvar)**		
Summer day	Solar PV	5	1.894	-	0.009755	89.32%
	DFIG	5	1.947	0.1847	0.01045	88.6%
Winter day	Solar PV	5	1.857	-	0.01981	80.3%
	DFIG	12	2.7314	0.2134	0.02269	77.47%
Summer night	DFIG	5	1.466	0.43	0.0128	74.88%
Winter night	DFIG	6	1.694	0.489	0.01629	77.3%

8. Conclusions and recommendations for future work

8.1 Conclusion

The review of grid integration of DGs as well as the studies conducted indicates that grid integration of DGs impacts the system's PQ, either negatively or positively. DG's impacts on network's PQ depend on the number of factors such as grid strength, DG location and penetration level, network loading and fault conditions in the network. The results obtained have indicated that indeed, a proper planning of grid integration of wind and solar farms has the capability to enhance PQ in both sub-transmission and distribution networks. The comparison of results obtained from grid integration of wind and solar farms under different scenarios have also indicated that wind and solar farms differ in their impacts and capacity to improve the system's PQ.

It was shown that PQ improvement in utility networks with DG integration can successfully be achieved by employing several approaches such as reactive power compensation, incorporating Battery Energy Storage (BES) at the PCC. PQ improvement in distribution networks can also be achieved by identification of optimal locations and sizes of wind and solar PV based DGs through application of optimization algorithms. This means that from knowledge of the characteristics of the network in question, the optimal buses and sizes of DG can be identified according to the DG type. The case studies conducted are crucial in future planning of grid integration DG technologies and will allow for compliance with the grid code requirements.

The integration of DGs into weak electrical networks is possible but requires certain measures in order to mitigate the adverse impacts they pose on the utility grids. Integration of wind and solar farms into weak utility grids was found to have detrimental impacts on the network's PQ. Their integration into strong grids on the other hand was found to enhance the performance of the network in terms of the system's PQ. Strong grids were found to have the capability to accommodate high penetration levels of DG without violating the grid code requirements in terms of acceptable voltage limits. The integration of DFIG based DGs in strong grids resulted in better voltage profiles in comparison with that resulting from integration of the same capacity of solar PV.

The proper planning of integration of DGs in electricity networks requires application of meta-heuristic techniques with properly formulated objective function to ensure that the system's PQ is enhanced. A significant improvement in bus voltage profiles and overall system's efficiency was achieved by application of GA technique to determine the optimal location and size of single and multiple DGs on the IEEE 9-bus sub-transmission and IEEE 33-bus distribution systems. The

significant improvement in voltage profiles was achieved when normal and varying seasonal load models of the distribution network were considered. The comparative analysis made between the optimal integration of solar PV and DFIG indicated the level of PQ improvement differ according to the DG type and number of integrated DGs.

8.2 Project Deliverables and Outcomes

As per the agreed deliverables, this research work included (a) the review of the aspects of planning of utility networks considering DG integration, (b) simulation studies for investigating the impacts of DG placement and sizing in utility networks with emphasis on PCC voltage profiles and overall active power losses of the networks, (c) investigation of PQ enhancement in utility networks with optimal DG placement and also including the STATCOM and SVC as well as battery energy storage at the PCC. The case studies carried out revealed that indeed, poor planning of DG integration can result in poor voltage profiles at the PCC and impacts network's efficiency.

The investigation of the optimal placement and sizing of DGs in utility networks also revealed that voltage profiles at different network buses are significantly improved by optimal solar PV and DFIG placement. The investigations were conducted under constant loads and when voltage variable load models defined by Equations C-1 and C-2 were considered. The results revealed that voltage profiles at different nodes of the networks are significantly improved by optimal DG placement and sizing, particularly when voltage dependency of loads is considered. The study also reveals that proper planning of DG integration such that the network PQ is enhanced can be achieved by applying appropriate tools.

8.3 Beneficiaries of this work

This studies conducted in this work have direct and indirect benefits to different entities and stakeholders. Some of the direct beneficiaries of this work are the electricity utility companies such as ESKOM which are seeking to connect RES to the grid. In the context of South African energy space, the participants of the REIPPPPs are also the direct beneficiaries of this work. Some of the fundamental findings which could benefit grid planners include:

- The ability of solar and wind farms to enhance the grid's PQ differ according to a number of factors such as DG location, capacity, network loading models, etc.
- It is feasible to connect DGs on to weak network, as long as necessary measures such as reactive power control at the PCC is adequate enough to provide support to PCC voltage

- The optimization techniques such as GA are capable of identifying the optimal location and size of DGs such the network's PQ and efficiency are enhanced.

8.4 Recommendations and future work

The following recommendations pertaining to grid integration of DGs are made:

- The network parameters such as line and bus data, load models and grid strength should accurately be modelled in network studies pertaining to planning of grid integration of DGs.
- The locations and penetration level of DGs in the network should be optimally determined such that the network's PQ does not deteriorate but rather enhanced in terms of voltage profile improvement.
- Voltage support through reactive power control should be included at the PCC to improve the transient behaviour of the network and ensure compliance with the grid code requirements.
- The study case results should be extended to grid integration of other RES such as biomass and concentrated solar plants (CSP) to broaden an understanding of PQ improvement by different DG types.
- The focus in the near future should develop a tool that is capable of deciding which DG technology is appropriate for integration to different network types.
- It is necessary to incorporate economics variables to quantify the financial implications of poor PQ in the network.
- Further research is also necessary for modelling and control of grid connected solar and wind farms such that their impacts on system's PQ are mitigated.

List of References

[1] " Renewables 2014 Global Status Report," REN21 Secretariat, Paris, 2014.

[2] B. A. Bossi, C. Delfino, B. Lewald, N. Massucco, S. Metten, E. Meyer, T. Silvesto and F. Wisiak, "Electrical Energy Distribution networks: Actual situation and perspective for Distributed Generation," in *17th international Conference on Electricity Distribution CIRED*, Barcelona, Spain.

[3] E. Coster, J. Myrzik, B. Kruimer and W. Kling, "Integration Issues of Distributed Generation in Distribution Grids," *Proceedings of the IEEE* |, vol. 99, no. 1, pp. 28- 39 , 2011 .

[4] I. E. A. (IEA), "Distributed Generation in Liberalised Electric," OECD/IEA, Paris, 2002.

[5] IEEE. [Online]. Available: www.ieee.org. [Accessed 17 March 2015].

[6] F. Gonzalez -Longatt and C. Fortoul, "Review of the Distributed Generation Concept: Attempt of Unification," in *Proceeding of International Conference on Renewable Energies and Power Quality*, España, 2005.

[7] P. .. P, P. N. P. and N. R.K., "Planning of grid integrated distributed generators: A review of technology, objectives and techniques," *Renewable and sustainable reviews,* vol. 40, pp. 557-570, 2014.

[8] A. Moreno-Munoz, J. de-la-Rosa, M. Lopez-Rodriguez, J. Flores-Arias, F. Bellido-Outerino and M. Ruiz-de-Adana, "Improvement of power quality using distributed generation," *International journal of Electrical Power and Energy Systems,* vol. 32, no. 10, pp. 1060 - 1076, 2010.

[9] G. Allan, I. Eromenko, M. Gilmartin, I. Kockar and P. McGregor, "The economics of distributed energy generation: A literature review," *International journal in renewable and sustainalble energy technologies reviews,* vol. 42, pp. 543 - 556, 2015.

[10] J. Paska, P. Biczel and M. Klos, "Hybrid power systems – An effective way of utilising primary energy sources," *Renewable energy,* vol. 34, no. 11, pp. 2414 - 2421, 2009.

[11] S. Chowdhury and T.Matlokotsi, "Role of grid integration of distributed generation in power quality enhancement: A review," in *2016 IEEE PES PowerAfrica*, Livingstone, 2016.

[12] C. SANKARAN, Power Quality, New York: CRC PRESS, 2001.

[13] S. &. B. Dwivedi2, "Power quality issues, problems, standards & their effect with correncitve means," *International Journal of Advances in Engineering & Technology,*, vol. 1, no. 2, pp. 1-11, 2011.

[14] L. M. J. D. A. de Almeida, "Power Quality Problems and New Solutions," in *International Conference on Renewable energy and power quality*, Vigo, 2003.

[15] M. S. S. Chattopadhyay.S, Electric power quality, Springer, 2011.

[16] Y. Zhao, *Electrical Power Systems Quality*, University Of Buffalo.

[17] H. KHAN, *Power quality improvement of distribution system with dispersed generation using novel algorithm for detection andcontrol of islanding process*, Doctoral Thesis, 2009.

[18] M. V. Sharad W. Mohod, "Power Quality Issues and its improvement in wind energy generation interface to the grid," *MIT International Journal of Electrical and instrumentation engineering*, vol. 1, no. 2, pp. 116-122, 2011.

[19] H. Markiewicz and A. Klajn, *Power Quality Application Guide-Voltage Disturbances,* Wroclaw: Standard EN 50160, 2004.

[20] A. Polycarpou, Power Quality and Voltage Sag Indices in Electrical Power Systems, Cyprus : InTechOpen, 2011.

[21] I. 1547, *Standard for Interconnecting Distributed Resources with Electric Power Systems,* IEEE, 2003.

[22] S. Std., "Grid connection code for renewable power plants(RPPs) connected to the electricity transmission and distribution systems in South Africa," 2014.

[23] R. P. Payasi, A. Singh and D. Singh, "Review of distributed generation planning: objectives, constraints, and algorithms," *International Journal of Engineering, Science and Technology,* vol. 3, no. 3, pp. 133 - 153, 2011.

[24] G. Murthy, S. Sivanagaraju, S. Satyanarayana and B. H. Rao, "Optimal Placement of DG in Distribution System to Mitigate Power Quality Disturbances," *International Journal of Electrical, Computer, Electronics and Communication Engineering,* vol. 7, no. 2, pp. 199 - 205, 2013.

[25] P. Georgilakis and N. Hatziargyriou, "A review of power distribution planning in the modern power systems era: Models, methods and future research," *Journal of Electric Power System Research,* vol. 121, pp. 89 - 100, 2015.

[26] EURELECTRIC, "Active Distribution System Management; A key tool for the smooth integration of distributed generation," 2013.

[27] J. Kennedy, P. Ciufo and A. Agalgaonkar, "Over-Voltage Mitigation within Distribution Networks with a High Renewable Distributed Generation Penetration," in *Energy Conference (ENERGYCON), 2014 IEEE International,* Cavtat, 2014.

[28] W. Tan, M. Hassan, M. Majid and H. Rahman, "Optimal ditributed renewable generation planning: A review of different approaches.," *Journal of Renewable and Sustainable Energy Reviews,* vol. 18, pp. 626 - 645, 2013.

[29] P. Georgilakis and N. Hatzaiargyriou, "Optimal Distributed Generation Placement in Power Distribution Network: Model, Methods, and Future Research," *IEEE Transactions on Power Systems,* vol. 28, no. 3, pp. 3420 - 3429, 2013.

[30] H. O. w. farm), "Using Wind power generation as an Alternative Energy Source," Domestic use of Energy, 2004.

[31] M. Reza, P. Schavemaker, J. Slootweg, W. Kling and L. van der Sluis, "Impacts of Distributed Generation Penetration levels on Power systems transient stability," in *Power Engineering Society general Meeting,* Denver, 2004.

[32] B. Alboyacy, "Grid Connection Requirements for Wind Turbine Systems in selected Countries - Comparison to turkey," *Electrical Power Quality & Utilization Magazine,* vol. 3, no. 2, 2008.

[33] J. Nye, J. Beukes and M. Bello, "Generation increase on distribution feeders using electronic voltage regulators," in *T&D Conference and Exposition, 2014 IEEE PES,* Chicago, 2014.

[34] A. Etxegarai, A. Etxegarai, E. Torres, A. Iturregi and V. Valverde, "Review of grid connection requirements for generation assets in weak power grids," *Renewable and Sustainable Energy Reviews,* vol. 41, pp. 1501-1514, 2015.

[35] S. Grunau and F. Fuchs, "Effect of wind-energy power injection into weak grids," Institute for Power Electronics and Electrical Drives Christian-Alberchts-University,, Kiel, 2012.

[36] A. Golieva, "Low Short Circuit Ratio Connection of Wind Power Plants," Master of Science Thesis, 2012.

[37] P. Kayal and C. Chanda, "Optimal mix of solar and wind distributed generations considering performance improvement of electrical distribution network," *Renewable energy,* vol. 75, pp. 173 - 186, 2015.

[38] D. Akinyele and R. Rayudu, "Review of energy storage technologies for sustainable power networks," *Sustainable Energy Technologies and Assessments,* vol. 8, pp. 74-91, 2014.

[39] D. Shi and R. Sharma, "Adaptive control of energy storage for voltage regulation in distribution system," in *Smart Energy Grid Engineering (SEGE)*, Oshawa, 2013.

[40] B. Zakeri and S. Syri, "Electrical energy storage systems: A comparative life cycle cost analysis," *Renewable and Sustainable Energy Reviews,* vol. 42, pp. 569 - 596, 2015.

[41] Z. Zeng, H. Yang, J. M. Guerrero and R. Zhao, "A Multi-Functional Distributed Generation Unit for Power Quality Enhancement," *E T Power Electronics,* vol. 8, no. 3, p. 467–476, 2015.

[42] G. Tabita and B. Satish, "A Control Strategy for Implementation of Enhanced Voltage Quality in Micro Grid," *International Journal of Engineering and Technical Research (IJETR),* vol. 2, no. 4, pp. 110 - 116, 2014.

[43] S. Naka, S. Toune, T. Genji and T. Yura, "Optimal Setting for Distribution Voltage Control Considering Interconnection of Distributed Generators," in *nternational Conference on Electrical Engineering,* Kitakyushu, Japan, 2000.

[44] A. Howlader, N. .. Urasaki, A. Yona, T. Senjyu and A. Y. Saber, "A review of output power smoothing methods for wind energy conversion systems," *Renewable and Sustainable Energy Reviews,* vol. 26, pp. 135-146, 2013.

[45] K. H.W., K. S.S and K. H.S., "Modeling and control of PMSG based variable-speed wind turbine," *Electric Power Systems Research,* vol. 80, pp. 46-52, 2010.

[46] M. Bollen and F. Hassan, Integration Of Distributed Generation in the Power System, New Jersey: A John Wiley & Sons, 2011.

[47] M. FARHOODNEA, A. MOHAMED, H. SHAREEF and H. ZAYANDEHROODI, "Power Quality Analysis of Grid-Connected Photovoltaic Systems in Distribution networks," *Elektrotechniczny (Electrical Review), 2013/2a,* p. 208–213, 2013.

[48] Z. Chen, "Issues of Connecting Wind Farms into Power Systems," in *IEEE/PES Transmission and Distribution Conference & Exhibition,* Dalian, 2005.

[49] D. Srinivas and M. R. S. Reddy, "Power Quality Improvement in Grid Connected Wind Energy System Using Facts Device and PID Controller," *IOSR Journal of Engineering (IOSRJEN)* , vol. 2, no. 11, pp. 19 - 26, 2012.

[50] M. Bollen, "Understanding Power Quality Problems,," Piscataway: IEEE Press IEEE Press, 1999.

[51] "Optimal sizing and location of SVC devices for improvement of voltage profile in distribution network with dispersed photovoltaic and wind power plants," *Applied Energy Journal,* vol. 134, pp. 114-124, 2014.

[52] D. Q. Hung, N. Mithulananthan and R. Bansa, “Integration of PV and BES units in commercial distribution systems considering energy loss and voltage stability,” *Applied Energy* , vol. 113 , p. 1162–1170, 2014.

[53] R. Sunny and R. Anto, “Control of harmonics and performance analysis of a grid connected photovoltaic system,” *International Journal of Advanced Research in Electrical Electronics and Instrumentation Engineering,* vol. 2, no. 1, pp. 37-45, 2013.

[54] J. Urbanetz, P. Braun and R. Rüther, “Power quality analysis of grid-connected solar photovoltaic generators in Brazil,” *Energy Conversion and Management,* vol. 64, pp. 8-14, 2012.

[55] R. Tonkoski and L. A. Lopes, “Impact of active power curtailment on overvoltage prevention and energy production of PV inverters connected to low voltage residential feeders,” *Renewable Energyn Journal,* vol. 36, pp. 3566 -3574, 2011.

[56] A. Samadi, E. Shayesteh, R. Eriksson, B. Rawn and L. Soder, “Multi-objective coordinated droop-based voltage regulation in distribution grids with PV system,” *Renewable Energy Journal,* vol. 71, pp. 315-323, 2014.

[57] D. Pandey and J. S. Bhadoriya, “Optimal Placement & Sizing Of Distributed Generation (Dg) To Minimize Active Power Loss Using Particle Swarm Optimization (Pso),” *Scientific & technology research volume,* vol. 3, no. 7, pp. 246-255, 2014.

[58] A. Madariaga, C. J. M. d. Ilarduya, S. Ceballos, I. M. d. Alegría and J. Martín, “Electrical losses in multi-MW wind energy conversion systems,” in *International Conference on Renewable Energies and Power Quality,* Santiago de Compostela, 2012.

[59] M. Arifujjaman, “A comprehensive power loss, efficiency, reliability and cost calculation of a 1 MW/500 kWh battery based energy storage system for frequency regulation application,” *Renewable Energy Journal,* vol. 74, pp. 158 - 169, 2015.

[60] M. Arifujjaman, “Reliability comparison of power electronic converters for grid-connected 1.5kW wind energy conversion system,” *Renewable energy journal,* vol. 57, pp. 348-357, 2013.

[61] M. A. S. Masoum, H. Dehbonei and E. F. Fuchs, “Theoretical and Experimental Analyses of Photovoltaic Systems With Voltage- and Current-Based Maximum Power-Point Tracking,” *IEEE TRANSACTIONS ON ENERGY CONVERSION,* vol. 17, no. 4, pp. 514 - 522, 2002.

[62] R. Yan, T. K.Saha, N. Modi, N. Masood and M. Mosadeghy, “The combined effects of high penetration of wind and PV on power system frequency response,” *Applied Energy Journal,* vol. 145, pp. 320 - 330, 2015.

[63] R. Shah, N. Mithulananthan, R. Bansal and Ramachandaramurthy, “A review of key power system stability challenges for large-scale PV integration,” *Renewable and Sustainable Energy Reviews,* vol. 41, pp. 1423 - 1436, 2015.

[64] X. H, L. Y, W. Z, G. D and Y. T., “A new frequency regulation strategy for photovoltaic system without energy storage,” *IEEE trans Sustainable Energy,* vol. 4, no. 4, pp. 985-193, 2013.

[65] K. Yang, M. H. Bollen, E. A. Larsson and M. Wahlberg, “Measurements of harmonic emission versus active power from wind turbines,” *Electric Power Systems Research Journal,* vol. 108, pp. 304-3141, 2014.

[66] S. Chen, N. Gao, H. Shena, Y. Quan, C. Wang, L. Zhu and J. Liu, "Affect Analysis of Power Grid Energy Quality for Coastal Wind Power Access," *Energy Procedia,* vol. 12, pp. 752-760, 2011.

[67] A. Latheef, D. A. Robinson, V. J. Gosbell and V. W. Smith, "Harmonic impact of photovoltaic inverters on low voltage distribution Systems," in *Australasian Universities Power Engineering Conference,* Australia, 2006.

[68] M. Sidrach-de-Cardona and J. Carretero, "Analysis of the current total harmonic distortion for different single-phase inverters for grid-connected PV-systems," *Solar Energy Materials & Solar Cells,* vol. 87, p. 529–540, 2005.

[69] M. Hossein and R. Baghipour, "Optimal Placement of DGs in Distribution System including Different Load Models for Loss Reduction using Genetic Algorithm," *Journal of advances in computer research,* vol. 4, no. 3, pp. 55-68, 2013.

[70] S. C. Reddy, P. V. N. Prasad and A. J. Laxmi, "Power Quality Improvement of Distribution System by Optimal Placement and Power Generation of DGs using GA and NN," *European Journal of Scientific Research* , vol. 69, no. 3, pp. 326-336 , 2012.

[71] R. S. Rao, K. Ravindra, K. Satish and a. S. V. L. Narasimham, "Power Loss Minimization in Distribution System Using Network Reconfiguration in the Presence of Distributed Generation," *IEEE TRANSACTIONS ON POWER SYSTEMS,* vol. 28, no. 1, pp. 317-326, 2013.

[72] B. A. Rad, "Optimum Design of DG-Based Distribution System Considering Power Quality and Reliability Indices Using PSO," *Middle-East Journal of Scientific Research,* vol. 18, no. 6, pp. 829-836, 2013.

[73] M. Kasaei, "Optimal placement of distributed generation and capacitor in distribution networks by ant colony algorithm," *Technical and Physical Problems of Engineering,* vol. 6, no. 20, pp. 52-56, 2014.

[74] M. Lolita, V. Reddy, N. Reddy and V. Reddy, "A Two Stage Methodology for Sitting and Sizing of DG for Minimum Loss in Radial Distribution Systems Using RCGA," *International Journal of Computer Applications,* vol. 25, no. 2, pp. 10-16, 2011.

[75] S. Ruiz-Romero, A. Colmenar-Santos, F. Mur-Perez and A. Lopez-Rey, "Integration of distributed generation in the power distribution network: The need for smart grid control systems, communication and equipment for a smart city-Use cases," *Renewable and sustainable energy reviews,* vol. 38, pp. 223-234, 2014.

[76] L. Collins and J. Ward, "Real and reactive power control of distributed PV inverters for overvoltage prevention and increased renewable generation hosting capacity," *Renewable Energy,* vol. 81, pp. 464-477, 2015.

[77] M. A. Mahmud, M. J. Hossain, H. R. Pota and A. B. M. Nasiruzzaman, "Voltage Control of Distribution Networks with Distributed Generation using Reactive Power Compensation," in *37th Annual Conference on IEEE Industrial Electronics Society* , Melbourne, 2011.

[78] T. Madangombe, "Integration of wind energy systems into the grid: Power quality and technical requirements," MSc Thesis, University of Cape town, 2010.

[79] M. V. D. Ilse, M. Zarghami and S. Vadhva, "Review of Concepts to increase Distributed Generation into the Distribution Network," in *Sixth Annual IEEE Green Technologies Conference*, Corpus Christi, 2014.

[80] P. T.N., U. K. and N. D.E, "An overview of the present grid codes for integration of distributed generation," in *Integration of Renewables into the Distribution Grid, CIRED 2012 Workshop*, Lisbon, 2012.

[81] S. Mali, S. James and I. Tank, "Improving low voltage ride-through capabilities for grid connected wind turbine generator," in *4th International Conference on Advances in Energy Research*, 2013.

[82] O. Ipinnimo, S. Chowdhury and S. Chowdhury, "Mitigation of Multiple Voltage Dips in a Weak Grid Using Wind and Hydro-based Distributed Generation," in *Transmission and Distribution Conference and Exposition (T&D)*, Orlando, 2012.

[83] O. Ipinnimo, S. Chowdhury and S. P. Chowdhury, "Application of Grid Integrated Wind Energy Conversion Systems for Mitigation of Multiple Voltage Dips in a Power Network," in *46th International Universities' Power Engineering Conference*, Soest, 2011.

[84] I. Perpinias, N. Papanikolaou and E. Tatakis, "Design Principles of Low Voltage Distributed Generation Units with Increased Fault Ride Through Capability," in *15th European Conference on Power Electronics and Applications (EPE),* , Lille, 2013.

[85] E. .D and S. Masri, "Challenges of integrating renewable energy sources to smart grids," *Renewable and Sustainable Energy Reviews*, vol. 52, pp. 770-780, 2015.

[86] X. Xu, M. Bishop, J. Sember, M. J. Edmonds and C. Hao, "Dynamic Modeling and Simulation of Distributed Static Compensators in System Impact Studies," in *IEEE PES Asia-Pacific Power and Energy Engineering Conference (APPEEC)*, Kowloon , 2013.

[87] I. Perpinias, N. Papanikolaou and E. Tatakis, "Fault ride through concept in low voltage distributed photovoltaic generators for various dispersion and penetration scenarios," *Sustainable Energy Technologies and Assessments*, vol. 12, pp. 15-25, 2015.

[88] J. Langstädtler, Schellschmidt, S. schrobsdorff, J. Scheffer and C. Kahlen, "Relevance of high-voltage-ride-through capability and testing," in *23rd International Conference on Electricity Distribution*, Lyon, 2015.

[89] C. Feltes, S. Engelhardt, J. Kretschmann, J. Fortmann, F. Koch and I. Erlich, "High Voltage Ride-Through of DFIG-based Wind Turbines".

[90] S. Hassan, "A review on voltage control methods for active distribution networks," *Electrical Review*, vol. 88, no. 6, pp. 304 - 312, 2012.

[91] P. M. S. Carvalho and P. F. Correia, "Distributed Reactive Power Generation Control for Voltage Rise Mitigation in Distribution Networks," *IEEE TRANSACTIONS ON POWER SYSTEMS*, vol. 23, no. 2, pp. 766 - 772, 2008.

[92] S.Sumankumar and S. Giri, "A Review of Voltage Control Technique of Grid Connected Distributed Generation," *International Journal of Innovative Research in Science, Engineering and Technology*, vol. 3, no. 1, pp. 1565 - 1571, 2014.

[93] G. Sulligoi and M. Chiandone, "Voltage Rise Mitigation in Distribution Networks using Generators Automatic Reactive Power Controls," in *Power and Energy Society General Meeting, IEEE*, San Diego, 2012.

[94] E. Mogos and X. Guillaud, "A voltage regulation system for distributed generation," *Power Systems Conference and Exposition*, vol. 2, pp. 787-794, 2004.

[95] S. Corsi, Voltage Control and Protection in Electrical Power Systems, London: Springer, 2015.

[96] F. Didactic, “Electricity and New Energy Static Var Compensator (SVC) Courseware Sample,” Festo Didactic , Canada , 2015.

[97] T. Masood, R. .. Aggarwal, S. Qureshi and R. Khan, “STATCOM Model against SVC Control Model Performance Analyses Technique by MATLAB,” in *International Conference on Renewable Energies and Power Quality*, Granada, 2010.

[98] T.tran-quoc, G. Rami, E.Monnot, A. Almeida, C. Kieny and N. Hadjsaid, “Intelligent voltage control in distribution network with distributed generation,” in *19th International Conference on Electricity Distribution*, Vienna, 2007.

[99] B. Blazic, T. Pfajfar and I. Papic, “Voltage control in networks with distributed generation — A case study,” in *IEEE PES/IAS Conference on Sustainable Alternative Energy (SAE)*, Valencia, 2009.

[100] C. Gao and M. A. Redfern, “A Review of Voltage Control Techniques of Networks with Distributed Generations using On-Load Tap Changer Transformers,” in *Universities Power Engineering Conference (UPEC)*, Cardiff, 2010.

[101] S. J. v. Zyl and C. Gaunt, “S. J. van Zyl and C. Gaunt,” in *IEEE Bologna Power Tech Conference Proceedings*, Bologna, 2003.

[102] S. K., N. Kumar and P. Renuga, “Optimal var planning using facts,” *International Journal of Power and Energy Systems*, 2012.

[103] H. Singh and L. Srivastava, “Recurrent multi-objective differential evolution approach for reactive power management,” *IET Generation, Transmission & Distribution*, vol. 10, no. 1, pp. 192-204, 2016.

[104] J. Hiscock, N. Hiscock and A. Kennedy, “Advanced voltage control for networks with distributed generation,” in *19th International Conference on Electricity Distribution*, Vienna, 2007.

[105] T. Bouktir and T. R. Guerriche, “Optimal Allocation and Sizing of Distributed Generation with Particle Swarm Optimization Algorithm for Loss Reduction,” *Science and technology*, vol. 6, no. 1, pp. 59-69, 2015.

[106] M. Sedighizadeh and A. Rezazadeh, “Using Genetic Algorithm for Distributed Generation Allocation to Reduce Losses and Improve Voltage Profile,” *World Academy of Science, Engineering and Technology 37* , vol. 37, pp. 251-256, 2008.

[107] S. Conti and A. Greco, “Active MV Distribution Network Planning Coordinated with Advanced Centralized Voltage Regulation System,” in *IEEE Power Tech* , Lausanne, 2007.

[108] M. Bollen and F. Hassan, “Overloading and Losses,” in *Integration of Distributed Generation in the Power System*, Hoboken, NJ, USA, John Wiley & Sons, Inc, 2011.

[109] H. Baghaee, M. Mirsalim, M. Sanjari and G. Gharehpetian, “Effect of type and interconnection of DG units in the fault current level of distribution networks,” in *Power Electronics and Motion Control Conference*, Poznan, 2008.

[110] S. Boswas, S. K. Goswami and A. Chatterjee, “Optimum distributed Generation placement with voltage sag effect minimization,” *Energy Conversion and Management*, vol. 53, no. 1, pp. 163-174, 2012.

[111] R. Garg and S. Mittal, "Optimization by Genetic Algorithm," *International Journal of Advanced Research in Computer Science and Software Engineering,* vol. 4, no. 4, pp. 587 - 590, 2014.

[112] C. G and P. F, ". Penetration level assessment of distributed generation by means of genetic algorithms," in *Proceedings of the IEEE power systems*, Clemson, 2002.

[113] D.White,"http://personal.denison.edu/~whiteda/files/ResearchPapers/SchemaOverview.pdf," 30 December 2009. [Online]. [Accessed 17 May 2017].

[114] M. G. Villalva, J. R. Gazoli and E. R. Filho, "Comprehensive Approach to Modeling and Simulation of Photovoltaic Arrays," *IEEE TRANSACTIONS ON POWER ELECTRONICS,* vol. 24, no. 5, pp. 1198- 1208, 2009.

[115] N. Hamrouni, M. Jraidi and A. Chérif, "New control strategy for 2-stage grid-connected photovoltaic power system," *Renewable Energy*, vol. 33, no. 10, pp. 2212 - 2221, 2008.

[116] D. Sulaiman, H. Ameen and I. Said, "Design of High Efficiency DC-DC Converter for Photovoltaic Solar Home Applications," *Energy and Power Engineering,* vol. 4, no. 11, pp. 43 - 51, 2010.

[117] S. Stallon, K. Kumar and S. Kumar, "Simulation of High Step-Up DC–DC Converter for Photovoltaic Module Application using MATLAB/SIMULINK," *I.J. Intelligent Systems and Applications,* vol. 7, pp. 72 - 82, 2013.

[118] G. Rampinelli, A. Krenzinger and F. C. Romero, "Mathematical models for efficiency of inverters used in grid connected photovoltaic systems," *Renewable and Sustainable Energy Reviews,* vol. 34, p. 578–587, 2014.

[119] F. Mahmood, "Improving the Photovoltaic Model In PowerFactory," Degree project in electric power systems, Stockholm, Sweden, 2012.

[120] I. Theologitis, E. Troester and T. Ackermann, "Aspects of generic photovoltaic model examined under the German Grid code for Medium voltage," in *1st International Workshop on Integration of Solar power into Power system*, Aarhus, Denmark, 2011.

[121] R. Ochieng, F. Onyango, J. Shichikha and A. Manyonge, "Mathematical Modelling of Wind Turbine in a Wind Energy Conversion System: Power Cofficient Analysis," vol. 6, p. 4528, 2013.

[122] M. Singh and S. Santoso, "Dynamic Models for Wind Turbines and Wind Power Plants," National Renewable Energy Laboratory, Colorado, 2011.

[123] M. Vijayalaxmi and a. N. ShanmugaVadivoo, "Identification of Doubly Fed Induction Generator based," in *Intelligent Systems and Control (ISCO), 2013 7th International* , 2013.

[124] N. S. Vadivoo and M.Vijayalaxmi, ""Identification of Doubly Fed Induction Generator based Wind Energy Conversion System using piecewise-linear Hammerstein Wiener model," in *7th International Conference on, Coimbatore*, Tamil Nadu, 2013.

[125] M. A. SNYDER, "Development of Simplified Models of Doubly-Fed Induction Generators(DFIG)," in *Master of science Thesis*, CHALMERS UNIVERSITY OF TECHNOLOGY, 2012.

[126] P. Sekhoto and S. C. O. Ipinnimo, "Voltage dip analysis of electricity networks on wind energy integration," in *Power Engineering Conference (UPEC)*, Dublin, 2013.

[127] A. D. Pilehvarani, M. Hakimzadeh, M. Far and R. Sedaghati, "Application of GAMS and GA in the Location and Penetration of Distributed Generation," *Electrical, Computer, Energetic, Electronic and Communication Engineering* , vol. 8, no. 11, pp. 1786-1790, 2014.

[128] S. Koohi-Kamali, V. Tyagi, N. Rahim, N. Panwar and H. Mokhlis, "Emergence of energy storage technologies as the solution for reliable operation of smart power systems: A review," *Renewable and Sustainable Energy Reviews,* vol. 25, p. 135–165, 2013.

[129] J. Z. Zhou and A. M. Gole, "Estimation of the Short Circuit Ratio and the Optimal Controller Gains Selection of a VSC System," in *nternational Conference on Power Systems Transients (IPST2013)* , Vancouver, 2013.

[130] A. K. Bohre, G. Agnihotri, M. Dubey and S. Kalambe, "Impacts of the Load Models on Optimal Planning of Distributed Generation in Distribution System," *Advances in Artifical Intelligence,* vol. 2015, no. Article ID 297436, pp. 1-11, 2015.

[131] J. D. Kramer and C. Jacky, "How to write biblos," vol. 1, no. 1, 2006.

[132] D. Powerfactory, "DIgSILENT Solutions-Power factory version 15," Germany.

[133] M. Molina and E. Espejo, "Modeling and simulation of grid-connected photovoltaic energy conversion systems," *international journal of hydrogen energy* , vol. 39, no. 16, pp. 8702 - 8707, 2014.

[134] L. Hassaine, E. OLias, J. Quintero and V. Salas, "Overview of power inverter topologies and control structures for grid connected photovoltaic systems," *Renewable and Sustainable Energy Reviews,* vol. 30, p. 796–807, 2014.

[135] R. Rajesh and M. C. Mabel, "A comprehensive review of photovoltaic systems," *Renewable and Sustainable Energy Reviews,* vol. 51, p. 231–248, 2015.

[136] W. Tsai-Fu, K. Chia-Ling, S. Kun-Han, C. Yu-Kai and L. Y.-D. C. Yung-Ruei, "ntegration operation of a single-phase bidirectional inverter with two buck/boost MPPTs for DC-distribution applications," *IEEE Transmission Power Electronics,* vol. 26, pp. 674 - 686, 2013.

[137] M. B. Latran and A. Teke, "Investigation of multilevel multifunctional grid connected inverter topologies and control strategies used in photovoltaic systems," *Renewable and Sustainable Energy Reviews,* vol. 42, pp. 361 - 376, 2015.

[138] H. Zhan, C. Wang, Y. Wang, X. Yang, X. Zhang, C. Wu and Y. Chen, "Relay Protection Coordination Integrated Optimal Placement and Sizing of Distributed Generation Sources in Distribution Networks," *IEEE Transactions onSmart Grid,* no. 99, pp. 1-11, 2015.

[139] P.Saravanan and R.Elavarasi, "Improvement of Voltage Profile in Distribution Network Using Distributed Generation," *International Journal of Innovative Research in Science, Engineering and Technology,* vol. 3, no. 1, pp. 1459 - 1467, 2014.

[140] R. Tyastuti, N. Hariyanto and M. Nurdin, "A Genetic Algorithm Approach Determining simultaneously Location and capacity of Distributed Generation in radial distribution system," in *5th International Conference on Electrical Engineering and Informatics 2015*, Bali, Indonesia, 2015.

[141] R. F. Tyastuti, N.Hariyanto, M. Nurdin and M. Yasunori, "A Genetic Algorith Approach Determining simulataneuosly Location and Capacity of Distributed Generation in Radial Distribution Networks," in *5th International Conference on Electrical Engineering and Informatics,* Bali, 2015.

[142] A. A. Seker and M. H. Hocaoglu, “Artificial Bee Colony Algorithm for Optimal Placement and Sizing of Distributed Generation,” in *Electrical and Electronics Engineering*, Bursa, 2013.

[143] N. T. L. a. D. X. Dong, “Optimal Location and Size of Distributed Generation in Distribution System by Artificial Bees Colony Algorithm,” *Information and Electronics Engineering*, vol. 3, no. 1, pp. 63-68, 2013.

[144] S. Kansal, V. Kumar and B. Tyagi, “Hybrid approach for optimal placement of multiple DGs of multiple types in distribution networks,” *Electrical Power and Energy Systems*, vol. 75, pp. 226-235, 2016.

[145] K. B. a. W. Phuangpornpitak, “Optimal Placement and Sizing of Distributed Generationfor Power Loss Reduction using Particle Swarm Optimization,” *10th Eco-Energy and Materials Science and Engineering* , vol. 34, pp. 307-317, 2013.

[146] A. Ibrahima, W. El-Khattama, M. ElMesallamy and H. T. a, “Adaptive protection coordination scheme for distribution network with distributed generation using ABC,” *Journal of Electrical Systems and Information Technology*, vol. 3, p. 320–332, 2016.

Conference papers published

- **D. Mabuggwe, T. Matlokotsi and S. Chowdhury:** Paper Tittle: "The Development of an Effective Restoration Scheme for a Ugandan Power System" – IEEE PES Power Africa Conference 2017, Accra, Ghana, May 2017 (Under review)
- **T. Matlokotsi, and S. Chowdhury:** Paper Tittle: "Role of grid integration of distributed generation in power quality enhancement-A review" IEEE PES Power Africa Conference 2016, Livingstone, Zambia, pp 1-5, June 2016
- **S. Mohammed, T. Matlokotsi and S. Chowdhury:** Paper Tittle: "Techno-Economic feasibility study of Solar PV and Biomass-based electricity generation for rural household and farm in Botswana" – IEEE PES Power Africa Conference 2016, Livingstone, Zambia, June 2016
- **T. Matlokotsi and S. Chowdhury**: Paper title: "Voltage and frequency profiles of Electricity networks with wind energy integration" – IEEE AFRICON 2015, Addis Ababa, Ethiopia, September 2015
- **K. Ramoreboli, T. Matlokotsi, and S. Chowdhury**: Paper tittle: "Comparison of the grid integration of wind farms and solar PVs in a utility grid" – South African Universities Power Engineering conference (SAUPEC2016), Johannesburg South Africa, January 2016

Appendix A: Parameters of networks used in the study

IEEE 9-Bus system data

Table A-1: The bus and load data for IEEE 9-bus system used in the study

Bus number	Voltage (kV)	Loads	
		Real power (MW)	Reactive power (MVar)
1	16.5	0	0
2	18	0	0
3	13.8	0	0
4	230	0	0
5	230	125	50
6	230	90	30
7	230	0	0
8	230	100	35
9	230	0	0

Table A-2: The line data for IEEE 9-bus sub transmission network used in the study

Line	Resistance (p.u)	Reactance (p.u)	Susceptance (p.u)
1-4	0.07173	0.0576	0.013
4-5	0.017	0.092	0.158
5-6	0.039	0.17	0.358
3-6	0.000	0.0586	0.000
6-7	0.0119	0.1008	0.209
7-8	0.0085	0.072	0.1490
8-2	0.000	0.0625	0.000
8-9	0.032	0.161	0.306
9-4	0.01	0.085	0.176

Table A-3: The parameters of the Synchronous generators of a 9-bus system

Parameter	Generator 1	Generator 2	Generator 3
Nominal voltage	16.5 kV	18 kV	13.8 kV
Nominal apparent power	100 MVA	150 MVA	100 MVA
Power factor	0.8	0.8	0.8
Active power	72MW	163MW	85 MW
Reactive power	28MVar	5MVar	-11 MVar
Nominal frequency	50 Hz	50 Hz	50 Hz
Connection type	YN	YN	YN
Stator resistance	0.01 p.u	0.01 p.u	0.01 p.u
Mode of voltage controller	Voltage	Power factor	Power factor

Rotor type	Round rotor	Round rotor	Round rotor

Transformer	Rated Power (MVA)	Rated voltage (kV)	X/R ratio	Technology	Connection
TR1					
TR2					
TR3					

IEEE 33-bus system data

Table A-4: Line data for IEEE 33-bus distribution network

From Node	To node	R(ohm)	X (ohms)
1	2	0.493	0.2511
2	3	0.0308	0.0157
3	4	0.0228	0.0116
4	5	0.0238	0.0121
5	6	0.0511	0.0441
6	7	0.0117	0.0386
7	8	0.1068	0.0771
8	9	0.0643	0.0462
9	10	0.0651	0.0462
10	11	0.0123	0.0041
11	12	0.0234	0.0077
12	13	0.0916	0.0721
13	14	0.0338	0.0445
14	15	0.0369	0.0328
15	16	0.0466	0.034
16	17	0.0804	0.1074
17	18	0.0457	0.0358
2	19	0.0102	0.0098
19	20	0.0939	0.0846
20	21	0.0255	0.0298
21	22	0.0442	0.0585
3	23	0.0282	0.0192
23	24	0.056	0.0442
24	25	0.0559	0.0437
6	26	0.0127	0.0065
26	27	0.0177	0.009
27	28	0.0661	0.0583
28	29	0.0502	0.0437
29	30	0.0317	0.0161
30	31	0.0608	0.0601
31	32	0.0194	0.0226
32	33	0.0213	0.0331

Table A-5: Load data for the 33-bus distribution network

Bus Number	Real Power (kW)	Reactive Power (kVar)
1	0	0
2	100	60
3	90	40
4	120	80
5	60	30
6	60	20
7	200	100
8	200	100
9	60	20
10	60	10
11	60	20
12	60	20
13	90	40
14	120	80
15	60	35
16	60	35
17	45	30
18	60	20
19	90	40
20	90	40
21	90	40
22	90	40
23	90	50
24	420	200
25	420	200
26	60	25
27	60	25
28	60	20
29	120	70
30	200	100
31	150	70
32	210	100
33	60	40

Appendix B: Solar and wind systems initialization parameters

DFIG system parameters

Table B-1: The parameters of the DFIG-based DG as modelled in PowerFactory

Parameter	Value	
	IEEE 9-bus system	IEEE 33-bus system
Nominal apparent power	10 MVA	1 MVA
Nominal voltage	230 kV	12 kV
Power factor	0.8	0.8
Frequency	50 Hz	50 Hz
Connection type	YN	YN

Table B-2: The parameters of the three windings transformer in DFIG system

Parameter	Value
Nominal apparent power	10 MVA
Nominal voltage	230 kV
Power factor	0.8
Frequency	50 Hz
Connection type	YN

Table B-3: The parameters of the converter used in DFIG system

Parameter	Value
Rated DC voltage	1.15 kV
Rated Power	5 MVA
Voltage set point	1.05 p.u
Reactive power set point	-0.5 MVAR
Control mode	$V_{DC}Q$

Solar PV parameters

Table B-4: The parameters of the converter used in DFIG system

Parameter	Value	
	IEEE 9-bus system	IEEE 33-bus system
Nominal apparent power	10 MW	1 MVA
Nominal voltage	230 kV	12 kV
Power factor	1	1
Frequency	50 Hz	50 Hz

Appendix C: Component models

Load models

Load modelling plays a significant role in the accuracy of results in power systems analysis. The loads in networks used for the study are modelled as normal loads that draw both real power and active power. The ratings of the respective loads of the two networks considered for this study are also presented in the appendices section. The load bus bars of the IEEE 9-bus system are located at the sub transmission part of the network and are considered as industrial load types. The loads of the 9-bus network are modelled in DIgSILENT as constant power load which are voltage-independent. The input parameters of the loads are entered on the window depicted in Figure C-1.

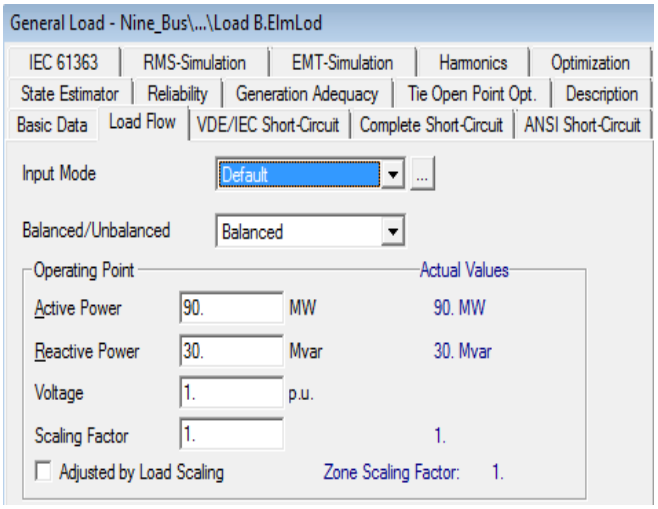

Figure C-1: The load parameter settings windows in DIgSILENT power factory

For the 33-bus distribution system, the loads are combined into groups and represented as residential, commercial and industrial loads. The loads at respective system busbars are made up sub-loads categorized by their voltage dependency. The conventional load flow studies assume that active and reactive power are constant values, independent of voltage magnitude at the bus. However, in actuality, different types of residential, commercial and industrial loads demand active and reactive power which are functions of system voltage at a particular instant. The active and reactive power ratings set for each load represents the combined power of individual loads supplied from the bus.

The mathematical representation of load models for any particular load can be expressed by equations (C-1) and (C-2) below:

$$P_i = P_{oi} V_i^{\alpha} \quad \text{(C-1)}$$

$$Q_i = Q_{oi} V_i^{\beta} \quad \text{(C-2)}$$

The real power, reactive power and voltage magnitude at bus i are P_i , Q_i and V_i ,respectively. The active and reactive operating points at bus i are represented by P_{oi} and Q_{oi}. The constants α and β are the exponents of the active and reactive power and are available as inputs in DIgSILENT PowerFactory as depicted in Figure C-2 below. For the constant load models used in both the 9 bus and 33-bus test systems, α and β are set to zero.

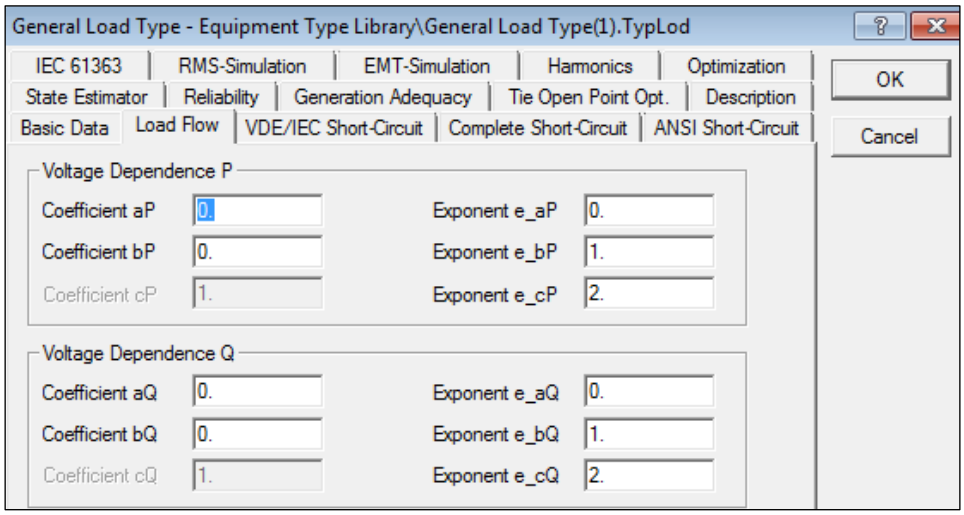

Figure C-2: The window for specifying the settings of the voltage dependent loads in PowerFactory

Synchronous generator models

Electrical power generators play a vital role in power system's operation since they are the source of electrical power used to power devices in the network. The conventional synchronous generators are considered to be the centralized generators in the 9-bus sub-transmission network of Figure 5-1. The proper settings of the generators are essential for power balancing and stability in an electrical network. The detailed parameters of generators used in this work are listed in Table A-3 in Appendix A. The windows depicting the parameters settings of generators as executed in DIgSILENT power factory are depicted in Figure C-3 below.

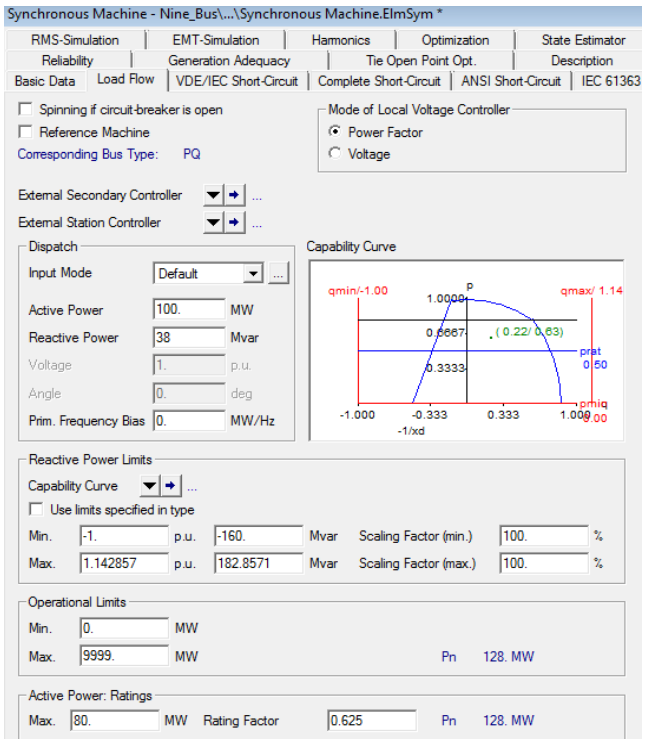

Figure C-3: The window for parameter settings of the synchronous generator's in DIgSILENT

Line models

The line models used for power delivery in transmission and distribution systems are important for understanding the active and reactive power flows in the networks. The transmission lines in this work are modelled as lumped parameter (PI) models. The significant line characteristics such as nominal voltage, impedance and rated currents are specified based on network type. The impedances of the 9-bus and 33-bus networks lines are presented in Table A-2 and Table A-5 in Appendix A respectively. The single line diagram of the lumped parameter model of the transmission lines is depicted in Figure C-4 below:

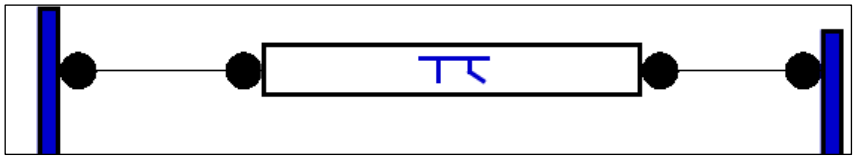

Figure C-4: The single diagram of the lumped parameter model of the lines

Transformer models

The transformers are included in the test networks above to interface the network portions of different voltage levels. The 9-bus system has a total of three, two-winding transformers used to step up the voltage level at generation before feeding power in to the sub-transmission system. The sub-transmission level voltage of the 9-bus system is 230 kV; therefore the three transformers will step up the terminal voltage of the respective generators to 230 kV. For the 33-bus system, there is one

step down transformer with the voltage ratio of 5.5 at the main substation feeding the rest of the network. The data of transformers for both the 9-bus and 33-bus networks are presented in Table A-4 and Table A-5 in Appendix A. In DIgSILENT, the settings of the transformers are entered on the window depicted in Figure C-5 below.

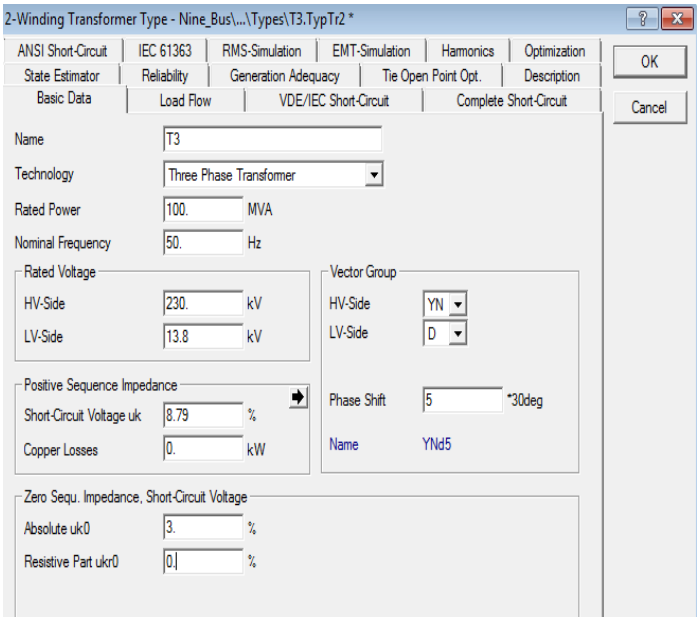

Figure C-5: Transformer power settings window for DIgSILENT

Appendix D: GA parameters

The flowchart of the GA optimization techniques applied is presented in Figure D-1 below. The parameters of GA algorithm used in different scenarios of the optimization processes are also listed in this section.

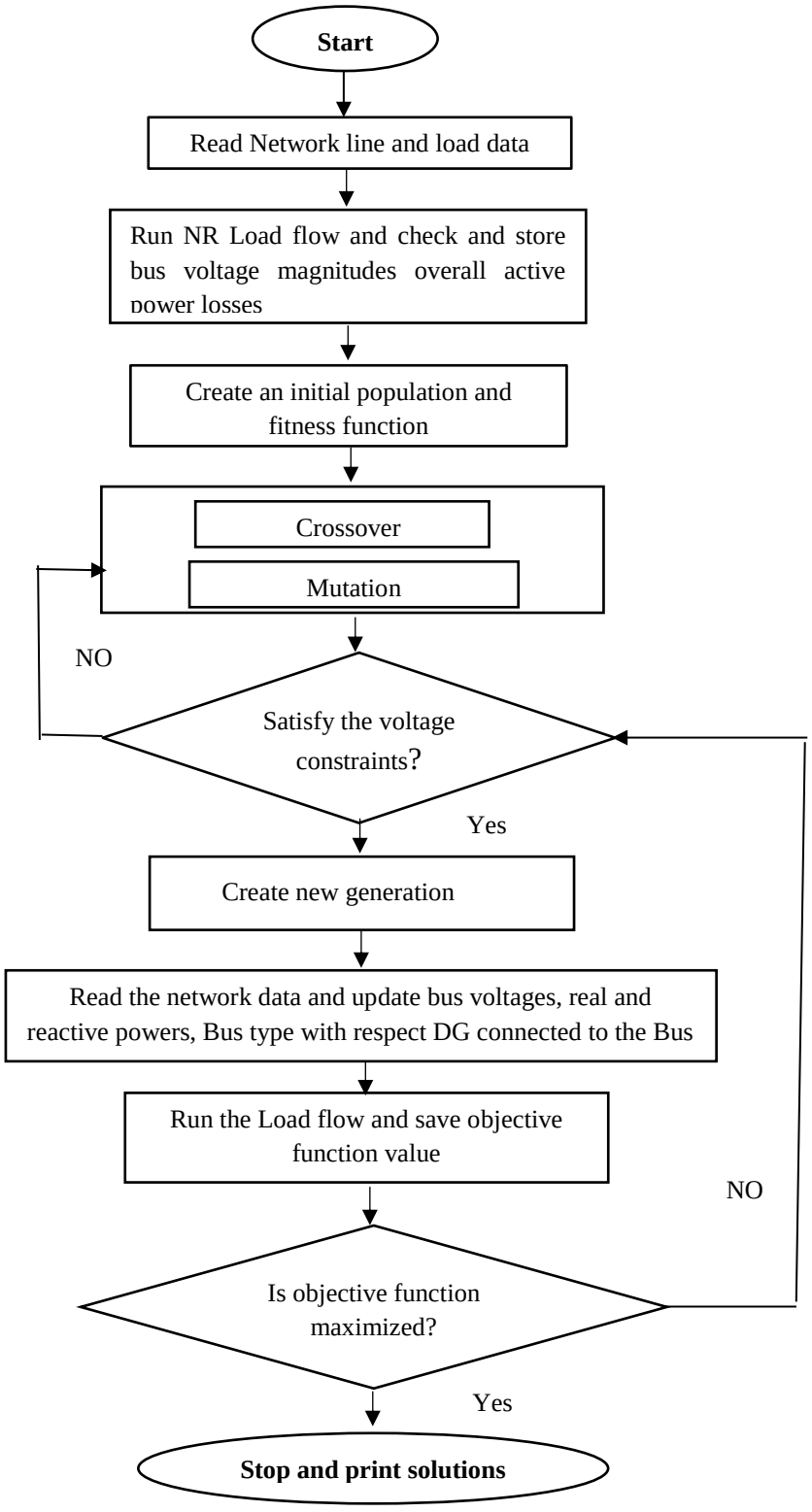

Figure D-1: The flow chart of the GA algorithm applied in this work

Table D-1: The general parameters of GA used throughout the optimization procedure

Parameter	Value
Initial Scores	90
Population size	25
Crossover function	0.8
Generations	10

Table D-2: Settings of GA dimensions for single DG optimal placement on 9-bus system

	Location	Capacity	
		Solar PV	DFIG
Lower bound	4	0.1 MW	0.1MW and 0.1 MVar
Upper bound	9	6.5 MW	6.5 MW and 5 MVar

Table D-3: Settings of GA dimensions for single DG optimal placement on a 33-bus system

	Location	Capacity	
		Solar PV	DFIG
Lower bound	2	0.1 MW	0.1MW and 0.1 MVar
Upper bound	33	2MW	2 MW and 1 MVar

Table D-4: Settings of GA dimensions for multiple solar PV optimal placement on a 9-bus network

	Location			Capacity		
	DG 1	DG 2	DG n	DG 1	DG 2	DG n
Lower bound	4	4	4	0.1MW	0.1 MW	0.1 MW
Upper bound	9	9	9	6.5 MW	6.5 MW	6.5 MW

Table D-5: Settings of GA dimensions for multiple DFIGs optimal placement on a 9-bus network

	Location			Capacity		
	DG 1	DG 2	DG n	DG 1	DG 2	DG n
Lower bound	4	4	4	0.1MW, 0.1 MVAr	0.1MW, 0.1MVAr	0.1MW, 0.1MVAr

Upper bound	9	9	9	6.5 MW, 5MVar	6.5 MW, 5MVar	6.5MW, 5MVar

Table D-6: Settings of GA dimensions for multiple solar PV optimal placement on a 33-bus network

	Location			Capacity		
	DG 1	DG 2	DG n	DG 1	DG 2	DG n
Lower bound	2	2	2	0.1MW	0.1 MW	0.1 MW
Upper bound	33	33	33	2 MW	2MW	2MW

Table D-7: Settings of GA dimensions for multiple DFIGs optimal placement on a 33-bus network

	Location			Capacity		
	DG 1	DG 2	DG n	DG 1	DG 2	DG n
Lower bound	2	2	33	0.1MW, 0.1 MVAr	0.1MW, 0.1MVAr	0.1MW, 0.1MVAr
Upper bound	33	33	33	2MW, 1MVar	2 MW, 1MVar	2MW, 1MVar

University of Cape Town is required to complete this form **before** collecting or analysing data. The objective of submitting this application *prior* to embarking on research is to ensure that the highest ethical standards in research, conducted under the auspices of the EBE Faculty, are met. Please ensure that you have read, and understood the **EBE Ethics in Research Handbook**(available from the UCT EBE, Research Ethics website) prior to completing this application form: http://www.ebe.uct.ac.za/usr/ebe/research/ethics.pdf

APPLICANT'S DETAILS		
Name of principal researcher, student or external applicant		Tlhoriso Gerard Matlokotsi
Department		Electrical Engineering
Preferred email address of applicant:		Mtltlh003@myuct.ac.za
If a Student	Your Degree e.g., MSc, PhD, etc.,	MSc
	Name of Supervisor (if supervised):	Dr. Sunetra Chowdhury
If this is a researchcontract, indicate the source of funding/sponsorship		UCT Mastercard Scholarship
Project Title		Power Quality Enhancement in Electricity Networks Using Grid-connected Solar and Wind Based DGs

I hereby undertake to carry out my research in such a way that:

- there is no apparent legal objection to the nature or the method of research; and
- the research will not compromise staff or students or the other responsibilities of the University;
- the stated objective will be achieved, and the findings will have a high degree of validity;
- limitations and alternative interpretations will be considered;
- the findings could be subject to peer review and publicly available; and
- I will comply with the conventions of copyright and avoid any practice that would constitute plagiarism.

SIGNED BY	Full name	Signature	Date
Principal Researcher/ Student/External applicant	Tlhoriso Matlokotsi		**28 Oct 2016**

APPLICATION APPROVED BY	Full name	Signature	Date
Supervisor (where applicable)	Dr. Sunetra Chowdhury		**28 Oct 2016**
HOD (or delegated nominee) Final authority for all applicants who have answered NO to all questions in Section1; and for all Undergraduateresearch (Including Honours).	Click here to enter text.		Click here to enter a date.
Chair : Faculty EIR Committee For applicants other than undergraduate students who have answered YES to any of the above questions.	Click here to enter text.		Click here to enter a date.